UNIVERSIDADE FEDERAL DE MINAS GERAIS
PROGRAMA DE PÓS-GRADUAÇÃO EM SANEAMENTO, MEIO AMBIENTE E RECURSOS HÍDRICOS

Developing a Seamless Medium- to Long-Range Flow Forecast to Improve the Prediction of Hydropower Generation in Brazil

Alberto Assis dos Reis

Belo Horizonte
2021

Alberto Assis Dos Reis

Developing a Seamless Medium- to Long-Range Flow Forecast to Improve the Prediction of Hydropower Generation in Brazil

Tese apresentada ao Programa de Pós-graduação em Saneamento, Meio Ambiente e Recursos Hídricos da Universidade Federal de Minas Gerais, como requisito parcial à obtenção do título de Doutor em Saneamento, Meio Ambiente e Recursos Hídricos.

Área de concentração: Recursos Hídricos

Linha de pesquisa: Modelagem de Processos Hidrológicos

Orientador: Wilson dos Santos Fernandes
Coorientadora: Maria Helena Ramos

Belo Horizonte
Escola de Engenharia da UFMG
2021

Reis, Alberto Assis dos.
R375d Developing a seamless medium-to-long-range flow forecast to improve the prediction of hydropower generation [recurso eletrônico] / Alberto Assis dos Reis. – 2021.
1 recurso online (232 f. : il., color.) : pdf.

Orientador: Wilson dos Santos Fernandes.
Coorientadora: Maria Helena Ramos.

Tese (doutorado) - Universidade Federal de Minas Gerais, Escola de Engenharia.

Bibliografia: f. 214-232.
Exigências do sistema: Adobe Acrobat Reader.

1. Engenharia sanitária - Teses. 2. Precipitação (Meteorologia) – Teses. 3. Vazão, Medidores de --Modelos matemáticos - Teses. I. Fernandes, Wilson dos Santos. II. Ramos, Maria Helena. III. Universidade Federal de Minas Gerais, Escola de Engenharia. IV. Título.

CDU: 628(043)

Ficha catalográfica elaborada pela Bibliotecária Letícia Alves Vieira - CRB-6/2337
Biblioteca Prof. Mário Werneck - Escola de Engenharia da UFMG

UNIVERSIDADE FEDERAL DE MINAS GERAIS
ESCOLA DE ENGENHARIA
COLEGIADO DO CURSO DE PÓS-GRADUAÇÃO EM SANEAMENTO, MEIO AMBIENTE E RECURSOS HÍDRICOS

FOLHA DE APROVAÇÃO

Developing a seamless medium- to long-range flow forecast to improve the prediction of hydropower generation in Brazil

ALBERTO ASSIS DOS REIS

Tese de Doutorado defendida e aprovada, no dia 10 de dezembro de 2021, pela Banca Examinadora designada pelo Colegiado do Programa de Pós-Graduação em Saneamento, Meio Ambiente e Recursos Hídricos da Universidade Federal de Minas Gerais constituída pelos seguintes professores:

Prof. Dr. Fernando Mainardi Fan

Membro Externo - UFRGS

Prof. Dr. Carlos Henrique Ribeiro Lima

Membro Externo - UnB

Profª. Drª. Letícia Santos de Lima

Membro Interno - UFMG

Profª. Drª. Maria Helena Ramos

Coorientador – INRAE

Prof. Dr. Wilson dos Santos Fernandes

Orientador - UFMG

APROVADA PELO COLEGIADO DO PPG SMARH

Sonaly Cristina Rezende Borges de Lima - Coordenadora

Belo Horizonte, 10 de dezembro de 2021.

Documento assinado eletronicamente por **Wilson dos Santos Fernandes**, **Servidor(a)**, em 13/12/2021, às 11:02, conforme horário oficial de Brasília, com fundamento no art. 5º do Decreto nº 10.543, de 13 de novembro de 2020.

Documento assinado eletronicamente por **Carlos Henrique Ribeiro Lima**, **Usuário Externo**, em 13/12/2021, às 15:26, conforme horário oficial de Brasília, com fundamento no art. 5º do Decreto nº 10.543, de 13 de novembro de 2020.

Documento assinado eletronicamente por **Leticia Santos de Lima**, **Professora do Magistério Superior**, em 14/12/2021, às 07:20, conforme horário oficial de Brasília, com fundamento no art. 5º do Decreto nº 10.543, de 13 de novembro de 2020.

Documento assinado eletronicamente por **Maria Helena Domingues Ramos**, **Usuário Externo**, em 16/12/2021, às 10:26, conforme horário oficial de Brasília, com fundamento no art. 5º do Decreto nº 10.543, de 13 de novembro de 2020.

Documento assinado eletronicamente por **Fernando Mainardi Fan**, **Usuário Externo**, em 16/12/2021, às 23:06, conforme horário oficial de Brasília, com fundamento no art. 5º do Decreto nº 10.543, de 13 de novembro de 2020.

Documento assinado eletronicamente por **Sonaly Cristina Rezende Borges de Lima**, **Coordenador(a) de curso de pós-graduação**, em 10/02/2022, às 09:08, conforme horário oficial de Brasília, com fundamento no art. 5º do Decreto nº 10.543, de 13 de novembro de 2020.

A autenticidade deste documento pode ser conferida no site https://sei.ufmg.br/sei/controlador_externo.php?acao=documento_conferir&id_orgao_acesso_externo=0, informando o código verificador **1138691** e o código CRC **8FA588BE**.

Referência: Processo nº 23072.263347/2021-56 SEI nº 1138691

Acknowledgement

I would like to acknowledge UFMG and CNPq for their collaboration on my PhD research. I also acknowledge Deltares (Albrecht H. Weerts, Jan Talsma and Jan Verkade), INRAE (Maria Helena Ramos, Charles Perrin) and ECMWF (Fredrik Wetterhall) for hosting me during the international visits to their institutes, and for the collaboration in this research project with many discussions and ideas during the development of this work.

I would like to acknowledge CEMIG (Nelson Benício, Marcelo de Deus, Ivan S. Carneiro, Luiz Cesar, Vanessa M. Rezende, Henrique N. Braga) for sponsoring the international visits at the institutes and the colleagues to for their collaboration on my PhD research.

I also would like to acknowledge my supervisor, Wilson dos Santos Fernandes, for the collaboration on this research, sharing ideas for the studies and helping to solve the problems during the period at UFMG.

I also would like to acknowledge my wife Regina and my daughters Lavinia and Marina for their support and patience during the development of the research, which took a big part of my time during nights, weekends, and vacations.

RESUMO

A gestão dos recursos hídricos é de grande importância para muitas atividades humanas, especialmente no contexto operacional no setor elétrico brasileiro, com predominância da geração hidrelétrica. Assim, a previsão de vazões é uma das principais informações para otimização do sistema. Este manuscrito descreve uma série de etapas para lidar com as incertezas nos dados, buscando-se obter uma previsão de vazão confiável. Os trabalhos desta pesquisa têm como objetivo desenvolver e avaliar uma cadeia de dados e modelos para a previsão hidrometeorológica de curto (vários dias) à longo (vários meses) prazo, que possa ser utilizada para a previsão da produção hidroelétrica no Brasil. O estudo é baseado em 41 bacias hidrográficas, que representam 30 hidrelétricas na América do Sul, com alto interesse para produção de energia. Para a incerteza na precipitação estimada a partir de dados observados, foram investigadas as diferenças entre TRMM_MERGE e CPC para diversas resoluções de tempo (precipitação diária, mensal e anual). Foram encontradas diferenças substanciais entre as duas fontes de dados, que parecem ser amplificadas no período 2008-2017. Foi encontrada uma tendência espacial, com valores de precipitação do TRMM-MERGE mais elevados que os do CPC ao se deslocar para norte e oeste na área de estudo. Baseado nessas incertezas observadas e buscando uma melhor estimativa da precipitação, foi avaliada também a combinação destas duas fontes. Assim, inspirado na equação do balanço hídrico modificada, foi identificada e quantificada a incerteza envolvendo o conjunto de dados de precipitação e utilizada a modelagem hidrológica para escolher e validar melhores dados de precipitação. Os resultados indicaram que a combinação da precipitação em tempo real (TRMM-MERGE e CPC), ponderada pela incerteza das fontes originais, tem um desempenho superior ao uso isolado de uma das fontes de dados. Outra fonte de incerteza analisada foi a previsão de precipitação. Nesta etapa, foi comparado o desempenho de dois métodos diferentes de correção de viés, o *QM - Quantile Mapping* e o *LS - Linear Scaling*. Em termos de previsão de precipitação sazonal (até 7 meses de horizonte de previsão), os resultados indicaram que os erros observados na previsão bruta são mais dependentes do mês do ano do que do horizonte de previsão, com uma superestimação sistemática durante a estação chuvosa e uma subestimação observada durante a estação seca, para a maioria das bacias estudadas. Os métodos de correção de viés foram eficazes, especialmente durante a estação chuvosa, com o método *QM* apresentando melhor desempenho. Baseado no bom desempenho obtido com este método, a correção de viés foi aplicada nas previsões de médio (até 45 dias) e curto (até 15 dias) prazo do centro europeu de previsão ECMWF, mas com uma diferente forma de aplicação. O modelo de médio prazo, à cada rodada (lançamento de uma previsão), gera também o *hindcast* dos últimos 20 anos, para os mesmos 46 dias do calendário. Assim, os parâmetros para a correção QM são recalculados à cada rodada, gerando uma correção *on-the-fly*, apenas dependente do horizonte de previsão. Esses mesmos parâmetros são utilizados para corrigir o modelo de curto prazo, apresentando resultados iguais ou melhores que os resultados obtidos com os parâmetros calculados apenas com o histórico de previsões do modelo de curto prazo. Esse método apresenta uma vantagem, pois não precisa de um longo histórico de previsões para calibração dos parâmetros de correção de viés, podendo acompanhar melhor as evoluções dos modelos meteorológicos (no caso desta tese, os modelos do ECMWF). Para construir a previsão de precipitação de maneira continua ("*seamless*"), baseada no acoplamento

dos três horizontes de previsão dos modelos do ECMWF (15 dias, modelo EPS; 45 dias, modelo "*extended*" e 7 meses, modelo sazonal), foram testados vários métodos de acoplamento, sendo escolhido o método membro-a-membro. Este apresentou o mesmo desempenho quando comparado aos métodos mais sofisticados também investigados nesta tese, mas com a vantagem de não necessitar de grande esforço matemático ou manipulação dos dados. O principal resultado obtido indicou que o maior número de inicializações dos modelos de curto e médio prazo (inicializados diariamente e a cada segunda e quita feiras, respectivamente) melhora o desempenho das previsões de precipitação, principalmente para o mês seguinte à data de inicialização da previsão. Esta previsão contínua de precipitação foi aplicada à modelagem hidrológica. Foram testadas duas técnicas de pós-processamento para tratar a incerteza da previsão hidrológica, sendo estas a assimilação dos dados de vazão em tempo real e a aplicação de uma correção autorregressiva (*AR output-error correction*) para ajustar a saída do modelo (previsões finais de vazão). A aplicação destas técnicas melhorou o desempenho das previsões, produzindo resultados mais confiáveis e com menor erro médio, principalmente nos dois primeiros meses do horizonte de previsão. A previsão de vazão proposta à partir das diferentes etapas de construção de previsões hidrometeorológicas de curto à longo prazo foi aplicada para prever a produção de energia hidrelétrica do sistema interligado baseada nas 30 usinas associadas às 41 bacias hidrográficas deste trabalho de tese. Os resultados mostraram um bom desempenho do sistema de previsão, sendo este capaz de prever quando a produção estaria acima ou abaixo da produção média para os horizontes de previsão mais distantes (previsão sazonal). O trabalho desenvolvido nesta tese propõe assim uma ferramenta que apresenta um grande potencial para ser aplicada no planejamento da operação hidrelétrica no Brasil, podendo auxiliar na otimização da operação do sistema elétrico e na gestão do uso da água de reservatórios.

Palavras-chave: Previsão de vazões; Correção de viés; Previsão de precipitação; Previsão contínua; Previsão de Geração hidrelétrica

ABSTRACT

The management of water resources is of great importance for many human activities, especially in the operational context of the Brazilian electricity sector, where we have a predominance of hydroelectric generation. In this context, streamflow forecasts are the main source of information for the optimization of the electric system. This PhD thesis describes a series of steps developed to deal with uncertainties in the forecasts, in order to obtain reliable flow predictions. This research work aims to develop and evaluate a chain of data and models for short (several days) to long (several months) term hydrometeorological forecasting, which can be used for forecasting the hydroelectric production in Brazil. The study is based on 41 river basins, which represent 30 hydroelectric plants in South America, with high interest for energy production. For the uncertainty in the observed precipitation data, we investigated the differences between the TRMM_MERGE and CPC datasets, considering different resolutions (daily, monthly and annual precipitation). Substantial differences were found between the two data sources, which seem to be amplified in the period 2008-2017. A spatial trend was found, with TRMM-MERGE precipitation values higher than those of the CPC dataset when moving towards north and west in the study area. Based on these observed uncertainties, and seeking a better estimate of precipitation, the combination of these two sources was evaluated. Inspired by the modified water balance equation, uncertainties involving the precipitation datasets were identified and quantified. Hydrological modeling was also used to choose and validate the precipitation datasets. The results indicated that the combination of real-time precipitation (TRMM-MERGE and CPC), weighted by the uncertainty of the original sources, outperforms the isolated use of only one of the data sources. Another source of uncertainty analyzed was the precipitation forecast. In this step, the performance of two different bias correction methods, QM - Quantile Mapping and LS - Linear Scaling, was compared. In terms of seasonal precipitation forecast (up to 7 months of forecast horizon), the results indicated that the errors observed in the raw forecasts are more dependent on the month of the year than on the forecast horizon, with systematic overestimation during the rainy season and underestimation observed during the dry season for most of the basins studied. The bias correction methods were effective, especially during the rainy season, with the QM method showing better performance. Based on the good performance obtained with this method, the bias correction was applied to the medium (up to 45 days) and short (up to 15 days) term forecasts of the European center ECMWF, but with a different application. At each initialization (time when a forecast is issued), the medium-term

model also generates the reforecast of the last 20 years, for the same 46 calendar days. Thus, the parameters for the QM correction were recalculated at each initialization, generating an on-the-fly correction, which depends only on the forecast horizon. These same parameters were used to correct the short-term model, and the results obtained were equal to or better than the results obtained with the parameters calculated only with the historic time series of short-term reforecasts. This method is advantageous as it does not need a long time series of reforecasts to calibrate the bias correction parameters, which allows to better follow the evolution of meteorological models (in the case of this thesis, the ECMWF models). To build the precipitation forecast in a continuous (seamless) way, based on the coupling of the three forecast horizons of the ECMWF models (15 days, EPS model; 45 days, extended model and 7 months, seasonal model), several coupling methods were tested. The member-by-member method was chosen as it presented equal performance when compared to the more sophisticated methods, but with the advantage of not requiring great mathematical efforts or data manipulation. The main result obtained indicated that the greater number of initializations of the short- and medium-term models (initialized every day and every 15 days, respectively) improves the performance of the precipitation forecasts, especially for the month following the start date of the forecast. The seamless precipitation forecast was applied to a hydrological modelling framework. Two post-processing techniques were tested to deal with the uncertainty of the hydrological forecasts, these being the assimilation of streamflow data in real time, and the application of an autoregressive correction (AR output-error correction) to adjust the model output (final streamflow predictions). The application of these techniques improved the performance of the forecasts, producing more reliable results and with lower average error, especially in the first two months of the forecast horizon. The streamflow forecasts obtained from the different stages of construction of the short to long-term hydrometeorological forecasting system were applied to predict the production of hydroelectric energy in the Brazilian electric system, based on the 30 plants associated with the 41 river basins of this thesis. The results showed a good performance of the forecasting system, which was able to predict when the production would be above or below the average production for the most distant forecast horizons (seasonal forecast). The work developed in this thesis proposes a tool that has great potential to be applied in the planning of the hydroelectric operation in Brazil, which can contribute to the optimization of the operation of the electrical system and the management of the use of the water stored in the reservoirs.

Keywords: Flow Forecast; Bias correction; Precipitation forecast; Seamless Forecast; Hydropower Generation Prediction

List of Publications

Journals

Published:

REIS, A. A.; FERNANDES, W. S.; RAMOS, M. H.: Assessing two precipitation data sources at basins of special interest to hydropower production in Brazil. *RBRH - Brazilian Journal of Water Resources*, RBRH-2019-0068 , 2019 - http://dx.doi.org/10.1590/2318-0331.252020190068

REIS. A. A.; WEERTS. A.; RAMOS. M. H.; WETTERHALL. F.; FERNANDES. W. S.: Hydrological modeling as a tool for selection and validation of precipitation data relevant to seasonal streamflow forecasting. *Journal of Hydrology Regional Studies*, EJRH-D-21-00413, 2021 (submitted, received 'major review' and the revised version is under preparation)

To be submitted:

REIS. A. A.; RAMOS. M. H.; WEERTS. A.; WETTERHALL. F.; FERNANDES. W. S.: The quality of seasonal precipitation and streamflow forecasts in Brazil over a large set of river basins. *HESS - Hydrology and Earth System Sciences Journal*

REIS. A. A.; RAMOS. M. H.; WETTERHALL. F.; WEERTS. A.; FERNANDES. W. S.: Improving the performance of ECMWF short range and subseasonal precipitation forecasts in South American Catchments: *Climate Services Journal - Special Issue*

REIS. A. A.; RAMOS. M. H.; WETTERHALL. F.; WEERTS. A.; FERNANDES. W. S.: Coupling the different ECMWF forecast models to build a seamless precipitation forecast for a group of South America Catchments. *Climate Services Journal- Special Issue*

REIS. A. A.; RAMOS. M. H.; WEERTS. A.; WETTERHALL. F.; FERNANDES. W. S.: Developing seamless medium- to long-range flow forecast to improve the prediction of hydropower production in Brazil. *HESS - Hydrology and Earth System Sciences Journal*

Symposiums and Congress

REIS, A. A.; FERNANDES, W. S.; RAMOS, M. H.; WETTERHALL, F.; WEERTS, A.; VERKADE, J. Performance of the new ECMWF seasonal forecast model SEAS5 in South American catchments with hydropower plants. *EGU2019 – European Geoscience Union General Assembly*, EGU2019-11264, 2019, https://meetingorganizer.copernicus.org/EGU2019/EGU2019-11264.pdf

LIST OF FIGURES

LIST OF TABLES

LIST OF ABBREVIATIONS and ACRONYMS

ACL - Free Contract Environment

ACR - Regulated Contract Environment

AMJ - April, May and June

ANEEL - National Electric Energy Agency

BS_{rel} - Brier Score Reliability

BS_{res} - Brier Score Resolution

CCEE - Electric Energy Commercialization Chamber

CDF - Cumulative Distribution Functions

CFSv2 - Climate Forecast System Version 2

CMO - Marginal Cost of Operation

CPC - Unified Gauge-Based Analysis of Global Daily Precipitation

CPTEC - Weather Forecast and Climatic Studies Center (Centro de Previsão de Tempo e Estudos Climáticos)

CRPS - Continuous Rank Probability Score

DECOMP - Short-Term Interconnected Hydrothermal Systems Operation Planning Model (Modelo de Planejamento da Operação de Sistemas Hidrotérmicos Interligados de Curto Prazo)

DELFT FEWS - Delft Flood Forecast and Warning System

DESSEM - Short-Term Hydrothermal Dispatch Model (Modelo de Despacho Hidrotérmico de Curto Prazo)

ECC - Ensemble Copula Coupling

ECDF - Empirical Cumulative Distribution Functions

ECHAM4.6 - Atmosphere General Circulation Model - ECHAM4.6 developed by Max Planck Institute for Meteorology

ECMWF - European Center for Medium-range Weather Forecast

ENA - Affluent Natural Energy

EPE - Energetic Research Company

EPS - Ensemble Prediction System

ERA5 - Interim Reanalysis version 5

ESP - Ensemble Streamflow Prediction

GCM - General Circulation Models

GEFS - Global Ensemble Forecast System

GloFAS - Seasonal forecasting System Around the Globe

GPCP-1DD - Global Precipitation Climatology Project - Daily

GPM - Global Precipitation Measurements

GTS - Global Telecommunications System

HEC-HMS - Hydrologic Engineering Center - Hydrologic Modeling System

HPP - Hydropower Plant

IMERG - Integrated Multi-satellitE Retrievals

INPE - National Institute of Spatial Research

JAS - Japanese Agricultural Standards

JAXA - Japan Aerospace Exploration Agency

JFM - January, February and March

KGE - The Kling-Gupta efficiency

LS - Linear Scaling

MAE - Mean Absolute Error

MGB - Big Basins Hydrological Model

MWSEP - Multi-Source Weighted-Ensemble Precipitation

NASA - US National Aeronautics and Space Administration

NCAR - US National Center for Atmospheric Research

NCEP - National Centers for Environmental Prediction

NEWAVE - Long- and Medium-Term Interconnected Hydrothermal Systems Operation Planning Model (Modelo de Planejamento da Operação de Sistemas Hidrotérmicos Interligados de Longo e Médio Prazo)

NOAA - National Oceanic and Atmospheric Administration

NSE - Nash- Sutcliffe efficiency

NWP - Numerical Weather Predictions

OND - October, November, and December

ONS - National Operator of the Electric System

PLD - Settlement Price of Differences

QM - Quantile Mapping

R^2 - Coefficient of Determination

RegCM4 - Regional Climatic Model System Version 4 developed by NCAR

RME - Relative Mean Error

RMSE - Root Mean Square Error

S2S - Subseasonal to Seasonal

SEAM - A merged system of ECMWF extended range forecast and seasonal forecast system SEAS4

SEAS4 - ECMWF seasonal forecast system 4

SEAS5 - ECMWF seasonal forecast system 5

SMA - Soil Moisture Accounting

SPPT3 - Stochastic Atmospheric Perturbations Version 3

TMPA 3B42 - Rainfall Estimate L3 3 hour 0.25 degree x 0.25 degree V7

TRMM - Tropical Rainfall Measuring Mission

TRMM-MERGE - Combination of IMERG and GPM data developed by CPTEC

WFDEI-CRU - WATCH Forcing Data ERA Interim

SUMMARY

CHAPTER 1:

INTRODUCTION

1 INITIAL CONSIDERATIONS

1.1 BACKGROUND AND JUSTIFICATION

Precipitation as a crucial variable for large-scale hydrological modelling

The quantification of precipitation and its spatiotemporal distribution in a certain area has high importance in hydrology, especially when we are assessing the impacts of the weather in human activities, like water resources management, irrigation, hydropower generation, urban planning and forecasting the extremes such as floods and droughts (Golding, 2009; Kucera et al., 2013; Pozzi et al., 2013; Serrat-Capdevila et al., 2013; Lettenmaier et al., 2015; Verkade, 2015 and Beck et al., 2017). In the Brazilian case, the electrical system is essentially hydrothermal, having more than 65% of its production from hydroelectric generation; therefore, it is crucial to have a robust and trustworthy streamflow forecasting system to forecast inflows to the power plants in order to maximize the production and optimize the management of multiple water uses in hydropower reservoirs.

Precipitation is however one of the most difficult variables to estimate and to forecast, mainly due to its heterogeneous distribution in space and in time, to the small-scale processes, such as convection, that are difficult to represent in numerical models, and to the measurement errors caused by sparse rain gauge networks, uncalibrated equipment, communication problems and human errors affecting the measured values, among others (Herold et al., 2015). With the constant search to improve the representativeness of the observed precipitation, mainly in areas with a low density of gauge of stations, gridded precipitation products, from satellite, radar or their combination with rain gauges, have emerged since the late 1990s (Huffman et al., 1997; Adler et al., 2003). These products have been constantly improved, as technology advances and new measurements are added. Within the experiment MSWEP, Beck et al. (2017) studied and compared a group of 22 gridded rainfall data products based on estimations of precipitation with a constellation of satellites, rain gauges and reanalyzes of meteorological models. The authors concluded that the product that merged all information available — Multi-Source Weighted-Ensemble Precipitation (MSWEPv1.0) — had better overall performance. From this group of 22 data sources, only two however had real-time data available, on a daily basis, with a spatial resolution equal to or higher than 0.5°, and covering the whole South America. These datasets are the CPC Unified Gauge-Based Analysis of Global Daily Precipitation of the US National

Center for Atmospheric Research (NCAR) (Chen et al., 2008) and the NASA's IMERG, Integrated Multi-satellitE Retrievals for GPM (Global Precipitation Measurements) data (Huffman et al., 2017), the successor of the Tropical Rainfall Measuring Mission (TRMM) data products. Particularly in the Brazilian case, we also have the TRMM-MERGE dataset, where the IMERGE information is coupled with data from Brazilian rain gauges to solve some problems of underestimation and overestimation observed in some regions (Rozante et al., 2010, 2018, 2020).

With this growing availability of information and precipitation products, with sometimes diverging spatial and temporal resolutions (Juárez et al., 2009; Demaria et al., 2011; Scheel et al., 2011; Falck et al., 2015; Mantas et al., 2015), it is a challenge for users to assess the quality of the datasets and select the best precipitation forcing for hydrological studies and river basin water management. This challenge has been explored by many researchers, including by using hydrological models as a tool to deal with the validation of precipitation products (e.g., Su et al., 2008; Collischonn et al., 2008; Voisin et al., 2008; Bitew et al., 2012; Li et al., 2013; Falck et al., 2015; Tang et al., 2016; Beck et al., 2017). Overall, the studies indicate that where there are good estimates of the observed flows at the outlet of the river basins, at least better than estimates of the precipitation, the use of hydrologic modeling can indirectly bring result in improvements to the estimations of the observed precipitation and help with data validation.

The transformation of precipitation data into runoff and flow information at the outlet of river basins is essential for many human activities. In the last years, large-scale hydrological simulation projects have been developed at continental and global scales, the majority using as precipitation forcing reanalysis data, as, for example, the HTESSEL offline model coupled to the CaMa-Flood (Balsamo et al., 2009; Yamazaki et al., 2011), the LISFLOOD model (van der Knijf et al., 2010) and the WaterGAP3 model (Doll et al.,2009). Siqueira et al. (2018) applied a distributed model (the MGB model) over South America and obtained good simulation results using also the reanalysis dataset MSWEP (Beck et al., 2017).

For hydrologic applications related to river flow forecasting, the simulation models have to be able to run continuously in real-time, with precipitation data also available in real-time or near real-time. Recently, GloFas, aGlobal ensemble streamflow and flood warning system (Alfieri et al., 2013; Shummann et al., 2018) has been developed for real-time flood forecasting at a global scale. It uses a hydrological model (LISFLOOD) to forecast flows up to 45 days ahead in major

river basins worldwide and seasonal ensemble forecasts for up to 16 weeks ahead since version 2.1 (ECMWF, 2019). In Australia, Bennett et al. (2017) present the developments carried out for seasonal forecasting by merging the meteorological models and the precipitation climatology to create an ensemble of futures scenarios, FoGSS – forecast guided stochastic scenarios (Bennett et al, 2017), which are then used as forcing in the hydrological model to generate an ensemble of streamflow forecasts up to for 12 months ahead.

The hydropower sector in Brazil and its needs for reliable forecast information

The Brazilian electric system has a hydrothermal structure with a centralized operation, where the ONS (System National Operator) defines the rules and the normalization in order to have an harmonic operation of the system countrywide to attend the energy demand at the lowest price. This set of rules are in the "Network Procedures", which organize all the information of the system's operation, with the obligations of all agents involved at the operation of the system, the optimization and forecast models used, the consistence of all information, etc. (ONS, 2021). To sell all the energy produced in Brazil, there are two main energy markets, the ACR (Regulated Contract Environment), where the Federal Government, with energy auctions, attend the structural demand of the electric system and the demand of the distribution companies responsible to sell energy directly to the captive consumers, and the ACL (Free Contract Environment), where the bigger consumers, with bilateral contracts, buy the energy directly from the generators (CCEE, 2021). The commercial part of the energy system is under the responsibility of the CCEE (Electric Energy Commercialization Chamber), where all the contracts are registered and also run the same models used by ONS to optimize the energy production, with a similar deck of information, but with the objective to calculate the PLD (Settlement Price of Differences), which is the price of the energy spot market, where all the energy produced attend the demand, but without contracts with the ACL or the ACR, which is remunerated by the PLD (CCEE, 2021). The optimization models take into account the predictions of the energy demand, the energy production of all available sources, hydraulic, thermal, solar, wind and others, the level of the reservoirs, and other information (Nascimento, 2021). Besides the Brazilian electric system be hydrothermal, and year after year it is increasing the participation of other sources as solar and wind power, the energy production and its price still strongly depend on the hydropower generation. Even during the sequence of drought years observed since 2013, the majority of the electricity production was still coming from hydropower, responsible for 76% of the energy production in 2016 (Paiva et al., 2020).

As shown in Figure 1.1, the needs of the hydroelectric system for accurate and reliable forecasts extent from forecasts up to 24-48 hours ahead for the balance of the electric grid (ONS, 2019), short-range from 1-7 days for flood control depending on the basin size, medium-range forecasts up to 7–30 days ahead for energy trading in the spot-market (CCEE, 2010), and seasonal (months ahead) streamflow forecasts for the electric system's optimization, maintenance planning, management of the multiple uses of water , and long-term energy trading strategies. Therefore, all forecast horizons have a great importance for the electric system. It becomes crucial to extract the best information of each forecasting system that targets a given forecast horizon.

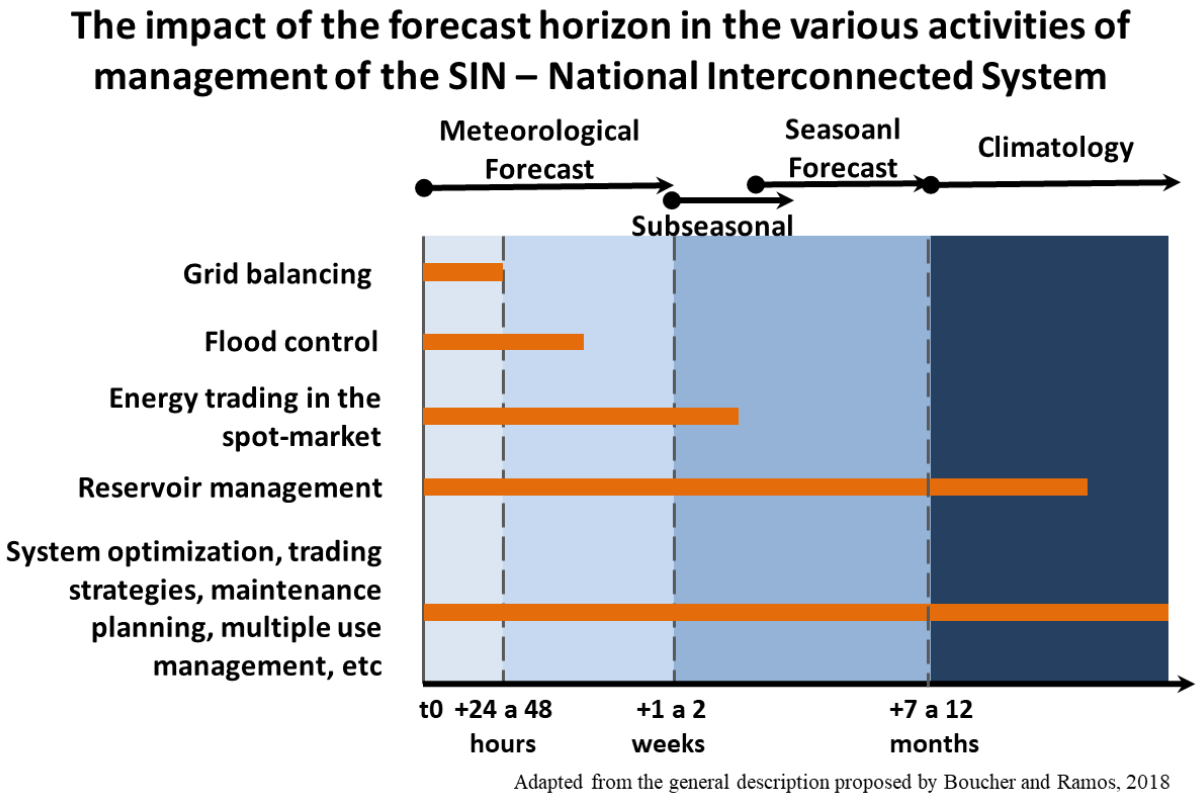

Figure 1.1 –The impact of the forecast horizon in the various activities of management of the SIN – National Interconnected System (adapted from the general description proposed by Boucher and Ramos, 2018)

Uncertainties in river flow forecasting

Uncertainty in hydrologic modeling may arise from several sources: model structure, parameters, initial conditions, and observational data as observed precipitation and streamflow used to drive and evaluate the model (Liu et Gupta, 2007). Uncertainty is part of the modelling process, as a result of the inherently chaotic behavior of the atmosphere (forcing uncertainty), the limitations in our ability to measure and model the different compartments of the hydrological cycle, and

the errors present in observational and model data (Gill et al. 2008). Therefore, working with river flow forecasting is a process where we have to constantly deal with uncertainties to achieve the goal of reducing the errors in the forecasts.

A major source of uncertainty in river flow forecasting is the meteorological uncertainty. Meteorological models are in constant evolution, aiming at improving their spatial and temporal resolution, incorporating new internal elements of the dynamics of precipitation formation and moving from deterministic models to probabilistic models (ensemble forecasts) with the representation of scenarios generated from perturbations of the initial conditions and stochastic parametrizations of the models (ECMWF, 2015). With this information, we can have a better knowledge of the future precipitation, which is one of the most important information when it comes to assess the availability of water in the future.

The European Centre for Medium-Range Weather Forecasts (ECMWF) precipitation forecast products can be divided in three products covering different temporal scales. The medium-range forecast model (until 15 days ahead) runs twice a day with 51 ensemble members. There is no ocean coupling for the first 10 days of the forecasts. From day 10 onwards, the atmospheric model is coupled with the ocean model (ECMWF, 2015). The ECMWF extended forecast (sub-seasonal forecast; until 46 days ahead) runs twice a week, every Monday and Thursday. The treatment of the ensemble members between day 15 and day 46 is the same as for the 10-15 day of the medium-range forecast model. The ECMWF extended forecast also provides an “on-the-fly” hindcast from the same calendar date for the last 20 years (ECMWF, 2015). The ECMWF seasonal forecast system (SEAS5) consists of an ocean analysis to estimate the initial state of the ocean, a global coupled ocean-atmosphere general circulation model to calculate the evolution of the ocean and atmosphere, and a post-processing suite to create forecast products from the raw numerical output. The seasonal forecast consists of a 51-member ensemble with up to seven months of forecast horizon. The ensemble is created using a combination of sea surface temperature (SST) and atmospheric initial condition perturbations and the activation of stochastic physics. The stochastic physics settings are identical to those used in the medium-range ensemble forecast (ECMWF, 2017).

Seasonal streamflow forecasts can help to take anticipatory measures for a range of applications, such as water supply or hydropower reservoir operation, energy trading and drought risk management. However, forecasts have a degree of uncertainty and can present systematic biases.

In order to improve the applications of forecasting systems, it is generally useful to apply bias correction techniques or statistical post-processors to the raw forecasts (Verkade, 2015; Crochemore et al., 2016). There are many methods for reducing bias in forecasts. These methods use reforecasts and observations to estimate the parameters of a statistical model that is applied to estimate the corrected probability distribution of the forecast. Techniques include linear regression (e.g. Hay and Clark, 2003; Gneiting et al., 2005; Hagedorn et al., 2008; Wilks, 2011), logistic regression (Hamill et al., 2008; Wilks, 2011), quantile mapping (Bremnes, 2004; Wood et al., 2004; Sharma et al., 2007; Sun et al., 2011; Verkade et al. 2013; Ratri et al., 2019) and indicator co-Kriging (Brown and Seo, 2010, 2013), among others.

Besides investing in the correction of the biases of the precipitation forecasts, hydrological modelers and forecasters also have to deal with the uncertainties related to the observed precipitation. These uncertainties affect the initial conditions of the models and, consequently, lead to errors in the flow forecasts, especially in the initial forecast horizons, which, for large basins, may exceed one month. Observational and initial conditions uncertainty can be treated in a lumped way, pulling it together with the other uncertainties, including the meteorological uncertainty (Regonda et al., 2013). Alternatively, it can also be treated separately, since observational and initial conditions uncertainty depends on the hydrological modeling process and can be caused, for example, by measurement and sampling errors, climate variability and the determination of the initial and boundary conditions (Kim et al., 2021), independently of the meteorological forecast model. Some authors apply this approach (separation of uncertainties) (Krzysztofowicz, 2002; Seo et al., 2006; Demargne et al., 2014). Different post processing techniques are available to improve model predictions. The Quantile mapping (QM) technique, also widely used for seasonal meteorological forecasts as seen previously, is commonly used in hydrological corrections approaches (Shi et al., 2008; Madadgar et al., 2014), but other approaches also exist, based, for instance, on Bayesian models (Krzysztofowicz and Maranzano, 2004; Brown and Seo, 2010, 2013), or the generalized linear regression (Zhao et al., 2011). Additionally to post-processing model outputs to correct forecast biases, data assimilation is another important component to address the errors of initial conditions and improve the accuracy of real-time forecasts. In general, Wu et al. (2012) group the data assimilation techniques into two approaches: those where the inputs are changed and, in some cases, also the parameters or internal states of the model are changed; and those that directly adjust the outputs of the model regardless of what is happening internally in the model. This last category is also associated with “output correction” techniques. Xiong and O'Connor (2002) studied several data assimilation

methodologies for error correction and concluded that Auto-Regressive (AR) models present better performance in correcting errors in flow predictions. Later, studies have shown that lower order models (2 or 1) fitted better to predictions (Wu et al., 2012).

Seamless forecasting

Whatever techniques of post-processing, data assimilation or output model error correction are applied, there is a growing interest from forecast providers and users to consider generating seamless forecasts. The seamless prediction is a concept widely used in climatic change projections (see, for example, the studies about projections of regional anthropogenic climate changes by Solomon et al., 2007). The idea could be translated into the simple concatenation of "the best" forecast at each lead-time (Palmer and Webster, 1993). The clear advantage of this off-the-shelf seamless prediction is that it utilizes products that are already in place, thereby avoiding the complications of new developments while generating forecast products to meet different types of needs (Pappenberger et al., 2013). The use of a seamless prediction system allows, for instance, probabilistic projections of climate change to be constrained by validations on weather or seasonal forecast timescales, which can also improve the initialization of the seasonal forecast models by adding, at each new run, better initial conditions (Palmer, 2008). Another example of seamless forecast application is the PROFORCE project, where forecasts from nowcasting (hours ahead) were coupled to medium-range forecasts (days ahead) providing a seamless forecast for decision makers and civil protection during extreme storms (Wastl et al., 2018). Since seamless forecasts can be used across a variety of forecast horizons, the application of this concept to the optimization of the hydropower production and the electric system's operation becomes an interesting application for this particular sector.

Tools for river flow forecasting and forecast performance assessment

Due to the great importance of future flows in the Brazilian electric system, the investment in flow forecasting using meteorological models has intensified in the past years, mainly for the operation of reservoirs in order to attend multiple uses and flood control. More recently, we have also observed in Brazil, the transition from a deterministic approach to a stochastic approach in the modeling of streamflows to be used as input to hydropower plants, with a particular focus on the potentials and open opportunities related to the use of ensemble forecasts (ONS, 2019). This approach, which attempts to take into account the uncertainties involved in flow predictions in a

more space-time coherent way by using ensemble members generated by meteorological modes as input to hydrological models (see Cloke and Papenberger, 2009, for a review), is still incipient in Brazil. Fan (2015) showed however that significant gains in reliability and accuracy in flow forecasts can be achieved with the adoption of probabilistic precipitation forecasts in conjunction with hydrological models to applications such as flood control or hydropower plants operation (Fan et al., 2014; Fan et al., 2016). More recently, Siqueira et al. (2021) provided a continental-scale assessment of the use of statistical post-processing on medium-range, ensemble streamflow forecasts over South America, based on ECMWF reforecast data and the MGB hydrological model. The authors highlighted current challenges and opportunities to improve the skill of medium-range forecasts, such as the use of better observational datasets for the calibration of post-processors and the use of data assimilation techniques for better model initial conditions.

The operationalization of hydrologic ensemble modeling and forecasting is a fairly laborious activity to perform manually, because it means repeating several times the data collection activities, the preparation of files for models and their application in hydrological models. Thus, the development of tools to automate this process is growing fast. Within this context of integrated modeling, the Delft-FEWS system has been developed (Werner and Heynert, 2006; Twigt et al., 2011; Werner et al., 2013; Schwanenberg et al., 2015; Gibertoni et al., 2017). It is a sophisticated system composed of a set of modules that can be used in a workflow, in order to build an operating system of water resources management adapted to the individual needs of each user (Gijsbers, 2010). In Brazil, CEMIG, the main electricity company of Minas Gerais, has adopted the Delft-FEWS system since 2015 (Gibertoni et al., 2017). The research presented in this PhD thesis relies on this system and brings additional novel components to it, mainly in terms of handling seamless ensemble meteorological forecast data, post-processing model outputs and assimilating data to improve hydrologic initial conditions and flow forecasts. Together with the DELFT FEWS-CEMIG System, this research also uses the EVS (Ensemble Verification System; Brown et al., 2010) to asses forecast performance. It is a flexible, user-friendly, software tool that is designed to verify ensemble forecasts of numeric variables, such as temperature, precipitation, and streamflow. For a better visualization and analyses of some specific results of this thesis, some complementary R codes were also developed.

Motivation, originality and research questions

This research is motivated by the following considerations:

- Ensemble flow forecasting in Brazil is still insipient. The ONS National Operator of the Electric System started to use ensemble forecasts in 2017, and recently has worked on improving the system through bias analysis and correction for the first 10 days of forecast horizon (ONS, 2019). The application of meteorological ensemble models, across different time horizons, from days to months ahead, can strongly contribute to enhance the performance of flow forecasts in Brazil and provide information for a better use of the water resources and a more efficient operation of the reservoirs, ensuring the safety of the electric system at the lowest cost to society;

- Beyond novel operational tools for a broader field of applications, there is also a need to better understand how post-processing techniques can be efficiently applied when dealing with forecasts and predictions from different models and targeting different lead times. Research is needed to better understand sources of uncertainty and systematic biases. This study also contributes to the development and expansion of knowledge of the techniques to perform flow forecasts and deal with some of the uncertainties inherent in the forecast process, in order to propose methods to improve the forecasts and extract the maximum of information from the data available;

- Although many studies have assessed global datasets of historic precipitation data worldwide, there is a need to investigate how a good-quality precipitation dataset that covers South America can be obtained following some essential criteria for flow forecasting: a long enough dataset to allow the estimation of regional climatologies and an easy-to-access dataset for real-time or near real-time operational applications. This study assess how good the available large-scale gridded real-time precipitation datasets are over South America, and proposes a combined precipitation dataset, which is an outcome that can be applicable in many research and operational areas;

- To the knowledge of the author, this study is the first to evaluate the performance of the three ECMWF forecast models available, covering different time horizons (precipitation forecasts from days to months ahead) and a large set of river basins with different climatic and physiographic characteristics over South America. This study investigates the different models separately but also in combination, with the aims to efficiently combine the available information and offer a methodology for generating seamless predictions. Such information is of great importance for decision-making in various socio-economic

fields, such as drought forecasting, agribusiness, energy, transport, tourism, multiple water uses, and others.

The originality of this research lies in the proposition of a methodology to generate seamless medium- to long-term forecasts, while dealing with a specific group of uncertainties described below, at a continental scale, and identifying spatial and temporal patterns of predictability. The first source of uncertainty assessed is the observed precipitation data, and a method is proposed to combine two different existing data sources for real time applications based on their uncertainty (chapters 2 and 3). The second source of uncertainty assessed is the precipitation forecast. Several forecast horizons, from days to months, are explored and different bias correction methods are applied to evaluate their ability to reduce biases and improve forecast quality (chapters 4 and 5). The research also investigates five different coupling methods to select the better way to build a seamless precipitation forecast, a novel work that is very incipient in Brazil and internationally (chapter 6). Finally, the seamless precipitation generated in the research is applied in a flow forecasting framework to evaluate its value in the hydrometeorological forecasting chain (chapter 7). At this point of the research, a flow data assimilation method and a flow post-processing technique are also explored to assess hydrologic initial conditions uncertainty and hydrologic model biases. The aim is to improve further the performance of the flow forecasts, especially at the first days of lead time, and open up opportunities towards future investigations on the value of the forecasts for hydroelectric production.

With this research, we aim to answer the following scientific questions:

1. *How to improve the representativeness of Brazilian climatology as an way of guaranteeing energy security in the context of hydroelectric generation?*

    a. *How representative of local climatology is the daily grid observed precipitation data provided by the TRMM-MERGE and by the CPC-NOAA for their use in rainfall-runoff models and inflow forecasting to a group of hydropower plants in Brazil?*

    b. *Can this information be blended to have a better precipitation forcing and reduce the uncertainty of the observed precipitation while providing a better initial condition for the hydrological models?*

   c. *Can this new observed precipitation data be used to perform bias correction to the meteorological forecasts?*

2. *How good is the performance of the weather forecasting models made available by the meteorological center of ECMWF (UK) for short (days to weeks) to long (months to seasons) forecast ranges in the Brazilian context of hydropower production?*

   a. *Can the application of bias correction techniques improve the performance of the forecasts for the Brazilian basins?*

   b. *For the short-term forecasts, does the 'on-the-fly' bias correction based on the seasonal hindcasts perform better than the structural bias correction based on the short-range reforecasts?*

   c. *How can we build a seamless hydrometeorological forecast for hydropower decision-making, ranging from short to seasonal scales?*

3. *Can the benefits of the seamless precipitation forecast be translated into a better seasonal flow forecast and even into a better driver for decision making in the electric sector?*

   a. *Can the Quantile Mapping bias correction method correct the systematic hydrological calibration bias?*

   b. *Can flow data assimilation improve the performance of the streamflow forecasts?*

   c. *Can the seamless forecasts help on building decision-making guidance for hydropower generation?*

To answer these scientific questions and to deal with uncertainties in the process to perform a seamless seasonal flow forecast, a general methodology is proposed, as shown in Figure 1.2. This general methodology will be detailed on the next chapters of the thesis.

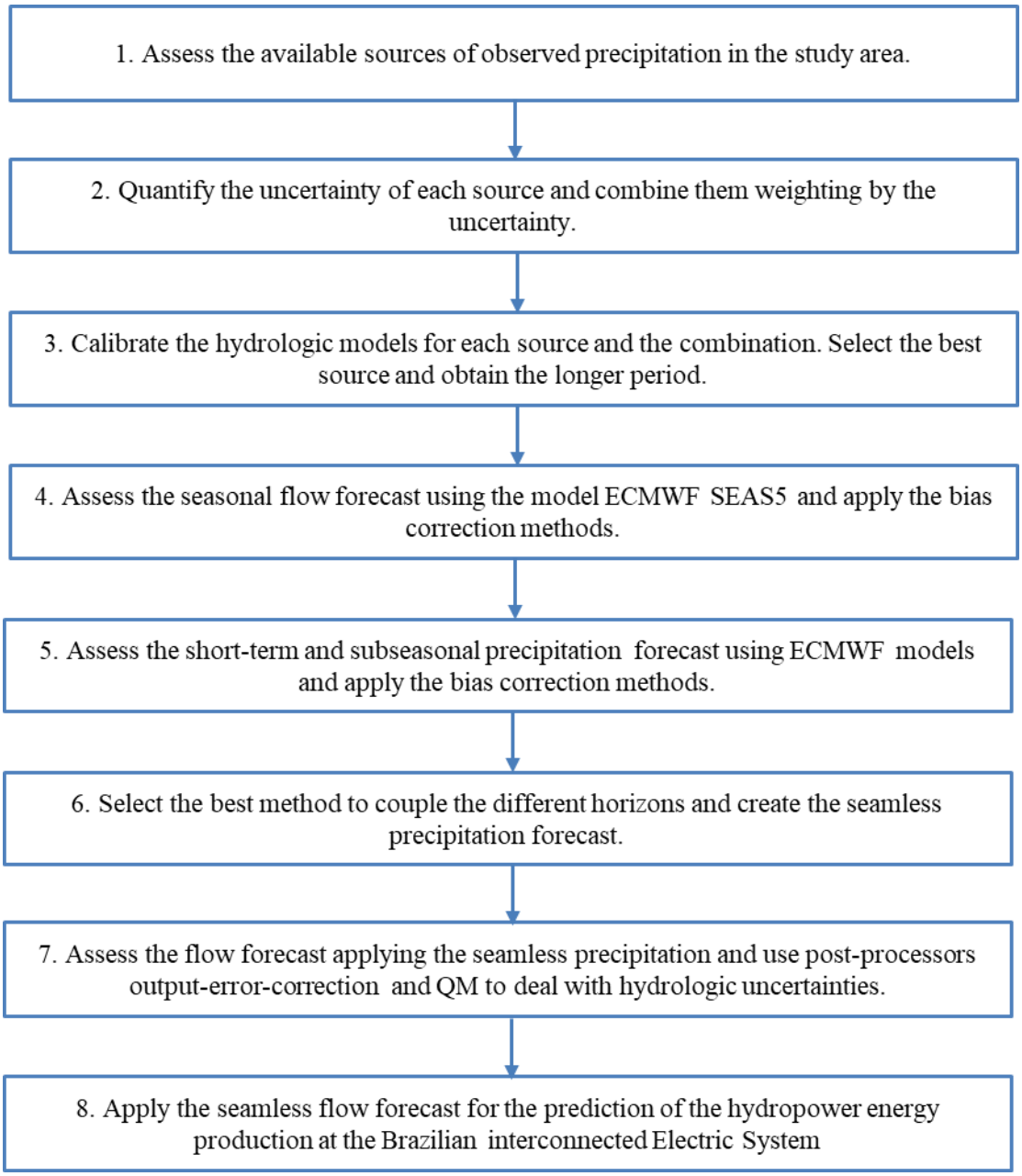

Figure 1.2 – General methodology to perform a seamless seasonal flow forecast for hydropower plants in the Brazilian interconnected electric system

1.1 OBJECTIVES

1.1.1 General objective

The general objective of this thesis is to develop a methodology to advance knowledge on seamless short to seasonal flow forecasting in order to improve energy security in the hydropower-dependent context of Brazil. This will be accomplished through a deep investigation of the sources and types of uncertainties that may affect commonly used precipitation datasets

and through the development of a novel technique to take into account (and potentially overcome) the impact of these uncertainty sources.

1.1.2 Specific objectives and research steps

I. To assess the quality and uncertainty associated with the real-time observed precipitation data from the TRMM-MERGE and CPC-NOAA sources and their applicability for predicting flows for hydropower plants in South America.

II. To assess the uncertainties of observed precipitation and use of hydrological modeling to define the best precipitation forcing.

III. To assess the seasonal flow forecast performance:

- To assess the performance of ECMWF SEAS5 ensemble seasonal precipitation forecast model and the benefit of bias correction methods;
- To apply this forecast in hydrological models and evaluate their performance.

IV. To assess the short-term and sub-seasonal precipitation forecasts and to develop the seamless precipitation forecast:

- To assess the performance of the ECMWF short-term and sub-seasonal ensemble meteorological models;
- To evaluate the benefit of forecast bias correction, and the use of the ‘on-the-fly’ hindcast from the sub-seasonal model to bias correct short-range forecasts;
- To compare the performance of the short-term, sub-seasonal and the seasonal forecasts at the different lead times;
- To develop the coupling strategies based on the similarities between the members for each forecast horizon and their comparison with the member-by-member approach.

V. To apply the seamless precipitation forecast on the hydrological flow forecast and compare to the original seasonal flow forecast:

- To test the QM method to correct the systematic bias in hydrological calibration;
- To define the parameters for auto-regressive (AR) model output correction for the flow forecasts, based on the technique of output-error-correction;
- To evaluate the seamless flow forecast performance and its application to the prediction of the hydropower energy production.

1.2 DOCUMENT STRUCTURE

This thesis is divided into 8 Chapters. The first, “Introduction” (this chapter) aims at presenting the background and the justification of this work, with scientific questions and the objectives of the research.

The second chapter, “Assessing two precipitation data sources at basins of special interest to hydropower production in Brazil.”, refers to specific objective I. The content of this chapter is in a paper published in the RBRH journal in 2019 - http://dx.doi.org/10.1590/2318-0331.252020190068).

The third chapter, “Hydrological modeling as a tool for selection and validation of precipitation data relevant to seasonal streamflow forecasting”, refers to specific objective II.

The fourth chapter, “The quality of seasonal precipitation and streamflow forecasts in Brazil over a large set of river basins”, refers to specific objective III.

The fifth chapter, “Improving the performance of ECMWF short range and subseasonal precipitation forecasts in South American catchments”, targets the specific objective IV.

The sixth chapter, “Coupling the different ECMWF forecast models to build a seamless precipitation forecast for a group of South American catchments”, aims to answer to the specific objective IV.

The seventh chapter, “Developing seamless medium- to long-range flow forecast to improve the prediction of hydropower production in Brazil”, targets the specific objective V.

Finally, the eighteenth chapter, “Final Considerations”, summarizes the conclusions obtained by this thesis, answering its scientific questions, and at the end we have all references used in the document.

CHAPTER 2:

ASSESSING TWO PRECIPITATION DATA SOURCES AT BASINS OF SPECIAL INTEREST TO HYDROPOWER PRODUCTION IN BRAZIL

This chapter is based on a paper published in the RBRH - Brazilian Journal of Water Resources: REIS, A. A.; FERNANDES, W. S.; RAMOS, M. H. Assessing two precipitation data sources at basins of special interest to hydropower production in Brazil. RBRH - Brazilian Journal of Water Resources, RBRH-2019-0068, 2019, http://dx.doi.org/10.1590/2318-0331.252020190068.

2 ASSESSING TWO PRECIPITATION DATA SOURCES AT BASINS OF SPECIAL INTEREST TO HYDROPOWER PRODUCTION IN BRAZIL

2.1 INTRODUCTION

Knowledge of surface precipitation is particularly important in hydrological research and operations. Accurate estimates of precipitation amounts are necessary to estimate river basin runoff, assess water-related risks (floods and droughts) and evaluate water availability for a broad range of water uses (e.g., water supply, agriculture, hydropower, and environmental protection).

At the global scale, gridded precipitation products have emerged since the late 1990s (Huffman et al., 1997; Adler et al., 2003). These products usually provide monthly estimates of surface precipitation from merged analyses that blend precipitation estimates from satellite data and in-situ rain gauge observations. While they can be useful for global climate change impact studies, finer space and temporal resolutions are often needed for hydrological applications that involve daily decision-making at continental or national scales, such as flood forecasting or hydropower operations (Alfieri et al., 2013; Fan et al. 2016; Emerton et al., 2016; Siqueira et al., 2018).

In Brazil, hydropower generation is responsible for 66,6% of the electric production (EPE – BEN, 2019). The inflows to hydroelectric plants have a considerable influence on planning the operation of the electrical system, as well as on setting energy prices in the short-term market. Computer models that optimize the system's operation, solving the hydrothermal dispatch problem, run once a week, every Thursday, providing forecasts of inflows on a daily and weekly basis for the first five weeks and on a monthly basis for the next months (ONS, 2016).

Currently, the National Operator of the Electric System (ONS) uses historical natural flow records in statistical models for monthly forecasts and daily precipitation data from rain gages to run hydrological models for daily flow forecasts at dozens of hydropower plants distributed around the whole Brazilian territory. Daily precipitation data is provided by the national electricity generators. When real-time precipitation data show gaps or inconsistencies, corrections have to be applied to have a better fit between simulated and observed flows during the warm-up phase of the hydrological models, i.e., before a forecast is issued (ONS, 2016). This is an important step to achieve accurate inflow forecasts to the hydropower plants.

Uncertainty in daily precipitation real-time data may come from various sources, such as the low density of the gauging network at some regions, human errors when reading the data, measurement problems at the gauging stations, data communication failures, among others. Observed real-time precipitation will therefore always be an approximation of the actual precipitation falling inside the river basins.

However, accurate real-time precipitation estimates are not the only challenge in hydropower operation. Long-term records of unbiased daily gridded-based observed precipitation data are also crucial when running sub-seasonal to seasonal forecasting systems. This is the case when using the Ensemble Streamflow Prediction (ESP) method, a widely applied technique to generate ensembles of possible future scenarios of streamflow over several weeks and months ahead. The method is based on using a continuous hydrological model to estimate initial hydrological conditions (using real-time meteorological data as input) and future meteorological forecasts (based on historical sequences of meteorological data) to obtain streamflow predictions several months ahead (see recent applications in, for instance, Crochemore et al., 2016; Bennett et al., 2017; Arnal et al., 2018; Harrigan et al., 2018). Reliable and consistent long-term historic meteorological data are therefore also crucial when running seasonal forecasting systems. For the operation of the Brazilian hydropower system at seasonal lead times, a necessary preliminary step to setting up an ESP system is to ensure that a homogeneous long-term precipitation time series over the whole country is available.

Beck et al. (2017) listed a group of 22 gridded rain datasets, but only a few of them have, simultaneously, a daily temporal resolution and a spatial resolution smaller than or equal to 0.5º covering the South America area. Among them, only two datasets were available in real time (or near-real-time), which is a necessary characteristic to use the data in forecasting systems. These datasets are the CPC Unified Gauge-Based Analysis of Global Daily Precipitation of the US National Center for Atmospheric Research (NCAR) and the NASA's IMERG, Integrated Multi-satellitE Retrievals for GPM (Global Precipitation Measurements) data, the successor of the Tropical Rainfall Measuring Mission (TRMM) data products.

Sun et al. (2017) also made a wide review of 30 currently available global datasets, based on gauging stations, satellite estimates and reanalysis. They compared 22 datasets from daily to annual time scales and found high discrepancies between them. The magnitude of the differences in annual precipitation estimates between two different data sources was found to be as high as

300 mm/yr. The discrepancy in precipitation amounts varied however from region to region and according to the time scale. According to the authors, important differences can limit the capacity of the products to be used for climate monitoring, attribution and model validation.

Another example is provided by Juárez et al. (2009), who analyzed six databases, some based on radar and others based only on gauging stations. They observed that the largest difference among the datasets over the Brazilian Amazon region was of 8% during the apex of the rainy season (December to March). Over the Brazilian northeast region, the maximum difference in the wet season rainfall total (February to April) was 30 mm, or 18%.

Many other authors have studied the uncertainties and the differences among different sources of observed precipitation data in different areas of the world, with some studies focusing on South America (e.g., Demaria et al., 2011; Scheel et al., 2011; Falck et al., 2015; Mantas et al., 2015). Overall, their main conclusion is that differences between different sources of observed precipitation data are common, and often vary in space and time.

The objective of this study is to evaluate two real-time (or near real-time) sources of gridded daily observed precipitation data available over the Brazilian and adjacent territory, namely the TRMM-MERGE (Rozante et al., 2010) and the CPC (Chen et al., 2008) datasets. The differences between these two datasets are investigated in space and time. We evaluated the datasets over 41 river basins of special interest to hydropower production. We also considered the evolution in time of the deviations and the deviations at different temporal resolutions (annual, monthly and daily time steps). The impact of using these different datasets in hydrological modelling is also presented for two case studies.

2.2 MATERIALS AND METHODS

2.2.1 STUDY AREA AND DATA

Study area

The study area covers 41 river basins that represent 31 main hydroelectric power plants in Brazil. These river basins vary in size, with drainage areas ranging from 9 300 km² to 38 2000 km². The study area extends from the north (Madeira River, Xingu River, Tapajos River, Tocantins River, and others) to the south of Brazil (Iguaçu River basin), and includes also river basins located at

the central part of the country (Paraná River, Grande River, São Francisco River). Figure 2.1 shows the study area, with the main hydropower plants indicated in the map and the basin areas associated with the hydropower plants delimited in red.

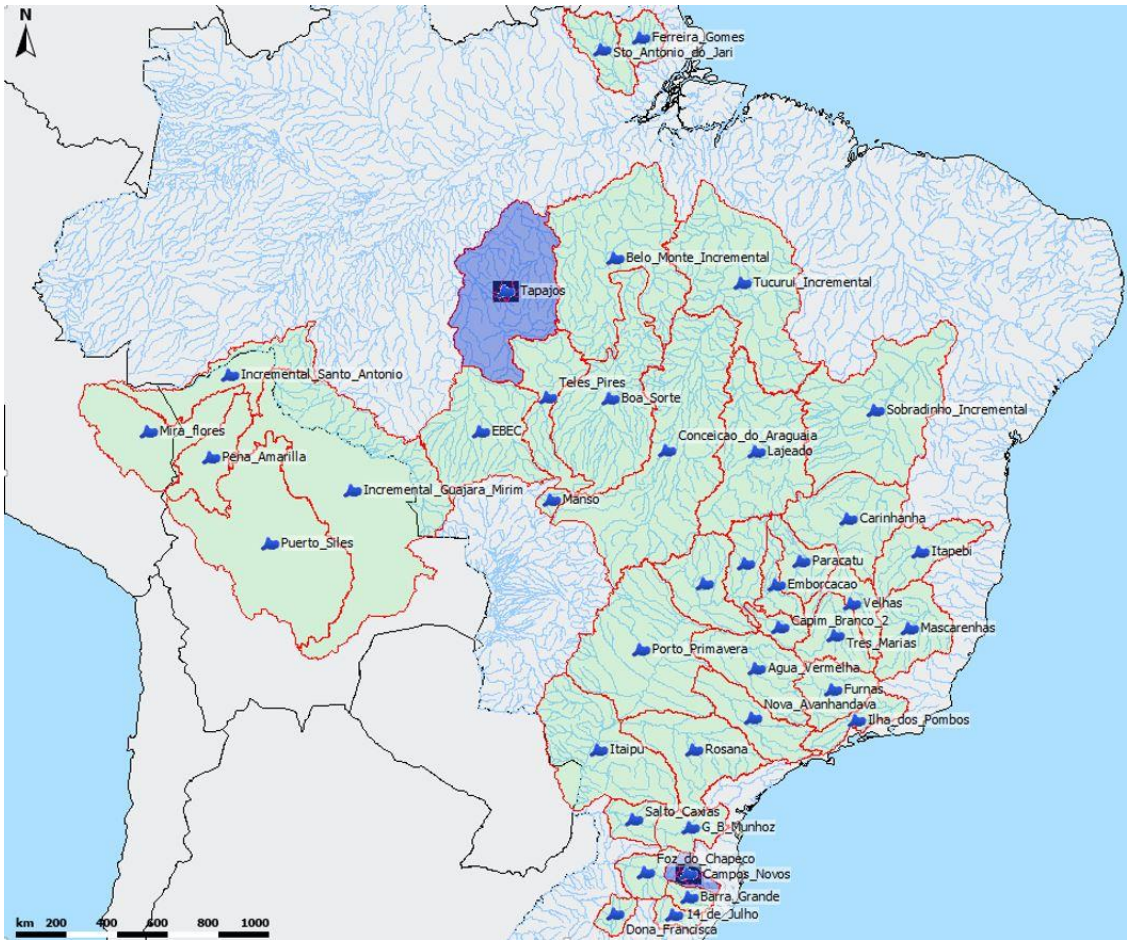

Figure 2.1 – Geographic distribution of the 41 basins of this study, with hydroelectric power plants in Brazil (the two basins in blue, Campos Novos and Tapajos, are used in an experiment to check impact of different precipitation dataset on flow simulations)

Observed precipitation datasets

Two datasets are evaluated in this study: the TRMM-MERGE and the CPC datasets.

The TRMM partnership project between the US National Aeronautics and Space Administration (NASA) and the Japan Aerospace Exploration Agency (JAXA) started in November 1997, with the main goal of studying and monitoring precipitation in tropical regions (Kummerow et al., 2000). The TRMM satellite uses several instruments to detect rainfall, including radar, microwave imaging, and lightning sensors (Maggione et al, 2016; Huffman et al., 2017). Although the TRMM products are considered valuable for numerical validation and simulations (Rozante et al., 2010), systematic errors have been detected, especially on the coast of the

northeast of Brazil and in the south region of Brazil, close to the triple frontier between Brazil, Argentina, and Paraguay.

The TRMM-MERGE data was developed by CPTEC/INPE to reduce the interpolation problems observed in regions of low-density of rain gages, causing under- and over-estimations in the TRMM products. It combines gauging station datasets from the Global Telecommunications System (GTS), telemetric stations from various agencies and companies in South America and the real-time TRMM rainfall product (3B42RT), providing an improved quality gridded dataset with a spatial resolution of 0.25° for evaluation of models and operational uses (Rozante et al., 2010). Basically, the merging technique consists in identifying the TRMM grid boxes where the observations are present, discarding the two adjacent grid boxes to the observation point, and, finally, interpolating the TRMM precipitation and the ground observations using the Barnes objective method (Barnes, 1973, apud Rozante et al., 2010).

The TRMM-MERGE daily precipitation data used in this study was obtained from the CPTEC FTP site (CEPTEC - INPE, 2018). The information is available in the grib2 format, 0.25º resolution, and the historic period covers 1997 to 2017

The CPC data (Mingyue et al., 2008) is a product developed by the US NOAA's Climate Prediction Center. It comes from a project created to develop a group of automatic procedures to do quality control for the GTS daily precipitation products, comparing historical gauge records, concomitant observations at nearby stations, satellite estimates and numerical model forecasts. As a product of this project, NOAA/NCEP provides a daily observed precipitation gridded dataset with 0.5° spatial resolution since 1979.

The CPC data used in this study was obtained from the NCEP/NOAA FTP site (NOAA, 2018). The information is available in a grib2 format, and was retrieved for the historic period that covers 1979 to 2017.

2.2.2 METHODOLOGY

Our methodology consists of two main analyses. First, we evaluate basic statistics from the two different precipitation data sources for the average precipitation over each river basin. Secondly, we investigate the impact of the differences in precipitation on streamflow simulations on two selected river basins, one with a low and another with a high difference between the two

precipitation data sources. For the flow analysis, we set up and calibrated the HEC-HMS model, as presented below.

Average precipitation for each river basin

The first step to obtain the average precipitation is to delimit the contour of the basins and generate the shapefile with the basins that will be superposed on the gridded data files. In this study, we used the DELFT FEWS-CEMIG System (Pinto et al., 2013; Werner et al., 2013; Schwanenberg et al., 2015; Gibertoni et al., 2017) to obtain the average precipitation at each basin and time step. We configured the FEWS system to read the shapefiles and to use the geographic information provided to extract the average precipitation. The system uses a workflow of routines to perform the calculations. The methodology used to obtain the average precipitation is the "Average Area", which takes the mean of the data points inside the shape of each basin.

Basic statistics of precipitation differences

We analyzed the daily, monthly and annual precipitation totals of the two data sources, and their basic statistics. We also evaluated the differences in percentage between TRMM-MERGE and CPC precipitation data:

$$\Delta P(t) = \frac{P1(t) - P2(t)}{P1(t)} * 100 \qquad (2.1)$$

where *P1* is the precipitation from TRMM-MERGE and *P2* is the precipitation from CPC at time *t*. A positive (negative) difference indicates higher (lower) value of precipitation for the TRMM-MERGE dataset.

In the annual analysis, we considered the hydrological year from October 1st to September 30th to calculate the annual totals. From the time series of the annual percent differences, we estimated the following basic statistics: the minimum, the first quartile, the mean, the third quartile, and the maximum (Naghettini et al., 2007). For the monthly analysis, we used box-plot representations of the monthly percent differences to display the distribution of differences in monthly precipitation.

For the daily analysis, we estimated the Empirical Cumulative Distribution Function ECDF ($F_n(y)$) (Naghettini et al., 2007) of the daily precipitation values for each dataset. We considered only the amounts higher than 1 mm/day over the basin areas. For observations x = (x1, x2, ... xn), F_n is the fraction of observations less or equal to y.

$$f_n(y) = \frac{1}{n}\sum_{i=1}^{n} 1_{x_i \leq y} \qquad (2.2)$$

$$F_n(y) = \int_{-\infty}^{y} f_n(y)dy \qquad (2.3)$$

where the indicator is ($x_i \leq y$) and n = number of data points.

Finally, to visualize the geographic impact of the differences between the datasets and their evolution in time, we used maps to represent the percent differences of the annual average precipitation for two decades: 1998-2007 and 2008-2017.

Flow analysis with the HEC-HMS model

Streamflow modeling for flow forecasting has to be performed using a continuous model for the simulations in order to evaluate the initial conditions at the onset of the forecasts. For this, it is necessary to choose a more sophisticated configuration of the HEC-HMS model (Feldman, 2000). Below, we describe the modules used and the method chosen for each module in order to build the hydrological modeling approach used in this study (Scharffenberg, 2016).

Canopy method: Simple Canopy - the precipitation is intercepted until the canopy storage capacity of the surface is filled. All excess of precipitation falls to the surface. The potential evapotranspiration is used to empty the canopy storage.

Surface method: Simple Surface - the precipitation that arrives on the soil is captured until the storage capacity of the surface is filled, then the runoff starts with the excess of precipitation. The water in the surface infiltrates into the soil, according to the soil's infiltration capacity.

Loss method: Soil Moisture Accounting - SMA - this loss method uses three layers (soil storage, upper groundwater, and lower groundwater) to represent the dynamics of the water movement in the soil. For the given precipitation and evapotranspiration the model calculates surface runoff of the basin, groundwater flux, losses and the deep percolation over the whole basin. The method

is capable to simulate wet and dry cycles and can be used for long periods of continuous simulation.Transformation method: Clark Unit Hydrograph - this method is a synthetic unit hydrograph and the principal components are the time of concentration defining the travel time in the sub-basin and the storage coefficient used to account for storage effects on the linear reservoir.

Base-flow method: Linear Reservoir - uses a linear reservoir to model the recession of the base-flow after a precipitation event, conserving the mass. The lateral outflow of the groundwater is connected with the infiltration from the soil moisture accounting loss method.

The HEC-HMS configuration selected has 26 free parameters to be calibrated against observed flow data. In our study, observed streamflow data comes from ONS (National Operator of Electric System). The calibration was performed manually, by comparing simulations with observations and minimizing volume errors.

For the analysis of the impact of the different precipitation data sources on the simulations of streamflow, we calibrated two selected basins. They represent the extremes of precipitation differences observed during the annual precipitation analysis. This basins are: i) the UHE Campos Novos, located at the south region, at Canoas River (Uruguay river basin), where the differences between the precipitation data sources are smaller than 5% and there is not a strong seasonality in precipitation, and ii) the UHE Tapajos, located at the north region, at Tapajos river (Amazon basin), with annual differences between precipitation data sources higher than 40%, and with a strong precipitation seasonality. These basins are full blue colored in figure 1.

In the flow analysis, we want to investigate what happens if we calibrate the hydrological model with one dataset and simulate it with another dataset. The hydrological model is first calibrated for the complete data period, from October 1997 to September 2017, with one climatic forcing and then run to simulate streamflow using the other climatic forcing, over the same period. Since we have two climatic forcing datasets, the calibration and simulation procedure is done twice.

In order to analyze the effects of the different precipitation datasets used as input to the hydrological models, we represented the ECDF of both TRMM-MERGE and CPC simulated time series. We also evaluated the simulated flows against observed flows using four numerical criteria as performance indicators: NSE, RMSE, KGE and R^2.

NSE – The Nash- Sutcliffe efficiency (Nash, 1970) measures how good the results of the model are when compared with a simulation represented by the mean observed flow. Values equal to 1 indicate a perfect fit and values smaller than zero indicate that the mean is a better predictor than the model.

RMSE – The Root Mean Square Error is a common measure of the accuracy of a model. It is calculated by taking the square root of the average of the sum of squared differences between observed and simulated values. It can be interpreted as the standard deviation of the model prediction error. A smaller value of RMSE indicates better model performance.

KGE – The Kling-Gupta efficiency (Gupta et al., 2009) is an alternative criterion to the NSE, and was proposed to assess the qualities of a model in terms of its ability to represent the water balance, flow variability and correlation. Values range between $-\infty$ and 1, and as for the NSE, values close to 1 indicate a more accurate model.

R^2 – The coefficient of determination is an indication of how well one variable correlates with the other. It is represented as a value between 0 and 1. The closer the value is to 1, the better the fit, or relationship, between the two variables.

2.3 RESULTS

2.3.1 Evaluation of annual precipitation totals

Table 2.1 shows the basic statistics of the percent differences for annual precipitation totals for each basin. From this table, we can see that differences in quantiles range between –31% and +42% in mm of total annual rainfall. High differences are more frequently observed towards positive differences. This means that when differences are high, it is more frequently due to higher values of rainfall given by the TRMM-MERGE dataset.

From table 2.1, we also note that the magnitude of the differences in annual precipitation varies according to the basin. Some basins tend to exhibit a similar behavior in terms of basic statistics of the percent differences between annual precipitation totals. We detected eight groups of similar behavior (Basin Groups I to VIII, hereafter, BGI to BGVIII). These groups are indicated in table 2.1. They are formed by the following basins: for north basins - Group I: Inc. Santo Antonio, Mira Flores, Pena Amarilla, Puerto Siles, and Guajara Mirim and Group II: Ferreira

Gomes, Santo Antônio do Jari, Belo Monte Inc., Boa Sorte, Tapajos, Ebec, Teles Pires, Manso, Tucurui Inc., and Conceição do Araguaia. For northeast and east Basins - Group III: Sobradinho Inc., Carinhanha, Paracatu, Velhas, Três Marias, Itapebi, and Mascarenhas. For the basins in the center-west and southeast regions - Group IV: Lajeado, Emborcação, Itumbiara, São Simão, Capim Branco 2, Ilha dos Pombos, and Furnas; Group V: Agua Vermelha, Nova Avanhandava and Rosana; and Group VI: Itaipu and Porto Primavera. For the basins in the south region - Group VII: Salto Caxias, G. B. Munhoz, Barra Grande, and Campos Novos; Group VIII: Foz do Chapecó, Quatorze de Julho, and Dona Francisca.

Table 2.1 – Basic statistics from the time series of percent differences between annual precipitation totals from TRMM-MERGE and CPC datasets

Basin	Min.	1st Qu.	Mean	3rd Qu.	Max.
GROUP I					
Mira_flores	27%	25%	34%	39%	38%
Puerto_Siles	22%	17%	27%	35%	36%
Pena_Amarilla	8%	2%	8%	11%	0%
Inc._Guajara_Mirim	17%	11%	12%	10%	14%
Inc._Santo_Antonio	19%	10%	10%	13%	9%
GROUP II					
Ferreira_Gomes	28%	21%	10%	5%	2%
Sto_Antonio_do_Jari	16%	4%	6%	8%	11%
Belo_Monte_Inc.	28%	15%	11%	7%	-1%
Boa_Sorte	30%	14%	13%	9%	0%
Tapajos	42%	16%	14%	10%	4%
EBEC	22%	13%	5%	-2%	2%
Teles_Pires	18%	4%	3%	-1%	-4%
Manso	26%	4%	5%	4%	-5%
Tucurui_Inc.	8%	9%	6%	6%	1%
Conceicao_do_Araguaia	16%	8%	6%	4%	1%
GROUP III					
Sobradinho_Inc.	6%	2%	0%	1%	-1%
Carinhanha	6%	9%	1%	-3%	0%
Paracatu	-4%	4%	0%	-2%	-1%
Velhas	3%	2%	-1%	-1%	-7%
Tres_Marias	1%	-6%	-4%	-4%	-9%
Itapebi	3%	2%	1%	-1%	4%
Mascarenhas	-1%	-1%	-3%	-5%	-4%
GROUP IV					
Lajeado	2%	1%	-1%	-4%	-3%
Emborcacao	-2%	-4%	-6%	-4%	-11%
Inc._Itumbiara	-3%	-1%	-5%	-2%	-9%
Inc._Sao_Simao	2%	-3%	-3%	-3%	2%
Capim_Branco_2	-7%	-2%	-4%	-9%	-1%
Ilha_dos_Pombos	5%	-9%	-7%	-8%	-6%
Furnas	2%	2%	-1%	-4%	-2%

GROUP V					
Agua_Vermelha	-5%	-10%	-5%	-6%	5%
Nova_Avanhandava	3%	-14%	-5%	1%	1%
Rosana	-8%	-4%	-3%	-2%	-3%
GROUP VI					
Itaipu	4%	-1%	2%	4%	6%
Porto_Primavera	11%	7%	4%	3%	5%
GROUP VII					
Salto_Caxias	28%	4%	5%	3%	11%
G_B_Munhoz	4%	0%	1%	-2%	5%
Barra_Grande	-31%	-6%	-2%	-1%	-2%
Campos_Novos	5%	1%	1%	0%	5%
GROUP VIII					
Foz_do_Chapeco	-3%	-4%	0%	0%	2%
Quatorze_de_Julho	1%	5%	3%	0%	6%
Dona_Francisca	9%	7%	4%	2%	2%

Figure 2.2 shows how the differences in annual precipitation totals between data sources evolve along the years. We selected one basin representative of each BG. We can see that the basins in the north region (BGI and BGII) display more often high positive differences, with values tending to increase with time, mainly after 2010. These BGs are generally affected by strong variations of one of the sources: either TRMM-MERGE presents very high annual precipitation totals all over the period (BGI) or CPC presents very low annual totals for a more recent period (BGII). These results illustrate how big the uncertainties in precipitation can be in this region, where the density of gauges is low. For the other regions, where the gauge density is higher, the variation of the differences is smaller and tends to be more linked to specific time periods. BGIII, BGIV and BGVI (northeast, central-west and southeast regions), for instance, display high values more often for the negative differences, with these occurring either at the initial years or at the final years of the study period. In the south region, BGVII and BGVIII present alternated years of positive and negative differences along the study period.

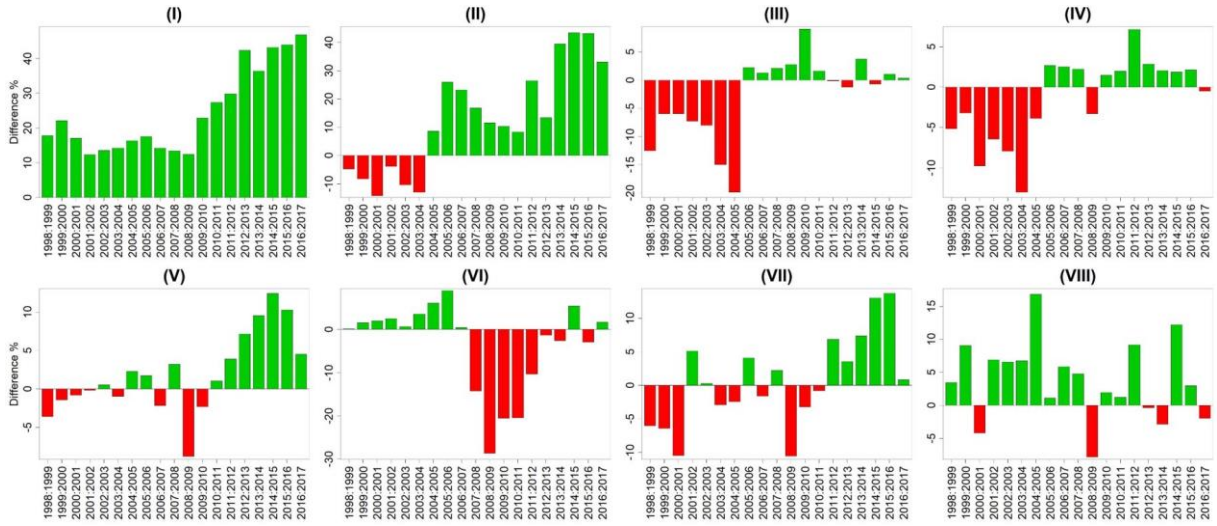

Figure 2.2 – Percent differences in annual precipitation totals between TRMM-MERGE and CPC datasets for a representative basin in each Basin Group (BGI to BGVIII) (period 1998-2017)

2.3.2 Evaluation of monthly and daily precipitation

Figure 2.3 shows the statistical distribution (boxplot) of the monthly differences. The line in red represents the monthly average precipitation of the TRMM-MERGE data. It provides a reference to compare the totals to the magnitude of the deviations. With this information, it is possible to visualize the differences along the months and the seasons in each of the eight groups of basins with similar behavior. We can see that monthly precipitation differences are higher for the basins of the north region (BGI and BGII). For these groups, the TRMM-MERGE data source presents more precipitation than the CPC data, in practically all months and especially during the rainy months (November to March). For the other regions, the differences vary around zero, with the higher variations occurring during the wet months. TRMM-MERGE dataset can display either wetter or dryer months than CPC, depending on the region.

Figure 2.4 shows the ECDF curves of the daily precipitation values greater than 1mm/day from the two data sources. The line in red represents the TRMM-MERGE data and the blue line, the CPC data. Each graph shows one basin representative of the basin groups defined in Table 2.1. We can see that the cumulative distribution functions of daily precipitation are very similar. Differences can only be seen in the basins in the north region (BGI and BG II) and in the extreme south region (BG VIII), where the TRMM-MERGE dataset presents higher values of precipitation for almost all probabilities. This analysis illustrates the tendency of the basins in the more central regions to present more similarity between the data sources than the basins located in the extreme north and south regions.

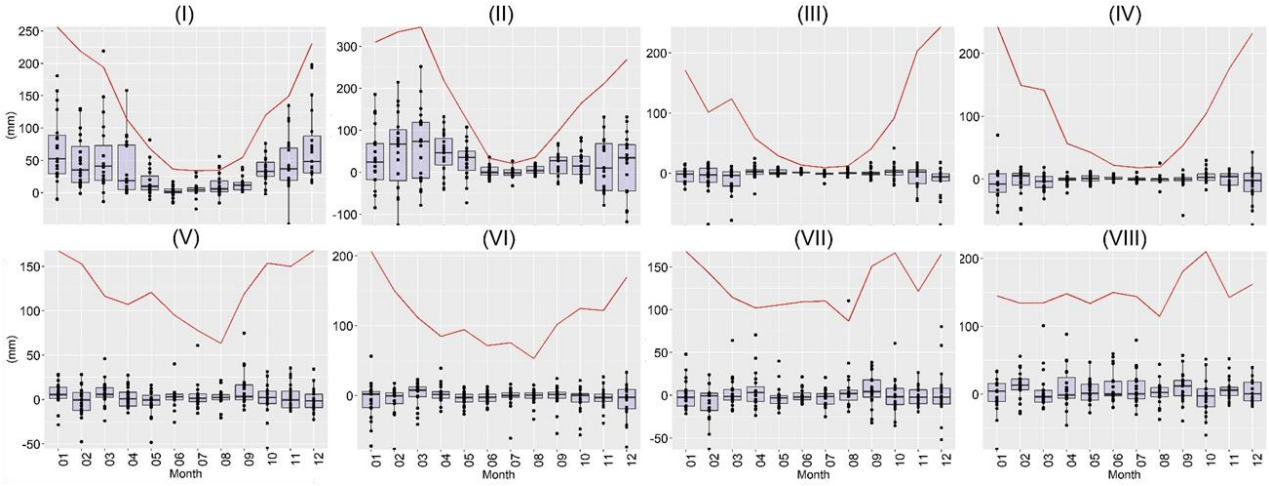

Figure 2.3 – Boxplots of percent differences (%) in monthly precipitation between TRMM-MERGE and CPC datasets for a representative basin in each Basin Group (BGI to BGVIII). The red line represents the monthly average precipitation (mm/month) of the TRMM-MERGE data (period 1998-2017)

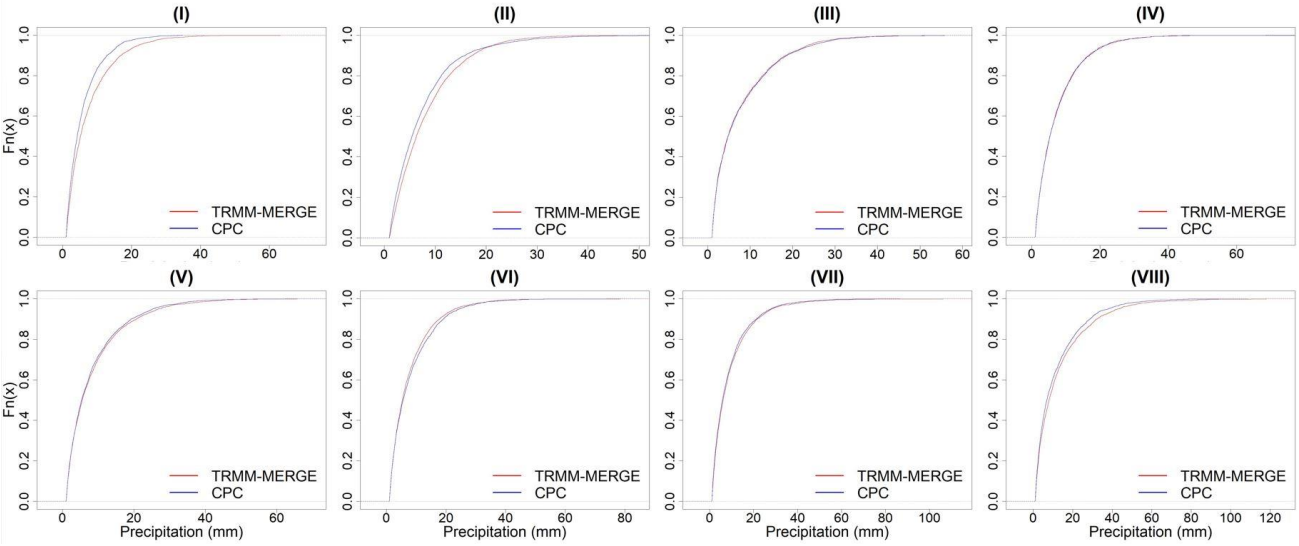

Figure 2.4 – ECDF of daily precipitation greater than 1mm/day for the TRMM-MERGE (red) and the CPC (blue) datasets for a representative basin in each Basin Group (BGI to BGVIII) (period 1998-2017)

Table 2.2 shows an example of the differences we can expect in precipitation quantiles (mm/day) for the probability of non-exceedance of P=0.9. The quantiles were extracted from the ECDF curves for all basins. The percent differences confirm, in numbers, the behavior showed in the ECDF plots (figure 4), i.e., a tendency of the extreme regions (north and south) to have higher differences (TRMM-MERGE daily precipitation greater than CPC precipitation) and the center regions to have similar values for the same probability.

Table 2.2 – Daily precipitation quantile (mm/day) for the probability of non-exceedance P=0.9 extracted from the ECDF curves of each basin and percent difference between TRMM-MERGE and CPC data sources

BG	Basin	Quantile (mm/day) P=0.9		
		TRMM	CPC	Diff
I	Inc._Guajara_Mirim	14.5	12.6	13%
	Inc._Santo_Antonio	18.0	16.2	10%
	Mira_flores	20.8	17.7	15%
	Pena_Amarilla	20.8	21.5	-4%
	Puerto_Siles	16.9	12.9	24%
II	Belo_Monte_Inc.	16.2	15.2	6%
	Boa_Sorte	17.6	16.2	8%
	Conceicao_do_Araguaia	15.7	15.0	4%
	EBEC	17.5	16.6	5%
	Ferreira_Gomes	20.9	19.5	6%
	Manso	20.6	19.4	6%
	Sto_Antonio_do_Jari	19.5	17.3	11%
	Tapajos	17.1	15.8	8%
	Teles_Pires	17.8	18.3	-3%
	Tucurui_Inc.	15.8	14.8	6%
III	Carinhanha	17.5	17.4	0%
	Itapebi	17.2	16.2	5%
	Mascarenhas	18.3	18.6	-1%
	Paracatu	19.2	19.0	1%
	Sobradinho_Inc.	13.9	14.5	-4%
	Tres_Marias	17.9	17.9	0%
	Velhas	19.0	17.9	6%
IV	Capim_Branco_2	21.0	19.4	8%
	Emborcacao	16.8	17.1	-1%
	Furnas	16.7	17.0	-2%
	Ilha_dos_Pombos	15.9	16.3	-3%
	Inc._Itumbiara	15.8	15.8	0%
	Inc._Sao_Simao	15.2	15.0	2%
	Lajeado	14.6	15.0	-2%
V	Agua_Vermelha	15.5	17.2	-11%
	Nova_Avanhandava	19.2	19.0	1%
	Rosana	17.8	19.1	-7%
VI	Itaipu	20.7	19.2	7%
	Porto_Primavera	15.3	14.5	5%
VII	Barra_Grande	26.4	25.3	4%
	Campos_Novos	25.9	25.2	3%
	G_B_Munhoz	21.5	21.2	2%
	Salto_Caxias	28.8	24.5	15%
VIII	Quatorze_de_Julho	29.0	25.5	12%
	Dona_Francisca	32.2	28.5	11%
	Foz_do_Chapeco	28.9	27.6	5%

2.3.3 Variation of annual precipitation differences in space and time

We investigated if the differences between precipitation data from TRMM-MERGE and CPC vary when considering two time periods: figure 2.5 shows a map with the average percent differences of annual precipitation for the period 1998-2007 and figure 2.6 shows the same but for the period 2008-2017. The shadows of green represent positive differences and the shadows of red represent negative differences. Table 2.3 shows the specific values for the average difference for each basin for each decade.

The differences between the TRMM-MERGE and the CPC data sources present a clear spatial and temporal behavior. For the first period (1998-2007), some basins in the north region (BGI and BGII) and in the extreme south region (BGVIII) display the most important positive average values of percent differences, while basins in the south-east region (BGIII and BGIV) display the highest negative differences. Positive average percent differences become higher and spread over the north and central regions in the last period (2008-2017). Negative average percent differences do not spread over the area in the second decade. They are however higher at the basins of the BGVI.

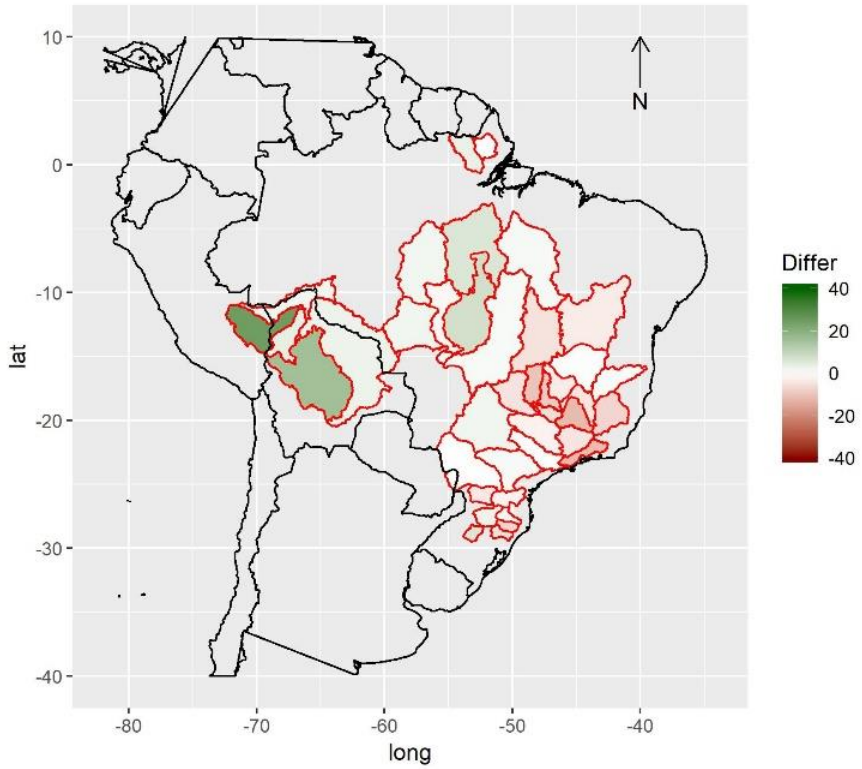

Figure 2.5 – Map of the average percent difference (%) of annual precipitation between TRMM-MERGE and CPC for the period 1998-2007

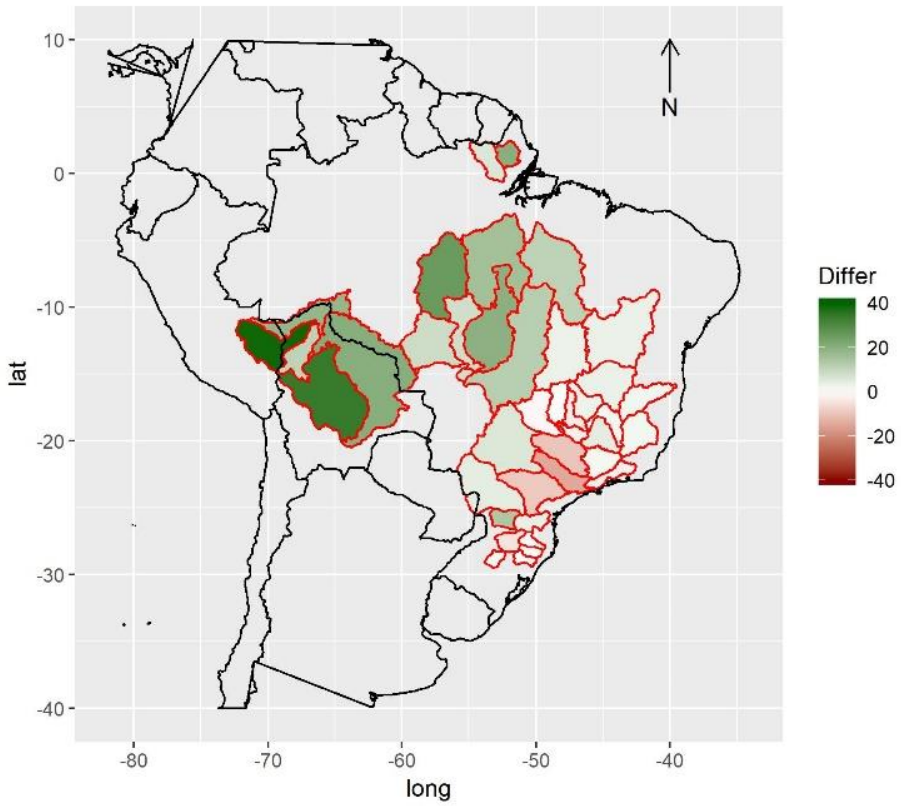

Figure 2.6 – Map of average percent difference (%) of annual precipitation between TRMM-MERGE and CPC for the period 2008-2017

Table 2.3 – Average percent difference (%) of annual precipitation between TRMM-MERGE and CPC for the study basins and for the periods 1998-2007 and 2008-2017

BG	Basin	1998-2008	2008-2017
I	Inc._Guajara_Mirim	2.9	20.3
	Inc._Santo_Antonio	1.8	18.0
	Mira_flores	24.9	39.0
	Pena_Amarilla	3.7	10.7
	Puerto_Siles	15.9	33.9
II	Belo_Monte_Inc.	6.0	15.7
	Boa_Sorte	7.7	19.6
	Conceicao_do_Araguaia	1.3	12.0
	EBEC	2.2	8.6
	Ferreira_Gomes	0.0	20.0
	Manso	1.8	7.9
	Sto_Antonio_do_Jari	3.3	5.7
	Tapajos	2.0	25.4
	Teles_Pires	-1.3	7.8
	Tucurui_Inc.	1.6	11.1
III	Carinhanha	0.4	3.2
	Itapebi	0.8	2.1
	Mascarenhas	-6.9	1.8
	Paracatu	-3.1	2.7
	Sobradinho_Inc.	-3.0	3.2
	Tres_Marias	-11.2	4.2
	Velhas	-4.0	1.7
IV	Capim_Branco_2	-5.4	-2.1
	Emborcacao	-8.4	-2.8
	Furnas	-4.2	1.7
	Ilha_dos_Pombos	-11.1	-2.1
	Inc._Itumbiara	-9.5	0.2
	Inc._Sao_Simao	-4.4	-1.1
	Lajeado	-4.7	3.1
V	Agua_Vermelha	-1.9	-9.5
	Nova_Avanhandava	0.3	-14.3
	Rosana	1.2	-8.9
VI	Itaipu	-0.1	4.2
	Porto_Primavera	2.3	5.9
VII	Barra_Grande	-6.5	-0.5
	Campos_Novos	1.7	0.2
	G_B_Munhoz	-1.8	3.4
	Salto_Caxias	-3.4	13.7
VIII	Quatorze_de_Julho	5.0	-0.5
	Dona_Francisca	5.7	1.6
	Foz_do_Chapeco	2.7	-4.2

2.3.4 Impact of different precipitation data on flow simulations

The results of the experiment with the HEC-HMS hydrological model calibrated for the UHE Campos Novos and the Tapajos basins are shown in table 2.4. It shows model performance when the model is calibrated with the TRMM-MERGE precipitation data and then used in simulation with the CPC precipitation data as forcing and vice versa. Both calibration and simulation runs are performed over the same period, 1997-2017. We can see that model performance is good in both basins, with NSE and KGE values ranging between 0.71 and 0.94 in calibration and between 0.45 and 0.79 in simulation. As expected, the performance of the model behaves according to the magnitude of the differences between the precipitation data sources: for the basin where the differences are small (Campos Novos), the performance in calibration is similar to the performance in simulation (differences in performance indicators are between -4% and -8% when calibrating with TRMM-MERGE, and simulating with CPC and between -1% and 3% when calibrating with CPC and simulating with TRMM-MERGE). For the basin with a high difference in precipitation datasets (Tapajos), the decrease in performance from calibration to simulation is clear, with stronger differences in performance indicators. The most important losses are in accuracy (RMSE).

Table 2.4 – Performance indicators (RMSE, NSE, KGE and R^2) and difference in performance (Diff) when calibrating the hydrological model HEC-HMS with TRMM-MERGE (TRMM cal) and CPC (CPC cal) precipitation and simulating river flows with the other dataset (CPC sim and TRMM sim, respectively) for two basins (Campos Novos and Tapajos) and considering the whole period 1997-2017 for calibration and simulation. Diff values indicate the percentage loss (negative values) or gain (positive values) in performance when moving from calibration with one dataset to simulation with the other dataset

Basin	Campos Novos			Tapajos		
Perf. indicator	TRMM cal	CPC sim	Diff.	TRMM cal	CPC sim	Diff
RMSE (m3/s)	203	214	-6%	1959	3578	-83%
NSE	0.73	0.70	-4%	0.88	0.61	-31%
KGE	0.83	0.79	-4%	0.94	0.70	-26%
R^2	0.65	0.60	-8%	0.87	0.50	-42%
	TRMM sim	CPC cal	Diff.	TRMM sim	CPC cal	Diff
RMSE (m3/s)	210	212	1%	3858	3383	-14%
NSE	0.71	0.72	-1%	0.55	0.66	-16%
KGE	0.82	0.79	3%	0.45	0.82	-44%
R^2	0.65	0.63	3%	0.67	0.60	11%

Figure 2.7 shows the ECDF of observed flows and of daily flows when calibrating the model with TRMM-MERGE and simulating with CPC. We can see that for the basin where the precipitation data of both sources are similar, the ECDF curves are also very similar. However, for the basin with a higher difference between the two sources, the ECDF curves show a clear

difference. For the same probability level, the flows simulated with the CPC data are lower than the observed flows and the flows simulated with the TRMM-MERGE data. The ECDF curves obtained when using the CPC data for calibration and the TRMM-MERGE for simulation present a similar behavior (not shown in this paper).

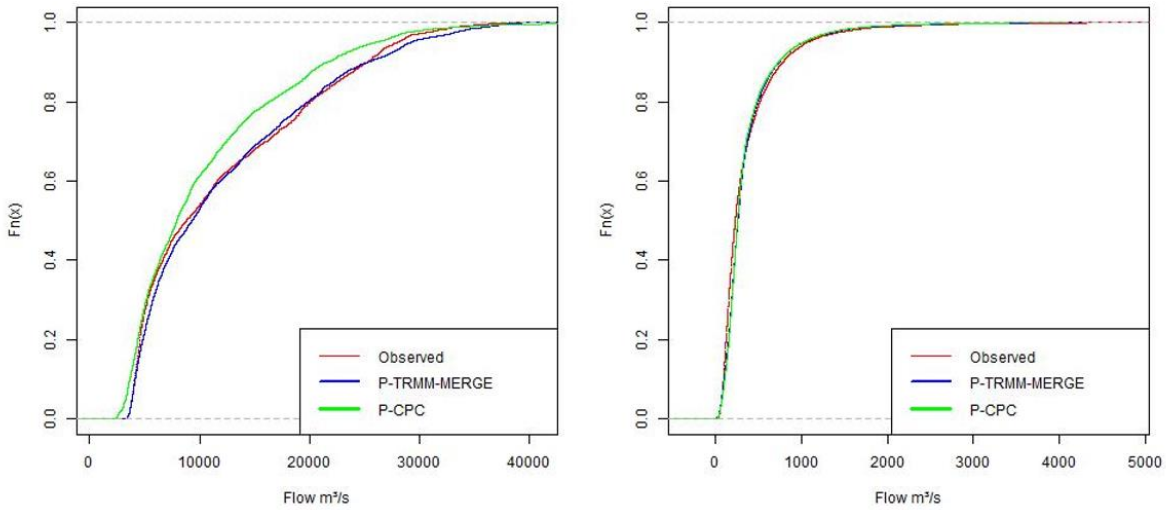

Figure 2.7 – ECDF curves of the observed (red) and simulated daily flows (m^3/s) with the TRMM-MERGE (blue) and the CPC (green) precipitation data as forcing in the HEC-HMS model for two basins (Tapajos, above, and Campos Novos, below)

Finally, in figure 2.8, we present a comparison between the percent differences of annual precipitation (TRMM-MERGE minus CPC) and the percent differences of annual streamflow simulations, when using TRMM-MERGE data in calibration and CPC data in simulation. The points in the first quadrant indicate the situations where the values of precipitation and simulated flow are smaller when using the CPC data. The third quadrant indicates the opposite, the situations where the CPC precipitation is more intense than the TRMM-MERGE and therefore also the streamflow simulations based on CPC data.

We can see that in the basin with small differences between the precipitation datasets (Campos Novos), the relation between the differences of precipitation and the differences of flow (orange lines) tends to be closer to the diagonal line, with a slope that is higher when the CPC precipitation is higher than the TRMM-MERGE precipitation. For the basin with the high difference in precipitation datasets (Tapajos), the slopes of the regression lines (blue lines) are higher than 1 for both quadrants, first and third. The angular coefficient of the line of the third quadrant is also bigger than the one of the line in the first quadrant. The graphs with the CPC data used in calibration and the TRMM-MERGE data used in simulation (not shown in this paper) present a similar behavior for the Campos Novos basin. For the Tapajos basin, where the

precipitation of the simulation dataset is more intense then the precipitation in the CPC calibration dataset, the differences in flows are amplified.

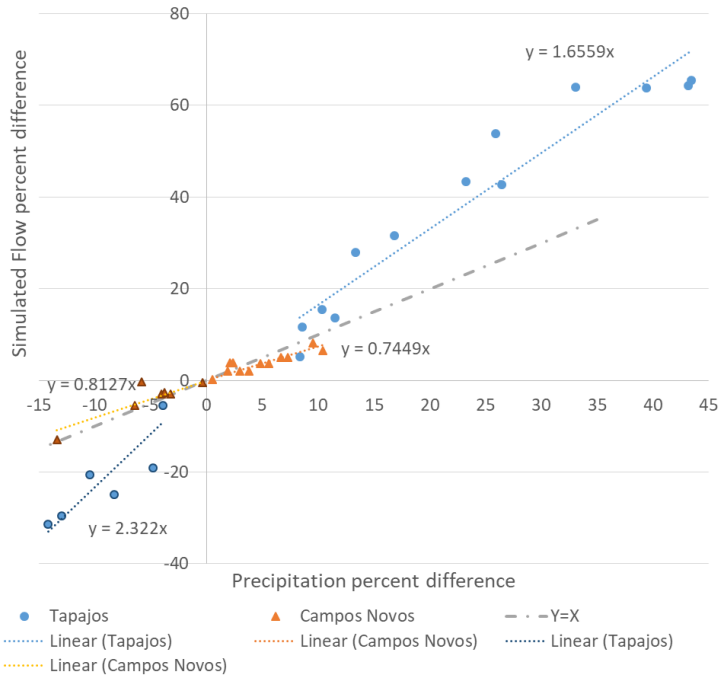

Figure 2.8 – Percent differences (%) in annual simulated flows as a function of percent differences in annual precipitation between TRMM-MERGE and CPC datasets for two basins (Tapajos in blue and Campos Novos in orange)

2.4 DISCUSSION

The TRMM-MERGE precipitation dataset uses raingauge data to calibrate the system. They have quality control of the sensors and use the telemetry rain data to improve the interpolation of the grid data (Huffman et al., 2017). The CPC precipitation data uses satellite information to perform the quality control of the rain gauge data and to create a better and trustworthy grid of precipitation data (Chen et al., 2008). Despite the fact that both sources use information from satellite and rain gauges in different degrees and ways, they both try to represent the same variable and one could expect they would provide similar datasets.

In our comparative study, the first signal of the differences between TRMM-MERGE and CPC precipitation datasets appears in the results from the basic statistics of annual precipitation totals. We found high differences, up to 42%, for the minimum annual precipitation, as well as for the first quartile (up to 25%). The other values (mean, third quartile and maximum) also show differences, but they are not as strong. This shows that, in the absence of a more accurate dataset of ground precipitation data, and considering that the observed precipitation in a certain basin is

an estimation of the actual precipitation, uncertainties are present in any dataset and, for our study, both datasets need to be considered.

Our study provides an extensive analysis of differences in precipitation data for a wide range of basins in South America, covering the continent from north (3ºN) to south (30°S) and a variety of climatic conditions. Our results show that the 41 basins studied can be grouped into eight groups of similar behavior. The results from the group I, the Madeira river basin, show that the precipitation values from the TRMM-MERGE are higher than the values obtained from the CPC dataset for all the study period (1997-2017), with differences that tend to increase in the last years. The analysis of monthly precipitation totals shows that the highest differences are observed during the wet season, which goes from November to April. During the wettest months, it is common to observe differences higher than 100 mm/month and some maximum values higher than 200 mm/month, which can be higher than the monthly average precipitation. The analysis of the statistical distribution of daily precipitation shows that the TRMM-MERGE daily precipitation quantiles tend to be higher than the CPC quantiles for the same probability of occurrence. This is observed for the majority of the probability quantiles.

The results from the group II, representing other basins in the north region, exhibit smaller differences between the precipitation datasets for the first decade of the data period (1998-2007), with alternation of positive and negative differences. However, in the last decade (2008-2017), the differences become more often positive, showing that CPC precipitation tends to be lower than TRMM-MERGE precipitation. These differences in the last decade translate into high variations during the wet season, from January to March. It is common to observe differences higher than 100 mm/month. The maximum differences occur at the basins in the extreme north, with values near to 200 mm/month, which can be around 70% and 80% of the monthly averages. The ECDF curves of daily precipitation also exhibit the tendency of TRMM-MERGE daily precipitations higher than the CPC values for the same probability of occurrence. The magnitude of the differences depends on the basin.

These results for the north region are coherent with the results obtained by Juarez et al. (2009). The authors show positive differences when comparing TRMM-MERGE and CPC precipitation data. Their differences were smaller, but the values were only computed considering the first decade of our data period.

The analysis of the northeast and east basins, group III, shows annual precipitation differences smaller than in the north region, with differences that, on the majority of the basins, are lower than 10%. The values tend to be slightly negative on the first decade of the study period and become slightly positive along the second decade. For the major part of the basins, the smaller differences are observed during the last five years, which can be an indication that both data sources may be getting more similar along the years in terms of annual precipitation totals. The differences in monthly precipitation show that the majority of differences in this group of basins are between -25 mm/month and 25 mm/month. The highest differences occur again during the wet season, November-March, but they are often smaller than 20% of the monthly average precipitation. In terms of daily precipitation, the ECDF curves do not indicate a great difference between the two data sources.

The basins in the center-west and southeast regions, group IV, show a tendency to have negative values of the differences between datasets in the first decade, varying from small values near 5% until higher values near 25% for some basins. In the second decade of the study period, the differences become positive (i.e., TRMM-MERGE precipitation data are higher than CPC data), but the values are smaller than 10%. For the monthly precipitation differences, the highest differences occur in November, December, January and February, with highlights for strong negative values that sometimes are close to -100 mm/month. For the daily precipitation values, the probability distribution curves do not indicate a great difference between the two sources of precipitation data.

The three basins in group V, in the southeast region, display a different behavior from the others. The differences in annual precipitation are slightly positive in the first decade and tend to be negative during the second decade. The highest differences occur between the years 2008-2013, with values near -30%. During the last five years of the study period, the differences become small again, near 5%. The monthly differences are higher from November to February. In terms of daily values, there is a tendency for TRMM-MERGE daily precipitation to be lower than the CPC precipitation for the same probability of occurrence.

In the group VI, basins on the neighborhood of the South region, the differences in annual precipitation are very small during the first-decade and become positive along the second decade, with values higher than 10%. The highest differences occur during the wet season, varying, in the majority of basins, between -50 mm/month and 50 mm/month. The ECDF curves show that

the daily precipitation from TRMM-MERGE tends to be higher than CPC precipitation for the same probability of occurrence.

The group VII, basins in the south region, displays small negative differences during the first decade, which then become positive along of the last decade, with some values higher than 10%. These basins do not have a clear seasonality and differences in monthly precipitations spread all over the year, with the majority of values between -50mm/month and 50mm/month. For daily precipitation values, the ECDF curves show that the TRMM-MERGE daily precipitations are higher than the CPC values for the same probability of occurrence.

Finally, at the extreme south region, the group VIII exhibits a change of behavior in terms of differences in annual precipitation, when compared with the other south basins. Differences are more often positive in the first decade and tend to reduce along the second decade. In terms of monthly values, this group has the same behavior as group VII, without a wet season with higher differences. For daily precipitation values, the statistical distributions show that the TRMM-MERGE daily precipitations are often higher than the CPC values for the same probability of occurrence.

Our analyses show clearly a regional pattern on the differences between the two precipitation data sources. As we move to the north and west regions of the study area, the annual differences tend to become more positive. This spatial variability in annual precipitation differences is amplified in the second and most recent decade of the study period. The basins located in the northeast, east, and southeast regions have smaller differences and these differences tend to become more positive in the second decade, although at a smaller degree. The exceptions are the basins of the group VI, which tend to display more negative differences in annual precipitation during the last decade.

We also evaluated the impact of the observed differences on the simulation of streamflows, using calibrated hydrological models in two basins (Campos Novos and Tapajos), representative of the lowest and highest differences between precipitation data sources. The analysis showed how the models are sensitive to changes in precipitation, confirming the general findings in Fan (2015). If the two precipitation data sources used in calibration and simulation are similar, model performance is also similar. However, when they are very different, the performance indicators showed that the hydrological model tends to lose performance. The amount of loss in

performance may vary according to the quality of the data source used in the calibration. In our study, in the Tapajos basin, where the differences between TRMM-MERGE and CPC data are high, the performance loss was stronger when calibration was performed with TRMM-MERGE and CPC was used in simulation, comparatively to the opposite situation. The empirical relationship between annual precipitation and flow values shows that the dispersion is higher when dealing with the CPC data. This indicates that CPC data has more uncertainty, which impacts the results when the CPC data is used to simulate flows in a model that was calibrated with another data source. More uncertainty in the CPC data in this basin can be explained by the low density of raingauge stations in this area. The use of satellite information may give more accuracy to the TRMM-MERGE dataset in this case.

Another result of our study is that the hydrological model seems to propagate and amplify the differences in precipitation data into differences in streamflow simulations. Small differences in precipitation result in similar small differences in streamflow. However, large differences in precipitation seem to result in even larger differences in streamflow.

2.5 CONCLUSIONS

This study aimed to evaluate the differences between precipitation data obtained from two sources over 41 river basins in South America, the TRMM-MERGE and the CPC datasets, for the period 1997-2017. We investigated differences for different time resolutions (daily, monthly and annual precipitation), at different locations and according to their impact on the simulation of streamflow.

The results show that differences vary in space and time, and according to the temporal aggregation of the precipitation values. The second decade tends to amplify the observed differences in the majority of the basins.

Some basins show considerable differences, notably in terms of daily and monthly precipitation values, with an expected impact on the simulation of daily streamflows, which are also affected by the uncertainty of each precipitation data source. In addition, a spatial behavior of the differences between the precipitation sources was detected, with differences becoming more positive (i.e., TRMM-MERGE values are higher than CPC values) as we move to north and west in the study area.

With the results of this study, we recommend being cautious when working with a unique source of historic precipitation data to calibrate hydrological models, since this source can display uncertainties and errors that vary in space and time. In our study, we showed that it is a complex problem to determine a precipitation data source that is the best for all situations, especially when no observed data set can be used as ground truth or reference, as in the case of large continental areas such as South America.

When it comes to maximize the performance of streamflow simulations, it becomes important to extract information from all data sources available. In this study, we illustrated how hydrological models can be sensitive to changes in the precipitation data, especially when these changes reflect high differences between different forcing data sources. The use of observed streamflow is an alternative to help selecting the best precipitation data source. The comparison between observed and simulated streamflows is an indirect way to carry out the precipitation data analysis, but it can, nevertheless, be useful in hydrological applications at large river basins.

Further research will focus on accessing the uncertainties and investigating how data sources such as TRMM-MERGE and CPC can be combined, with varying weights according to basin location and time of the year, to provide a more robust long time series of precipitation data for hydrological model calibration and simulation. The goal is to have time series of forcing data that minimize the errors between observed and simulated flows in the past, so that these time series can be used for seasonal forecasting in the hydropower sector within the traditional ESP (Ensemble Streamflow Prediction) method, where hydrological models and historical precipitation are used to generate a set, or an ensemble, of possible flow scenarios dependent on the initial states of a given basin in real-time.

CHAPTER 3:

HYDROLOGICAL MODELING AS A TOOL FOR SELECTION AND VALIDATION OF PRECIPITATION DATA RELEVANT TO SEASONAL STREAMFLOW FORECASTING

This chapter is based on a paper submitted to the Journal of Hydrology: Regional Studies (EJRH), which received three reviews, with final editor's decision as "major revision"; the revised version was prepared and is being reviewed by the co-authors before re-submission: REIS. A. A.; WEERTS. A.; RAMOS. M. H.; WETTERHALL. F.; FERNANDES. W. S.: Hydrological modeling as a tool for selection and validation of precipitation data relevant to seasonal streamflow forecasting. *Journal of Hydrology: Regional Studies*, EJRH-D-21-00413, 2021.

3 HYDROLOGICAL MODELING AS A TOOL FOR SELECTION AND VALIDATION OF PRECIPITATION DATA RELEVANT TO SEASONAL STREAMFLOW FORECASTING

3.1 INTRODUCTION

Time series of quantitative precipitation estimates is crucial for calibrating and running hydrological models to be used in research and operational applications such as water resource management, irrigation planning, hydropower operations, and forecasting of floods and droughts. However, in large river basins or on countrywide and continental scales, it is often difficult to have consistent and accurate time series of spatially distributed precipitation data available over a long period of time. Precipitation is one of the climate variables most difficult to estimate because of its heterogeneous distribution in space and high variability in time (Herold et al., 2015). It is also susceptible to measurement errors caused by wind, evaporation, wetting, splashing and drifting effects, and human errors, such as uncalibrated gauge equipment, acquisition, and data communication problems (Michelson, 2004). Therefore, it is a major challenge to produce consistent precipitation products in space and time over large areas and long periods, especially if such products should be continuously used in real-time operations in hydrology (Golding, 2009; Kucera et al., 2013; Pozzi et al., 2013; Serrat-Capdevila et al., 2013; Verkade et al., 2013; Lettenmaier et al., 2015; Van Osnabrugge et al., 2017).

The main sources of precipitation data are the gauges, weather radars, and the satellite instruments (Gilewski and Nawalany, 2018). The first two sources, besides to be more accurate, have limitations because their dependence on spatial distribution, otherwise the satellite data emerges as a potential source because its higher resolution and capacity to cover big areas, but needs to be unbiased (Cassalho et al., 2020). The main sensors used to estimate the precipitation are the passive microwave, the calibrated infrared, and a combination of them (Hong et al., 2018). With the evolution of the sensors where added the active microwave sensors at the satellites as the Ku-band Cloud Profiling Radar (DPR) on the TRMM Satellite (Simpson et al. 1988), the W-band Cloud Profiling Radar on the CloudSat (Chen et al., 2008b), and Ku-/Ka-band Dual-Frequecy Precipitation Radar (DPR) on the GPM satellites (Huffman et al., 2017). To extract the precipitation information from this constellation of satellites where developed different algorithms, since the simplest IR-based GOES Precipitation Index (GPI) (Arkin and Meisner, 1987) until the most recent and sophisticated NASA GPM (Global Precipitation Measurements) Integrated Multi-satellite Retrievals (IMERGE) (Huffman et al., 2017).

On a global scale, gridded precipitation products have been available since the late 1990s (Huffman et al., 1997; Adler et al., 2003; Sun et al., 2017; Beck et al., 2017). However, only a few are produced in near real-time, such as the CPC Unified Gauge-Based Analysis of Global Daily Precipitation from the U.S. National Oceanic and Atmospheric Administration (NOAA) (Chen et al., 2008), and the IMERG for GPM dataset from the U.S. National Aeronautics and Space Administration (NASA) (Huffman et al., 2017), which is the successor of the Tropical Rainfall Measuring Mission (TRMM) data products. For South America, the TRMM-MERGE product developed by the Brazilian Centre for Weather Forecast and Climatic Studies (Centro de Previsão de Tempo e Estudos Climáticos, CPTEC), is also available in near real-time (Rozante et al., 2010). It combines gauging station datasets from the Global Telecommunications System, automatic stations from various agencies in South America, and the near real-time TRMM precipitation product, providing a gridded dataset of daily precipitation at 0.25° of spatial resolution for operational applications. In May of 2020, after the TRMM data be discontinued, CPTEC started to provide the GPM-MERGE, built with the GPM dataset based on the IMERG-E algorithm in (the substitute of TMPA-V7 in TRMM mission), maintaining the same gauge stations and the algorithm MERGE (Rozante et al., 2010), now in a higher resolution of 0.1° (Rozante et al., 2018, 2020).

When different precipitation products are available over an area, the question arises whether it would be better to select one product or combine different products. Beck et al. (2017) investigated 22 gridded global and tropical precipitation datasets and concluded that the product that merged all information available — Multi-Source Weighted-Ensemble Precipitation (MSWEPv1.0) — had better overall performance. Recently, Reis et al. (2019) carried out a study comparing the CPC-NOAA and TRMM-MERGE real-time precipitation datasets over 41 river basins, mostly located in Brazil. The authors found considerable differences in space and time between these two datasets, with a tendency to increase differences when moving from south to north and from east to west. For the majority of the studied river basins, the recent decade of data (2008–2017) presented the biggest differences in terms of areal precipitation over the river basins. The authors also highlighted the fact that the differences between the precipitation datasets were propagated, and often amplified in simulated streamflow when used to force a hydrological rainfall-runoff model.

Hydrological models can be useful tools for analyzing precipitation datasets. By comparing simulated and observed streamflows, the quality of a precipitation dataset used to force the model

can be indirectly assessed and the uncertainties evaluated. This strategy has been used in numerous previous studies to evaluate the quality of precipitation datasets at regional or global scales (e.g., Su et al., 2008; Collischonn et al., 2008; Voisin et al., 2008; Bitew et al., 2012; Li et al., 2013; Falck et al., 2015; Tang et al., 2016; Beck et al., 2017). Overall, the studies indicate that, once there are better estimates of observed flow than precipitation, the use of hydrological modeling can inversely bring better estimations of the observed precipitation and help in data validation.

Hydrological models can also be used to define and evaluate the best combination of multiple data sources. The MSWEPv1.0 product is an example of a combined product that uses river discharge observations from stations across the globe and hydrological simulations to correct systematic terrestrial precipitation biases (Beck et al., 2017). It is a fully global, historic precipitation dataset (1979–2014) available at daily and three-hourly temporal resolutions and 0.25° spatial resolution. It is based on data from gauge stations, satellite remote sensing, and atmospheric model reanalysis. The hydrological model used to evaluate the performance of the MSWEP product and compare it with other state-of-the-art gauge-adjusted datasets (i.e., WFDEI-CRU, GPCP-1DD, TMPA 3B42, and CPC Unified) was the HBV model (Bergström, 1995). Flow simulations using MSWEP showed better performance (median NSE of 0.52) than simulations with the other precipitation datasets (NSE values of 0.29 to 0.39). The median correlation obtained when using the MWSEP product was the best correlation for 60% of independent precipitation gauges from FLUXNET tower stations used for validation (for more details, see Beck et al., 2017). The MSWEP product is in constant evolution, in the version 2 the product added new algorithms to improve the accuracy, increased the resolution to 0.1°, included ocean areas, added new precipitation dataset at the analysis, and extended the MSWEP dataset until 2017 (Beck et al., 2019). Actually, MSWEP is in the version 2.8, with the resolution of 0.1° and 3-hourly dataset, under the platform GloH2O, available under requestion to the providers (MSWEP, 2021). Recently, Siqueira et al. (2018) applied the MSWEP precipitation product with the distributed MGB hydrological model over South America to simulate streamflows. They reported good overall performance of the simulations, with NSE > 0.6 in 55% of the flow stations. The performance was better in large rivers and wet regions, decreasing in drier climates, where timing errors in rivers with floodplain effects had been reported.

Reliable historical datasets are needed, but the datasets also need to be consistent over time and must represent the statistical variability of the climatology of the region. Therefore, consistent

long time series of spatially distributed precipitation over large areas are very useful for seasonal streamflow forecasting, being used to calibrate the hydrological models, to warmup the flow forecast models, calibrate bias correction of the global climate models (GCMs) (Crochemore et al., 2016). The ECMWF SEAS5, the most recent version of the European Weather Center seasonal model, has a hindcast of 35 years (1981-2016) (ECMWF, 2017), demanding a long time series of observed precipitation to access its performance and calibrate an eventual bias correction. As an alternative to using dynamic climate forecasts from GCMs as input to hydrological models for streamflow seasonal forecasting, the ensemble streamflow prediction (ESP) method is traditionally applied in hydrological forecasting (Twedt et al., 1977; Day, 1985; Wood and Lettenmaier, 2006). The method relies on using historic precipitation and temperature data as future possible climate scenarios in a continuous hydrological model, which is used to estimate the initial hydrological conditions of the catchments at the time of issuing a forecast. Historic meteorological data are useful for determining an ensemble of future scenarios, while real-time meteorological data are crucial for evaluating the initial conditions of the catchment. The ESP method has been widely used to provide skillful long-term ensemble predictions for a variety of hydrological applications, either alone or in combination with GCM-based predictions (see, for instance, Crochemore et al., 2016; Beckers et al., 2016; Bennett et al., 2017; Arnal et al., 2017; Harrigan et al., 2018). Emerton et al. (2018), for instance, used the latest ECMWF reanalysis product, ERA5, to generate a reference climatology to evaluate the GloFAS-Seasonal forecasting system around the globe. In Australia, a seasonal forecasting system was proposed by merging meteorological models and precipitation climatology to create an ensemble of future precipitation scenarios, the Forecast Guided Stochastic Scenarios (Bennett et al., 2017), which was later used to force a hydrological model and generate an ensemble of streamflow forecasts up to 12 months ahead.

In Brazil, gridded large-scale precipitation products are of particular importance to the real-time operations of the hydropower sector (Schwanenberg et al., 2015; Gibertoni et al., 2017). The anticipation of hydrological conditions can strongly influence the centralized operation of the electrical system and energy prices (ONS, 2016). Given the lack of a reference observational dataset based on ground rainfall measurements from gauges or radar, a methodology is proposed that uses a hydrological model and observed discharge time series to quantify uncertainties from the precipitation datasets, combine them, and select the best final product. It has been shown that direct empirical comparisons between rainfall and streamflow can be useful for evaluating rainfall dataset performance across multiple scales, in addition to helping identify and quantify

the magnitude of the uncertainty involving the dataset used in hydrologic modeling (Levi et al., 2017). Based on the water balance equation, and assuming that a catchment hydrologically behaves like a reservoir system, it is possible to invert the reservoir model equation and express the rainfall as a function of the streamflow and then use this relationship to estimate the uncertainty of the rainfall data (Kirchner, 2009; Henn, 2015).

Real-time precipitation datasets are usually subject to errors that affect their homogeneity through space and time. Because of its great importance for human activities, many studies are caring out to improve this information and provide a better real-time precipitation dataset, developing different algorithms to process the new satellite data and quality control tools to have a reliable rain gauge information, evolving many researchers in this process. The MERGE existing products are developed with analysis in a grid scale. As a novelty, we suggest in our research a different approach, where we make use of the knowledge existing behind the spatialized data, and blend them based on its uncertainty, in a catchment scale, to have a more robust estimation of the mean precipitation on the studied basins. This blend solution makes it possible to take advantage of the individual quality of the datasets and smooth eventual errors from one dataset or the other, ultimately resulting in better performance in hydrological modeling. Therefore, this paper addresses the following research questions: i - How can we blend this different observed precipitation dataset and validate the combination, taking the advantage of the collective intelligence behind each source, to have a better precipitation forcing for their use in rainfall-runoff models, precipitation forecast bias correction and flow forecasting? ii - How can we extend the combined precipitation dataset for a period longer than the coincident between both time series?

This paper aims to propose a method to produce a long and reliable real-time precipitation dataset that can be used to perform seasonal streamflow forecasts and as a reference of observed precipitation to assess the performance of precipitation forecasts issued by meteorological and global climate models. We use hydrological modeling as a tool for the selection and validation of the dataset over a large set of 41 river basins, that are relevant to the hydropower sector in Brazil and neighboring countries. The two real-time, station, and satellite-based precipitation products are TRMM-MERGE and CPC datasets, and the combined dataset is compared with the benchmark MSWEP. In Section 3.2, the methodology and dataset used in the experiment are presented. In Section 3.3, the results obtained are provided. Section 3.4 is a discussion of the results, and the conclusions and planned future studies are presented in Section 3.5.

3.2 MATERIALS AND METHODS

3.2.1 Study area and data

The methodology was applied to 41 river basins distributed in different climatic regions within Brazil and neighboring countries (Fig. 3.1). The river basins vary in size, with areas ranging from 9,300 to 382,000 km². The study area extends from the north (Jari River, Madeira River, Xingu River, Tapajos River, Tocantins River, and others) to the south of Brazil (Iguaçu River, Uruguay River, and others) and includes river basins located in the central part of the country (Paraná River, Grande River, São Francisco River, etc.). The 41 river basins provide inflow to 30 hydropower plants (HPPs).

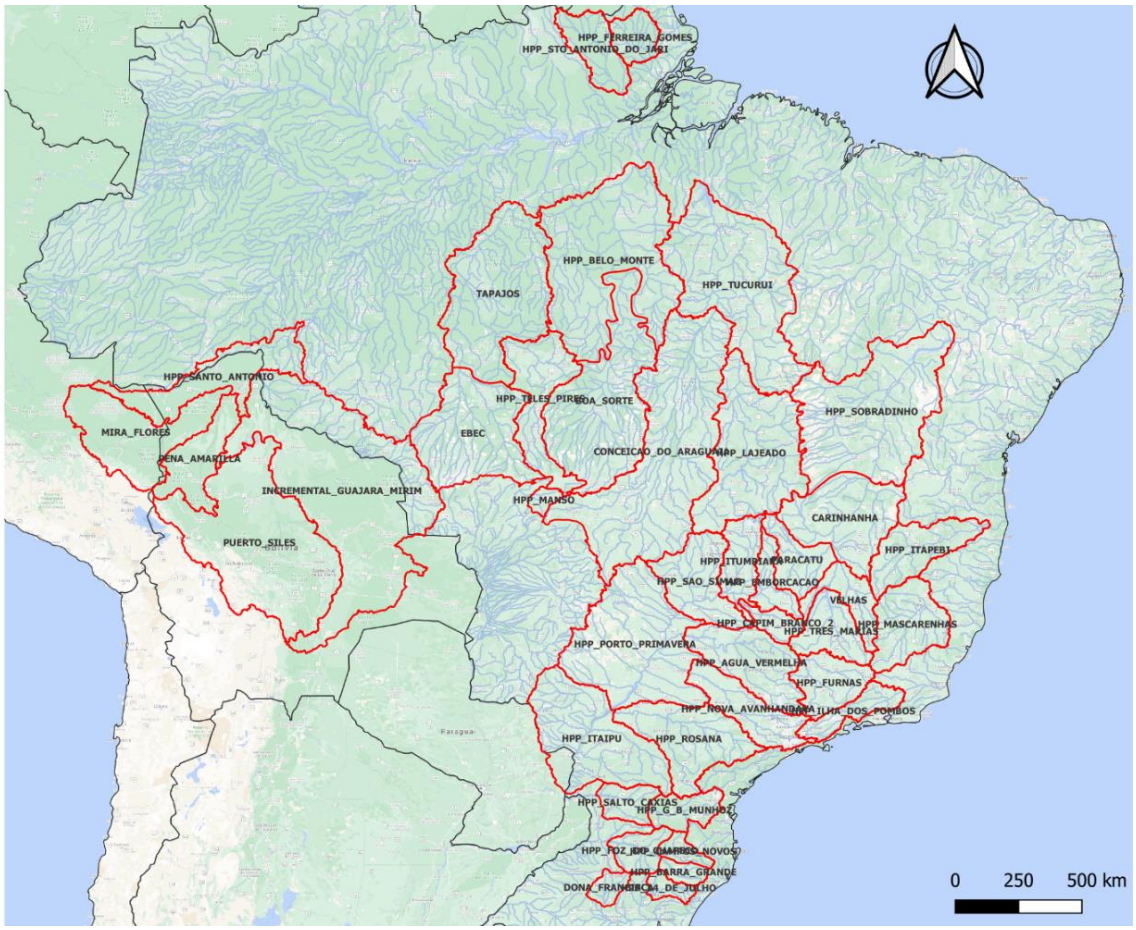

Figure 3.1 – Geographic location of the study area with the 41 river basins (red contours).

For each river basin, daily areal precipitation was obtained from the TRMM-MERGE, the CPC-NOAA, and the MSWEP datasets. Daily areal precipitation time series were calculated using the shapefile of the basins and averaging all grid data points falling inside each river basin considered. Table 3.1 presents the main information of each dataset.

Table 3.1 – Summary of the precipitation dataset main information.

Dataset	Spatial resolution	Time resolution	Time period covered	Download URL	Main references
TRMM-MERGE	0.25°	Daily	1997 - 2020	ftp:ftp1.cptec.inpe.br/modelos/io/produtos/MERGETRMM-MERGE/	Rozante et al. (2010)
GPM-MERGE	0.1°	Daily and 30 minutes	2000 - present	http://ftp.cptec.inpe.br/modelos/tempo/MERGE/GPM/DAILY/	Rozante et al. (2018, 2020)
CPC	0.5°	Daily	1979 - present	ftp://ftp.cpc.ncep.noaa.gov/precip/CPC_UNI_PRCP/GAUGE_GLB	Chen et al. (2008)
MSWEP	0.1°	Daily and 3 hourly	1979 - 2020	http://www.gloh2o.org/mswep/	Beck et al. (2019) and MSWEP, (2021)

Daily discharge data were obtained from the ONS (the National Operator of the Electric System). They correspond to the official HPP natural flow time series and are compiled annually by the national operator. Where the ONS takes of the regularization effects of the reservoirs and adds evaporation and other water uses to obtain the natural flows of the reservoir, these flows are also validated by the generators involved at the process (for more details, see ONS, 2005). Overall data availability depends on each river basin. The data can be downloaded at the URL: https://sintegre.ons.org.br/sites/9/13/84/paginas/servicos/produtos-pasta.aspx?RootFolder=/sites/9/13/84/Produtos/427/01-12-2020_022612. For this study, the discharge dataset used covers the period 1979-2018 for all studied river basins.

3.2.2 Methodological steps

To select a better real-time precipitation dataset among the two available independent data sources and a dataset that is a combination of the two, and to validate the selection and blending procedure using a hydrological model and observed streamflows, an experiment was designed with six basic methodological steps as showed in Figure 3.2.

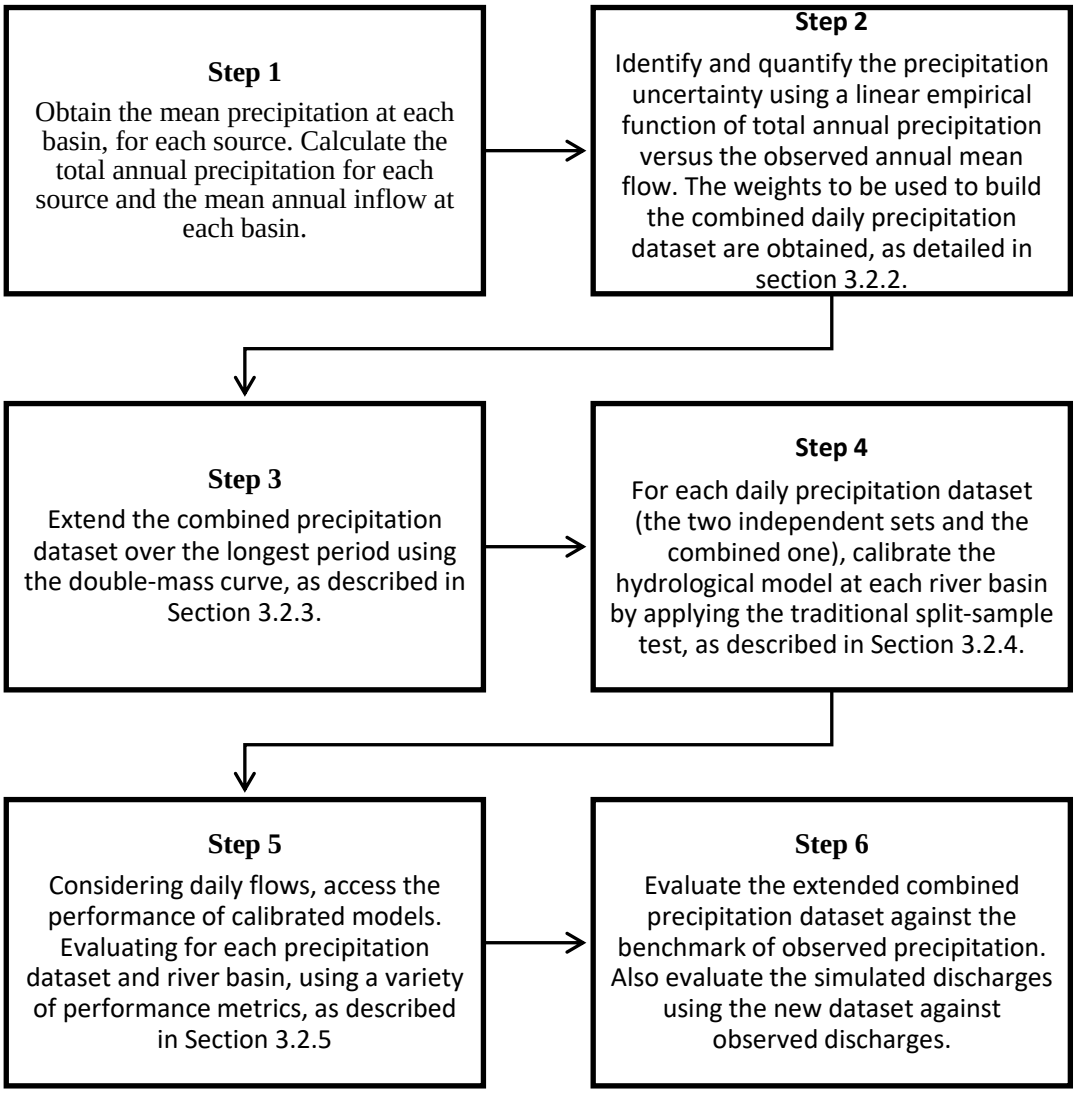

Figure 3.2 – Summary schema of the experiment.

Step 1: For each river basin, the daily areal precipitation time series (average over the area of the river basin) is estimated for each precipitation data source. The daily observed flow data are extracted for the same period at each basin. In addition, the total annual precipitation, and the annual mean of observed daily flows are calculated to perform the analysis based on the water balance relationship (Step 2).

Step 2: The uncertainty of each precipitation data source is identified and quantified by using empirical functions that relate the total annual precipitation amounts and the observed annual mean flows. The weights used to build the combined daily precipitation dataset are obtained based on the uncertainty quantified from the annual water balance, as detailed in Section 3.2.2.

Step 3: Because the two independent precipitation data sources cover different time periods, a procedure is used to extend the combined precipitation dataset over the longest period, using the double-mass curve, as described in Section 3.2.3.

Step 4: For each daily precipitation dataset (the two independent sets and the combined one), the hydrological model is calibrated at each river basin by applying the traditional split-sample test, which divides the time series into two periods for calibration and validation, and a calibration procedure over the entire data period, as detailed in Section 3.2.4.

Step 5: The performance of calibrated models is evaluated for each precipitation dataset and river basin, using a variety of performance metrics, as described in Section 3.2.5. The performance is accessed considering daily flows, with the parameters calibrated for the complete period (Oct1998 - Sep2017), for each of the three precipitation datasets.

Step 6: The extended combined precipitation dataset is evaluated against a benchmark of observed precipitation, and simulated discharges using the new dataset are evaluated against observed discharges.

3.2.3 Combining two precipitation data sources using the annual water balance

The water balance equation is used in hydrology to describe the flow of water in and out of a system. The period used to calculate the water balance is usually the hydrological year, which is a 12-month period that starts at the end of the dry season. For any given year, the water balance can be written as:

$$\Delta S = P_i - Q - ET \qquad (3.1)$$

where P_i is the annual precipitation for the given year (total precipitation over the hydrological year) of the precipitation data source i, Q is the annual mean flow, ET is the annual evapotranspiration, and ΔS is the annual variation of storage in the river basin, with all variables expressed in millimeters.

We are not focused into obtain the perfect relation P x Q, but only interested in knowing how the uncertainty varies when we use different precipitation sources in the same basins. We consider the hydrological year and at the end of the dry period the storage is near to the minimum. For

long time periods, usually more than 12 months, the ΔS term can be considered negligible (Shao et al, 2012, Beck et al., 2020). The ET term depends on physical factors, such as the vegetation type, soil cover, and land use, as well as on climate factors, such as temperature, solar radiation, humidity, and wind speed, this is clear on the Penman-Monteith method used to calculate the evapotranspiration (Allen et al., 1998). Therefore, this term can be considered independent of the precipitation source. Therefore, it is assumed that the variation of uncertainty in the water balance resulting from the different precipitation data sources is a function of the precipitation only. Equation (3.1) can be simplified, and the precipitation can be written as a function of the flow and the error term that will translate the uncertainties:

$$P_i = f\,(Q) + \varepsilon_i \qquad (3.2)$$

where $f\,(Q)$ is the empirical function between the precipitation (in millimeters) and the flow (in millimeters), and ε_i is the annual error associated with the precipitation source P_i.

The error ε_i is evaluated for each given year using the empirical function that relates each annual precipitation P_i to the annual flow Q. The evaluation is based on the standard deviation of the errors of each precipitation source P_i, and is computed over the time series of annual errors. The standard deviation estimates obtained were used to weight the proportion of each precipitation data source to create a combined precipitation dataset. The weights were based on the proportion of the standard deviation of the errors of one source with respect to the sum of standard deviations of the errors of both sources. The weights were obtained from the following equations:

$$W_j = 1 - \frac{\sigma\varepsilon_j}{\sigma\varepsilon_j + \sigma\varepsilon_k} \qquad (3.3)$$

$$W_k = 1 - W_j \qquad (3.4)$$

where W_j is the weight of the precipitation data source $P_{i=j}$, W_k is the weight of the precipitation data source $P_{i=k}$, $\sigma\varepsilon_j$ is the standard deviation of the annual errors of $P_{i=j}$, and $\sigma\varepsilon_k$ is the standard deviation of the annual errors of source $P_{i=k}$.

The main idea behind this methodology is not to identify the precipitation data source that displays the best correlation between P_i and Q. The goal is to access the uncertainty of each

source to make it possible to give a higher weight to the source with smaller uncertainty when the two sources of precipitation data are combined in one unique dataset.

Once the weights of each precipitation data source are obtained, they are applied to the daily precipitation time series to generate the combined daily precipitation dataset, according to Equation (3.5):

$$DP_{WC} = DP_j . W_j + DP_k . W_k \qquad (3.5)$$

where DP_{WC} is the daily precipitation of the weighted combination of the two precipitation data sources.

3.2.4 Double-mass curve method to extend the combined precipitation dataset

Once the combined precipitation method is applied to the two different precipitation data sources, a combined precipitation dataset for the same period of the shorter precipitation data source is obtained. It is thus necessary to extend, in a consistent way, this combined precipitation time series to also cover the period of the longer available data source. In this study, the double-mass curve method developed by the US Geological Survey was used (Searcy et al., 1960). The method is commonly used in data analyses to check the consistency of hydrometeorological data and adjust the data for any inconsistencies. It is based on comparing the time series of accumulated values at a single data station (or a given data source) with those given by data from other stations in a surrounding area (or other data sources) during the same period. The theory of the double-mass curve is based on the fact that a graph of the accumulation of one time series against the accumulation of another time series, during the same period, plots as a straight line as long as the data are proportional; the slope of the line represents the constant of proportionality "*b*" between them. Applied to this study, it gives Eq. (3.6):

$$P_c = P_k . b \qquad (3.6)$$

where P_c represents the precipitation variable of the combined precipitation dataset, and P_k is the precipitation variable coming from the longer time series of the two sources of precipitation used to produce the combined dataset. A break in the slope of Equation (3.6) indicates a change in the constant of proportion and the presence of inconsistencies.

In this study, for each river basin, daily precipitation was obtained from the TRMM-MERGE dataset for the period of 1997–2017 and the CPC-NOAA dataset for 1979–2017. Data from the reanalysis precipitation dataset MSWEP was used as benchmark (Beck et al., 2017). It covers the period 1979–2014. The double-mass curve was applied to annual values of total precipitation as follows.

- For each river basin, for the common period of TRMM-MERGE and CPC-NOAA data (1998–2017), the graph of accumulated annual values of the combined dataset is plotted against the graph of the CPC-NOAA dataset, which is the longer precipitation dataset.

- The years with a wide discrepancy around the normal tendency are removed, with the objective of having the most representative parameter to extend the time series.

- The constant of proportionality obtained with this correlation is used to multiply the past period of the longer data source, obtaining thus a complete time series of daily precipitation back until 1979, in order to represent the extension of the combined precipitation dataset.

To compare the combined precipitation dataset with the benchmark precipitation (MSWEP dataset), and also to evaluate how the dispersion of the error varies in time, the standard deviation of the annual precipitation errors (observed precipitation minus the value calculated with the empirical functions of Equation (3.2)) were calculated for 1980–2014 (full hydrological years of benchmark data available) in a five-year moving window. To improve the analysis and avoid scale distortions caused by differences in wetter or drier years between MSWEP and the combined precipitation dataset, the standard deviation error was normalized by dividing its value by the average precipitation of each five-year window.

3.2.5 HEC-HMS modeling and flow analyses

To validate the combined precipitation dataset obtained, a hydrological model was used to evaluate the accuracy of the simulated discharges when this dataset drives the model. The hydrological model used in this study is the one proposed in the suite of the HEC-HMS model (Feldman, 2000). It is a flexible and user-friendly suite of models, that can be used for many hydrological simulations like urban and rural flooding, flood warning systems, water uses planning, etc. The model can be applied since a quite simple event simulation to a semi-

distributed model in a continuous simulation. The modules can be chosen according to the needs of the user, application, and expected accuracy (Feldman, 2000; Najim, 2013). For the application at flow forecast activities, the model must be able to run in a continuous simulation, the HEC-HMS model has this capacity when we choose a more sophisticated configuration, selecting specific modules at the loss method, transformation method and base-flow method (Scharffenberg, 2016).

In this study, the HEC-HMS modeling framework was run at the daily time step, and the main modules chosen to satisfy a continuous simulation were the following: interception was modeled using the simple canopy (Bennett, 1998) and the simple surface (Bennett, 1998) methods, where occur the interception of part of the precipitation, the excess that arrives on the soil is captured until the storage capacity of the surface is filled then the runoff starts with the excess of precipitation. The water in the surface will infiltrate into the soil; to representing the rain-flow transformation, the soil moisture accounting method is the unique module able to run a continuous simulation, this loss method uses three layers to represent the dynamics of the water movement in the soil. For a given precipitation and evapotranspiration the model computes basin surface runoff, groundwater flow, losses and the deep percolation over the entire basin. (Bennett, 1998); to represent the shape of the hydrograph, was used the Clark unit hydrograph, the principal components are the time of concentration, defining the travel time in the sub-basin and the storage coefficient, used for accounts storage effects on the linear reservoir. (Kull and Feldman, 1998); the linear reservoir method (Kull and Feldman, 1998) was used to represent the base flow, it uses a linear reservoir to model the recession of base-flow after a storm event, conserving the mass of the basin. The lateral outflow of the groundwater is connected with the infiltration from the soil moisture accounting loss method. For the routing method, were used two options depending on the complexity of the basin and the reach extension: Lag method or Muskingum-Cunge Routing.

The split-sample approach (Klemes, 1986) was used to calibrate the hydrological model and test its robustness (validation). The time series is split into two and both parts are used for calibration and validation. The results in terms of model performance are evaluated for the two validation periods and compared with the performance results obtained over the same periods but with the calibration based on the complete period. The main objective of these various calibration and validation periods is to certify that the calibration of the total period, which is used in the next steps, is robust and has equivalent performance to that of the split-sample approach. Figure 3.3 illustrates the periods of calibration and validation of the HEC-HMS model.

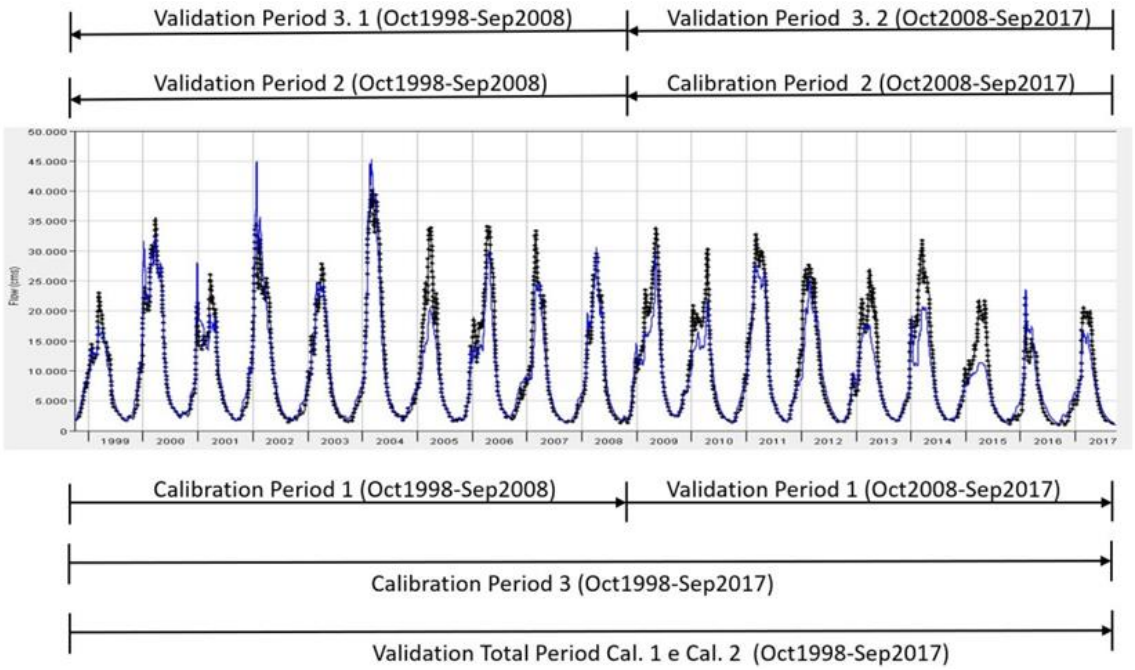

Figure 3.3 – Split-sample test method used in this experiment with two split periods with 10 years each of calibration/validation and the total period of calibration with 19 years and its validation separated into two decades to match the size of the split-sample validation periods. The blue hydrograph is the simulated flow, and the black is the observed flow.

The models were calibrated in a daily time step and for each of the three sources separately. Large basins, which have different climatic characteristics along the main river, was divided to better represent the average precipitation in each region and produce a better runoff transformation. In total, there are 26 parameters to be calibrated in the HEC-HMS model, the most sensible are the time of concentration and the storage coefficient, linked with the transformation module; and the maximum infiltration rate, soil total storage, soil tension storage, and the maximum soil percolation rate, linked with the loss method. An initial manual calibration is performed to obtain the first parameter set. Then, the automatic calibration procedure, available in HEC-HMS model, is applied to obtain optimal parameters using the Univariate-Gradient Search Algorithm. For the Clark unit hydrograph parameters, the objective function was the Minimum of Peak-Weighted RMS Error, and for the loss parameters the Minimum Sum of Squared Residuals (Diskin and Simon, 1977) was applied. Since the objective functions are more sensitive to the volumes and peaks of the hydrographs, it is sometimes necessary to adjust the baseflow parameters to have a better fit at the recession of the hydrograph after running the model optimization. The calibration process is repeated three times (calibration period 1, period 2, and total period), for each precipitation data source and for the combined precipitation, and for each river basin.

3.2.6 Evaluation metrics

To analyze the performance of the hydrological models run in this study (HEC-HMS model calibrated with the different observed precipitation datasets), the Nash–Sutcliffe efficiency - NSE (Nash, 1970), Kling–Gupta efficiency - KGE (Gupta et al, 2009), Mean Absolute Error - MAE, and R^2 (coefficient of determination) were used as performance indicators. These metrics are used to compare the simulated flows with the observed flows and were evaluated for the independent time periods defined in Figure 3 (October 1998 to September 2008; October 2008 to September 2017). In our evaluation, the performance indicators obtained for the validation periods 1 and 2 were used to evaluate the performance of the hydrological model at each river basin. The performance obtained during the total calibration period was used to define the best precipitation data source for each river basin.

NSE: measures how good the results of the model are compared with the mean observed discharge. Values equal to 1 indicate a perfect fit, and values smaller than zero indicate that the mean discharge is a better predictor than the hydrological model.

$$NSE = 1 - \frac{\sum_{i=1}^{n}\left(Y_i^{sim} - Y_i^{obs}\right)^2}{\sum_{i=1}^{n}\left(Y_i^{obs} - \bar{Y}^{obs}\right)^2} \qquad (3.7)$$

where Y_i^{sim} is the simulated value at time step *i*, Y_i^{obs} is the observed value at time step *i*, $\bar{Y}^{obs}$ is the mean of the observed value, and *n* is the number of time steps.

KGE: was developed to provide a decomposition of the Nash–Sutcliffe efficiency analysis. Values close to 1 indicate a more accurate model.

$$KGE = 1 - \sqrt{(r-1)^2 + \left(\frac{\mu_{sim}}{\mu_{obs}} - 1\right)^2 + \left(\frac{\sigma_{sim}}{\sigma_{obs}} - 1\right)^2} \qquad (3.8)$$

where, in the first part, r is the linear correlation between simulations and observations. In the second part (a measure of error variability), μ_{sim} is the mean of the simulations Y_i^{sim}, and μ_{obs} the mean of the observations Y_i^{obs}. In the third part (a bias term), σ_{sim} is the standard deviation of the simulations, and σ_{obs} is the standard deviation of the observations.

MAE: gives the average deviation between the simulated and the observed discharge. Values closer to zero indicate better performance.

$$MAE = \frac{1}{n}\sum_{i=1}^{n}\left|Y_i^{sim} - Y_i^{obs}\right| \quad (3.9)$$

where definitions are the same as in Equation (3.7).

R^2: is the proportion of the variance in the dependent variable that is predictable from the independent variable. A value close to 1 indicates a better fit of simulations to observations.

$$R^2 = \frac{\sum_{i=1}^{n}\left(Y_i^{sim} - \bar{Y}^{obs}\right)^2}{\sum_{i=1}^{n}\left(Y_i^{obs} - \bar{Y}^{obs}\right)^2} \quad (3.10)$$

where definitions are the same as in Equation (3.7).

3.3 RESULTS

3.3.1 Standard deviation of the annual precipitation errors

Figure 3.4 shows the boxplot distribution of the standard deviation of the annual precipitation errors (ε_i from equation (3.2)) obtained from the two sources of precipitation data and the combined precipitation dataset. The standard deviation values were evaluated over all 41 river basins and 19 years of data (Oct-1998 / Sep-2017), and in all basins the linear function was the best fit, this make sense once the water balance in an annual scale, was represented by a linear function (equation (3.1)). The standard deviation of annual precipitation errors from the benchmark MSWEP dataset, for all river basins and the period from 1998 to 2017, is also shown as reference. Table 3.2 shows the results for each river basin, as well as the weights applied when combining the two precipitation data sources.

The dispersion of the annual precipitation errors is reduced when the different precipitation data sources are combined. The combined precipitation dataset shows a lower standard deviation of the annual precipitation errors than the original datasets on 15 out of 41 river basins, and its boxplot distribution is closer to the reference MSWEP dataset. Although the median value of the error standard deviation is close to the TRMM-MERGE dataset median value, the interquartile range between the 75th and 25th percentiles is smaller in the combined dataset. This measure of dispersion of the precipitation errors around the empirical function gives an idea of the uncertainty of each precipitation dataset. In the combined dataset more weight is given to the precipitation dataset with lower uncertainty. In Table 3.2, we can see that the TRMM-MERGE

dataset has more weight than the CPC dataset in 30 out of 41 river basins, and both have equal weight in 2 river basins.

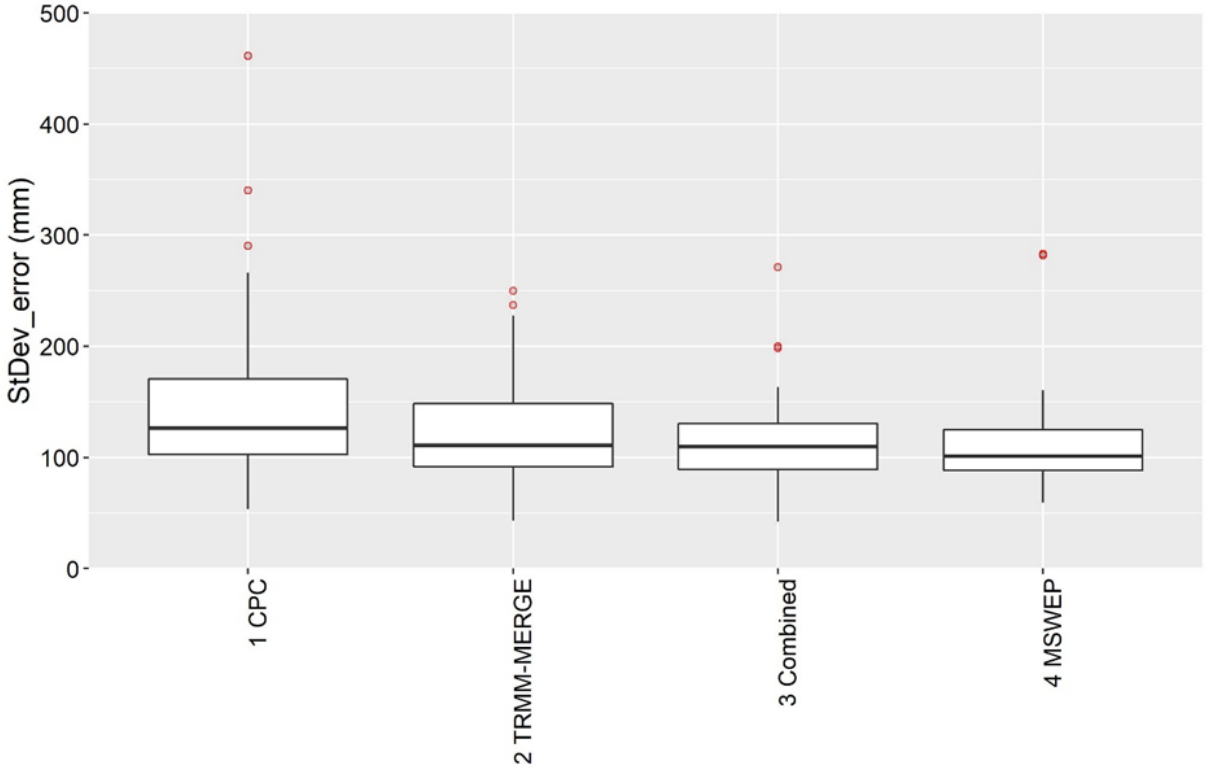

Figure 3.4 – Box-plot of the standard deviation of the annual precipitation errors (in mm) for areal precipitation over 41 river basins and for each precipitation dataset: CPC, TRMM-MERGE, Combined CPC and TRMM-MERGE and the reference MSWEP.

Table 3.2 – Standard deviation of the annual precipitation errors (in mm) for each river basin and precipitation dataset (TRMM-ERGE, CPC and Combined TRMM-MERGE and CPC) and weights used for the combined precipitation dataset. The dataset with the best performance is colored.

RIVER BASIN	Standard Deviation of annual precipitation errors			Weights used in the combined dataset	
	TRMM-MERGE	CPC	Comb.	TRMM-MERGE	CPC
1) HPP 14_DE_JULHO	128	100	101	**0.44**	**0.56**
2) HPP DONA_FRANCISCA	163	180	163	**0.53**	**0.47**
3) HPP BARRA_GRANDE	196	124	134	**0.39**	**0.61**
4) HPP CAMPOS_NOVOS	141	135	130	**0.49**	**0.51**
5) HPP FOZ_DO_CHAPECO	237	181	198	**0.43**	**0.57**
6) HPP G_B_MUNHOZ	111	161	122	**0.59**	**0.41**
7) HPP SALTO_CAXIAS	149	290	159	**0.66**	**0.34**
8) HPP ITAIPU	115	126	116	**0.52**	**0.48**
9) HPP ROSANA	116	80	75	**0.41**	**0.59**
10) HPP PORTO_PRIMAVERA	95	106	90	**0.53**	**0.47**
11) HPP NOVA_AVANHANDAVA	199	126	138	**0.39**	**0.61**
12) HPP AGUA_VERMELHA	169	101	120	**0.38**	**0.62**
13) HPP FURNAS	85	121	96	**0.59**	**0.41**
14) INC_HPP SAO_SIMAO	99	100	94	**0.50**	**0.50**
15) INC_HPP ITUMBIARA	120	150	124	**0.56**	**0.44**
16) HPP CAPIM_BRANCO_2	93	98	89	**0.51**	**0.49**
17) HPP EMBORCACAO	97	146	110	**0.60**	**0.40**
18) HPP ILHA_DOS_POMBOS	89	115	79	**0.56**	**0.44**
19) HPP MASCARENHAS	85	93	80	**0.52**	**0.48**
20) HPP ITAPEBI	43	54	42	**0.55**	**0.45**
21) HPP TRES_MARIAS	110	153	110	**0.58**	**0.42**
22) VELHAS	92	124	99	**0.57**	**0.43**
23) PARACATU	93	103	89	**0.52**	**0.48**
24) CARINHANHA	95	109	99	**0.54**	**0.46**
25) HPP SOBRADINHO_INC	122	135	127	**0.52**	**0.48**
26) HPP LAJEADO	76	100	72	**0.57**	**0.43**
27) CONC_DO_ARAGUAIA	78	119	70	**0.60**	**0.40**
28) HPP TUCURUI_INC	121	162	125	**0.57**	**0.43**
29) BOA_SORTE	101	227	114	**0.69**	**0.31**
30) HPP BELO_MONTE_INC	135	259	142	**0.66**	**0.34**
31) HPP MANSO	198	266	200	**0.57**	**0.43**
32) HPP TELES_PIRES	87	190	102	**0.69**	**0.31**
33) EBEC	69	171	68	**0.71**	**0.29**
34) HPP TAPAJOS	89	340	106	**0.79**	**0.21**
35) PUERTO_SILES	72	81	73	**0.53**	**0.47**
36) PENA_AMARILLA	152	136	139	**0.47**	**0.53**
37) MIRA_FLORES	148	105	110	**0.41**	**0.59**
38) INC_GUAJARA_MIRIM	93	93	89	**0.50**	**0.50**
39) INC_ HPP_SANTO_ANTONIO	111	131	104	**0.54**	**0.46**
40) HPP STO_ANTONIO_DO_JARI	228	257	137	**0.53**	**0.47**
41) HPP FERREIRA_GOMES	250	461	271	**0.65**	**0.35**

3.3.2 Hydrological model performance

The three precipitation datasets (TRMM-MERGE, CPC and Combined) were used to calibrate and validate the HEC-HMS hydrological model in all 41 river basins. Figure 3.5 shows the density functions representing the distribution of the four performance metrics analyzed: KGE, NSE, MAE (calculated in terms of specific discharge, in l/s.km² to permit comparison of the values in basins with different sizes), and R². The values obtained in calibration (validation) are in red (blue). Table 3.3 shows the median values of the metrics when considering all river basins, calibration and validation periods (as defined in Figure 3.3), and for each precipitation dataset.

Table 3.3 – Median values of the performance metrics NSE, KGE, MAE and R² for the simulated flows in calibration and validation periods from the hydrological model HEC-HMS applied over 41 river basins with the TRMM-MERGE, CPC and Combined CPC and TRMM-MERGE precipitation datasets. Calibration and validation periods come from the split-sample test of the total 1998-2017 data period.

Metric		Median values		
		TRMM-MERGE	CPC	Combined
NSE	Calibration	0.73	0.71	0.77
	Validation	0.71	0.68	0.75
KGE	Calibration	0.81	0.79	0.81
	Validation	0.78	0.75	0.78
MAE (l/s.km²)	Calibration	3.87	4.07	3.45
	Validation	3.94	4.33	3.64
R²	Calibration	0.69	0.66	0.70
	Validation	0.67	0.64	0.69

For most of the basins, the difference in performance metrics between calibration and validation is less than 10%. The calibrated models can be considered to perform well over the large river basin dataset of this study. For most of the 41 river basins, the NSE and KGE criteria are higher than 0.60, and the R^2 coefficient is higher than 0.55. Table 3.3 shows that median values of NSE and KGE vary from 0.71 to 0.81 in calibration, and from 0.68 to 0.78 in validation. Median values of R^2 coefficient in calibration and validation are also very close. These results indicate that the model calibration is sufficiently robust to represent the characteristics of the basins in different periods. Figure 5 also shows that the combined dataset results in a more consistent calibration and validation performance, with sharper curves and fewer outliers of performance. The combined dataset is also the one that presents the highest median values of NSE, KGE and R^2 and the lowest median values of MAE (Table 3.3). These results can also be another indicator of the robustness and good performance of the combined precipitation dataset.

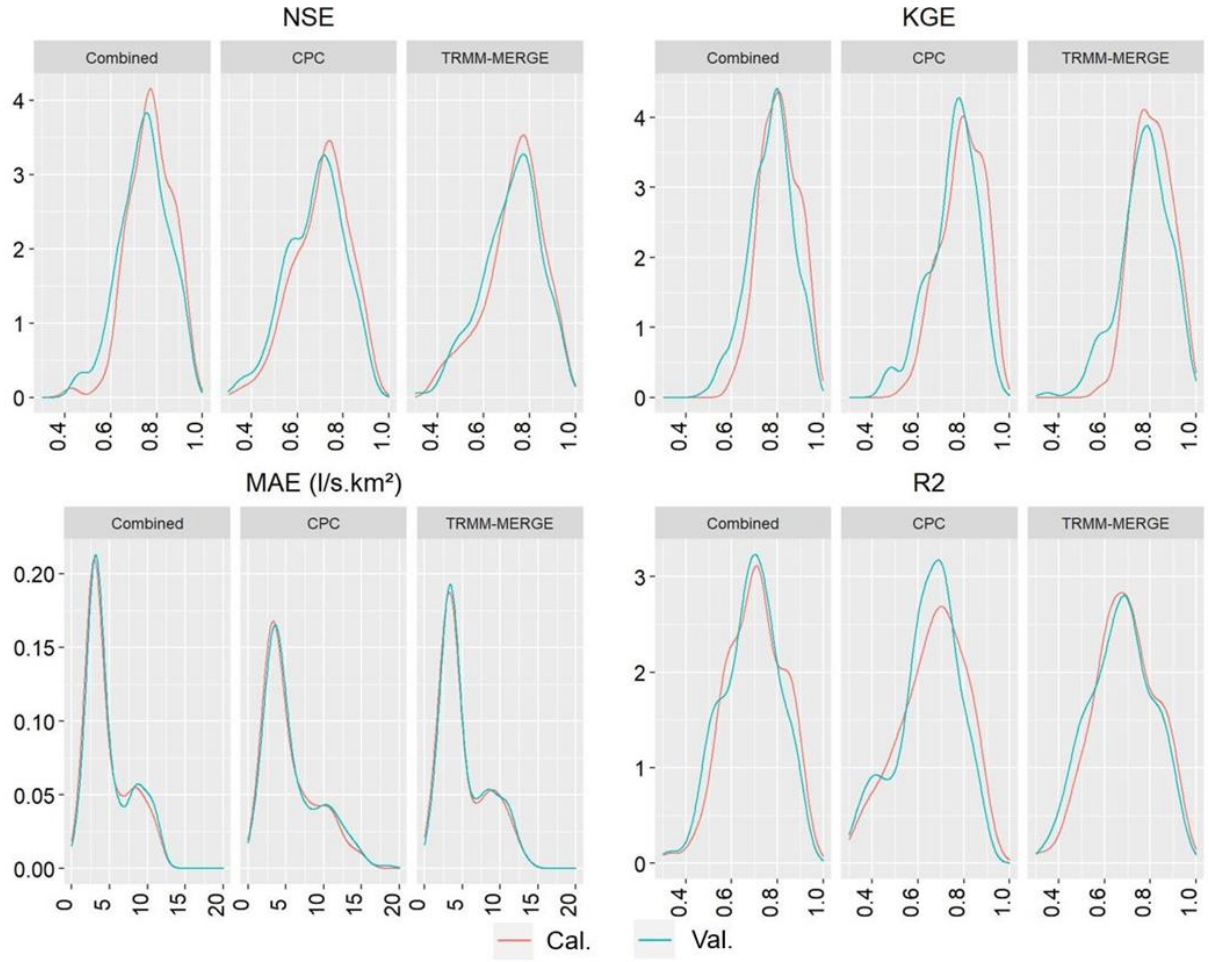

Figure 3.5 – Density functions of the values of the performance metrics NSE, KGE, MAE and R^2 for the simulated flows in calibration (line in red) and validation (line in blue) periods from the hydrological model HEC-HMS applied over 41 river basins with the TRMM-MERGE, CPC and Combined CPC and TRMM-MERGE precipitation datasets. Calibration and validation periods come from the split-sample test of the total 1998-2017 data period.

3.3.3 Selection of the best precipitation dataset

After the evaluation and validation of the performance of the hydrological model for each river basin, the best performing precipitation dataset was evaluated in terms of simulated discharges. The simulations were made using the model with parameters calibrated with each precipitation dataset and over the entire period (Oct1998–Sep2017). Figure 3.6 shows the MAE, KGE, NSE, and R^2 performance metrics obtained for the 41 river basins and the three sources of precipitation data (TRMM-MERGE, CPC, and the combined precipitation dataset).

In general, the simulated discharges using the CPC precipitation dataset clearly performed worse for the four indicators analyzed. The simulated discharges using the combined precipitation dataset performs best for almost all basins. When the scores are not the best for this dataset in a river basin, the differences are less than 10% in the majority of the cases (not shown). The best

performance of the combined dataset is clearly shown with the NSE, MAE and R^2 criteria. In terms of the KGE criterion, 50% of the river basins present values higher than 0.79 when using the combined and the TRMM-MERGE precipitation datasets. There are small differences in KGE between these two datasets, although the use of the combined dataset resulted in fewer outliers in terms of performance and notably less river basins with low values of KGE. For individual river basins showing the lowest values of KGE with the combined dataset, the differences regarding the KGE with the TRMM-MERGE are lower than 8%.

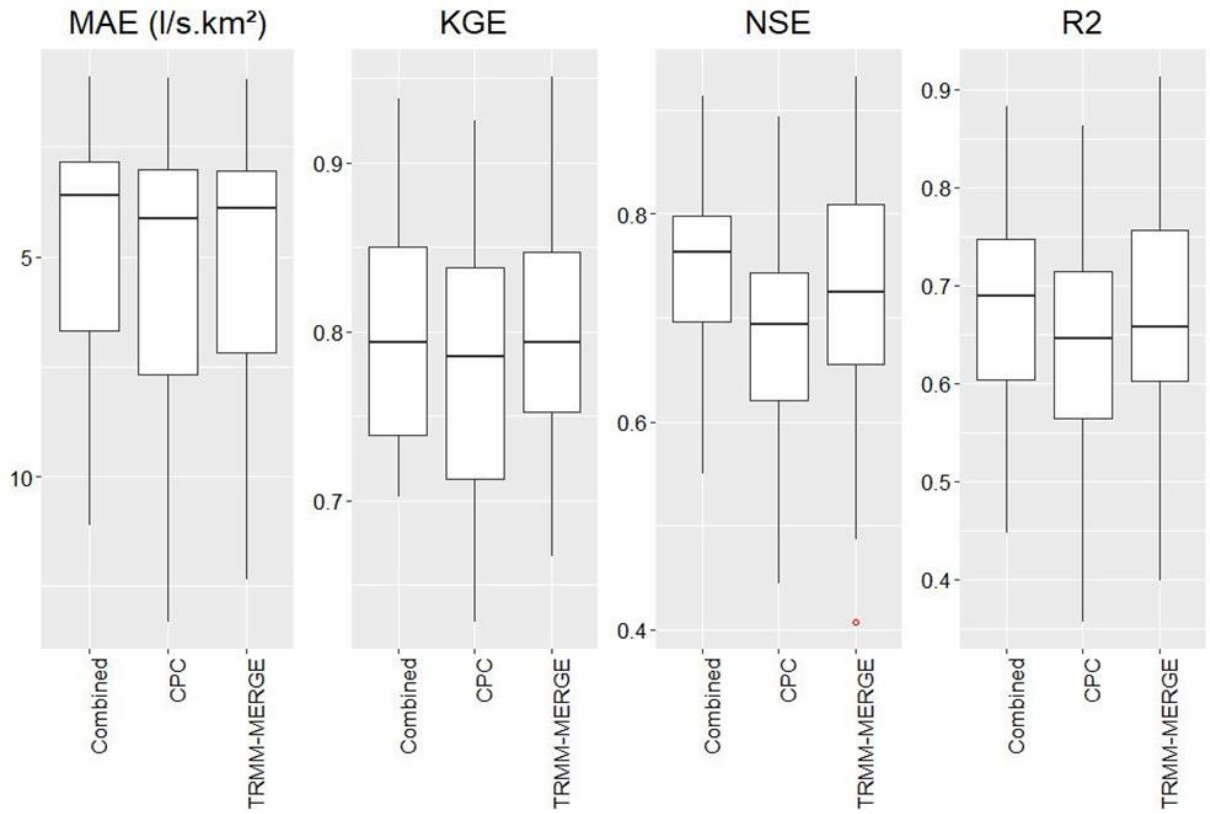

Figure 3.6 – Performance metrics MAE, KGE, NSE and R^2 for the simulated flows in the calibration period 1998-2017 from the hydrological model HEC-HMS applied over 41 river basins with the TRMM-MERGE, CPC and Combined CPC and TRMM-MERGE precipitation datasets.

3.3.4 Extension of the combined precipitation dataset

Once the evaluation showed that the combined precipitation of the two precipitation data sources achieved the best performance over the common period of data (Oct1998–Sep2017), the next step was to use the double-mass procedure (Section 3.2.3) to extend the combined dataset. The correlation of the double-mass curve between the longest dataset (CPC) and the combined dataset was used to extend the period of the combined dataset until 1979 (first year of data available in the longest CPC dataset). To validate the extended dataset obtained, the hydrological models were run for each river basin, with parameters calibrated for the period 1998–2017. The

performance of the streamflow simulations of this recent period was compared with the performance of the simulations obtained over the extended (validation) period of 1979–1997. Figure 3.7 shows the distribution of streamflow performance metrics (MAE, NSE, and R2) over the 41 river basins of this study.

In terms of accuracy of the streamflow simulations (MAE), the average error for the extended (validation) period (1979–1997) is slightly lower than the average error of the recent (calibration) period (1998–2017). Considering the NSE criterion, the extended period has, on average, better performance (higher NSE values) than the recent period. For the R^2 correlation, the values obtained over the extended period are clearly higher than the values obtained over the recent period. These results validate the extension of the combined precipitation dataset in terms of its ability to provide streamflow simulations in the extended earlier period that match the observed streamflows as well as in the more recent period of the combined precipitation dataset.

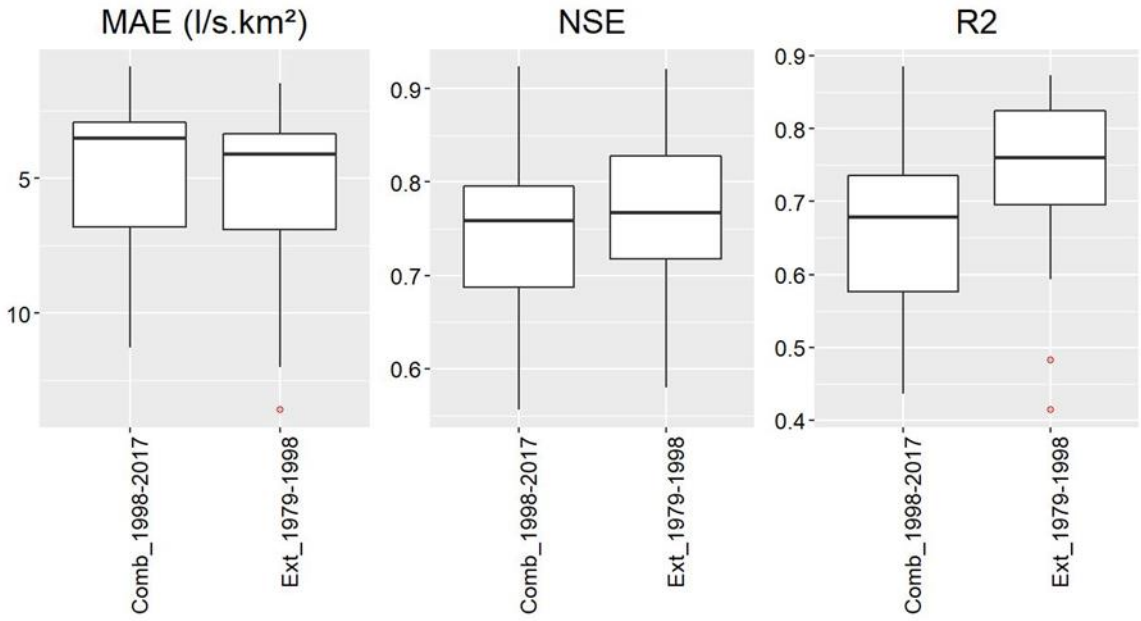

Figure 3.7 – Performance metrics MAE, NSE and R^2 for the simulated flows from the hydrological model HEC-HMS applied over 41 river basins with the Combined CPC and TRMM-MERGE precipitation datasets in the calibration period 1998-2017 and in the validation extended period 1979-1998.

3.3.5 Comparison of the combined precipitation dataset with the benchmark

The combined precipitation dataset was evaluated against the benchmark MSWEP dataset. Figure 3.8 shows the evolution in time of the normalized standard deviation of the annual precipitation errors obtained for 1980–2017 in a five-year moving window. The thickest lines

represent the median of the values for all river basins and the shadowed areas show the 25th and 75th percentiles (variability among river basins).

Figure 3.8 – Normalized standard deviation of the annual precipitation errors with the combined precipitation dataset (red) and the benchmark MSWEP dataset (blue). Median values (lines) and 25th and 75th percentiles (shadowed areas) are calculated in a five-year moving window and over 41 river basins.

The extended period of the combined precipitation (before 1998) tends to have a behavior closer to the benchmark. It shows similar standard deviation of annual precipitation errors, but higher values: median values are closer to 6% versus median values closer to 5% for the benchmark. The combined precipitation dataset does not exhibit a visible temporal trend. However, the standard deviation of the precipitation errors decreases after the year 2000, to increase again just a few years later.

The standard deviation of the MWSEP annual precipitation errors is smaller and more stable over time comparatively to the combined precipitation dataset. It also shows less variability among river basins. After around 1998, there is a reduction in the MSWEP error standard deviation, probably due to the use of satellite observations to improve the estimates of precipitation. After 2008, median values tend to increase again to values similar to those before 1998, although the variability among river basins remain reduced.

When the entire period (1980–2017) is considered, the combined precipitation dataset has a higher median and variability among river basins than the benchmark, but the difference can be considered small, especially considering that the combined precipitation is a real-time dataset, subject to errors that might be corrected afterwards, and the level of consistency is not comparable to a reanalysis dataset such as MSWEP.

In terms of spatial distribution of the errors, there is no evidence of a pattern or regions with a clear higher normalized standard deviation of the errors (not shown). For almost all basins, the combined precipitation dataset displays values between 4% and 9%. Only a few basins have values higher than 11%, and they are not concentrated in the same region..

3.3.6 Examples of simulated hydrographs using the combined precipitation dataset

As showed in Sections 3.3.2 and 3.3.3, the combined precipitation dataset displayed good performance for the period used to build it from the two existing data sources, i.e., 1998–2017, with NSE and KGE values above 0.75. Figure 3.9 shows some examples of the simulated flows using the combined precipitation dataset for the complete period generated from this study, i.e., from October 1st, 1979 to September 30th, 2017. Three river basins were selected to represent the southern region (HPP Foz do Chapecó at the Uruguai River), the southeast region (HPP Emborcação at the Paranaíba River), and the north region (HPP Santo Antônio at the Madeira River).

In the southern region, the weather does not present a clear seasonality and peaks of flow may occur in any month of the year. The simulated flows tend to underestimate the highest peaks and overestimate the lowest flows (NSE = 0.78). In the southeast region, seasonality is present, and the wet season is from November to March. The simulated flows tend to overestimate the flow peaks for the period 1983–1993 and underestimate them for 2005–2010. Despite these tendencies, this river basin also presents a good statistical fit, with NSE value of 0.76. In the north region, the biggest basin of our dataset is shown. A clear seasonality is observed, with the wet season from December to May. The simulated flows display an overall better and more stable performance, with a good fit to flow peaks and flow recession periods (NSE = 0.87).

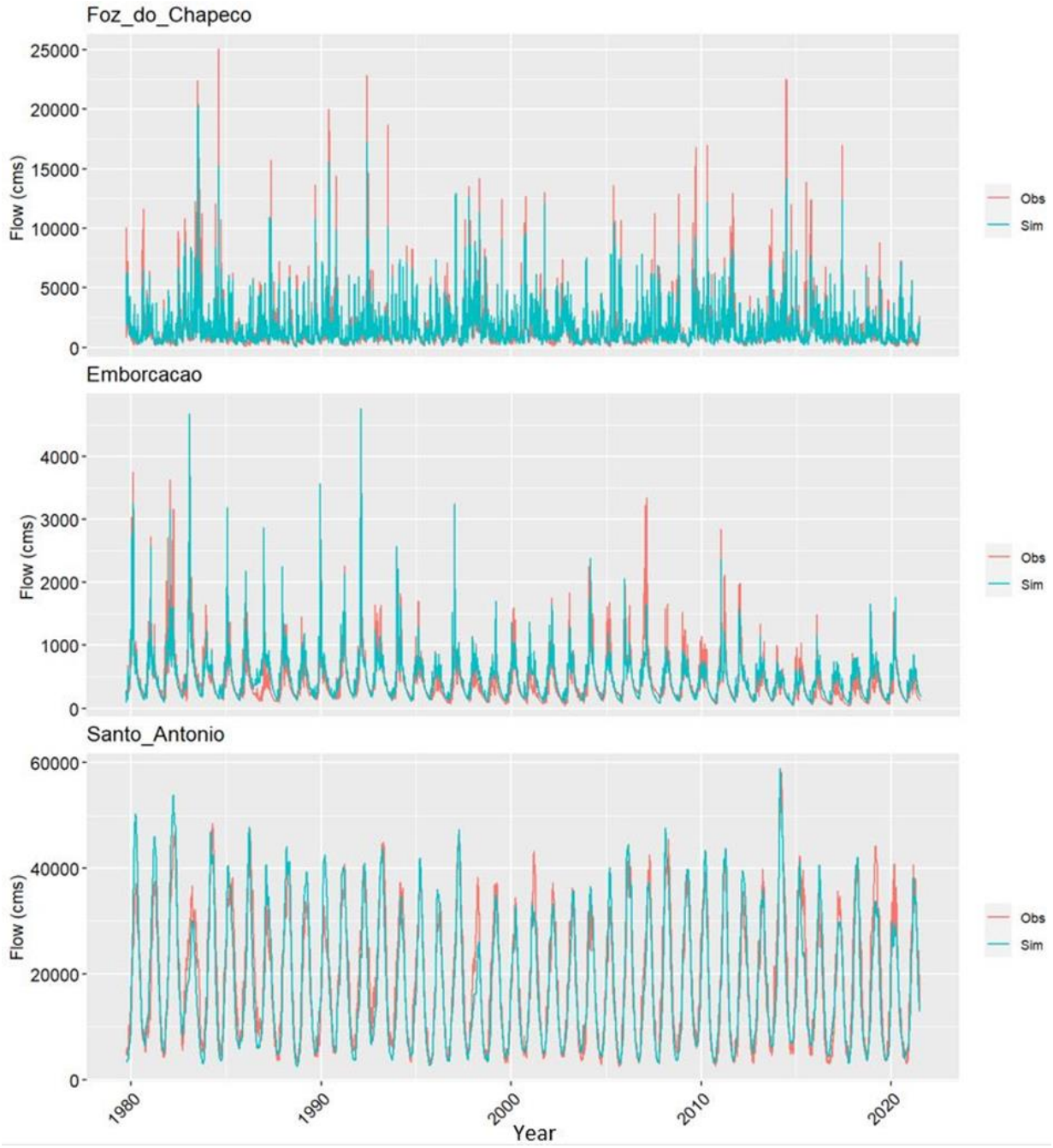

Figure 3.9 – Simulated (blue) and observed (red) daily streamflows for three representative river basins from October 1st, 1980 to September 30th, 2017: Foz do Chapecó (Uruguai River) in the south region (top pannel), Emborcação (Paranaíba River) in the southeast region (middle panel), and Santo Antônio (Madeira River) in the north region (bottom panel).

3.4 DISCUSSION

The study area has a continental dimension exhibiting diverse patterns of weather and climate governed by large scale climate phenomena (Garreaud et al.,2009). We find climates with a clear precipitation seasonality, as the drier semi-arid weather at the northeast region (Tinôco et al., 2018), the South America monsoon system responsible to the high precipitations at the southeast

and central-western Brazil (Ferreira and Gan, 2011), and the intense convective storms from tropical weather at the Amazon region with (Garreaud et al.,2009). It is possible to find a weather with no seasonality, presenting wet and dry periods in any month of the year, the subtropical weather at the south region of the continent (Garreaud et al.,2009).

The first part of this study is an evaluation of the precipitation uncertainty in two raingauge and satellite-based products (CPC and TRMM-MERGE), covering the study area of 41 river basins in Brazil and neighboring countries. This is an important step before performing any hydrological analysis or using available data in real time flow forecasting (Levi et al., 2017). The uncertainty is evaluated and used to combine the two precipitation data sources available in near real time. As a novelty the method proposed was applied in basins scale, therefore is possible to find a combination that satisfies the hydrological and weather specificity of each region, besides to take advantage of the quality control and knowledge already developed in each precipitation source, as the five levels quality control at the CPC dataset (Chen. M, et al., 2008). It was found that the uncertainty, as measured by the standard deviation of annual precipitation errors, had the highest values in the CPC dataset for most of the basins. This result agrees with the finds of Rozante et al. (2010), when comparing the performance of TRMM-MERGE product with the gauge based product OBS90, showing a superior quality of the MERGE product over the gauge based product. When the precipitation data sources were combined, the new dataset displayed remarkably similar annual uncertainty to the one evaluated from the source which had the smallest standard deviation values. However, the uncertainty variability among the river basins was reduced in the combined dataset and became more similar to the one displayed by the reference, non-real time MSWEP precipitation dataset. This result is in line with results obtained by Beck at al. (2017), when comparing the results of a merged areal product based on satellite, rain gauge and reanalysis found a superior quality of the observations against the other individual sources.

The data source presenting the lower standard deviation of annual precipitation errors is usually the one with the higher weight when combining the daily precipitation data. Due the fact of the method proposed blends the precipitation in a daily time step, and in a basin scale, the reduction of the annual uncertainty is captured at the shorter time scales. In several cases, large errors of each data source were smoothed during the combination process, and the resultant precipitation dataset displayed lower standard deviation of annual precipitation errors for 15 of the 41 basins. However, in a daily scale, where the hydrological models are calibrated and validated, the performance is better for almost all basins, reflecting a lower uncertainty also in a daily time step.

These results are the first indication that the combination of the different sources of data can lead to a precipitation forcing dataset that is more robust and display lower uncertainty in different time scales. This is relevant because lower uncertainty can result in better and more robust calibration of the hydrological model, with fewer differences in performance of flow simulations when comparing validation and calibration periods. Robustness in hydrological modelling is crucial for real time flow forecasting, when future events that were not experienced in the past, and hence were not included in the model calibration process, might occur and generate extreme situations of interest for hydrological risk and water resources management.

When calibrating the hydrological models, we generated nine simulations, three for each precipitation forcing (TRMM-MERGE, CPC, and their combination). Following the traditional split-sample test, there were two calibration-validation procedures applied each to half of the sample. Additionally, one calibration covered the entire data period of almost twenty years. The results were evaluated using performance indicators (NSE, KGE, MAE, and R^2) and it was shown that, for most of the basins, the results in terms of performance of simulated flows are similar among the different periods. This enabled the use of the hydrological model as a tool for the selection and validation of the precipitation datasets, including the combined precipitation dataset. Such procedure is relevant to seasonal streamflow forecasting, since the traditional method of ESP (Ensemble streamflow prediction) for issuing reliable hydrological forecasts requires long series of homogeneous historic precipitation data available at real time or near-real time.

For the validation and selection of the best precipitation dataset, the model calibration over the complete period was used. Since the treatment of the model parameters uncertainty in not scope of this study, are not applied any treatment as the simulation and sampling based method (Monte Carlo) (Kuczera and Parent, 1998) or other. It is assumed that the application of the split sample test and the use of a long time series, to have the calibrations/validations can satisfactorily deal with the uncertainty of the parameters and bring parameters robust enough for the application, it is confirmed below, when we compare the performance results with other models. The combination of the two available precipitation sources showed the best performance for the majority of river basins in a daily time step. This result is in agreement with the conclusions drawn by Beck et al. (2017). The authors evaluated a large group of observed precipitation data sources and concluded that the combination of data sources into one reanalysis dataset provided better estimates of precipitation. The unique MSWEP (Multi-Source Weighted-Ensemble

Precipitation) dataset of global terrestrial precipitation dataset provides a high-resolution (daily and 3-hourly temporal and 0.1° spatial resolution) reanalysis dataset. While it was used in our study as a reference dataset to evaluate (and validate) the combined dataset built, its direct use for real time operations is not possible given the fact that this dataset it is not processed to be available in real time. Combined precipitation datasets are particularly useful when water managers have to operate over large areas, from tens to hundred square kilometers, and cannot compile different data sets in real time for each river basin under their management. The use of a unique and robust precipitation dataset is an asset in operational settings and continental-wide applications.

The performance results of this study can be compared with other large-scale model experiments in terms of overall performance. For the NSE criterion, our results show the performance is higher than 0.60 for 97% of the basins and the average NSE over the study area is 0.75. The KGE criterion is also higher than 0.60 for all basins and the average value is 0.77. The average coefficient of correlation is 0.67 for the study basins. Siqueira et al. (2018), using a distributed hydrological model (MGB) and the MSWEP data from Beck et al. (2017) as precipitation forcing, obtained NSE values for discharge and water levels higher than 0.60 for 55% of the studied cases and KGE values higher than 0.60 in 70% of the studied cases of streamflow simulation. According to the authors, the global models (WaterGap, LISFLOOD, and HTESSEL/CaMaFlood) showed more than 40% of the basins in South America with an NSE and a KGE lower than zero. When comparing the HEC-HMS models calibrated in this study with the other experiments realized in South America, we can see that the results and the performance of the HEC-HMS models are robust and sufficient for the next step of the study, which is the application of the combined precipitation dataset and the calibrated model for seasonal streamflow forecasting.

The combined precipitation dataset has a similar evolution of precipitation uncertainty (standard deviation of annual areal precipitation errors) as the reference MSWEP dataset, notably in the periods before late 1990s and early 2000s. The median values are however higher (generally, 1% higher), as well as the variability of standard deviation of annual areal precipitation errors among river basins. Although differences in median values are more important in the period 2005-2010, median values become comparable in the more recent period. Despite having more information available in the recent period, since satellite data is added to the TRMM-MERGE dataset, the uncertainty of the combined precipitation dataset is not reduced, as can be seen in the MSWEP

dataset, which presents a decrease in the variability of the standard deviation of the errors among the river basins in the period after 1998. These differences can be explained by the fact that the MSWEP dataset uses more information and more consistent data than real time datasets. Errors and inconsistencies are often present in real time datasets, such as the ones used to build the combined dataset in this study, so it is expected that this impacts the quality of the precipitation data. Despite these issues, an important aspect of the combined precipitation dataset is that it provides a more homogeneous dataset over the region, since no regions in the study area displayed specific patterns of errors. Patterns were identified previously in the CPC and TRMM-MERGE precipitation datasets (Reis et al., 2019), with differences between the datasets growing toward the northwest of Brazil. After the combination of the datasets, the uncertainty did not show any clear dependency on the spatial location of the river basins.

The TRMM-MERGE data-set used in this study was discontinued in May 2020, and now CPTEC provide a merge product called GPM-MERGE, based on the GPM satellite product which uses the new IMERGE retrieval algorithm which "fuses the early precipitation estimates collected during the operation of the TRMM satellite (2000 - 2015) with more recent precipitation estimates collected during operation of the GPM satellite (2014 - present) (Rozante et al., 2018, Skofronik-Jackson et al., 2018). The new CPTEC GPM-MERGE dataset, maintain the same gage stations used at the TRMM-MERGE product and the same MERG algorithm (Rozante et al., 2010), which give privilege of the station data over the satellite information (Rozante et al., 2020), According Rozante et al. (2018), in a study comparing the old product the TMPA-V7, based on the TRMM mission, with the new products IMERGE and the GSMaP-G from JAXA, they found that the IMERG-E and TMPA-V7 show a similar behavior in terms of Critical success index - CSI, Adjusted Equitable Threat Score - ETS, Probability of Detection - POD, False Alarm Ratio - FAR and Bias, with a better performance for IMERGE. These characteristics makes the new GPM-MERGE the natural substitute of the discontinued TRMM-MERGE, with similar behavior, but with a better performance and higher resolution of 0.1° x 0.1°. Therefore, due the similarity of the both products we believe the results obtained at this research with the TRMM-MERGE, still valid with the use of the new GPM-MERGE available after May of 2020.

The MSWEP (Beck et al., 2019) dataset used at this study, as benchmark, is the V2.2 daily precipitation data, with 0.1° special resolution, the MSWEP is in constant evolution and now is in the version 2.8, with the daily and 3 hourly time resolution and with the same spatial resolution, but the complete version still not in real time, due the latency of some of the products used

(MSWEP, 2021). However, this latency is reducing year after year, and we believe in the next years we will have some new real time products, adding these new products with high quality we believe it is possible to improve even more the results obtained until this moment of the research.

3.5 CONCLUSIONS

At this chapter, we access real-time precipitation datasets in an area with different weather patterns, as the convective storms at the Amazon region, the South America monsoon system responsible for the precipitations at the center area of the continent, the semi-arid weather at the north-east region, and the subtropical weather at the south region, we worked with a variety of basin sizes since 9300 km² until 382000 km², to have a good representation of the region for hydrological modeling.

A sequence of steps was described that can be used to blend different real-time precipitation datasets, validate the results, and obtain a better near real-time observed precipitation forcing dataset for Brazilian river basins, with a long historical period to be used in future studies of streamflow forecasting. The main conclusion of this study is that a combination of existing precipitation datasets, weighted by the annual uncertainty of each original source, in a basin scale, reduces the uncertainty in a yearly basis, adapting the proportion of the precipitation sources for the characteristics of each basin and its specific weather. This yearly uncertainty reduction is potentialized when we analyze it in daily scale, the hydrological modeling demonstrate that this approach is able captures the quality control and intelligence behind the individual dataset, giving better results in terms of daily hydrological simulation than the performance of each source running individually. Therefore, providing a more trustworthy precipitation dataset also with a lower daily uncertainty.

A drawback of combining data sources is the fact that datasets are often not available for the same period. In this study, we show that a possible practical solution is to extend the period of the combined precipitation dataset to cover the longest possible period, given the original datasets, by using the double-mass curve correlation. The validation of such extension is illustrated also using a hydrological model. The model allows users to evaluate, in terms of simulated discharges, if the performance of a precipitation dataset in the extended period, where not all data sources are available, remains similar and consistent to the one in the original period, where all data sources were available to build the combined precipitation dataset. Hydrological modeling proved to be a useful tool to evaluate the performance of different sources of

precipitation data, as also suggested recently by Levy et al. (2017), who highlighted the importance of the problem of “data selection uncertainty” when analyzing nine datasets in Brazil..

Finally, a comparison of the combined precipitation with the reference MSWEP, our benchmark dataset, showed that the combined dataset obtained in this study has a level of uncertainty compatible with the benchmark and can be potentially useful for real time seasonal streamflow forecasting. The examples of simulated flows showed that the calibrated models can correctly represent the long-term flow variations in different regions and climates in the study area. The areal precipitation products are reducing the latency and probably on the next years, will be possible to add new real time datasets and combine them, with potential to improve even more the results obtained until this moment.

This study is limited to basins with big dimensions, higher than 9000 km², where a daily simulation makes sense and for the South America region, where the TRMM-MERGE (after 2020 is GPM-MERGE) is available. For other regions, the method is applicable for the local products available, being necessary to evaluate the local results. For small basins, where hourly simulations are necessary, this approach also can be used to blend ground radar dataset, rain gauge data and satellite precipitation. But is necessary to compare with other merge algorithms and compare the hydrological results at this shorter time step.

CHAPTER 4:

THE QUALITY OF SEASONAL PRECIPITATION AND STREAMFLOW FORECASTS IN BRAZIL OVER A LARGE SET OF RIVER BASINS

This chapter will be submitted as a paper to HESS - *Hydrology and Earth System Sciences Journal*, with the following co-authors: REIS. A. A.; RAMOS. M. H.; WETTERHALL. F.; WEERTS. A.; FERNANDES. W. S.

4 THE QUALITY OF SEASONAL PRECIPITATION AND STREAMFLOW FORECASTS IN BRAZIL OVER A LARGE SET OF RIVER BASINS

4.1 INTRODUCTION

The optimal management of water resources is of great importance for many human activities. This is especially true in Brazil, where the majority of the electricity production comes from hydraulic sources (hydropower reservoirs and run-of-the river power plants). The Brazilian electric system is essentially hydrothermal, with hydraulic generation being responsible for approximately 67% of the electricity generation (EPE, 2019). With the increasing use of other renewable, but intermittent, sources of energy, such as wind and solar power, the role of hydropower plants (HPPs) is also becoming more relevant in terms of maintaining the stability of the interconnected power grid system, given their capacity to respond quickly under load variations (Schmidt et al., 2016).

In Brazil, hydropower generation takes advantage of the diversity of climatic regions and the complementarity of seasonal river flows, as the rainy season occurs in different periods of the year from northern to southern parts of Brazil (ONS, 2016). Planning hydropower generation is therefore intrinsically related to predicting future river flows and seasonal inflows to reservoirs. The inflows to HPPs play a role in the planning of the electrical system operation as well as influence the energy price setting in the short-term market. Errors in the forecasts, for instance, can lead to the activation of thermal power plants in the wrong moment, increasing the prices of energy and also air pollution.

Traditionally, seasonal climate and hydrological forecasts can benefit from the prediction of large-scale climate indexes (ENSO, NAO, etc.). For instance, Rimbu et al., (2005) use correlations with the SST (Sea Surface Temperature) for the seasonal forecasting of river flows in the Danube river basin; studies of droughts in the Amazon region have shown the usefulness of correlating the SST of the ENSO region to forecast the severe periods of low precipitation and high temperature (Lima and AghaKouchak, 2017); studies in Africa have explored the use of SST-based statistical indices in prediction models for precipitation forecast (Bahaga et al., 2019). In hydrology, an alternative approach is the ESP (Ensemble Streamflow Prediction) method (Twedt et al., 1977; Day, 1985; Wood and Lettenmaier, 2006). It is a well-established technique to generate an ensemble of possible future scenarios of streamflow several weeks and months

ahead. The method is based on using a continuous hydrological model to estimate initial hydrologic conditions (using real-time meteorological data as input) and future meteorological forecasts based on historical sequences of meteorological data from past years to obtain streamflow predictions (see, for example, Crochemore et al., 2016; Anghileri et al., 2016; Beckers et al., 2016; Bennett et al., 2017; Arnal et al., 2017; Prudhomme et al., 2017; Harrigan et al., 2018). The ESP method is widely used alone or, in some cases, in combination with large-scale climate indexes or information coming from a GCM (General Circulation Model) (e.g., Crochemore et al. 2017 and references therein).

With the increase in computational capacity, GCMs are constantly evolving, improving their spatial and temporal resolutions, incorporating new internal elements of the dynamics of precipitation formation, and moving from deterministic to probabilistic models, with the representation of scenarios generated from perturbations of the initial conditions (ECMWF, 2015). Increasingly, GCM predictions have been used to provide global precipitation predictions (Zhao et al. 2020), and sometimes also input to hydrological models to generate global river flow predictions (Emerton et al., 2018) several months ahead. The system SEAS5 is the latest generation of the operational seasonal forecasting system of the European Centre for Medium-Range Weather Forecasts (ECMWF). Since its introduction in November 2017, some studies have been carried out to investigate the performance of the model's raw and bias corrected predictions in different regions of the world (e.g. Johnson et al., 2019; Ratri et al., 2019; Sánchez-García et al., 2019). Recently, Gubler et al. (2020) evaluated the performance of ECMWF SEAS5 over South America by investigating the quality of 3-monthly means of categorical forecasts of temperature and precipitation when compared against homogenized ground meteorological station data. The authors show that the dynamical SEAS5 predictions outperform statistical predictions based on a regionally-adapted ENSO index in most of the region, with lower performance observed for precipitation than for temperature. They also highlight the strong variability in space and time of the performance of precipitation predictions as well as the influence of quality problems detected in the observation ground data. Both aspects make it difficult to identify patterns of the SEAS5 prediction performance, although the authors suggest that SEAS5 predictions are reliable enough to be usefully applied in many regions in South America.

In Brazil, diverse patterns of weather and climate governed by large-scale climate phenomena can be found (Garreaud et al.,2009), such as the South America monsoon system responsible for

high amounts of precipitation in the south-east and central-west regions in Brazil (Ferreira and Gan, 2011), the tropical weather at the Amazon region with intense convective storms (Garreaud et al.,2009), and the semi-arid weather at the northeast region (Tinôco et al., 2018). Although these weather patterns are marked by a clear precipitation seasonality, patterns with no seasonality, i.e., presenting wet and dry periods in any month of the year, can also be found in the subtropical weather in the south region (Garreaud et al.,2009). This diversity brings challenges for reliably predicting precipitation and river flows months ahead, and raises the question of which approach performs better when it comes to a user that has to issue predictions over a large set of river basins that are spread all over the country, such as hydropower water managers.

The use of statistical approaches to predict precipitation in southern Brazil has shown good results for the extreme terciles (Viana and Sansigolo, 2016). A recent study has shown good performance for precipitation and temperature predictions from dynamical models, and, particularly, the added value of nesting regional climate models (RegCM4) with global models (CPTEC and CFSv2) to reduce prediction biases (Reboita at al., 2017). Biases and uncertainties in long-term precipitation predictions impact river flow forecasts and influence also the decisions on which approach should be used for seasonal hydrological prediction. Pilz et al. (2019) compared the performance of a statistical model with the performance of a process-based hydrological model (forced by meteorological hindcasts of the GCM ECHAM4.6, downscaled using empirical quantile mapping; Delgado et al., 2018) to forecast reservoir levels and droughts in the semi-arid northeast of Brazil. They concluded that statistical methods can perform well at regionally and monthly aggregated scales, but process-based methods (dynamical approaches using climate and hydrological models) are better when applications concern finer spatial and temporal scales, such as reservoir inflow forecasting.

In seasonal hydrological prediction, the ESP approach, which uses hydrological models without climate models, may not be a good reference for water management when, depending on the period of the year, the climate forcing dominates the variability of the river flows over the hydrologic initial conditions, reducing the prediction capacity of the model (Shukla and Lettenmaier, 2011). In this case, the use of climate models, together with hydrological models, is an asset. This, however, introduces an additional source of uncertainty and can hence also introduce systematic biases in the predictions. In order to remove biases, it is generally useful to apply bias correction (BC) techniques or statistical postprocessors to correct the raw climate

forecasts (e.g., Verkade, 2015; Zhao et al., 2017). Crochemore et al. (2016) compared eight simple bias correction methods to correct precipitation seasonal forecasts (ECMWF SEAS4) and investigated how they affect the skill of streamflow forecasts over catchments in France that displayed a pluvial regime. The study showed that the empirical distribution mapping of daily values calibrated for each calendar month (EDMD-m) was particularly efficient for increasing the reliability of precipitation and streamflow forecasts, while linear scaling (LS-m) led to higher improvements in sharpness and accuracy. When looking at all monthly lead times of the forecast range, they also observed that the biases vary more with the calendar month of the forecast horizon than with the lead time. In Norway, Gudmundsson et al. (2012) compared a group of statistical transformations to correct the precipitation bias from the HIRHAM RCM forced with the ERA40 reanalysis and classified them into (1) distribution-derived transformations, (2) parametric transformations, and (3) nonparametric transformations, each differing with respect to the underlying assumptions. The methods included distribution mapping based on fitted theoretical or empirical distributions and linear scaling. The study highlighted the differences between the bias corrections and the necessity of testing methods prior to their application. The authors recommended using nonparametric methods because these methods were the most effective in reducing the bias and did not require any approximations of the empirical distributions.

To our knowledge, similar studies at the catchments scale have not yet been carried out in Brazil. The aim of this paper is to investigate the quality of seasonal precipitation forecasts (from SEAS5 ECMWF) and seasonal streamflow forecasts in Brazil over a large sample of river basins. Our goal is to gain insights on the quality of forecasts when using SEAS5 forecasts to drive a hydrological model and issue reservoir inflow forecasts for the operation of reservoirs that accommodate multiple uses, including hydropower and flood control. More recently, in Brazil, the hydrological modeling of river inflows to HPPs has been moving from a deterministic to a probabilistic approach using ensemble forecasting (ONS, 2019). However, this approach is still incipient and acquiring knowledge on the quality of seasonal ensemble predictions is crucial to guide the choice of techniques, data and approaches. With this context in mind, our objective is to answer to the following scientific questions: i) How do the precipitation forecasts from the SEAS5 ECMWF forecasting model perform in the Brazilian context of large river basins? i) Can the application of bias correction techniques improve the accuracy and the reliability of the precipitation forecasts for the Brazilian basins? iii) How does the precipitation bias correction reflect on the quality of the streamflow forecasts?

In Section 4.2, the methodology and dataset used are presented. In Section 4.3, the results obtained are provided. Section 4.4 is a discussion of the results, and the conclusions and planned future studies are presented in Section 4.5.

4.2 MATERIALS AND METHODS

4.2.1 River basins and observed hydrometeorological data

The study area covers a large part of Brazil and parts of some neighboring countries in South America. It comprises 41 river basins, associated with 30 hydropower dams and HPPs of high importance for hydroelectric generation in Brazil. The basins display different climates and land uses, and have areas varying from 9,300 to 382,000 km². Figure 1 illustrates the study area, with the basins delimited in red and the groups (G1 to G8) with similar climatic and flow behavior delimited in black dashed lines.

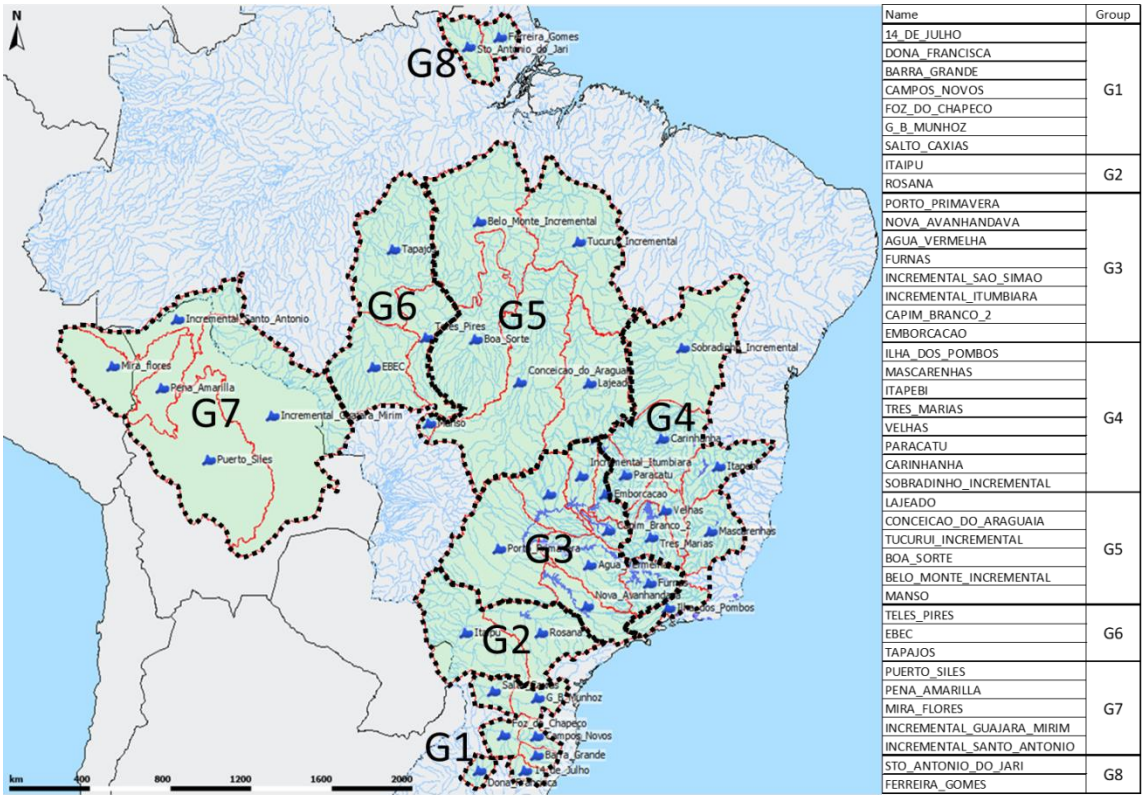

Name	Group
14_DE_JULHO	G1
DONA_FRANCISCA	
BARRA_GRANDE	
CAMPOS_NOVOS	
FOZ_DO_CHAPECO	
G_B_MUNHOZ	
SALTO_CAXIAS	
ITAIPU	G2
ROSANA	
PORTO_PRIMAVERA	G3
NOVA_AVANHANDAVA	
AGUA_VERMELHA	
FURNAS	
INCREMENTAL_SAO_SIMAO	
INCREMENTAL_ITUMBIARA	
CAPIM_BRANCO_2	
EMBORCACAO	
ILHA_DOS_POMBOS	G4
MASCARENHAS	
ITAPEBI	
TRES_MARIAS	
VELHAS	
PARACATU	
CARINHANHA	
SOBRADINHO_INCREMENTAL	
LAJEADO	G5
CONCEICAO_DO_ARAGUAIA	
TUCURUI_INCREMENTAL	
BOA_SORTE	
BELO_MONTE_INCREMENTAL	
MANSO	
TELES_PIRES	G6
EBEC	
TAPAJOS	
PUERTO_SILES	G7
PENA_AMARILLA	
MIRA_FLORES	
INCREMENTAL_GUAJARA_MIRIM	
INCREMENTAL_SANTO_ANTONIO	
STO_ANTONIO_DO_JARI	G8
FERREIRA_GOMES	

Figure 4.1– Spatial distribution of the river basins, with the HPP basins delimited in red and the groups (G1 to G8) with similar climatic and flow behavior in black dashed lines.

Discharge data come from the ONS, the national operator of the electric system in Brazil. They are the natural flow time series for HPPs in Brazil. Actual flow is naturalized for each reservoir by the ONS by considering the regularization effects of the reservoirs and adding evaporation

and other water uses to obtain the natural flow time series of each reservoir (for more details, see ONS, 2005).

The observed precipitation data are a blend of the TRMM-MERGE dataset, a real-time data provided by the CPTEC/INPE Meteorological Center of Brazil on a daily basis with 0.25° grid resolution (Rozante et al. 2010, Hufman, 2017; Harrigan et al., 2018), and the CPC dataset, which provides real-time observed data from the U.S. National Oceanic and Atmospheric Administration Climate Prediction Center, with 1° grid resolution and on a daily basis (Mingyue et al., 2008). These datasets were combined by merging the two sources, for each basin, weighted by the uncertainty of each dataset, based on the standard deviation of the errors of the observed precipitation versus the empirical function of annual flow and yearly precipitation (Reis et al., 2019; Reis et al., 2021, submitted). This combination makes it possible to smooth the errors inherent in each source, producing more-trustworthy information (see Chapter 3).

4.2.2 SEAS5 ECMWF precipitation forecasts

ECMWF long-range forecasting system SEAS5 is based on a coupled ocean–atmosphere model. It consists of an ocean analysis system to estimate the initial state of the ocean, a global coupled ocean–atmosphere general circulation model to calculate the evolution of the ocean and the atmosphere, and a post-processing suite to create forecast products from the raw numerical output. Compared to its predecessor, System 4, the vertical and horizontal resolutions were increased and new physical modules were added to improve the ocean model,. The atmosphere model is based on the new ECMWF Integrated Forecast System (IFS), which was introduced in the medium-range forecasting system in November 2016. In SEAS5, some parameterizations and forcing are different from the IFS to better represent the processes that most affect the seasonal forecasting skill (ECMWF, 2017).

The real-time seasonal forecast system SEAS5 consists of a 51-member ensemble with a seven-month forecasting horizon. The ensemble is created using a combination of sea surface temperature, atmospheric initial condition perturbations, and the activation of stochastic physics. The stochastic physics settings are identical to those used in the medium-range ensemble forecast (ECMWF, 2017). The EMCWF SEAS5 is initialized every first of the month. Hindcasts are available from 1981 to 2016, on a daily basis, with an ensemble of 25 members and a spatial resolution of 0.4°. These data are made available to users to allow them to analyze the

performance of the systems and to calibrate the bias correction methods to be applied to the real-time forecasts.

4.2.3 Precipitation bias correction methods

Were investigated two methods for bias correction (BC) of the precipitation forecasts from ECMWF SEAS5: LS – linear scaling and QM – quantile mapping.

The LS is a simpler method, and consists of correcting the monthly mean values of the forecasts to match the monthly mean values of the observations (Teutschbein and Seibert, 2013). A scaling factor is calculated considering the ratio between the observed and forecast (ensemble median in this study) values. The scaling factor obtained through calibration, for each month, location and lead time, is then applied as a multiplicative factor to correct daily precipitation forecasts in each basin and for each forecast ensemble member.

The QM is a more-sophisticated method, classified as distribution-derived transformation (Déqué et al., 2007; Block et al., 2009; Piani et al., 2010; Johnson and Sharma, 2011; Sun et al., 2011; Kim et al., 2016). It involves correcting the precipitation forecasts so that their statistical distribution becomes closer to the statistical distribution of the observations. There are several ways to adjust the forecast and observed distributions or quantiles, and existing techniques mainly differ in terms of how the cumulative distribution functions (CDFs) are considered (Crochemore et al., 2016). In this study, the empirical CDFs (ECDFs) are used to build the probability distributions of the observed and forecast datasets. Then, the functions are used to make the ECDF of the forecast ensemble match the observed ECDF. The correction function is a nonlinear equation with the parameters calibrated for each location, month, and lead time.

In both BC techniques, the correction is a transformation function of the raw forecast precipitation, with parameters calibrated from the use of hindcasts and observed precipitation. The methods are applied on areal precipitation at each basin. The parameters are dependent on the location, month, and lead time.

$$BCPF_{\alpha,\beta,\gamma} = f\left(RawPF_{\alpha,\beta,\gamma}\right) \qquad (4.1)$$

where $BCPF_{\alpha,\beta,\gamma}$ is the bias-corrected daily precipitation forecast and $RawPF_{\alpha,\beta,\gamma}$ is the raw daily precipitation forecast at the α location, β month, and γ lead-time.

4.2.4 Quality assessment of precipitation and flow forecasts

Evaluation through a precipitation perspective

The SEAS5 reforecast dataset (section 4.2.2) and the combined observed precipitation dataset (section 4.2.1) were used to evaluate the performance of areal precipitation forecasts over the river basins. Firstly, the raw forecasts were used to extract the mean precipitation for each of the 41 studied basins. Metrics were used to evaluate how well the forecasts matched the observed precipitation in terms of reliability, resolution, correlation, the error of the median of the ensemble and overall performance (see below). All metrics were calculated using monthly precipitation values and forecasts were compared against the combined observed precipitation dataset. This evaluation of raw forecasts allowed us to identify patterns of performance and biases. Secondly, the BC methods LS and QM (section 4.2.3) were applied to investigate how these techniques can improve forecast performance and determine which technique is more efficient according to each metric analyzed.

Evaluation through a hydrologic perspective

The model used to generate the hydrological forecasts was the HEC-HMS, provided by the Hydrologic Engineering Center of the U.S. Army Corp of Engineers (https://www.hec.usace.army.mil/software/hec-hms/). It is a flexible and user-friendly hydrological model, which includes several hydrologic rainfall-runoff functions such as infiltration, unit hydrographs, and hydrologic routing. The configuration applied in this study uses a soil moisture accounting function to account for infiltration losses and evaluate excess precipitation. The transformation into surface runoff uses the Clark unit hydrograph (Kull and Feldman, 1998), and the Linear Reservoir method is used to represent baseflow (Feldman, 2000; Scharffenberg, 2016). The models for the 30 HPPs were built in a lumped mode, considering hydrologic homogeneous regions. Where the climate or land uses are very different, the basin was divided in sub-basins, which resulted in the 41 basins considered in this study (section 4.2.1). The calibration of the model was performed at a daily time step for the period 1998–2017, using the combined precipitation dataset as observed precipitation and observed flow data. Once the models were calibrated, we ran all the ensemble members of the SEAS5 seasonal precipitation forecast for all the basins using the DELFT FEWS-CEMIG system (Werner et al., 2006; Werner et al., 2013; Schwanenberg et al., 2015; Gibertoni et al., 2017). The ensemble seasonal precipitation forecast is used as input to the models, and the flow forecasts are obtained for all

basins to assess their performance. Similar to the precipitation analysis, the daily flows obtained are aggregated in monthly flows. They were analyzed with the same metrics (see below) and up to seven months of forecast horizon. Flow forecasts were compared against the simulated flows (obtained using the combined observed precipitation dataset as input to the hydrological model) in order to check exactly the effect of the precipitation bias correction at the flows.

Metrics for forecast quality evaluation

To assess the performance of the monthly-aggregated forecasts, the ensemble verification system (Brown et al., 2010) was used. The metrics presented below were calculated.

To analyze the overall performance of the forecasts, we used the CRPS – Continuous Rank Probability Score (Hersbach, 2000). It measures the integrated square difference between the cumulative distribution function (CDF) of the forecast variable, $P_i(x)$, and the corresponding CDF of the observed variable, $H(x - y_i)$. In practice, the CRPS is averaged over a number of cases (pairs of forecast-observation in the time series):

$$\text{CRPSi} = \int_{-\infty}^{\infty} [P_i(x) - H(x - y_i)]^2 \, \text{dx} \qquad (4.2)$$

$$\overline{CRPS} = \frac{1}{M} \sum_{i=1}^{M} \text{CRPS}\, i \qquad (4.3)$$

where $P_i(x)$ is the predictive distribution at time step i, $H(x - y_i)$ is a step function that assumes a probability of 1 for values of the forecast greater than or equal to the observation y_i, and zero otherwise, and M is the number of pairs of forecast-observation.

To assess the accuracy of the forecasts, we used the RME - Relative Mean Error. It measures the mean difference between a set of forecasts and the corresponding observations, divided by the mean of the observations. A positive RME implies overestimation and a negative RME, an underestimation.

$$RME = \frac{\sum_{i=1}^{n} (\bar{Y}_i - x_i)}{\sum_{i=1}^{n} x_i} \qquad (4.4)$$

where $\bar{Y}_i$ is the mean forecast at time step *i*, x_i is observation, and *n* is the number of pairs of forecast-observation.

In terms of reliability, we used the decomposition of the BS – Brier Score (Murph, 1973). The BS measures the average squared probability error of probability forecasts, and is applicable to a set of mutually exclusive discrete outcomes or classes (Brier, 1950). It can be decomposed into three terms: reliability, resolution and uncertainty. The reliability term (BS_{rel}) measures how close the predicted probabilities are to the true probabilities, given that forecast. If the reliability is 0, the forecast is perfectly reliable.

$$BS_{rel} = \frac{1}{N}\sum_{k=1}^{K} n_k \, (f_k - \bar{o}_k)^2 \qquad (4.5)$$

where N is the number of forecast-observation pairs, n_k is the number of forecasts with the same probability category k , $\bar{o}_k$ is the observed frequency (actual outcome: 0 if it does not happen and 1 if it does happen) and f_k is the forecast probability (based on the percentage of ensemble members).

To evaluate the degree to which forecasts can separate different situations, we used the resolution term of the decomposed Brier Score (Murph, 1973). The resolution term (BS_{res}) measures how much the conditional probabilities given the different forecasts differ from the sample climatology. The higher the resolution term is (the closer to 1), the better (i.e., the ensemble forecast has resolution enough to produce very high and very low probability forecasts). When the forecasts always give the climatological frequency as forecast, the resolution term is zero (i.e., ensemble forecasts with low resolution) (Murphy 1996).

$$BS_{res} = \frac{1}{N}\sum_{k=1}^{kK} n_k \, (\bar{o}_k - \bar{o})^2 \qquad (4.6)$$

$$\bar{o} = \sum_{t=1}^{N} \frac{o_t}{N} \qquad (4.7)$$

where N is the number of forecast-observation pairs, n_k is the number of forecasts with the same probability category k , $\bar{o}_k$ is the observed frequency (actual outcome: 0 if it does not happen and 1 if it does happen) and $\bar{o}$ is the observed frequency of the event (sample climatology).

To measure the strength of the relationship between the observed data and the median values of the ensemble forecasts, we used the Correlation Coefficient (r), where values close to 1 denotes a strong linear correlation between forecasts and observations.

$$r = \frac{Cov(x,\bar{Y})}{\sigma(x)\sigma(\bar{Y})} \quad (4.8)$$

where $Cov(x,\bar{Y})$ is the sample covariance between $\bar{Y}$, the median of the members of the ensemble forecasts and x, the corresponding observations, $\sigma(x)$ is the standard deviation of the observations and $\sigma(\bar{Y})$ is the standard deviation of the forecasts.

Finally, to assess the capacity of the ECMWF SEAS5 system to forecast low-precipitation periods during the wet season, we calculated the probability of detection (PD), i.e., the probability of precipitation values below the average precipitation for each basin, month, and lead time. The PD is the ratio between the number of hits (observed and forecast events) and the number of observed events (forecast and missed events). It ranges from zero to one; one represents a perfect score. We considered two levels of detection: the system's capacity to detect values below the average, and the system's capacity to detect droughts, defined as values below the third quartile of exceedance (value below which 75 % of the observed values are situated). This threshold is the same considered by Sant'Anna Neto (1990) for Brazilian basins.

Skill scores were used when comparing the ensemble forecast system against a reference forecast. In the case of precipitation forecasts, the climatology of the combined precipitation dataset (Reis et al., 2021, submitted) was used as a reference forecast to benchmark the performance of the ECMWF SEAS5 precipitation forecasts. For the streamflow forecasts the reference was the simulated flows. Skill scores were calculated according to the following equation:

$$Skill\ Score = \frac{Score_{forecast} - Score_{reference}}{Score_{perfect} - Score_{reference}} \quad (4.9)$$

4.3 RESULTS

4.3.1 How raw precipitation forecast skill varies over climatic zones and seasons

Figure 4.2 shows the maps for the metric RME of the median raw catchment precipitation forecasts of the ensemble ECMWF SEAS5 (period 1981-2016), for the lead-times 1, 4 and 7

months, and for the wet (October, November, and December – OND, and January, February, and March - JFM) and dry (April, May, and June – AMJ, and July, August, and September - JAS) seasons. We can see that forecast performance depends more on the season of the year than lead-time. For the same season, catchment precipitation forecasts show the same tendencies of overestimation (positive RME) or underestimation (negative RME) along the forecast horizon.

During the wet seasons (OND and JFM), a great part of the basins, represented by the groups G1 to G3, the south part of group G4 and group G7, show forecasts that tend to overestimate the observations, while the basins in the north and northeast region (groups G5 and G8 and part of groups G4 and G6) show a tendency towards underestimation, especially for the trimester OND. During the period JFM, the number of basins with overestimation increases, and, at longer lead-times, only basins from group G8 and part of G5 and G6 still present an underestimation tendency.

During the drier months AMJ and JAS, when the basins from groups G2 to G7 receive very low amounts of precipitation, it is possible to see a generalized underestimation tendency, with exception of the basins from group G7, Madeira river, where forecasts tend to overestimate the observations. For all seasons, it is also possible to see that the intensity of the underestimation increases to the northeast direction. For the basins from group G1, where there is no precipitation seasonality, with possibility of both below-average precipitation and severe precipitation periods during AMJ, the underestimation persists along this semester.

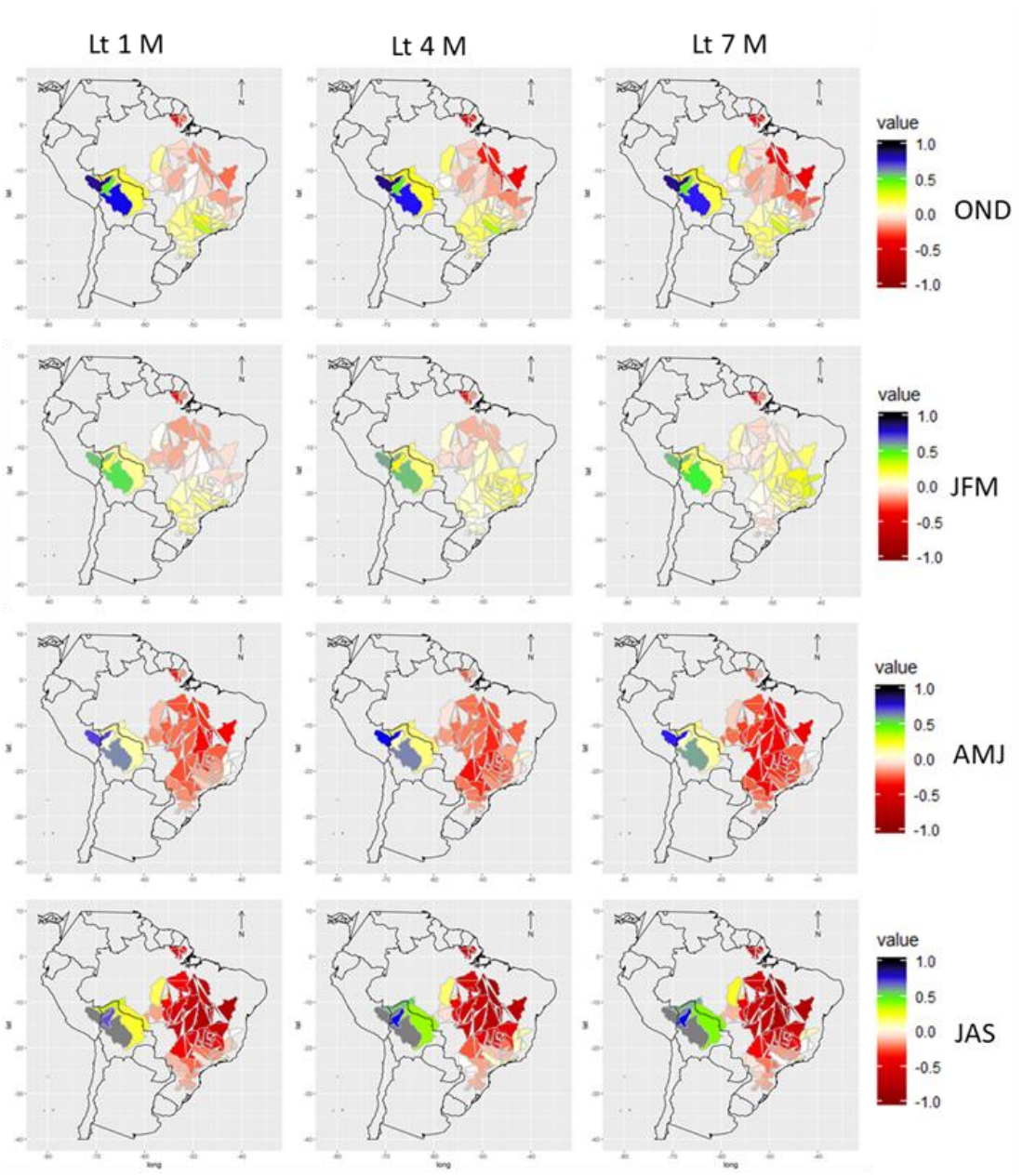

Figure 4.2 – RME of the median raw catchment precipitation forecast of the ensemble ECMWF SEAS5 (period 1981-2016), for the lead-times 1, 4 and 7 months, and the wet (OND and JFM), and dry (AMJ and JAS) seasons.

Figure 4.3 shows the bias (forecast ensemble median/observed precipitation; Mbias) evaluated over monthly totals of the raw catchment precipitation forecasts of ECMWF SEAS5. Months are represented by the numbers 01 (January) to 12 (December) and for all seven lead times. To visualize the patterns more clearly, the basins were grouped by similarity of behavior and climate (groups G1 to G8). For most of the basins, the monthly bias presents a clear seasonal pattern with an overestimation (Mbias greater than 1, in blue) for most of the months during the rainy season of each group and an underestimation (Mbias smaller than 1, in red) during the low precipitation period, independent of the lead time. The exceptions are the Madeira River basin (group G7),

where the forecasts present an overestimation bias in all months, and the two basins above the equator line (group G8), where the opposite behavior is found, with an underestimation forecast bias observed year-round.

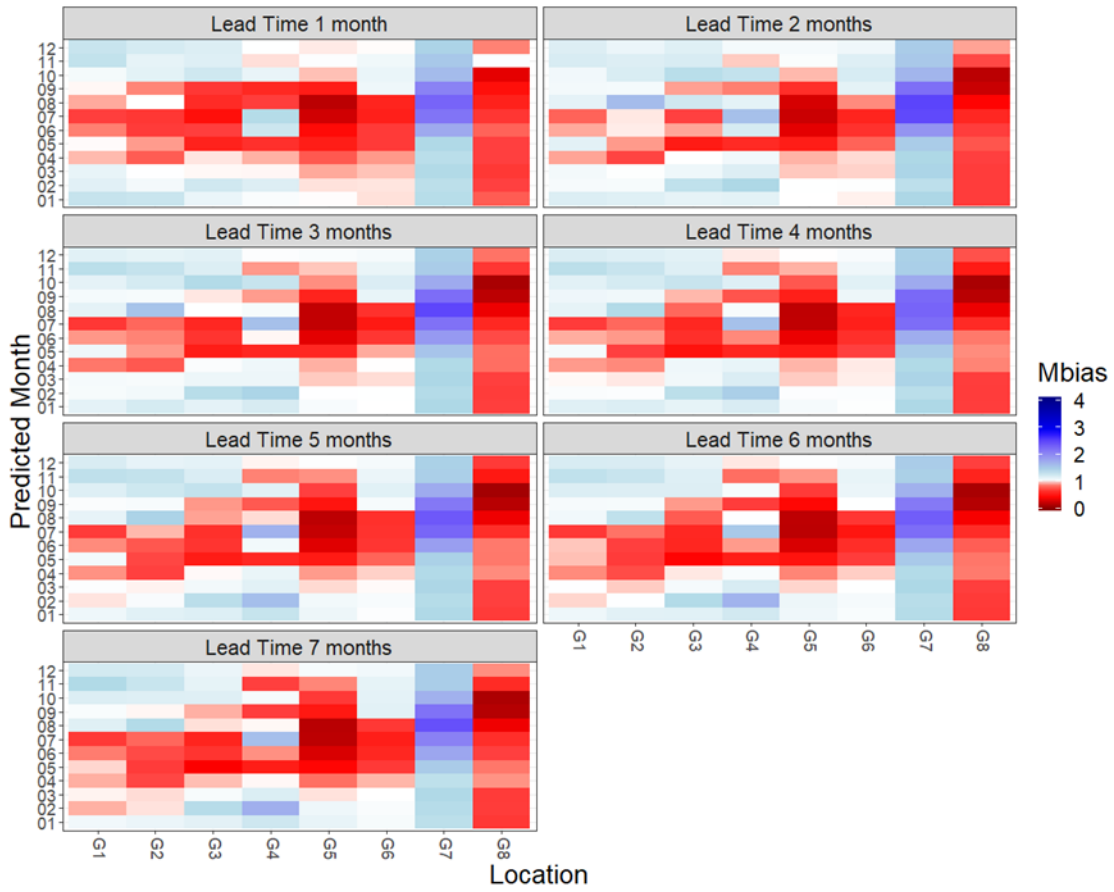

Figure 4.3 – Monthly bias (Mbias) of the median raw catchment precipitation forecasts of the ensemble ECMWF SEAS5 (period 1981-2016), for lead-times 1 to 7 months, for each calendar month (vertical axis) and the 8 groups (G1 to G8, horizontal axis; see Figure 4.1) of river basins (blue indicates forecast overestimation and red, underestimation).

Figure 4.4 shows a group of heat graphs for the metrics CRPSS, correlation coefficient, resolution (BS_{res}), and reliability (BS_{rel}). The graphs are separated by trimester from wet to dry season (OND, JFM, AMJ, and JAS) and for each lead-time (1 to 7 months).

In terms of overall performance (CRPS Skill score, CRPSS), the results shows that the raw precipitation forecasts present a performance superior to the climatology for the first month at most of the basins in all seasons; the exceptions are the basins from groups G7 and G8, which shows a poor performance in all seasons at almost all lead times. For the basins in the south region (G1 and G2), performance decreases from the second month, and become worse than the climatology until the last month of the forecast horizon (month 7). For the other basins (G3, G4,

G5, and G6), the forecasts are better than the climatology in all lead-times for almost all seasons; the exception is JFM, the trimester most difficult to forecast, where forecasts are skillful only in the first month lead-time.

The results for the correlation coefficient show that the basins of the south region (G1 and G2) have a good performance only at the first month of lead time, with R^2 values higher than 0.5. For the trimester OND, the basins from groups G3 to G8 present values higher than 0.6 at all forecast horizons. On the other hand, the trimester JFM only shows good performance at the first month; from the second month ahead there is practically no correlation between precipitation forecasts and observations.

In terms of resolution, the forecasts present lower values (better performance) only at the first month, losing resolution as lead time increases. The trimester JFM is clearly the most difficult to forecast, with a low resolution of the ensemble forecasts from the second month onwards in all basins (BS-SHA closer to zero).

Concerning reliability, the worse results appear in almost all lead times for the basins of the groups G7 and G8, with values far from zero (best score). For the other basins, the best values are around 0.03 and 0.1, and better performance is seem at the first two months of forecast horizon.

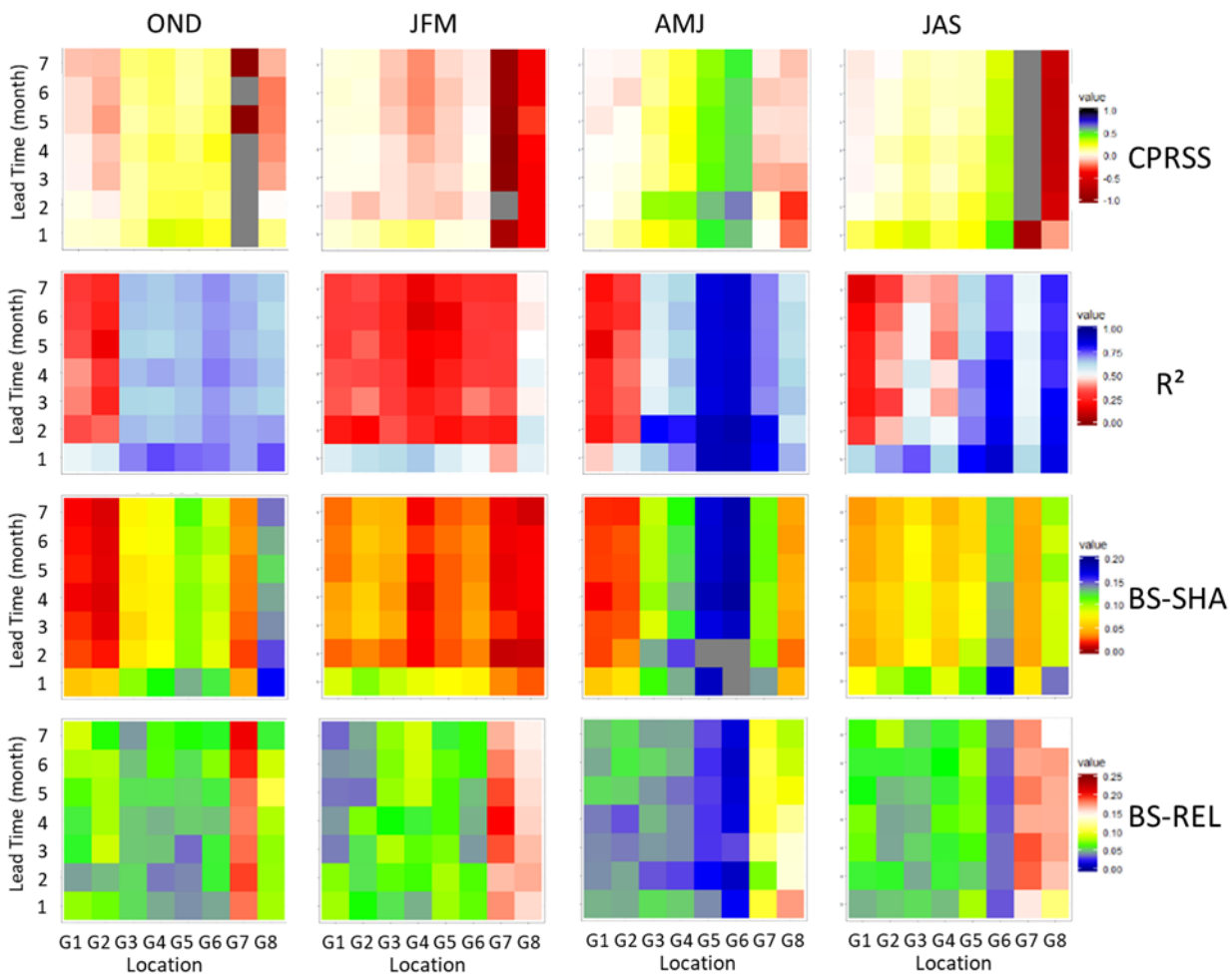

Figure 4.4 – CRPS Skill score (CRPSS), correlation coefficient (R^2), BS resolution (BS-SHA), and BS reliability (BS-REL) performance of the raw catchment precipitation forecasts of the ensemble ECMWF SEAS5 (period 1981-2016), for lead-times 1 to 7 months and the 8 groups of river basins (G1 to G8). Graphs are separated by trimester from wet to dry season (OND, JFM, AMJ, and JAS).

4.3.2 How bias correction affects the quality of precipitation forecasts

The LS and QM bias correction methods were applied to the raw catchment precipitation forecasts and scores were computed over the bias corrected forecasts. In Figure 4.5, the maps with the RME values for the wet season (trimesters OND in the first six maps on the top, and JFM in the last six maps on the bottom) are shown for the raw forecast (first column) and for the bias-corrected forecasts (LS and QM). The analysis shows that bias correction strongly improves accuracy already at the first month of lead time; the performance achieved at the first month is then slightly improved or remains the same at the subsequent forecast lead times (months 2 to 7). The spatial pattern of the errors after bias correction shows that both correction methods bring the RME values closer to zero in all basins, indicating a very good efficiency of these methods.

Overall, the efficiency of the QM BC method is slightly better over the basins and across lead times.

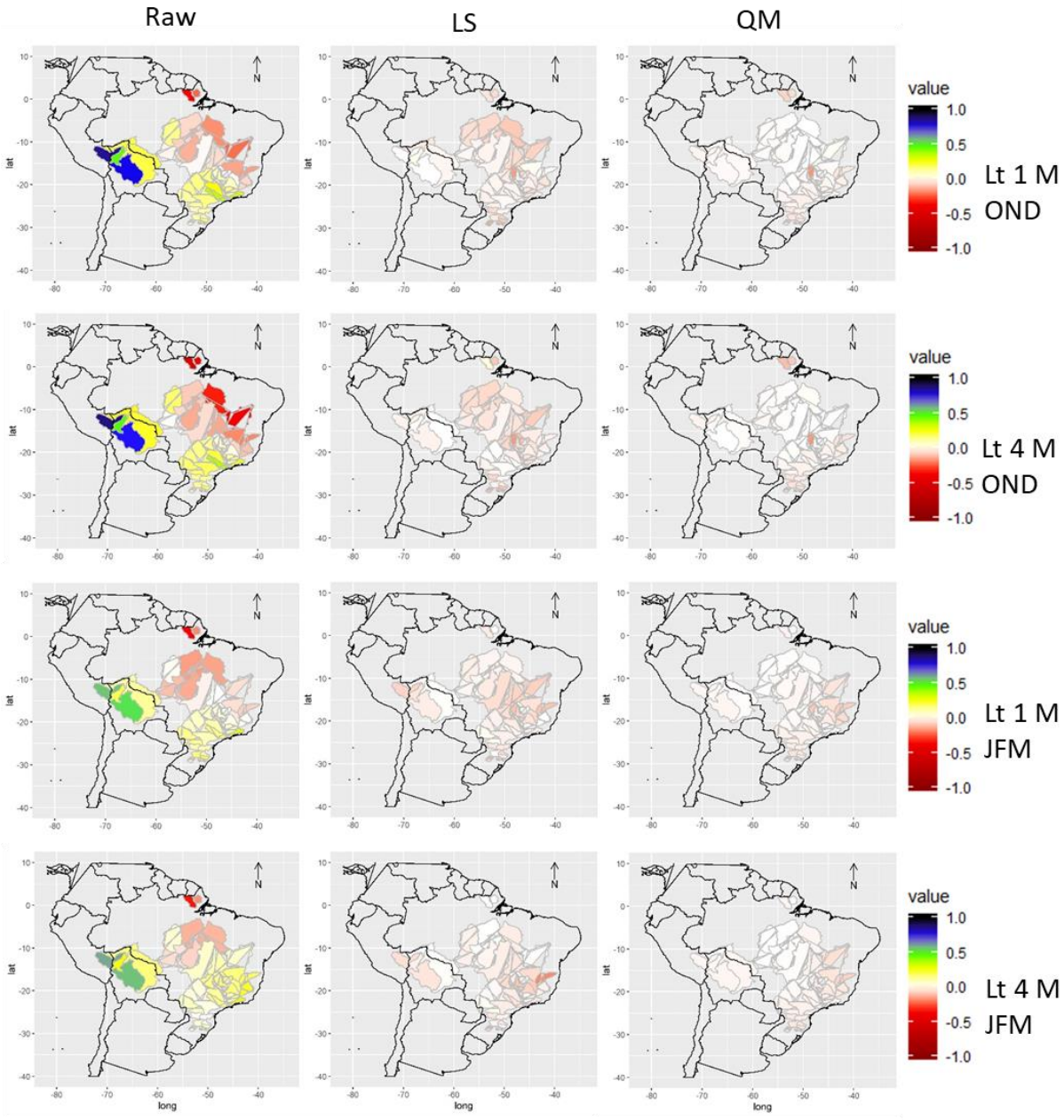

Figure 4.5 – RME of the median raw (left) and bias corrected (LS, center and QM, right) catchment precipitation forecast of the ensemble ECMWF SEAS5 (period 1981-2016), for the lead-times 1 and 4 months, and the wet periods OND (first six graphs on top) and JFM (last six graphs on bottom).

The correlation coefficient analysis showed that forecast performance did not change after the application of bias correction to the raw forecasts (not shown here). In terms of CRPS skill score (CRPSS), figure 4.6 shows the results for the eight groups of basins, the four 3-month periods of the year and the seven monthly forecast lead times. The application of the bias correction

improves the skill of the forecasts for all basins and lead times. In terms of seasons, the improvements are more important for the periods OND (G1, G2, G7 and G8), JFM (G3 to G8), and JAS (G7 and G8). The results are similar for both bias correction methods. It is worth noting that the QM method produces bias corrected forecasts that have less skill than the reference climatology at some specific situations: JAS, G5, lead times 6 and 7 months ahead). This is an indication that the method is not performing correctly, as, at worst, it should give bias corrected forecasts with performance at least equal to climatology (Zhao et al., 2017).

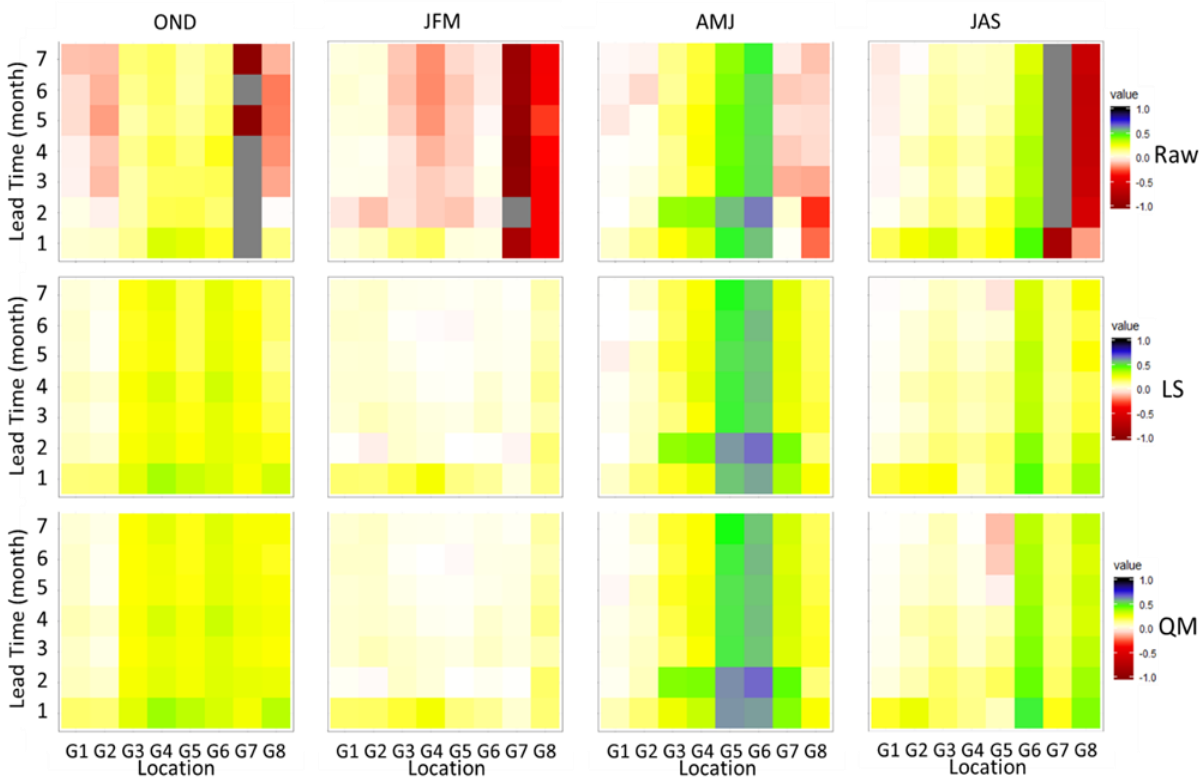

Figure 4.6 – CRPSS of the raw (top) and bias corrected (LS, center and QM, bottom) catchment precipitation forecast of the ensemble ECMWF SEAS5 (period 1981-2016), for lead times 1 to 7 months, all the river basins groups (G1 to G8), and the periods OND, JFM, AMJ, and JAS.

To evaluate the gain in performance in terms of forecast reliability and resolution, figure 4.7 plots the skill score of both metrics (BS_{rel} and BS_{res}), with the raw forecast used as a reference forecast: i.e., positive (negative) values of the skill score indicate that the bias corrected forecasts perform better (worse) than raw forecasts. Equally performing forecasts will display skill scores equal to 1. The results show that, for most of the cases, there is a gain in reliability, with values close to 100% improvement. In terms of resolution, values vary around −10% to 10%, and they seem to be independent of a gain or loss in reliability. The results are similar with both bias

correction methods. In addition, no spatial pattern (not shown) was found, with all basins displaying a similar result.

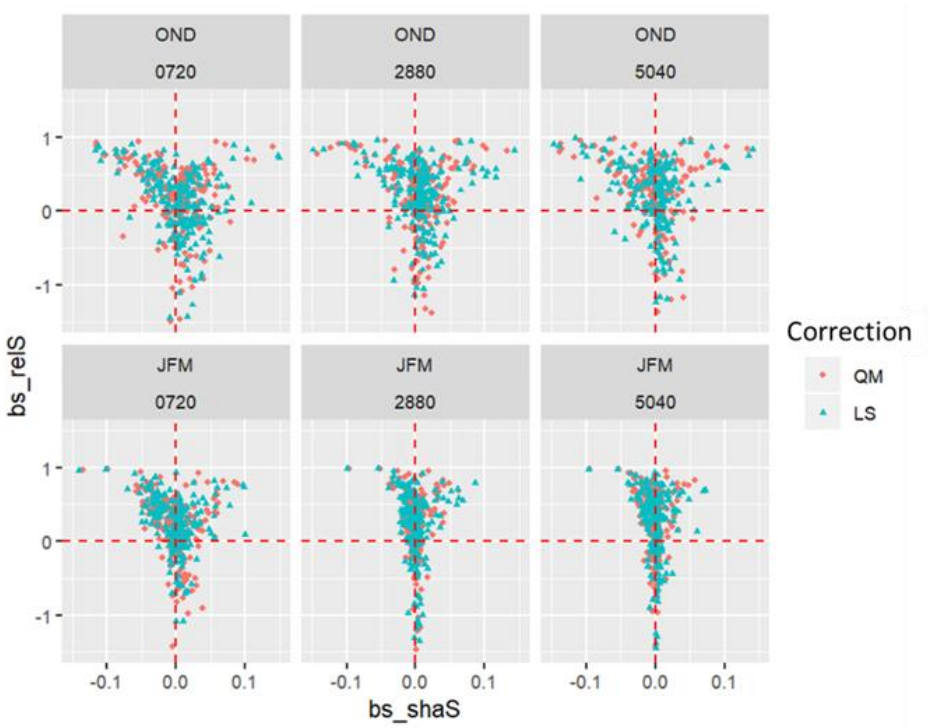

Figure 4.7 – BS reliability Skill Score (bs_rel2) versus BS resolution Skill Score (bs_sha2) of the bias corrected (LS in green and QM in red) catchment precipitation forecasts of the ensemble ECMWF SEAS5 (period 1981-2016), for lead-times 1 month (0720), 4 months (2880) and 7 months (5040) and the 41 river basins. The skill cores use the raw forecasts as reference forecast.

Since the overall results in performance were quite similar for both bias corrected methods, we carried out an analysis that focused on the wet, rainy seasons only (OND and JFM), with all metrics used in this study (BS reliability, BS resolution, Correlation coefficient, CRPS and RME) evaluated as skill scores, with the raw forecast as the reference. Figure 4.8 shows bar graphs with the percentages of the cases (over all basins and lead times) where each method (LS and QM) showed a better performance. Red (green) bars show the cases where the QM method scores better (worse) than the LS method. Blue bars contain the cases where both methods perform equally ('TIE'). Here, we consider that performances are different if the scores differ by more than 0.05 points. As the figure shows, in terms of reliability (BS-rel), overall performance (CPRSS) and accuracy (RME), the QM method is more effective and performs better than the LS method for most cases during the wet season. In terms of resolution (BS-res), the LS method is slightly better. Regarding the linear correlation, in the trimester OND, there is a large number of cases (more than 60%) where both methods perform equally. In the JFM period, most cases

are either associated with better performance from the QM method or equal performance (around 35% of cases in each situation).

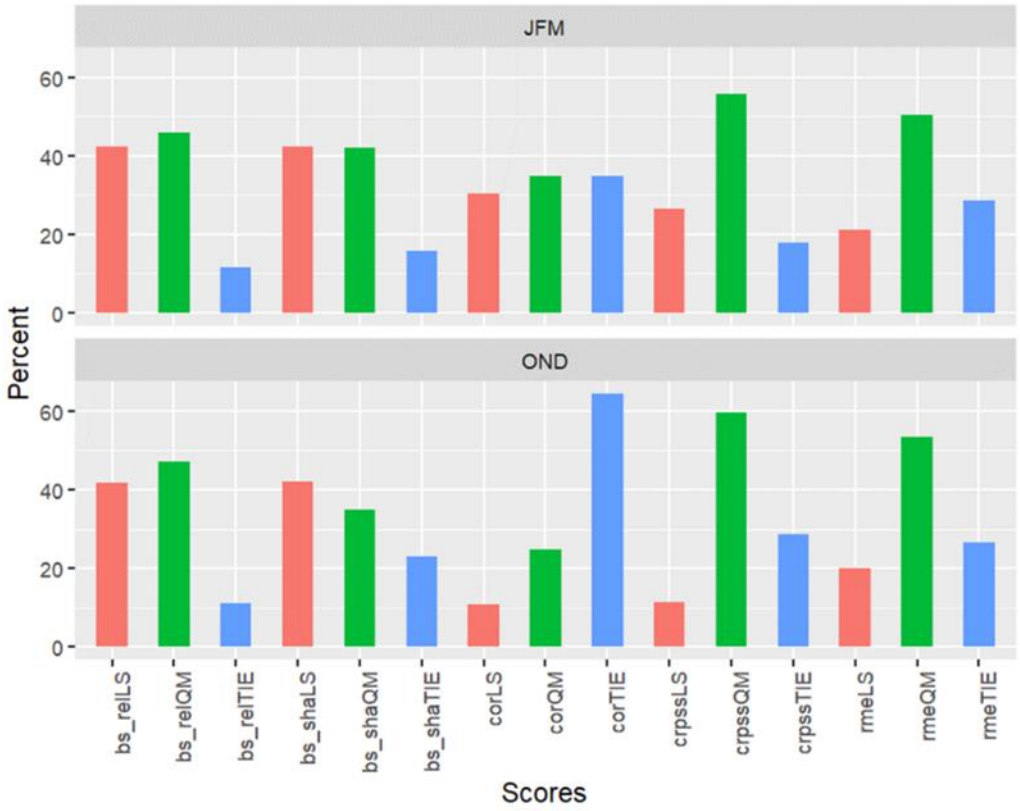

Figure 4.8 – Percentage of cases where each bias correction method performs better than the other (red bars when LS method performs better; green bars when QM method performs better) or when both performs equally (blue bars; 'TIE') for catchment precipitation forecasts of the ensemble ECMWF SEAS5 (period 1981-2016) and the wet seasons (OND and JFM). Scores are: BS reliability (bs_rel), BS resolution (bs_sha), Correlation coefficient, CRPS Skill score (CRPSS) and RME (rme). Percentage of cases include all 41 basins and 7 monthly lead times.

To evaluate the capacity of the model to forecast low monthly precipitation amounts during the wet season, two situations of precipitation deficit were considered: i) precipitation below the average monthly precipitation, and ii) precipitation below the quartile 0.75 of probability of exceedance. It was seen (not shown here) that the raw forecasts exhibit a low capacity to predict values below the average for the majority of the basins, even at the first month of lead time with POD – Probability of Detection skill scores below zero for many basins. Concerning the very low precipitation deficit situation (below quartile 0.75), forecast skill is limited to the first month of lead time, and this for both raw and bias corrected forecasts, with, in general, the QM method displaying better results than the LS method (not shown here). Specifically for the performance of the QM method, Figure 4.9 a heat graph with the performance of the bias corrected precipitation forecasts for the 7 lead times (0720 corresponds to month 1 and 5040 to month 7;

vertical axes) and for precipitation deficits during months JFM (01, 02, 03) and OND (10, 11, 12) for all 41 basins (horizontal axis). The skill score in the plots refers to the first situation of precipitation deficit (i.e., capacity to forecast below average monthly precipitations). Blue (red) colors indicate that the bias corrected forecasts are better (worse) than the climatology (the reference forecast) in terms of forecasting precipitation below the average. For all basins, except two (basin #31 and #33), the bias corrected forecasts are skillful at the first month lead time. In many basins, they remain skillful until the maximum lead time of seven months. The efficiency of the QM method to improve the performance of the raw precipitation forecasts is confirmed. .

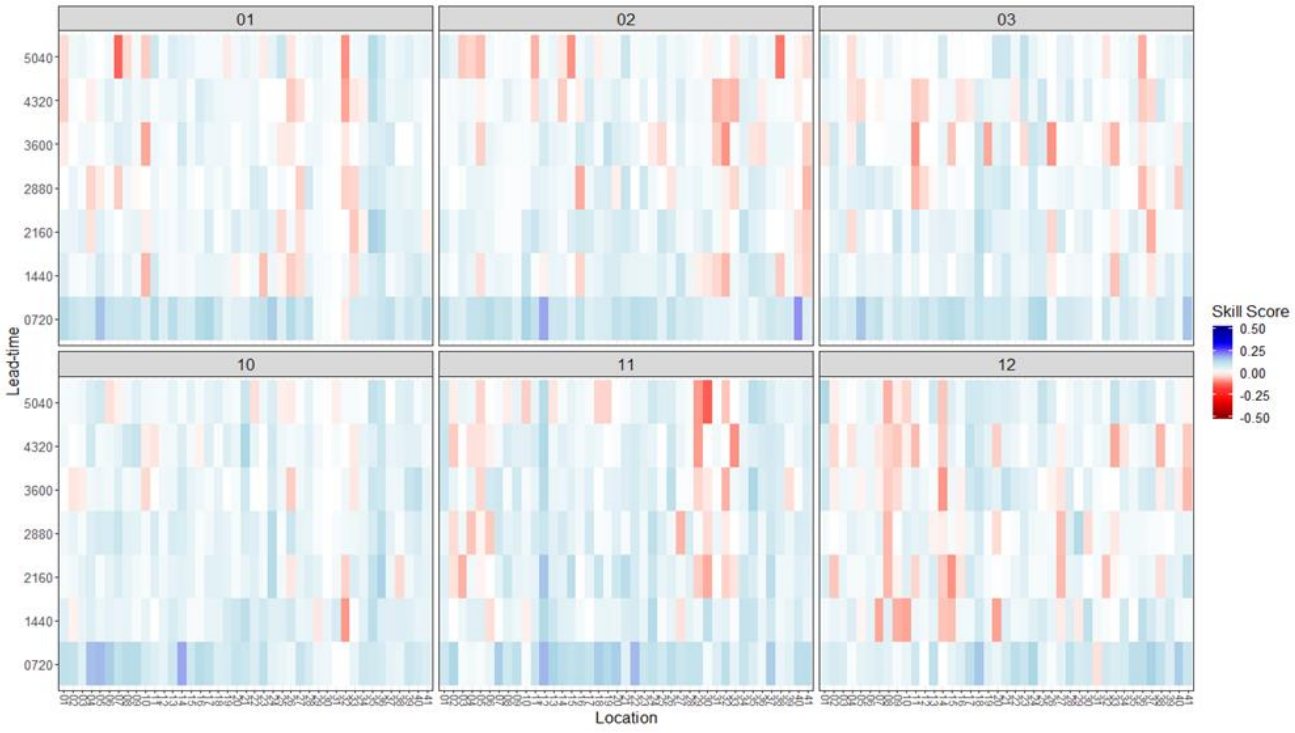

Figure 4.9 – POD Skill Score for detecting monthly precipitation amounts below the average for the months of January, February, March, October, November, and December (01, 02, 03, 10, 11, 12), lead time 1 to 7 months (vertical axis) and the 41 basins (horizontal axis).

4.3.3 Impact of bias correction of precipitation forecasts on streamflow forecasts

To understand the specific effect of precipitation bias correction on the streamflow forecasts, the performance of the streamflow forecasts is evaluated when running the hydrological model with raw and bias corrected precipitation forecasts. The quality of the forecasts is evaluated against the simulated streamflows obtained when using the observed precipitation (combined precipitation dataset) as forcing. Figure 4.10 shows the monthly biases (Mbias) of the median ensemble streamflow forecasts when using raw and bias corrected (LS and QM) catchment precipitation forecasts of the ensemble ECMWF SEAS5 (period 1981-2016). We show the

results for lead times 1, 4 and 7 months, for each calendar month of initialization of the forecasts and for the 8 groups of river basins. The effects of the LS and QM bias correction methods on the quality of streamflow forecasts can be clearly seen, as the initial bias is strongly reduced after bias correction. The results of the LS and QM bias correction methods are very similar.

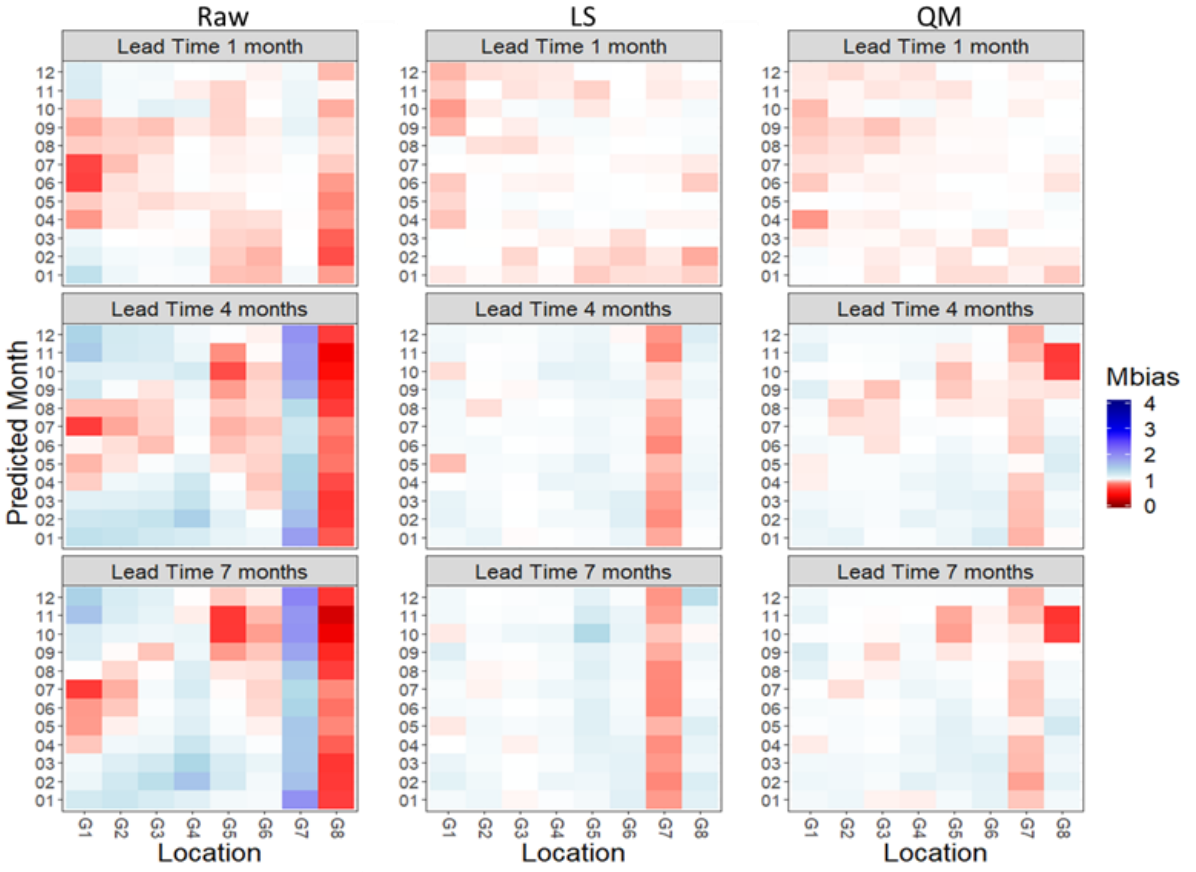

Figure 4.10 – Monthly bias (Mbias) of the median streamflow forecasts when using raw (left) and bias corrected (LS, middle; QM right) catchment precipitation forecasts of the ensemble ECMWF SEAS5 (period 1981-2016), for lead times 1, 4 and 7 months, for each calendar month (vertical axis) and the 8 groups (G1 to G8, horizontal axis; see Figure 4.1) of river basins (blue indicates forecast overestimation and red, underestimation).

The analysis of RME (not shown here) indicated similar results. The RME was significantly reduced in all basins and for all seven months horizon. Only in group G6, Madeira River, the systematic overestimation becomes a small underestimation, although, in absolute values, flow forecast accuracy is improved by the correction of biases in the raw precipitation forecasts. The analysis of the BS reliability and resolution (not shown here) showed that the reliability is improved for all basins and lead times, with the QM method displaying a better performance than the LS method, while the resolution did not significantly change with the application of bias correction. The same was observed for the correlation coefficient (not shown here). The results

were similar to those obtained for the precipitation forecasts, i.e., the correlation did not change after the application of the bias correction methods.

Figure 4.11 shows the performance results obtained with the CRPS Skill Score (CRPSS) of the median of the ensemble streamflow forecasts, using as reference forecast the simulated flow, while Figure 4.12 provides a spatial representation with a focus on the wet season (OND, first six upper panels, and JFM, last six bottom panels) and lead times 1 and 4 months.

We can see that, after bias correction, the performance is improved, resulting in better forecasts for almost all basins and seasons across the seven months of lead time (figure 4.11). The exception is the season JFM, when the forecasts for groups G1 to G4 were improved only until 3 months of lead time. In general, the results of the QM method are slightly better than those of the LS method. For the dry season, the forecasts after the bias correction have higher quality than the climatology in the April, May, and June (AMJ) trimester for all basins for the seven months forecast horizon. When the transition to the wet season begins, the ability is reduced, being usable around the second-month lead time for groups G1–G3 and for the complete forecast horizon for groups G4–G8.

From Figure 4.12, we can see that, at the beginning of the wet season (OND), the raw and bias corrected forecasts produce streamflow predictions with better quality than the climatology of the simulated flows. The benefits of the corrections applied to the precipitation forecasts are more noticeable after the second month of lead time, when the hydrological initial conditions have less influence on the flow forecasts. This is shown by the maps for a lead-time of four months ahead, which show an improvement in the quality of the forecasts, especially in the southern region. The second part of the wet season (JFM) is the most difficult to forecast, with the raw flow forecasts demonstrating more skill than the climatology only at the first month of lead time for most of the basins. The bias correction shows a visible improvement only after the second month of lead time, with its impact becoming clear at the fourth month of lead time, as shown in Figure 4.12, with values better than the climatology for all basins. The bias correction of precipitation forecasts was able to generate streamflow forecasts with a CRPSS superior or equal to the climatology of the simulated flows (positive values of CRPSS in Figure 4.12) for most of the basins and up to seven months ahead. The QM correction was again more effective than the LS method

It is important to notice that streamflows are strongly influenced by the hydrological initial conditions at the first month of lead time, especially in the case of large river basins. In this situation, the performance of the streamflow forecasts is not strongly impacted by the performance of the precipitation forecasts and, as a result, the values of the CRPSS practically do not change after the application of the bias correction methods to the precipitation forecasts, as shown in Figures 4.11 and 4.12. The performance at the first month of the flow forecasts only reflects the impacts of the bias correction applied to the precipitation forecasts in the small basins located in the southern region (group G1). In this group, the time of concentration of the basins is approximately one week, therefore the benefits of the bias correction appear more clearly already in the first month. For the other basins, the improvements produced by the bias correction appear only after the second month of lead time, and increases along the forecast horizon.

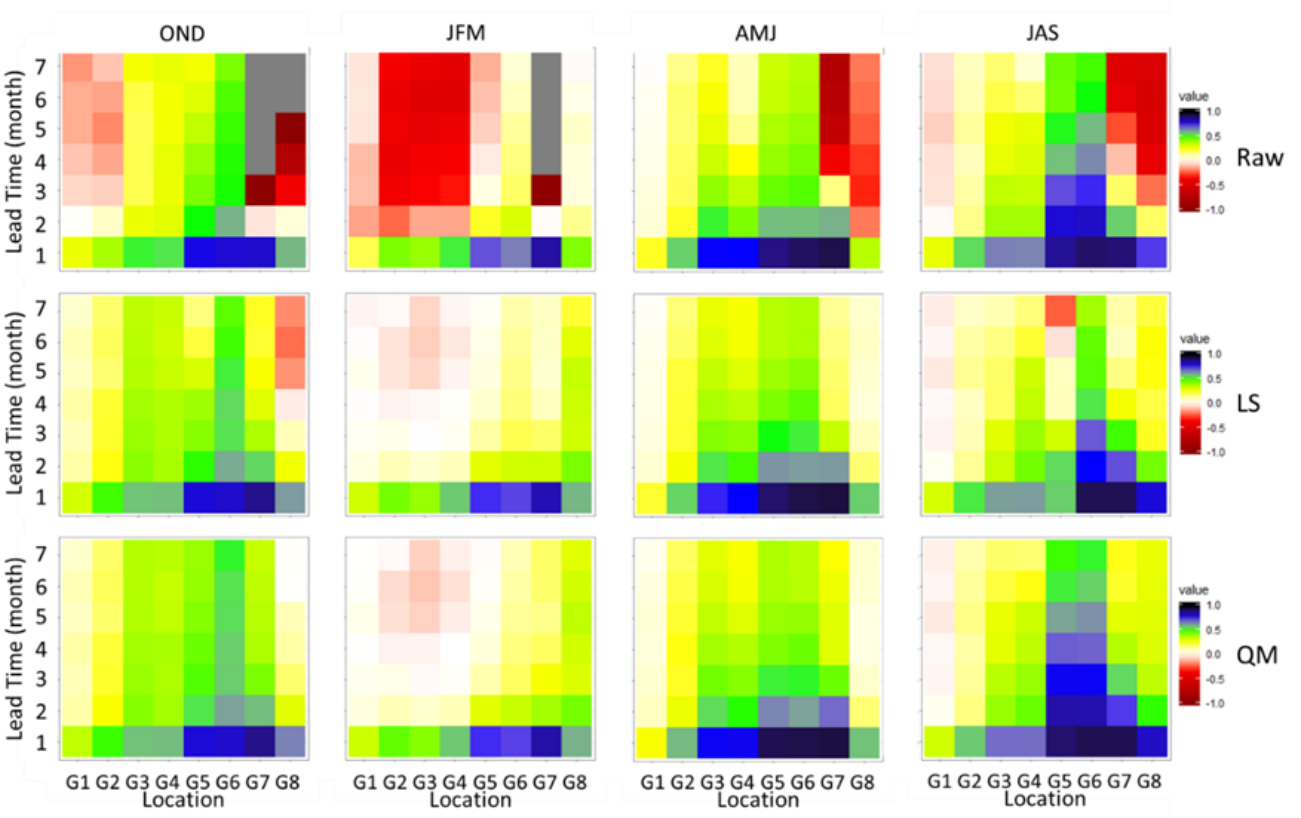

Figure 4.11 – CRPSS of the streamflow forecasts when using raw (top) and bias corrected (LS, middle; QM bottom) catchment precipitation forecasts of the ensemble ECMWF SEAS5 (period 1981-2016), for lead times 1 to 7 months, all the river basins groups (G1 to G8), and the periods OND, JFM, AMJ, and JAS.

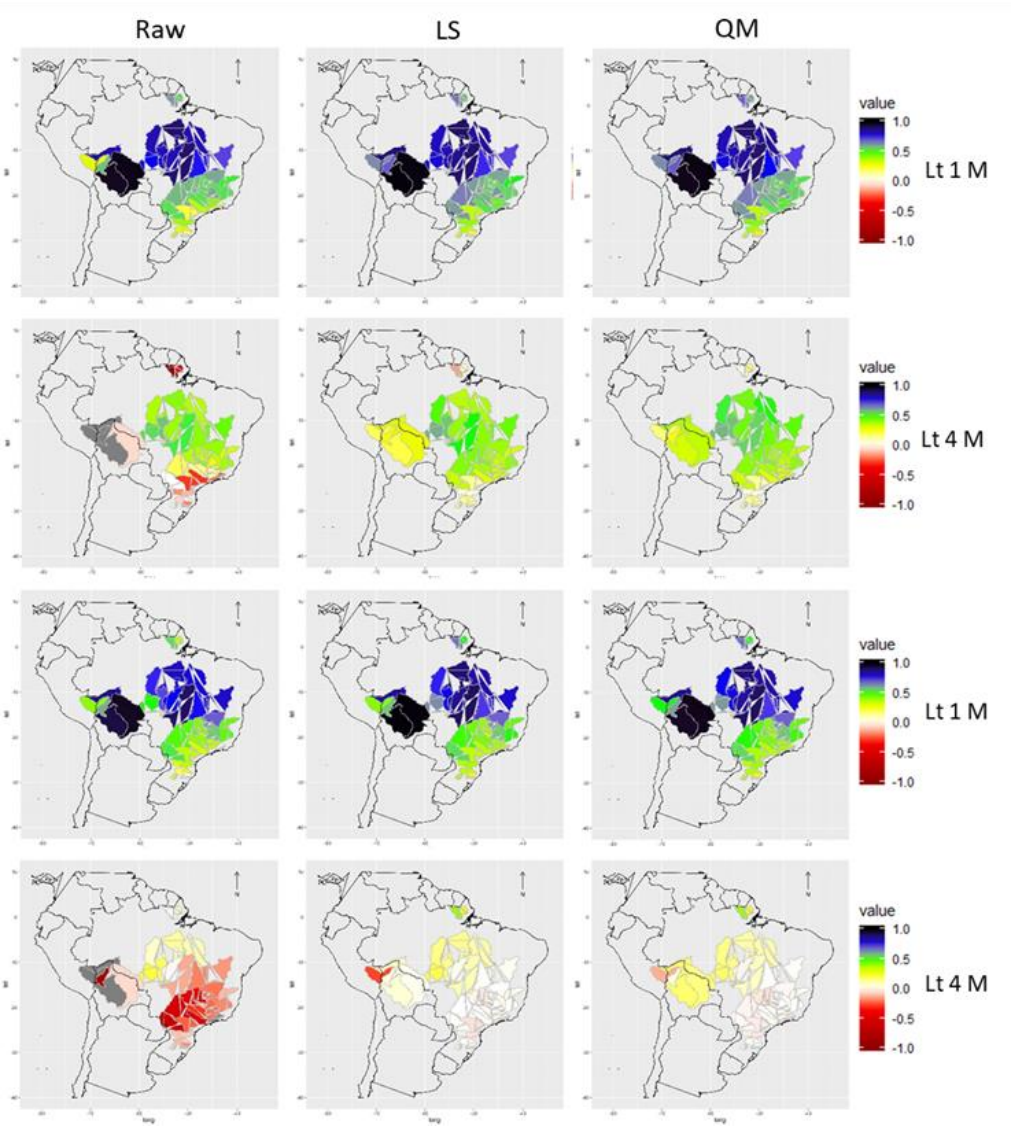

Figure 4.12 – CRPSS of the streamflow forecasts when using raw (left) and bias corrected (LS, center and QM, right) catchment precipitation forecast of the ensemble ECMWF SEAS5 (period 1981-2016), for the lead-times 1 and 4 months, and the wet periods OND (first six graphs on top) and JFM (last six graphs on bottom).

4.3.4 Validating the bias correction using an independent period in real-time forecasting

The parameters of the bias correction methods were calibrated for the period 1981–2016, with ensembles of 25 members coming from the hindcast made available by ECMWF. The real time ECMWF SEAS5 precipitation forecasts have however 50 members. In order to visualize the effect of the bias correction on real-time streamflow forecasts, we present an example where we apply the bias correction to an independent time series of real-time forecasts. The real-time validation period considered is 2017–2019. Figure 4.13 shows the application of the QM bias corrected precipitation to the forecast of streamflows in three selected HPPs. The black line is the observed flow; the red line is the median of the raw forecast, with, in light red the envelop

corresponding to the percentiles 20 and 80 of the raw ensemble; and in blue, we show the median and the same 20 and 80 percentiles for the flows generated using the QM bias corrected precipitation forecast. For visualization purposes, all forecasts are initialized every three months and the hydrographs correspond to a lead time of 1 to 3 months.

The first graph shows the 1 to 3 months ahead hydrograph of the HPP Ferreira Gomes, located in the northern region of Brazil. In this basin, the raw precipitation and streamflow forecasts showed a systematic underestimation during the BC calibration period. This underestimation is also visible in the graph for the raw forecasts during 2017–2019. The precipitation bias correction was able to improve the forecasts, reduce errors, and deliver flow forecasts that are closer to the observed values.

The second graph shows the HPP Santo Antonio, in the northwest region at the Madeira River. This basin presents the opposite behavior, with a systematic overestimation of the raw precipitation and streamflow forecasts. The bias correction was also able to correct this positive bias, reduce the errors and drive the forecasts to values closer to the observed flow in the calibration-independent period shown here (2017–2019).

The last graph shows the hydrographs for HPP Itaipu, in the southeast region. This HPP shows a mixed bias, with overestimations during the wet season and underestimations during the dry period. The application of the bias correction reduced the flows during the wet season and increased those during the dry season, decreasing the errors of the forecasts. However, the improvements in forecast performance were smaller than those observed in the two previous cases.

The graphs show clearly that the main biases coming from the uncertainty of the precipitation forecasts can be treated with post-processing of raw precipitation forecasts. However, along the forecasting chain, errors coming from the observed precipitation data, the initialization of the hydrologic model and the hydrologic model itself (calibrated parameters and structure) can also affect the performance of the flow forecasts. This indicates the need to also investigate post-processing techniques to apply to the flow forecasts in the future.

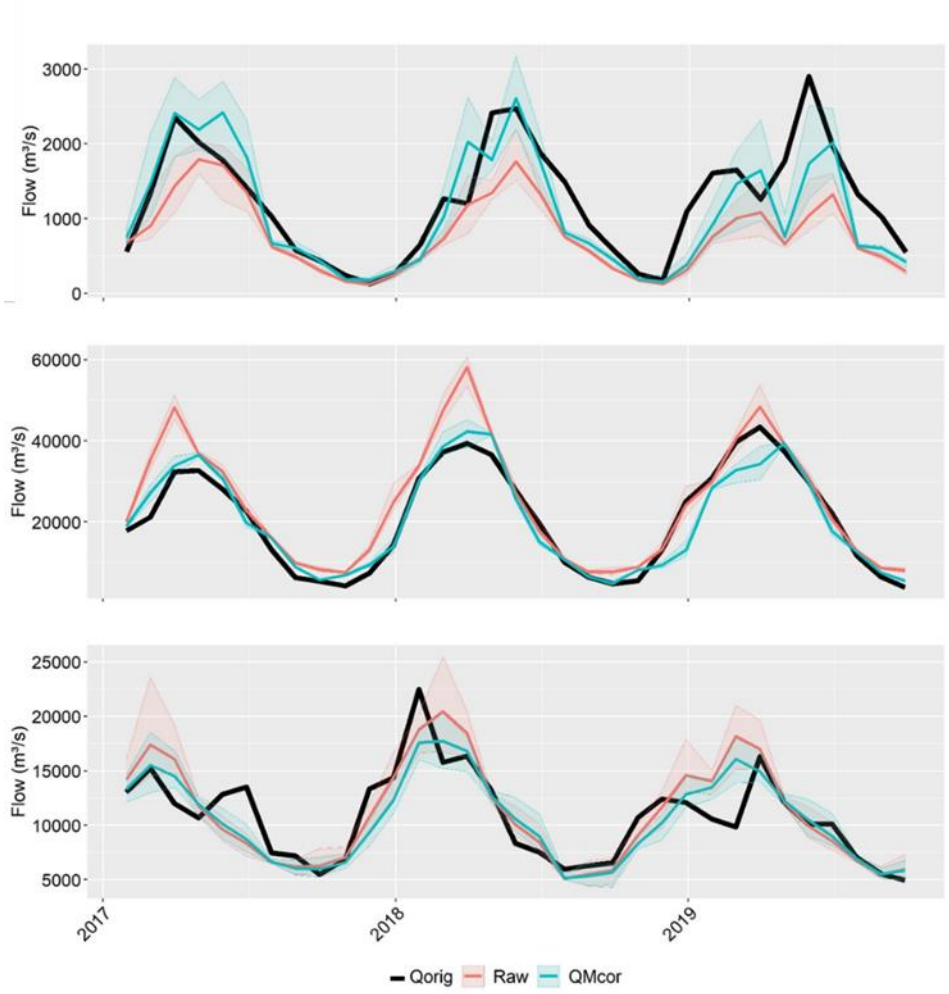

Figure 4.13 – Comparison of mean monthly flow hydrographs, with forecast initialized every month, when using raw (red) and QM bias corrected (blue) catchment precipitation forecast of the 50-member ensemble ECMWF SEAS5 over the period 2017-2019. Observed flows are indicated (black), as well as the percentiles 20-80 for the ensemble forecasts (shadowed areas). Graphs are for the HPP Ferreira Gomes (top), HPP Santo Antonio (middle), and HPP Itaipu (bottom).

4.4 DISCUSSION

Performance of raw precipitation over climatic zones and seasons

The results of the analyses of the bias behavior show similar results to those of Crochemore et al. (2016), with a bias that is not strongly dependent on the lead time, but with a clear pattern linked to the calendar month (initialization of the forecast). For basins from the south region, groups G1 and G2, raw precipitation forecasts display good performance in terms of reliability, resolution and correlation only at the first month of lead time, decreasing strongly at the longer horizons. The basins from groups G3-G6 exhibit the best performance at the first month, with performance still higher than the climatology up to seven months ahead, in almost all seasons.

The exception is the trimester JFM, the hardest period for the forecast model, when forecast performance decreases strongly after the second month of lead time. During this period, the forecasts have a very low resolution, which is a problem already observed in seasonal forecasts (Barnston and Mason, 2011). For the basins in groups G7 and G8, which display systematic overestimation and underestimation of the precipitation, respectively, there is a low performance in all horizons and seasons. In summary, when the analyses were divided in trimesters, to have a clear visualization of the variability of performance according to the seasons of the year, the overall performance of the raw precipitation forecast showed low scores mostly during the wet season, especially for longer lead times.

When we analyze performance with a spatial perspective, we notice, as also observed by Gubler et al. (2020) and Zhao et al. (2020), that the performance of the raw forecasts vary strongly, depending on the region studied, which highlights the need to separate the basins in clusters to drive the analysis towards the identification of spatial patterns. During the wet season, the basins from south and western area in groups G1-G3, part of G4 and G7 show a pattern of raw forecasts that overestimate the observed precipitation. The groups G4-northeast part, G5, G6 and G8 present a clear underestimation of the precipitation. During the dry season, almost all basins present a tendency of underestimation, with exception of those in the group G7. The raw forecast performance analysis showed, in general, an underestimation tendency going towards the north and east regions, as revealed in the RME maps. The overestimation of the catchment precipitation in the Madeira River, especially for basins closer to the Andes Mountains, is probably caused by the orographic effects that tend to produce more rain in the forecast models, and can also be affected by the lack of information on observed precipitation in the region. In general, the basins from the southeast and north region (groups G3-G6), where we have a clear seasonality of the precipitation signal, tend to present a better performance in all forecast horizons in terms of reliability, resolution and correlation. The south region G1 and G2, with no clear precipitation seasonality, only exhibits a reasonable performance at the first month horizon. The basins in groups G7 and G8, because of their systematic bias during the whole year, show the worse performance.

The impact of bias correction on the quality of precipitation forecasts

After the application of the bias correction methods, there is a clear improvement in the performance of the precipitation forecasts in all basins and lead times for both the LS and QM

correction methods. This shows that the methods were effective in bringing the forecast precipitation closer to the observed data.

The results in terms of accuracy showed that the bias correction methods were very effective in removing the error of the median of the precipitation ensemble, especially during the wet season, bringing the RME to values close to zero in all basins and for all lead times for both correction methods. They also showed that the QM method was more effective in correcting the bias of the forecasts (similar results were obtained in other regions by, for instance, Piani et al., 2010; Mehrotra and Sharma, 2016; Crochemore et al., 2016; Ratri et al, 2019). The evaluation of the correlation coefficient showed that the correlation of the bias corrected precipitation forecasts with the observations remained similar to the correlation of the raw forecasts with the observations. This is an expected result since the methods applied do not target corrections to the temporal correlation between the variables. In terms of forecast reliability, the results showed a general gain in performance during the wet season, in all basins and for all lead times after bias correction, with similar results for both techniques. In terms of resolution, the analysis did not show significant changes after the application of bias correction. When evaluating the tradeoff between reliability and resolution, it was shown that the highest gains in reliability imply only a small change in resolution, varying between −10% and 10%. Therefore, in our case, the gain in reliability brought by the bias correction methods does not imply a significant loss in resolution.

Although the LS method is simpler than the QM method, the results obtained in terms of performance of bias corrected catchment-scale precipitation forecasts were similar in many cases. The QM method showed to be more effective in improving the performance in a large percentage of cases in terms of overall skill (CRPSS), reliability (BS-reliability), accuracy (RME), and linear correlation (correlation coefficient).

The bias correction methods also showed ability to improve the forecast of precipitation deficits below average values during the wet season. Knowing that the precipitation in the future months might be below the monthly average provides valuable information for reservoir operation and energy trading. Extreme conditions are also important for reservoirs, particularly when the multiple uses of the water (agriculture, water supply, tourism, etc.) increase the pressure over water use for electricity production. In our analysis, when looking at stronger deficits (below percentile 75), the capacity to forecast drier conditions during the wet season was not improved with the bias correction. This may be due to the limitations of the seasonal climate forecasting

models to forecast extreme events and to remain sharp (i.e., avoid a large ensemble spread) at longer lead times (ECMWF, 2015). As a result, forecasts tend to stay closer to the average of the climatology at longer lead times. The limited efficiency of the bias correction methods when forecasting extreme precipitation deficits may also be linked to the scales adopted in this study (monthly aggregations and catchment-scale precipitation values). Higher time resolution (daily scale) or the analysis of smaller basins may provide more insight in terms of the ability of seasonal predictions to forecast extreme weather conditions.

The impact of precipitation forecast bias correction on streamflow forecasts

For the streamflow forecast performance, the results showed that the bias correction of the raw precipitation forecasts improves also the skill of the flow forecasts for all the metrics considered in this study. This cascade of improvement in performance, from precipitation to streamflow, due the correction of precipitation biases is aligned with the results of other studies (e.g. Hagemann et al., 2011; Zalachori et al., 2012, Lucatero et al., 2017). However, in our study at the seasonal scale, and given the size of the studied basins, the differences in performance between the streamflow forecasts issued when using the raw and the bias corrected precipitation forecasts is more clearly visible from the second month of lead time only, when the forecast becomes less sensitive to the initial conditions of the hydrological model and more sensitive to the precipitation forcing. Streamflow forecasts are strongly affected by the hydrological initial conditions (Lucatero et al., 2017), but also by errors from the hydrological model and the observed precipitation used to calibrate and run the model. If model and observations were perfect, the same benefit observed in the precipitation forecasts from the bias correction would probably be automatically observed in the streamflow forecast. This raises the question on the need to bias correct also hydrological model outputs before their use in decision-making.

Between the two bias correction methods investigated in this study, when taking into account all the skill metrics computed, the QM method performed best. The QM corrected flow forecasts were tested against the simulated flows. In terms of CRPSS, the results are superior for all seasons and basins, improving the performance and extending the reliable forecast horizon. As also observed in the precipitations forecasts, the trimester JFM exhibits the lowest performance. In terms of accuracy, the performance was improved in all basins, especially at the wet season, reducing the overestimations.

In general, the performance of the forecasts displayed a spatial trend. For the basins in the southern region of Brazil, where there is no seasonality, without a clear wet and dry season, and with the possibility of heavy rains in any month, the forecasts had the worst performance, with good skill only in the shorter horizons, generally two months ahead. In the basins in the north region, the forecasts showed better performance and up to longer horizons. In this basins, the climate is more determinant to the skill of the forecasts than the size of the basin. For example, the forecasts in the basin associated with the HPP Manso, located in the center-north region, which is a small basin in our experiment, had a forecast performance like the one observed in the large basins of the northern region, showing higher skill and for a longer horizon than the basins in the southern region with similar area.

Finally, the study showed how the corrected precipitation forecasts can affect the operational flow forecasts, which were run over an independent period from the period used to calibrate the bias correction methods. The changes are clear, especially in basins with systematic bias of under- or over-estimation. For basins where the errors are lower or can be related to both under- and over-estimation, the benefit is less striking.

4.5 CONCLUSIONS

The main conclusions after addressing the forcing uncertainties in the seasonal streamflow forecasts by applying bias correction methods to improve the precipitation forecasts from the ECMWF SEAS5 seasonal ensemble forecasting system to 41 basins in Brazil are presented below.

- In terms of precipitation forecast, the errors observed in the raw forecast depend more on the calendar month than the lead time, with a systematic overestimation during the wet season and an underestimation during the dry season for most of the basins.

- A spatial pattern was also noted during the wet season (OND–JFM), showing an underestimation going to the north and east regions and an overestimation in the direction of southern and west regions.

- The LS and QM bias correction methods are highly effective in correcting the biases of the raw precipitation forecasts, especially during the wet season.

- Although the BC methods provide both good results, the QM bias correction presents the best performance in the majority of cases (basins, lead times and scores, all together).

- The QM bias correction particularly improved the capacity of the model to forecast wet months or precipitation deficits below the monthly averages, which are both important information for reservoir operation and energy trading.

- The precipitation bias correction affects the performance of the streamflow forecasts, reducing the errors and presenting good forecast performance along the seven months of forecast horizon for almost all basins. As observed in the precipitation forecasts, the trimester JFM is also the most difficult for the flow forecasts.

- The climate showed to be more determinant in the flow forecast performance than the size of the basin in the small basins located in the regions with a strong precipitation seasonality; in this basins the forecasts performed better than in the larger basins in the south region, where there is not a marked seasonality of precipitation and precipitation variability along the year is higher.

- The parameters calibrated for bias correction, using 35 years of 25-member precipitation hindcasts, were effective to correct precipitation forecast biases and improve the performance of streamflow forecasts in an independent period of validation that reflects the current period (2017-2019). The ensemble with 50 members displayed flow forecasts closer to the observed flows when the bias corrected precipitation forecast was used in the hydrological model.

All the results, performances, and the calibration of the parameters of the bias correction methods and of the hydrologic models were based on a specific observed precipitation dataset available in real-time (developed in chapter 3). If the analyses were done with other proxy to observed (ground station) precipitation , as reanalysis precipitation data, different conclusions might be reached.

CHAPTER 5:

IMPROVING THE PERFORMANCE OF ECMWF SHORT RANGE AND SUBSEASONAL PRECIPITATION FORECASTS IN SOUTH AMERICAN CATCHMENTS

This chapter contains material for a paper to be submitted to the journal ***CLIMATE SERVICES***, with the following co-authors: REIS. A. A.; RAMOS. M. H.; WETTERHALL. F.; WEERTS. A.; FERNANDES. W. S.

5 IMPROVING THE PERFORMANCE OF ECMWF SHORT RANGE AND SUBSEASONAL PRECIPITATION FORECASTS IN SOUTH AMERICAN CATCHMENTS

5.1 INTRODUCTION

Precipitation is one of the most important information for many economic activities related with water resources and uses, such as agriculture, recreation, transportation, energy production, among others. An important source of precipitation forecast information are the numerical weather prediction (NWP) models, which provide predictions from the short range (several days or weeks ahead, multiple times per day) up to global seasonal forecasts (several months ahead, once a month). NWP models have shown advances during the last decades (Hamill et al., 2013), with notable improvements on their physics, the estimation of forecast uncertainty (ensemble forecasting), predictability and predictive skill (Bauer et al., 2015). As a result, NWP data, weather forecasting products and climate services have been increasingly used in many areas to support operations and decision-making.

Forecast users are many, and theirs needs may involve forecasts at different spatial resolution and for different time horizons. Although the concept of seamless prediction of the Earth system across scales has been widely investigated in the past decade (WMO, 2015), when it comes to the operational use of weather forecasts and climate predictions, users often have to handle outputs coming from different models. Forecasts associated to short and medium range models are specially affected by the atmospheric initial conditions (Kalnay, 2003; ECMWF, 2015). On the other hand, seasonal forecasts from coupled ocean-atmosphere general circulation models (GCM) are predominantly influenced by inertial variations of the initial conditions, such as sea surface temperature (SST), soil moisture and snow cover (Shukla, 2014; ECMWF, 2017). In both cases, models have migrated from deterministic to probabilistic forecasting in order to better estimate forecast uncertainty and allow users to assess risks more accurately. Based on perturbations of the initial conditions and stochastic model parametrizations, an ensemble of members is generated from the forecast model. Ensemble forecasts can deliver a probabilistic forecast to the users, and the dispersion of the ensemble members can provide information on the predictability of the phenomena being forecast. Users such as flood forecasters, water reservoir operators or agricultural planners can use all ensemble members in their operational models or decide on probability thresholds of interest to make their decisions.

Among the existing ensemble forecasting systems in the world, those developed and run by the European Center for Medium-range Weather Forecast (ECMWF) have been acknowledged as presenting consistently the best results in many regions worldwide (Hamill et al., 2006; Su et al., 2008; Medina et al.; 2019). They consist of three main products: the medium-range ECMWF ENS Ensemble Prediction System (EPS) runs twice a day for forecast horizons up to 15 days; the extended range system focuses mainly on the week-to-week changes in the weather and covers lead times up to 46 days; the long range, seasonal forecasting system (SEAS5) runs on the 1st of each month and extends up to 7 months. The EPS and SEAS5 products have been widely investigated for their use in hydrological models and water-related risk assessment (e.g., Fan et al. 2015, 2016; Johnson et al. 2019; Emerton et al. 2018), while studies investigating the value of the extended range system to hydrological applications are still rare (e.g., Wetterhall et al., 2018).

Extended range forecasting systems were created to investigate how predictability could be enhanced in the time range of 10 to 46 days, covering the gap between the short-term forecasting and the seasonal prediction. The World Weather Research Programme and the World Climate Research Programme implemented the Subseasonal to Seasonal (S2S) prediction project with the participation of operational centers and researchers around the world (Vitart et al., 2012). The ECMWF S2S datasets have being used in many different modeling and scientific studies around the world (e.g. Wang et al. 2017, Vigaud et al. 2017 a and b, Liu et al. 2017, Olaniyan et al., 2018, Andrade et al., 2018, Coelho et al., 2018). Despite the many improvements of the NWP and GCM models uncertainties and systematic biases remain, particularly when it comes to key variables used in hydrological models and applications such as precipitation and surface temperature. The application of bias corrections or statistic post-processors is a needed step to improve the predictability of the models (Verkade et al., 2013; Crochemore et al. 2016).

In Norway, Gudmundsson et al. (2012) compared a group of statistical transformations to correct the bias of precipitation forecasts. They classified the approaches into (1) distribution derived transformations, (2) parametric transformations and (3) nonparametric transformations, each differing from the other with respect to their underlying assumptions. The methods included distribution mapping based on fitted theoretical or empirical distributions. The authors recommended using non-parametric methods, since these methods were the most effective to reduce the bias and did not require any approximations of the empirical distributions. Their study highlighted the differences between the bias correction methods and the necessity to test them

prior to their application in an operational context. There are many other studies in the literature, from different regions and using different techniques of post processors, that apply bias correction techniques to improve the quality of precipitation forecasts (e.g. Piani et al. 2009; Gudmundsson et al., 2012; Teutschbein and Seibert, 2013; Crochemore et al. 2016; Mehrotra and Sharma, 2016; Kim et al., 2016; Zhao et al., 2017; Yang et al., 2020). In the context of bias correction, two procedures stand out: one that uses a fixed, historic time series of hindcasts (or reforecasts) to calibrate the bias correction parameters ('structural' bias correction), and another that applies calibration corrections 'on-the-fly', i.e., the full hindcast set is run every time a new real-time forecast is produced ('conjunctural' bias correction).

The 'structural' bias correction procedure is the most common approach found in the applications of post-processors in hydrology to correct systematic biases of the meteorological forecasts before running an operational hydrological model. In this case, a long period of meteorological hindcasts, often computationally expensive, is generated, with the same (fixed) version of the operational forecasting model, and used to evaluate forecast biases and skill, and calibrate the bias correction parameters. The errors between the forecasts and the observations (from gauge stations, satellite, radar or reanalysis data) are evaluated and considered in the setup of the post-processor, which is then systematically applied in real-time to the operational forecasts.

The 'conjunctural' or 'on-the-fly' bias correction procedure relies on parameters that are calibrated at each run of the operational forecast, at the user's request. In this case, the hindcasts are generated every time a new forecast is produced (in practice, slightly in advance of the real-time forecasts) using the same version of the model that is used to run the operational forecast (which can change over time and, therefore, the hindcasts can also come from different model versions, contrary to the fixed-model hindcast of the 'structural' procedure). The advantage of this procedure is that there is no need to have a long reforecast period before using the forecasts in real-time applications. On the other hand, one has to keep in mind that the parameters calibrated 'on-the-fly' with a short period of hindcasts might not be representative enough of the climatology of the weather of the region under study (e.g. Fan and Van de Doll, 2011; Jiang-Shan et al., 2014; ONS, 2019; Medina et al., 2019).

The aim of this study is to assess the performance of ECMWF short range EPS and extended range sub-seasonal S2S precipitation forecasts in river basins in Brazil and neighboring countries in South America. We focus on investigating how best can bias correction techniques be applied

to improve the quality of both sets of forecasts, while also analyzing the benefits of using the 'on-the-fly' S2S hindcast to calibrate the short-range EPS forecasts in a real-time, operational context. Our case study is the Brazilian hydroelectric system. In Brazil, the needs of the hydroelectric system for accurate and reliable forecasts extent across several forecasting horizons. The system relies on forecasts up to 48 hours ahead for the balance of the electric grid (ONS, 2019). Short-range forecasts, from 1 to 7 days ahead, depending on the basin's size, are applied to flood control, while medium-range forecasts, up to 7–30 days ahead, are crucial for energy trading in the spot market (CCEE, 2016). Additionally, seasonal (months ahead) streamflow forecasts are used to guide the system's optimization, to plan infrastructure maintenance, to manage multiple water uses, and to set up long-term energy trading strategies. Therefore, all forecast horizons have a great importance for the sector, being necessary to extract the best information of each one.

In the previous chapter (Chapter 4) we assessed the performance of the precipitation forecast from the seasonal model ECMWF SEAS5. We found systematic biases and investigated the use of the LS (Linear scaling) and QM (Quantile Mapping) bias correction methods to improve forecast performance. The conclusions drawn from the analysis indicated that the QM method provides the best results to correct the forecast biases and extend the predictive skill of the precipitation and streamflow forecasts. Therefore, in this part of the research, we focus on the use of the QM method only. Additionally, we also explore the use of the 'on-the-fly' hindcast of the sub-seasonal model to calibrate the parameters of the bias correction method and apply bias correction also to the short-range ENS forecasts. The idea is that if the 'on-the-fly' calibration performs well, it will then be possible to correct the short-term model without the need of using a fixed long historic hindcast. This is crucial issue since reforecasts need to be done every time a new model is implemented, i.e., every time important modifications are brought to the NWP models. In this chapter, as in Chapter 4, we evaluate the forecasts against the near real-time observed precipitation dataset developed in Chapter 3.

Considering the aims of this chapter, we focus on the following research questions:

i. How good is the performance of the ECMWF S2S precipitation forecasts, before and after the QM bias correction in the studied basins, considering the 'on-the-fly' hindcast?

ii. How good is the performance of the ECMWF EPS precipitation forecasts, before and after the QM bias correction, considering its historical 10-year hindcast?

iii. Does the bias correction using the 'on-the-fly' ECMWF S2S hindcast perform better than the bias correction using the 10-year historical ECMWF EPS reforecast to correct the short term ECMWF EPS forecasts?

The materials and methods are presented in section 5.2. Section 5.3 describes the results and section 5.4 presents the discussion. Finally, section 5.5 draws the conclusions of the study .

5.2 MATERIALS AND METHODS

5.2.1 River basins and observed precipitation data

The case study (41 river basins) and the observed precipitation data, averaged over the river basins' areas, used here are the same that were presented in chapter 4, section 4.2.1. The reader is invited to refer to it. We also remind that the combined real-time observed precipitation dataset was developed in chapter 3, by blending the gauged observed precipitation from CPC - NOAA (Chen et al., 2008) and the precipitation from TRMM-MERGE (Rozante et al., 2010). The combined precipitation, weighted by the uncertainty of the individual data sources, presented better results than the isolated use of each. The availability of the dataset is for the period from 1979 to 2020. This combined dataset was used in this chapter to evaluate the ECMWF precipitation forecasts.

5.2.2 ECMWF precipitation forecasts

ECMWF EPS – 15 days horizon, using the 00 GMT initialization with daily precipitation

The medium-range forecasting system runs every day with 51 ensemble members (one control plus 50 perturbed members) and up to 15 days of forecast horizon. Ensemble hindcasts (reforecasts) are available from 2006 to 2020. According to ECMWF previous analyses, in spite of the coarser resolution of the ensemble forecasts, which is half that of the deterministic forecast (ECMWF HRES; one single member), the ensemble control member, which has the same initial conditions as the deterministic forecast, performs very similarly to the deterministic forecast with respect to synoptic patterns. Differences are most noticeable for small scale extreme weather events, where the deterministic forecast is able to generate, for example, stronger winds and

higher precipitation values. There is no ocean coupling for the first 10 days of the forecasts. From day 10 onwards, the atmospheric model is coupled with the ocean model. To account for initial uncertainties, the oceanic control temperature analysis, including the SST and the deep ocean temperature, is complemented by four alternative analyses. They are produced by adding randomly wind perturbations to the ocean data assimilation, driven by five slightly different meteorological fields based on the control analysis, slightly and randomly perturbed. The resulting five ocean analyses are then distributed among the control member and the ensemble members (ECMWF, 2015).

ECMWF S2S – 46 days horizon, twice a week initialization (Monday and Thursday) with daily precipitation

The ECMWF extended forecasting system runs twice a week, every Monday and Thursday, with 51 members and up to 46 days of forecast horizon. As it runs, it also produces the 'on-the-fly' hindcast for the same calendar date covered by the run but for the last 20 years (see section 5.2.3). Data from the operational run is available from May 2015 to June 2020. The treatment of the ensemble members between day 15 and day 46 is the same as for the 10-15 day range described earlier for the ECMWF EPS. In order to estimate and compensate for any model drift, a five-member ensemble is integrated from the same calendar date for the last 18 years. This results in "back statistics", based on a 90-member ensemble of reforecasts from which systematic errors can be calculated. Systematic errors are then corrected during post-processing after the forecast run (ECMWF, 2015).

5.2.3 Methodology to assess the performance of the ECMWF S2S precipitation forecasts and apply the QM bias correction with the 'on-the-fly' hindcast

The methodology comprises four steps:

i) the first step is to assess the performance of the raw daily precipitation forecasts at the scale of the river basins (i.e., average precipitation over the river basin areas). This is done by calculating the performance metrics (see section 5.2.5) of the forecasts against the observed precipitation dataset;

ii) the second step is to calibrate the bias correction method using the precipitation forecasts of the hindcasts. For this study, we did all the bias correction analysis at the daily precipitations in a weekly lead times;

iii) the third step is to apply the QM method over the daily precipitation forecasts of the operational run, which covers the period May 2015 to 2020 June;

iv) the fourth step is to assess the performance of the bias-corrected daily precipitation forecasts at the scale of the river basins, and analyze it in comparison to the performance obtained in step i) for the raw forecasts.

The QM method is a more-sophisticated method, classified as distribution-derived transformation, (e.g. Block et al., 2009; Piani et al., 2010; Johnson and Sharma, 2011; Sun et al., 2011; Kim et al., 2016). It is based on correcting the precipitation forecasts aiming that their statistical distribution fits to the statistical distribution of the observations. There are several ways to adjust the forecast and the observed distributions or quantiles, and existing techniques mainly differ in terms of how the cumulative distribution functions (CDFs) are considered (Crochemore et al., 2016). In this study, the empirical CDFs (ECDFs) are used to build the probability distributions of the observed and forecast datasets. The QM method is already presented in chapter 4, section 4.2.3, and the reader is invited to refer to it.

The conjunctural bias correction was applied to the ECMWF S2S precipitation forecasts, using the ‘on-the-fly’ hindcast. It consists of an ensemble with 11 members (one control plus ten perturbed members), covering the previous 20 years of the same calendar dates of the operational run period (May 2015 to June 2020). For the calibration of the bias correction parameters, we take the ‘on-the-fly’ hindcast that are associated with exactly the same 46 calendar days of the operational forecast run. Therefore, this bias correction is only lead time dependent. It is applied to the daily precipitation of each river basin. The parameters are calibrated at each run, from week one to week six, and for each basin, considering the daily precipitation of the last 20 years on the same calendar days.

For example, the operational (raw) forecast run of 1 June 2020 covers the forecast range from 1 June 2020 to 16 July 2020 (46 days) with its 51 members. The ‘on-the-fly’ hindcast available to calibrate the parameters of the bias correction method corresponds to reforecasts for the period from 1 June to 16 July for the years 1999 to 2019 (the year of the operational forecast run is not

included). Each 46-day period has 11 ensemble members. Therefore, for each (operational forecast) run, we have a new set of hindcast and a new set of calibrated parameters. These parameters are then applied to the (raw) operational forecast to generated the bias corrected forecast. Both raw and bias corrected forecasts are then evaluated against the observed precipitation dataset, so that improvements due to the QM bias correction can be assessed. We note that, the QM bias correction is calibrated using daily precipitation in a weekly lead time, .i.e., there are six sets of calibrated parameters, one per each week of lead time.

5.2.4 Methodology to assess the performance of the ECMWF-EPS precipitation forecasts and apply the QM bias correction with the 10-year historical reforecast

At this step, the performance of the 15-day ECMWF EPS model is assessed for the period 2007-2016, using the forecast evaluation metrics CRPSS and RME, presented in section 5.2.6. Both raw and QM bias corrected forecasts are evaluated against the observed precipitation dataset, so that improvements due to the bias correction can be assessed.

The calibration of the parameters of the QM bias correction method (structural procedure) is done using a weekly time step (2 weeks of lead time for the forecast horizon of 15 days) and the historical reforecast period from 2007 to 2016. The correction method is lead-time and month dependent, i.e., a different correction is applied according to the month when the forecast was issued and the lead time for which the forecast value is valid. Therefore, there are 24 sets of parameters for each basin (12 months * 2 weeks of lead time). The calibrated parameters obtained are then applied to the raw daily precipitation forecast values according to the day of the forecast (on which month it falls) and the lead time. We use an independent period from the calibration of the QM method, running from January 2017 to June 2020.

5.2.5 Methodology to assess the performance of the bias corrected ECMWF EPS precipitation forecasts using the ‘on-the-fly’ sub-seasonal hindcast

The performance of the conjunctural (‘on-the-fly’) bias correction on the ECMWF EPS precipitation forecasts is assessed. The ‘on-the-fly’ hindcast from the S2S model (only lead time dependent; section 5.2.3) is used to correct the forecast bias of the short-term ECMWF EPS forecast model. The correction is applied to the daily precipitation forecast values for the same period used to assess the structural bias correction (section 5.2.4), from January 2017 to June 2020.

The parameters for the QM bias correction method obtained from the ECMWF S2S precipitation forecasts (section 5.2.3) are only available for the dates of the runs of the S2S forecasts, i.e., Monday and Thursday. However, the ECMWF EPS forecasts are issued every day, from Monday to Sunday. In this way, the parameters obtained from the Monday's run of the ECMWF S2S 'on-the-fly' hindcast will be used to correct the short-term ECMWF EPS runs from Monday to Wednesday, while the parameters obtained from the ECMWF S2S Thursday's run will be used to correct the short-term runs from Thursday to Sunday. Moreover, since the short-term model has only two weeks of lead time, only the bias correction parameters for the first two lead times of the sub-seasonal 'on-the-fly' hindcasts are used. Figure 5.1 shows the example of one week of bias correction of the short-term model using the sub-seasonal 'on-the-fly' bias correction parameters. The week starts on 1 June 2020 (Monday), and ECMWF ENS forecasts of Monday (1 June), Tuesday (2 June) and Wednesday (3 June) are bias corrected with the parameters that come from ECMWF S2S run of 1 June 2020 for lead time 1 (first week, in black) and lead time 2 (second week, in red). The other weeks of lead time are not used. On 4 June 2020 (Thursday), a new set of parameters from ECMWF S2S is available. They are used to bias correct ECMWF ENS forecasts of Thursday (4 June), Friday (5 June), Saturday (6 June) and Sunday (7 June).

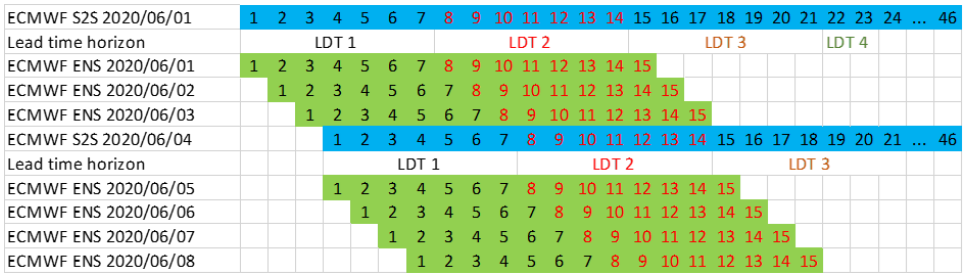

Figure 5.1– Example of one week of bias correction of the short-term forecast model (ECMWF ENS) using the 'on-the-fly' sub-seasonal (ECMWF S2S) hindcast. The days in black (red) indicate the first (second) week of lead time (LDT) that shares the same bias correction calibrated parameter.

5.2.6 Metrics to assess forecast performance

The metrics used are the same that were presented in Chapter 4, section 4.2.4 for the evaluation of the precipitation forecasts, i.e., CRPS, RME, BSrel, BSres, Correlation coefficient. The reader is invited to refer to it.

5.3 RESULTS

5.3.1 Performance of the sub-seasonal precipitation forecasts using the 'on-the-fly' hindcast (conjunctural bias calibration)

Figure 5.2 shows the overall performance of the ECMWF S2S model, in terms of the CRPSS metric, for the period May 2015 to May 2020, considering the 41 basins, grouped by climatic similarity in eight groups, for six week lead times. The analysis was divided in four seasons represented by the trimesters OND, JFM, AMJ and JAS to improve the understanding of the effects of the wet and dry seasons on performance. The graphs indicate the raw precipitation forecasts ('Raw') and the bias corrected forecasts using the QM method ('QM'). The shadows of red represent the results when the forecasts have a performance that is worse than the climatology forecast.

We can see that the raw forecast presents a good performance for almost all basins for the first two weeks horizon. The second trimester of the wet season (JFM) presents the lowest predictability of all seasons, with good forecasts at the first week and performance clearly degrading from the second week onwards. On the other hand, the first trimester of the wet season (OND) displays good performance up to six weeks ahead for the majority of the basins, with an exception for the basins from the south region groups G1 and G2, where the CRPSS values become negative after week 3, indicating a loss of skill comparatively to the benchmark climatology. After the application of the QM bias correction method, it is possible to see an improvement of forecast performance for the OND period, except for the Madeira river, represented as group G7, where the bias corrected forecasts became worse than the raw forecast. In the trimester JFM, only the basins of group G8 present a clear improvement after bias correction at all lead times. For the dry seasons (AMJ and JAS), the bias correction only slightly impacts the raw forecasts, often bringing them to a performance that is closer to the climatology (CRPSS values closer to zero).

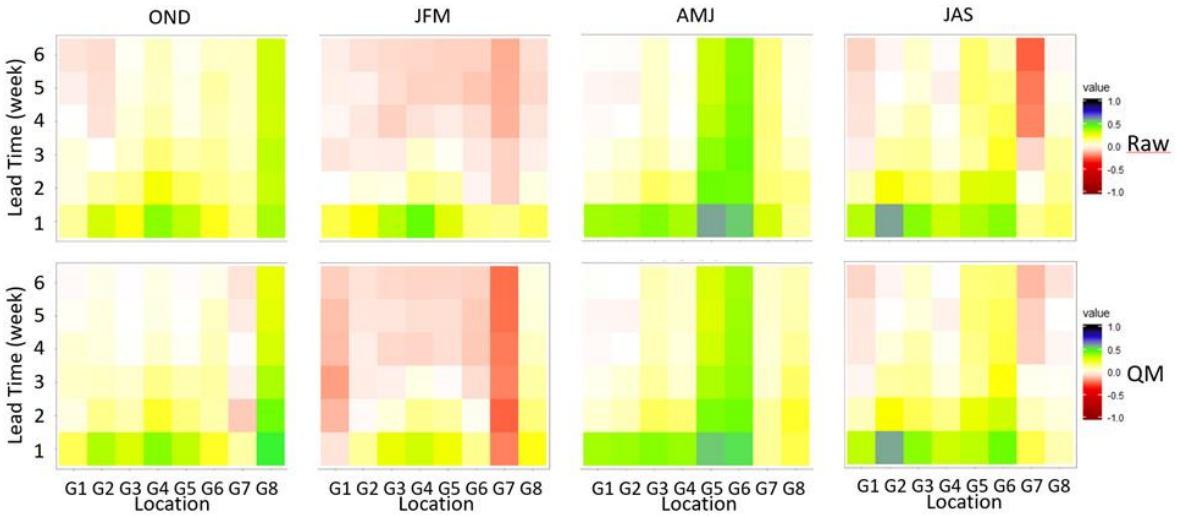

Figure 5.2– CRPS Skill score (CRPSS) of the raw (top) and QM bias corrected (bottom) catchment precipitation forecasts of the ensemble ECMWF S2S model (period 2015-2020), for lead-times 1 to 6 weeks and the 8 groups of river basins (G1 to G8). Graphs are separated by trimester from wet to dry season (OND, JFM, AMJ, and JAS).

Figure 5.3 shows the spatial representation of the ECMWF S2S performance for the CRPSS metric and the first two weeks of lead time for the wet seasons (OND and JFM), for the raw and the bias corrected precipitation forecasts. There is a spatial pattern of CRPSS performance that shows better performance when we move towards the northeast direction, with basins in the north presenting a better performance than those in the west and south regions. In all regions, the results degrade at the second week of lead time, with the period JFM presenting the stronger decrease in performance. After the application of the QM bias correction, it is possible to see a small improvement in some basins (G1, G2, and G6). Improvements are higher at the second week of lead time, when the trimesters present the higher number of basins with improvements, especially the trimester OND.

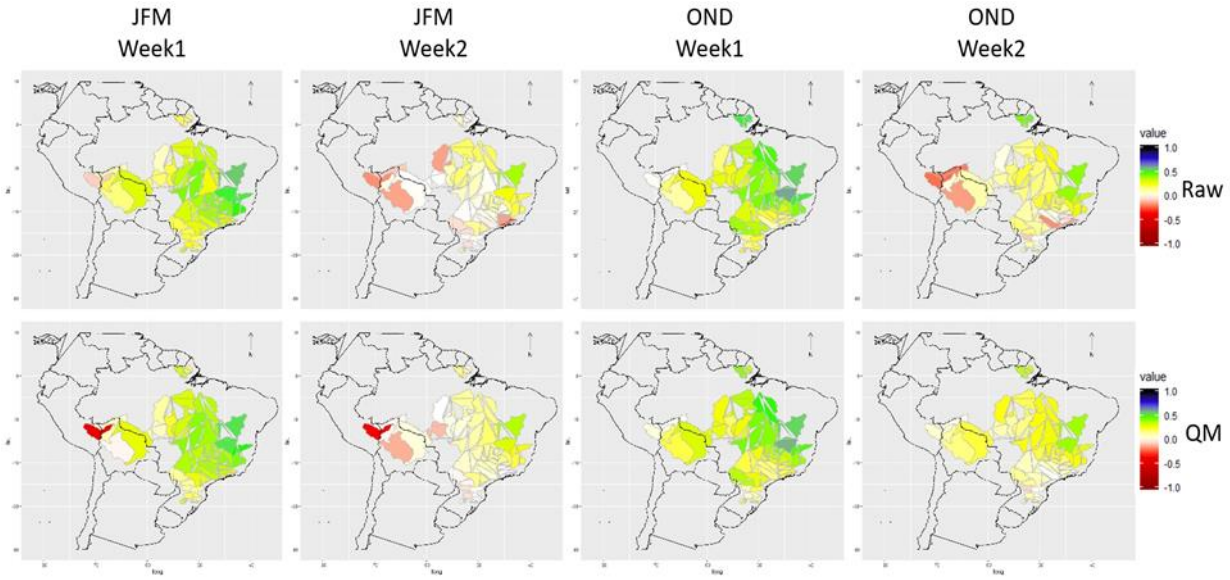

Figure 5.3 Spatial distribution of the CRPS Skill score (CRPSS) of the raw (top) and QM bias corrected (bottom) catchment precipitation forecasts of the ensemble ECMWF S2S model (period 2015-2020), for lead-times 1 and 2 weeks, all river basins and the wet seasons (JFM and OND).

Figure 5.4 shows the accuracy of the raw and bias corrected ECMWF S2S precipitation forecasts, as represented by the RME metric. Results are shown for the four seasons, the six weekly lead times, and the eight groups of climatic similar river basins. For the analyzed period (2015-2020), the raw forecasts show a tendency to underestimate the observed precipitation (negative RME values) at the first week for the majority of the basins, except those in the group G7. Considering only the wet seasons (OND and JFM), the tendency is inversed for groups G3 to G7 after the second week of lead time and raw forecasts tend to slightly overestimate the precipitation until the week 6. For the basins in group G8, at the extreme North region, the forecasts tend to underestimate the observed precipitation at all horizons and seasons. After the application of the QM bias correction method, the underestimation tendency of the first week is not corrected and, in some cases, it even increases in intensity. The forecast tendency to overestimate after the second week in the wet seasons for groups G3 to G6 becomes neutral or revert to a slight underestimation. For the basins in the group G7, the tendency revert to a slight underestimation of the precipitation, while for those in the group G8 the underestimation is reverted to a slight tendency to overestimate the observed precipitation.

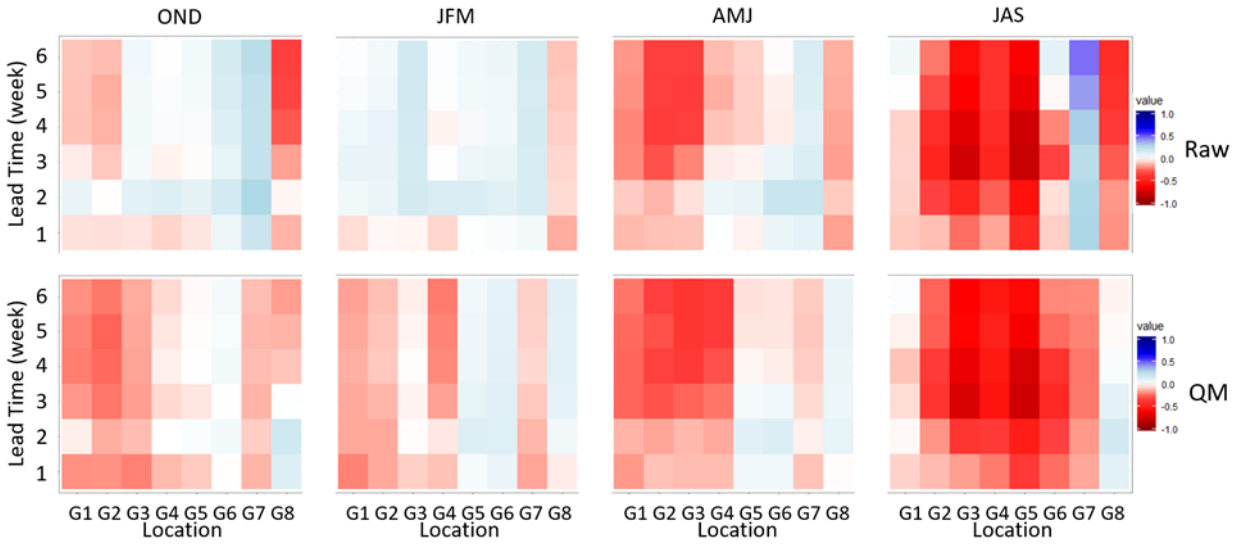

Figure 5.4– RME of the raw (top) and QM bias corrected (bottom) catchment precipitation forecasts of the ensemble ECMWF S2S model (period 2015-2020), for lead-times 1 to 6 weeks and the 8 groups of river basins (G1 to G8). Graphs are separated by trimester from wet to dry season (OND, JFM, AMJ, and JAS).

We also analyzed the impact of the bias correction of the raw forecasts on their reliability and resolution using the decomposition of the BS score (graphs not shown here). The application of the QM bias correction method did not visibly change the performance of the forecast model. Forecasts present better performance in terms of resolution at week 1 of lead time in all basins and seasons, with results degrading from week 2 onwards. The analysis of the correlation coefficient (also not shown here) also indicated no visible impact of the bias correction method. Correlation coefficients were higher than 0.7 for all basins at the first week of lead time and higher than 0.5 for the majority of the basins at the second week. For longer horizons, the values become lower than 0.25 for the majority of the basins.

5.3.2 Performance of the short-term precipitation forecasts using the historic hindcast (structural bias calibration)

Figure 5.5 shows the overall performance of the raw and bias corrected ECMWF EPS precipitation forecasts with the metric CRPSS, for the four seasons, week 1 and week 2 lead times and for the eight groups of river basins. The period 2007-2016 and the historic hindcast (structural bias calibration) were used to calibrate the bias correction parameters of the QM method. We can see that almost all basins have a good performance at the first week of lead time, which is reduced at the second week, with the exception of group G7, the Madeira river, which presents a performance that is worse than that of the climatology already at the first week lead

time, especially at the wet seasons (OND and JFM). After the application of the bias correction, we have an improvement in forecast performance in all basins and lead times.

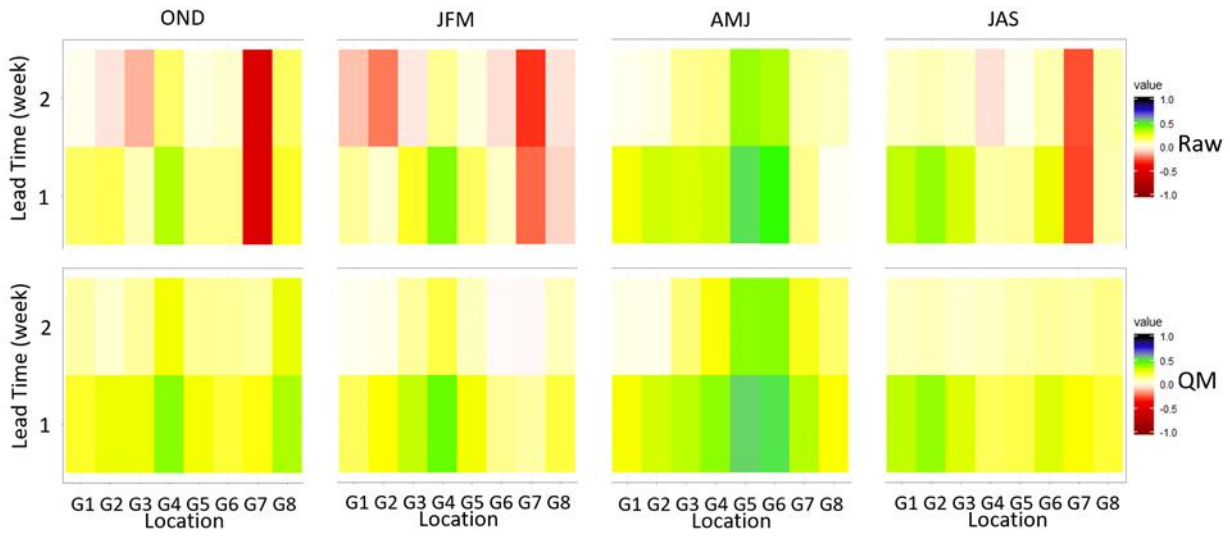

Figure 5.5 – CRPS Skill score (CRPSS) of the raw (top) and QM bias corrected (bottom) catchment precipitation forecasts of the ensemble ECMWF EPS model (period 2007-2016), for lead-times 1 to 2 weeks and the 8 groups of river basins (G1 to G8). Graphs are separated by trimester from wet to dry season (OND, JFM, AMJ, and JAS).

Figure 5.6 shows the results for the RME score. We can see that raw forecasts tend to overestimate the precipitations during the wet season (OND and JFM), for the majority of the basins. The exceptions are the basins from group G8, at the extreme North region, where a tendency towards underestimation is seen in all seasons and lead times. Raw forecasts tend to underestimate precipitations during the dry season (AMJ and JAS). After the application of the bias correction, the overestimation tendency of the basins during the wet seasons becomes a slight underestimation, and the overestimation from the forecasts in the basins from group G8 is reduced. The tendency of overestimation during the dry season persists even after the bias correction. Since the precipitation values are very small during this season, at some places almost near to zero, this tendency might not be a problem for flow forecasting and water resources management.

Figure 5.6 – RME of the raw (top) and QM bias corrected (bottom) catchment precipitation forecasts of the ensemble ECMWF EPS model (period 2007-2016), for lead-times 1 to 2 weeks and the 8 groups of river basins (G1 to G8). Graphs are separated by trimester from wet to dry season (OND, JFM, AMJ, and JAS).

Here again, the application of the QM bias correction method did not change the performance of the forecast model in terms of reliability, resolution and when considering the correlation coefficient (not shown). Forecasts tend to present better performance at week 1 of lead time in all basins and seasons, with results degrading from week 2 onwards. For instance, the BS resolution score shows values superior to 0.5 at the first week lead time, and values lower than 0.2 from the second week onwards during the wet season. The analysis of the correlation coefficient (also not shown here) also indicated no visible impact of the bias correction method. Correlation coefficients were higher than 0.6 for all basins at the first week of lead time, with a clear reduction during the second week, and with worse results observed at the wet season for the trimester JFM.

5.3.3 Performance of the short-term precipitation forecasts using the 'on-the-fly' hindcast of the sub-seasonal model (conjunctural bias calibration) and comparison with the structural bias calibration

Figure 5.7 compares the performance of the bias correction methods for the short-term precipitation forecasts (week 1 and week 2 of lead time) when following the conjunctural (section 5.2.3) and structural (section 5.2.4) procedures. Here, the validation period is different from the QM calibration periods of the previous sections. In this section, we apply the bias correction to short-range forecasts from an independent period, 2017-2020. The eight graphs on the left side of figure 5.7 show the CRPSS results, with the first column showing the performance when the

QM bias correction is applied with parameters calibrated with the historical reforecast (2007-2016; section 5.2.4) (noted, ‘QM’), and the second column showing the performance when the QM bias correction is applied with parameters calibrated with the ‘on-the-fly’ hindcast of the sub-seasonal model (section 5.2.3), (noted, ‘QM - Hind’). The other eight graphs on the right side of figure 5.7 show the RME results, following the same presentation as in the CRPSS.

In general, the performance of the bias correction using the ‘on-the-fly’ hindcast is equal or superior to the performance of the bias correction using the historic reforecasts for the majority of the basins. In terms of accuracy (RME), the bias correction using the ‘on-the-fly’ hindcast performs better especially during the wet seasons, with a reduction of the errors in the majority of the basins.

Finally, we note that the performances were very similar, showing no visible difference between the two bias correction procedures, for the other skill scores analyzed (BS relative reliability, BS relative resolution and correlation coefficient; not shown here).

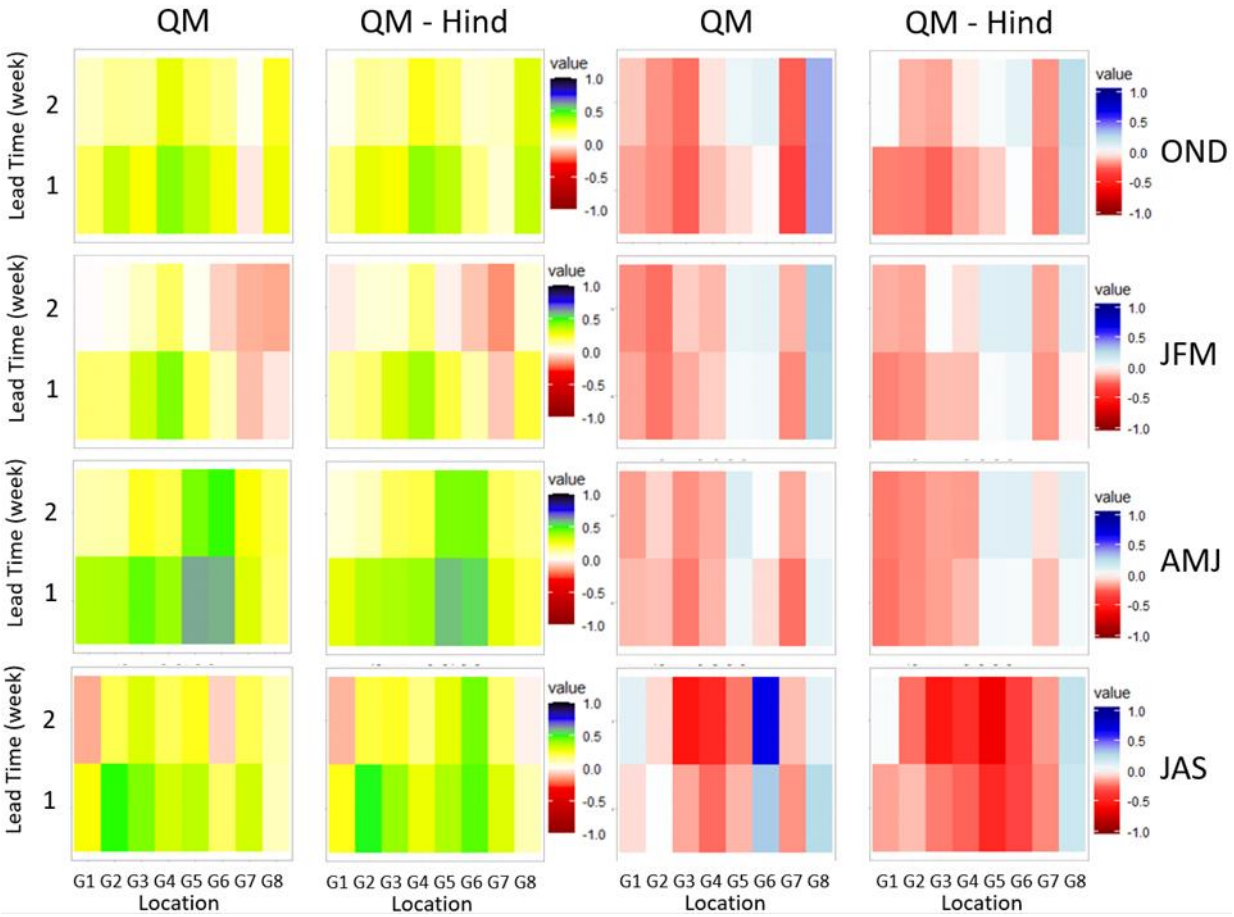

Figure 5.7 – CRPS Skill score (CRPSS) of the structural bias correction QM (first column) and conjunctural QM-Hind (second column), RME of the structural bias correction QM third

column) and conjunctural QM-Hind (fourth column) catchment precipitation forecasts of the ensemble ECMWF EPS model (period 2017-2020), for lead-times 1 to 2 weeks and the 8 groups of river basins (G1 to G8). Graphs are separated by trimester from wet to dry season (OND, JFM, AMJ, and JAS).

In order to analyze how the climatology of the observed precipitation period can impact the calibration of the bias correction parameters and, consequently, the analysis of the bias correction performance on the validation period (2017-2019) that is shorter than the calibration period (1996-2019), we present in figure 5.8 the monthly mean precipitation during the calibration period (top) and the validation (middle) periods, and the differences in precipitation between both periods (bottom) for the observed precipitation and all the river basins, ordered from South to North.

We can see that the wet season of the recent period (2017-2019) presents lower precipitation monthly values than the long period from 1996-2016. The wet months of December and January show a negative anomaly for the basins 10 to 25 (groups G3 and G4). The basins 26 to 34 (groups G5 and G6) and the basins 40 and 41 (group G8) present a negative anomaly for almost all months of the wet season. The basins 35 to 39 (group G7) show the first three basins with a positive anomaly and the last two basins with a negative anomaly. The basins 1 to 9 (groups G1 and G2), representing the basins of the south region, with no clear seasonality, also present more months with negative anomaly in the recent period when compared with the past period.

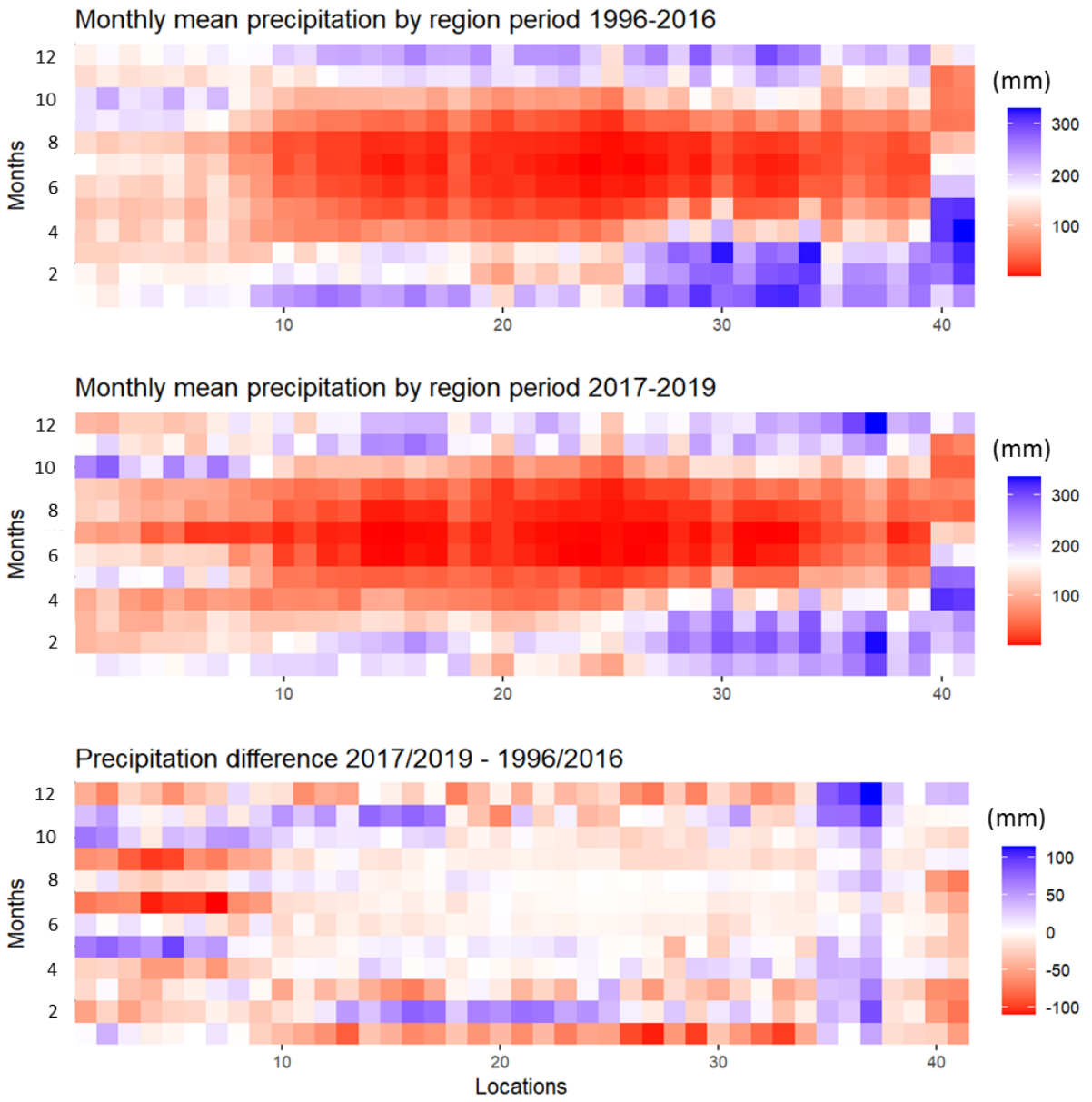

Figure 5.8 – Monthly mean observed precipitation during the calibration (1996-2016; top) and the validation (2017-2019; middle) periods, and differences in observed precipitation between both periods (bottom). The 12 months of the year are represented in the y-axis and the 41 river basins, ordered from South to North, in the x-axis.

5.4 DISCUSSION

Sub-seasonal precipitation forecast analysis

The performance of the ECMWF S2S was analyzed for its six weeks of lead time and considering the five-year period from May 2015 to Jun 2020. The overall performance of the raw forecasts assessed showed a good performance, with predictability superior to the observed climatology

until the third week of lead time for all basins in almost all seasons, but with a clear reduction after the second week. The exception is the JFM trimester, the most difficult to forecast, with a good performance only at the first week. There is a visible reduction of the reliability at the second week for this trimester, with practically all basins showing worse performance than the climatology after the third lead time week. The results also showed a slightly underestimation for the first week of lead time for most of the basins, with this behavior inverted at the second week lead time. For the basins located at the south region, the underestimation returns again and persists until the end of the forecasting horizon, at week six. The basins from group G7 present a tendency of overestimation in the whole forecast horizon and the basins from group G8 present exactly the opposite behavior. Our results are in line with the results presented by Coelho et al. (2018), where the authors assessed the performance of the ECMWF S2S and its hindcast with a framework of verification over the South America region, considering weekly accumulated precipitations. They evaluated the forecasts against the CPC observed precipitation, and their results also showed a reduction of the performance of the forecasts after the third week of lead time.

After the application of bias correction, the performance of the ECMWF S2S improved for most of the basins at the first week. However, for the next weeks of the forecast horizon, the results were very similar or, in some cases, even worse than the raw forecasts, especially for the trimester JFM (wet season). The overestimation biases were corrected and, in some cases, became a slight underestimation. At some basins (G1 to G6), the underestimation observed in the raw forecasts was not corrected, and it even became stronger in some cases.

These counter intuitive results, after the application of the bias correction, where the bias correction was not effective and, in some cases, bring even worse results, can be explained by the differences in the climatology of the observed precipitation during the longer, hindcast period 1996-2019 (in 20 years windows of the ECMWF on-the-fly hindcast), and the shorter, bias corrected period (2015-2020). When we look at the hindcast period, the model presents a tendency to overestimate the precipitations in most of the basins, and this tendency was also observed by Andrade et al. (2019) over South America. In addition, the past period of the hindcast was wetter than the recent period 2015-2020. Therefore, after the application of the bias correction, the results, in some cases, become worse, with the small overestimation of the raw forecasts becoming an underestimation, and also the underestimations being amplified.

Short-term precipitation forecast analysis

The analysis of the ECMWF-EPS precipitation forecasts, with 15 days of forecast horizon and data available from June 2006 to June 2020, also showed that the raw forecasts present skill superior to the observed climatology for the first week in most of the basins and seasons, with a reduction of the skill at the second week. The exception is the basins from the group G7 (Madeira river), which presented non-skillful forecasts even at the first week horizon. Forecast overestimation was detected for most of the basins during the wet season, and forecast underestimation was detected during the dry season, with the exception of the basins from group G8, at the extreme north region, where the forecasts tend to overestimate the observed precipitation during the whole year. After the application of the bias correction, the skill was improved in all basins and horizons and the over- or underestimations were reduced, following the same pattern as observed for the first weeks of the sub-seasonal forecasts.

Short-term bias correction comparison

One of the objectives of this study was to evaluate the possibility to correct the ECMWF EPS model with the parameters calibrated with the 'on-the-fly' hindcast of the ECMWF S2S model. This facilitates the use of the ECMWF EPS model in operational settings, without the need of changing a fixed bias correction procedure every time the meteorological model changes. The 'on-the-fly' bias correction, although it might be better, it is not necessary to have a long reforecast period of the operational forecast model to calibrate the parameters for the bias correction. This is because the 'on-the-fly' model automatically produces 20 years of hindcast at each run. Therefore, if the atmospheric model changes, to add new physics or configurations, it is possible to use the 'on-the-fly' hindcast to calibrate the parameters to correct both models (EPS and S2S), while one waits for a long term reforecast to be produced. With the 'on-the-fly' procedure, the user can bias correct (or not, it is their choice; for instance, they could apply bias correction during the wet seasons but skip the procedure during the dry season if this is in their interest) as the operational forecasts run in real-time.

We remind that the first bias corrected forecast is based on the parameters calibrated with the long term hindcast of the ECMWF EPS, with 51 members and a ten-year period (2007-2016). The second bias correction uses the parameters calibrated with the 'on-the-fly' hindcast of the ECMWF S2S, with 11 members, and 20 years of data. The analysis was performed over an independent validation period, 2017-2020.

The results showed that the ‘on-the-fly’ correction has performance equal or superior to the performance of the traditional correction with long term reforecasts. The ‘on-the-fly’ correction provides forecasts with smaller errors for the majority of the basins. Although this correction operates with less ensemble members, it performed better due to the longer historical period available (20 years as opposed to 10 years of the fixed, long term hindcast). Coelho et al. (2018) observed a similar behavior during their experiment, where they analyzed the performance of the ‘on-the-fly’ hindcast and the operational forecasts of the ECMWF S2S. The reduced number of members has not impacted the quality of the forecasts. In addition, the higher number of hindcast years, 20 in the on-the-fly, allows to capture better the variability of the climatology of the observed precipitation, and hence generate more robust parameters for the bias correction. This results highlighted the importance of the time window used to calibrate the parameters of the bias correction method, which seems to be more important than the number of members used to obtain the empirical density functions of the precipitation forecast used to calibrate the parameters.

5.5 CONCLUSIONS

This study presented an analysis of the performance of the ECMWF EPS and ECMEF S2S precipitation forecasts, assessing the capacity of these models to forecast weekly precipitation amounts in the 41 basins of this study, with special interest to energy production in Brazil and covering basins in practically the whole South America, from the subtropical to equatorial climate zones. The quality of the precipitation forecasts was analyzed in terms of the overall performance, accuracy, reliability, resolution and correlation, covering the lead times of one to two weeks for the ECMWF EPS and one to six weeks for the ECMWF S2S. The results of the application of the QM bias correction method to the forecasts of both models were also presented. We applied two procedures: the structural procedure for the bias correction of the ECMWF EPS using a long-term, fixed reforecast dataset, and the conjunctural procedure for the bias correction of the ECMWF S2S using its ‘on-the-fly’ hindcast dataset. Additionally, we applied the ECMWF S2S bias correction parameters to correct the ECMWF EPS short-term forecasts, comparing the results with the traditional (structural procedure) of bias correction. The main conclusions drawn from this study are presented below.

Sub-seasonal precipitation forecast analysis

- The ECMWF S2S model was able to produce skillful forecasts at least for the first three weeks of forecast horizon, and the ‘on-the-fly’ bias correction was able to improve the

quality of the precipitation forecasts, especially at the cases where systematic biases of overestimation or underestimation of the precipitations were observed in the raw forecasts.

- Spatially, the forecast model presented better results when moving towards the north-east direction in Brazil, and this was independent of the lead time.

Short-term precipitation forecast analyzes

- The short term ECMWF EPS model was analyzed for the period 2007-2016. It showed raw forecasts that tend to overestimate the observed precipitation during the wet season and underestimate it during the dry season. The raw forecasts were skillful at the first week horizon only, and, after the application of the QM bias correction, skillfulness was extended to the two weeks of forecast horizons, with also lower biases of under- or overestimation.

- When we compare the performance of the bias correction of the ECMWF EPS precipitation over the recent period 2017-2020, using parameters from both the long-term reforecasts (fixed period 2007-2016) and parameters from the 'on-the-fly' ECMWF S2S (moving window of 20 years prior to the forecast date), the bias correction using the 'on-the-fly' exhibited results equal or superior than the traditional fixed-period bias correction, based on ten years of reforecasts.

- The results obtained for the recent period (2017-2020) showed that the bias correction was not always very effective when compared to the performance of the bias correction over the longer 2007-2016 period. It was shown that this is probably because the shorter and recent validation period is not long enough to represent the variability of the climatology. The fluctuations of the interannual variation of the precipitation can affect the results of the performance metrics of skill. It is expected that, when we will have a longer period available for the validation of the bias correction over the operational forecasts (using forecast data after 2020), it will be possible to have a more robust analysis of the effectiveness of the bias correction.

Finally, it is necessary to take in account that the precipitation forecasts were compared against a near real-time observed precipitation dataset (see chapter 3). Although this dataset corresponds

to the best combination of two sources of precipitation, both based on satellite and gauge stations, uncertainties on the estimated precipitation remains over the basins, especially over areas with a sparse distribution of ground rain gauges as the North region of Brazil. Future studies with longer forecast periods and in-depth studies at specific regions or river basins with dense raingauge stations could be useful to confirm the predictive skill of the forecast models and the capacity of the bias correction to improve the quality of the precipitation forecasts coming from both ECMWF EPS and S2S models.

CHAPTER 6:

COUPLING THE DIFFERENT ECMWF FORECAST MODELS TO BUILD A SEAMLESS PRECIPITATION FORECAST FOR A GROUP OF SOUTH AMERICAN CATCHMENTS

This chapter will inspire a paper to be submitted to an international journal.

6 COUPLING THE DIFFERENT ECMWF FORECAST MODELS TO BUILD A SEAMLESS PRECIPITATION FORECAST FOR A GROUP OF SOUTH AMERICAN CATCHMENTS

6.1 INTRODUCTION

The seamless forecast idea could be translated into the simple concatenation of "the best" forecast at each lead time (Palmer and Webster, 1993). Pappenberger et al., (2013) wrote that "*the clear advantage of this off-the-shelf seamless prediction is that it utilizes products that are already in place, thereby avoiding the complications of new developments while generating forecast products to meet different types of needs*". As stated by Wetterhall and Di Giuseppe (2017), "*there is, however, an underlying complexity in this simplification, the substantial difference in design between the various forecasting systems makes the concatenation a task technically difficult. As systems are designed for different users, they often have non-matching temporal and spatial resolutions, different hindcast, different initialization frequency, and different ensemble sizes.*".

The concept of seamless forecast has applications in a wide range of time horizons, starting from very short-term forecasts, sometimes also known as nowcasting forecasts (Wang et el., 2017), generated with hourly updates nested with medium-term models, as the ECMWF EPS model (ECMWF 2015), or other intermediate models with different spatial and temporal resolutions, to build a seamless forecasting system, to be especially applied to civil protection (Wastl et al., 2018). Long term applications as climate change projections can also apply the seamless forecast concept (Solomon et al., 2007). Palmer et al. (2008) showed that the link between climate forcing and climate impact involves processes acting on different time scales, and the use of a seamless prediction system allows projections of climate change scenarios to be limited by validations on meteorological or seasonal forecast horizons.

In Europe, Wetterhall and Di Giuseppe (2018), with the objective of generating seamless hydrological forecasts with the European Flood Awareness System – EFAS (Thielen at al., 2019), compared the ECMWF seasonal forecasting system (SEAS4) and a merged system that assembled the ECMWF extended range forecasts (sub-seasonal) and the seasonal forecasting system SEAS4. The seamless system showed a better overall skill over most areas in Europe, with skillful lead times up to seven weeks. This increase in skill could be attributed to better

initial conditions of the hydrological and meteorological models, as well as a better atmospheric model version used in the sub-seasonal model of the seamless system.

Although seamless applications have been discussed since 1993, there is still a gap in the knowledge of the way to couple different models with different forecast horizons, number of ensemble members, spatial and temporal resolutions, frequency of initialization and target applications. Examples in the literature investigate how to apply a randomly selection to concatenate different models with different ensemble sizes to join the ECMMWF sub-seasonal and seasonal models (Wetterhall and Di Giuseppe, 2017); how to join the ensemble mean of the short-term model GEFS with the ensemble of the CFS seasonal forecasts (Yuan et al. 2014, Ye et al., 2017); or how to join models with different forecast horizons with a nowcasting model, by working with the probabilistic information of the time window that display the best performance of each of the models and extracting the most likely and other scenarios (Wastl et al., 2018). It is also possible to cluster the ensemble members of the models with different forecast horizons and distinct ensemble sizes and then generate an ensemble with a specific number of members, using a ranking method to order the ensemble members in a coherent way. This ranking can be based on a simple member-to-member coupling or on more sophisticated similarity methods that uses distance metrics, such as the Euclidean distance (Elmore and Richman, 2001).

Regardless the coupling technique used to generate seamless forecasts, it is crucial to ensure that the final system is coherent in space and time and provides a consistent forecast to users. Techniques using random selection for coupling ensemble members of different forecasting systems or techniques of statistical post-processing of model outputs (such as those used in chapters 4 and 5) can in certain cases result in incoherent forecasts. According to Schefzik (2017), many post-processing approaches for bias correction apply to a single weather quantity, at a single location, and for a single lead time only. Hence, they are incapable of taking inter-variable and spatial and temporal dependence structures into account. The rank dependence of the raw ensemble needs to be retrieved by combining the univariate post-processing techniques with specific ranking techniques such as the ensemble copula coupling (ECC; Schefzik et al., 2013). Essentially, ECC is used in ensemble calibration to preserve correlations. It aggregates samples from univariate post-processed predictive distributions obtained for each weather variable, location, and lead time separately, by reordering each individual sample according to the rank dependence pattern of the corresponding raw ensemble forecast. ECC has been a popular technique to issue physically realistic and consistent (in space and time) post-processed ensemble

weather and hydrologic forecasts (e.g., Bellier et al., 2018; Cassagnole et al., 2021). It can also be useful when coupling systems for seamless prediction.

In the context of the Brazilian electric system, where inflows to hydroelectric plants have a considerable weight in the planning of the electrical system operation, as well as a large weight in the energy price, computer models that optimize the system's operation, solving the hydrothermal dispatch problem (ONS, 2016), uses weekly flow forecasts for the first two operational months and monthly stochastic models from the third month to five years ahead (ONS, 2019). In our research work, we propose to use the ECMWF seasonal precipitation forecasting model (chapter 4) as input at a hydrological model to forecast flows two months ahead in a group of 41 South American river basins. However, the model issues daily forecasts every first of the month and, as the days pass, the initialization of the seasonal model becomes increasingly distant and the model loses performance until the next initialization. In this case, the solution to improve the results, until the next monthly run, is to couple the seasonal model with other models that have a shorter distance between two initializations. This is the case of the ECMWF EPS model (15 days ahead; initialized every day) and the ECMWF sub-seasonal model (46 days ahead; initialized twice a week), as seen in chapter 5. A seamless forecast can take the advantage of the higher frequencies of initialization of the short-term and sub-seasonal forecasts models, while also benefiting from the longer lead times of the seasonal model, in order to increase the capacity of the forecasting system to anticipate the changes in the atmosphere and better forecast the more intense precipitation events or the dryer periods occurring during the wet season.

In this chapter, we explore some techniques to couple the members of the different ECMWF precipitation forecasting systems, at their different forecast horizons, and investigate how to define a better way to build a seamless precipitation forecast. The idea is to couple the best part of each forecast horizon, aiming to obtain a better seasonal forecast, especially until two months of forecast horizon, that can be applied in hydrologic models.

Accordingly, the objective of this study is to answer the following research questions:

i. How can we create a seamless precipitation forecast with the three available ECMWF models (EPS, sub-seasonal, seasonal)?

ii. Does a more sophisticated coupling method perform better than the simple member-to-member coupling?

iii. Is it possible to improve the predictability of high anomalies of precipitation (positive or negative) for the next month by applying the seamless precipitation forecast?

This chapter is organized with the following sequence: materials and methods are presented in section 6.2; section 6.3 describes the results and section 6.4 presents the discussion. Finally, section 6.5 draws the conclusions of the analysis.

6.2 MATERIALS AND METHODS

6.2.1 Coupling structure

When coupling different forecast horizons from different forecast sources, there is a risk of changing the sharpness and the reliability of the coupled forecast by joining the same event of precipitation or drought forecasted at different times by the models and, as a result, to create a forecast with a dispersion that is higher or smaller than the dispersion of the original sources. The schemas in figure 6.1 illustrate two examples of what could happen when considering the evolution of accumulated precipitations in time: the shorter horizon model (in blue) and the model with the longer horizon (in red), both starting at the same time, are shown in the first graph (a); the second graph (b) shows a coupling order that creates a very wide dispersion of the precipitation at the end; the third graph (c) shows a coupling that, on the contrary, creates a sharper distribution of the precipitation at the end.

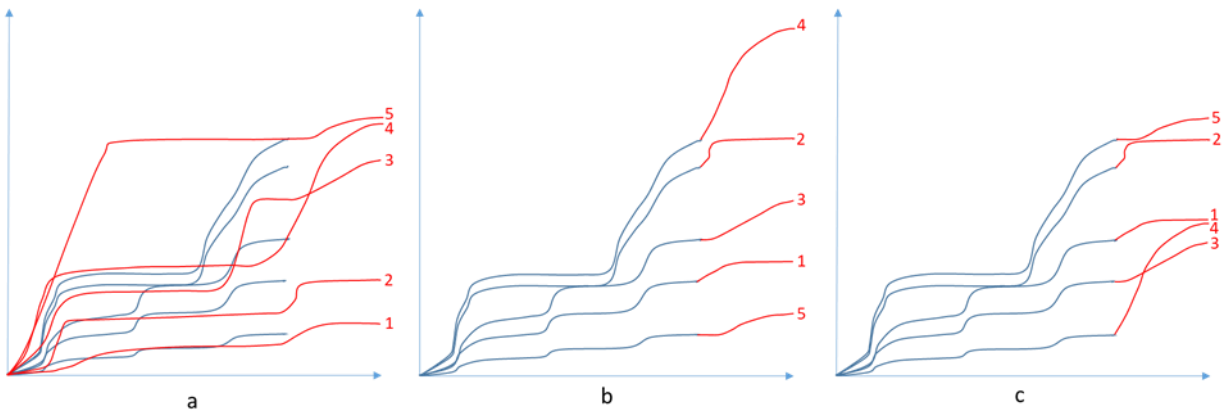

Figure 6.1 – Examples of the effects of coupling a shorter horizon model (in blue) with a longer horizon model (in red) with the same start time (a): we can have a coupling order that creates (b) a very wide dispersion of the accumulated precipitation, or (c) a too sharp distribution of the accumulated precipitation.

In this research, we will couple the three horizons of the ECMWF EPS, sub-seasonal and seasonal forecast models. Figure 6.2 shows an example of coupling the three forecast horizons along the 31 forecast days of January 2020. We have 31 initializations of the daily ECMWF EPS model (green), nine initializations of the ECMWF S2S model (blue) and one initialization of the ECMWF seasonal SEAS5 model (red). The last two colored lines indicate a seamless coupling for two forecast dates (5 January 2020 and 31 January 2020). On January 5th, the day of the month when each seasonal model run becomes available (in an operational mode), the seamless forecast has 211 days horizon, when we join the available runs of ECMWF EPS from January 5th, the ECMWF S2S runs from January 2nd and the ECMWF seasonal runs from January 1st. The last seamless run of January, on the 31st, is composed of the ECMWF EPS from this day, the sub-seasonal from January 30th and the seasonal run that is still the one from January 1st, resulting a seamless forecast with 185 days of forecast horizon.

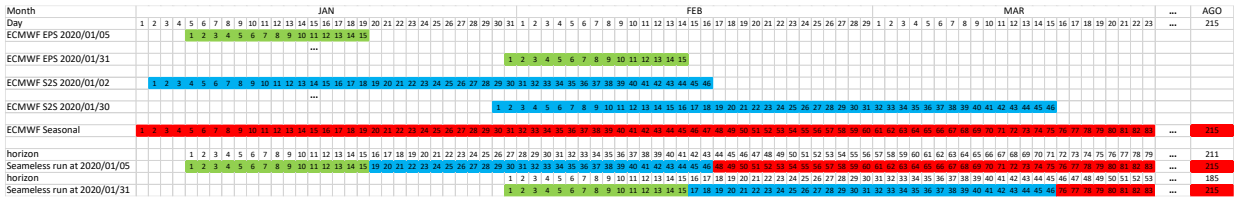

Figure 6.2 – Coupling scheme of the three ECMWF forecast models, EPS (green), sub-seasonal (blue) and seasonal (red), by joining their different forecast horizons to form a seamless run, with illustration for 5 January 2020 and 31 January 2020 (bottom lines).

6.2.2 Application of different methods to couple the models and build a seamless precipitation forecast

Based on the fact that the ECMWF EPS and ECMWF S2S forecasts are the same for the first 15 days (i.e., member 1 of ECMWF EPS is the same as member 1 of ECMWF S2S, with the same model structure and parametrization), and given that the forecast models lose skill as lead time increases (see chapter 5), there is an improvement in performance that can be expected by the more frequent daily model initialization of ECMWF EPS. Therefore, the models will be coupled every day member-to-member (0-0, 1-1, …, 50-50). This generates, every day, a 51-member ensemble forecast up to 46 days ahead, with ECMWF EPS in the first 14 days and ECMWF S2S from 15 to 46 days.

To couple the ECMWF sub-seasonal and the ECMWF seasonal forecast models, five blending methods are considered to build a seamless seasonal forecast. The methods are presented below

and vary from the simplest (a) to the most sophisticated (e) methods used to combine the models while avoiding the possible coupling problems shown in figure 6.1.

a) The first coupling method is the simpler member-to-member, where the control member of the sub-seasonal model is coupled to the control member of the seasonal model, member 1 of sub-seasonal coupled with the member 1 of seasonal, and so sequentially until the last member, considering the raw and bias corrected precipitation forecasts;

b) The second coupling consists of coupling the members of the raw sub-seasonal forecast, ordered by the volume of the last 15 days, with the accumulated precipitation of the same calendar days of the raw seasonal forecast;

c) The third coupling consists of coupling the members of the raw sub-seasonal forecast, ordered by the volume of the last 30 days, with the accumulated precipitation of the same calendar days of the raw seasonal forecast;

Methods b) and c) are based on the volumes of the last days of the sub-seasonal model. Two windows of accumulated precipitation are tested to calculate the volumes, the last 15 days and the last 30 days of the sub-seasonal model, considering the same calendar days of the seasonal model. We consider the raw precipitation forecasts, with members ordered from the wettest to the driest to obtain the order of the members of the coupled system. The wettest member of the sub-seasonal is coupled with the wettest member of the seasonal and so on, sequentially, until the driest members of the models. This order is used to build the raw and the bias corrected seamless forecast;

d) The fourth coupling consists of coupling using the Euclidean distance to calculate the similarity between the members to be blended considering the last 15 days.

$$d = \sum_{i=1}^{n} \sqrt{P_{Seasoi-}^{2} P_{S2Si}^{2}} \qquad (6.1)$$

where P_{Seasoi} is the accumulated precipitation of the seasonal model of day *i*, P_{S2Si} is the accumulated precipitation of the subseasonal model of day *i*, and *n* is the total number of days considered to calculate the Euclidean distance *d* between the accumulated precipitations.

e) The fifth coupling consists of coupling using the Euclidean distance to calculate the similarity between the members to be blended considering the last 30 days.

The last two methods d) and e) are the most sophisticated methods and are based on the daily similarity, using as a parameter the Euclidean distance between the member of each model, of the accumulated precipitation of the raw ub-seasonal forecast and the correspondent calendar period in the raw seasonal forecast, following the steps described below:

- To avoid scale distortions during the coupling process, the precipitation sum is standardized, dividing the values by the mean of the totals of the 15 and 30 days precipitation for each model;

- We then order the sub-seasonal from extremes, alternating the wetter and drier members until the median member (to reduce the chance to have a wet member of one model coupled with a dry member of the other, and to try to preserve the original sharpness of the forecast);

- Starting by the extremes (wettest, driest, second wettest, second driest, etc.), we obtain the sequence to couple the sub-seasonal forecast to the seasonal forecast, by calculating the Euclidean distance, as a reference of similarity. Starting by the distance between the wettest sub-seasonal member and the other 51 seasonal members, we select the smallest value and save the couple member numbers. The number of members available to couple will reduce at each coupling run, eliminating progressively the coupled members. At the next run, we use the driest sub-seasonal to calculate the Euclidean distance between the other 50 seasonal members available, and so sequentially until the last sub-seasonal member is coupled with the last member from the seasonal model. At the end of the interactions, we have a table coupling each sub-seasonal member with a corresponding member from the seasonal model.

6.2.3 Schema to evaluate the performance of the coupling methods

To evaluate the skill of the different coupled forecasts, the climatology of the combined observed precipitation dataset (see chapter 3), at each of the 41 basins, is used as a reference forecast (see details in section 2.6). The following strategy is used to evaluate the performance of the coupling methods that use the ECMWF sub-seasonal and ECMWF seasonal models:

- we compare the skill of the proposed blending methods by checking the performance at the second month lead time, considering the 30 days coupling period (first 15 days from sub-seasonal and last 15 days from seasonal) and the 10 days coupling period (5 days from sub-seasonal and 5 days from seasonal);

- we compare the inter-quantile distance considering the 10, 20 and 30 days coupling periods, with the values made dimensionless by the mean precipitation of the coupled ensemble, in order to allow us to compare different seasons and basins;

- we then evaluated the degree of coincidence of coupled members between the methods, in order to verify how different they are;

- we finally define the method to be used for the creation of the seasonal seamless forecast, by considering the computational costs and the benefits in terms of additional forecast performance.

After selecting the best method, the seamless forecast is compared with the seasonal forecast model according to the strategy below:

- we compare the performance by season of the first 10 days of the seamless forecast with the corresponding calendar period of the seasonal model;

- we compare the performance by season of the first 30 days of the seamless forecast with the corresponding calendar period of the seasonal model;

- we compare the performance by season of the second lead time month of the seamless forecast with the corresponding calendar period of the seasonal model

6.2.4 Application of the selected seamless forecast to predict precipitation anomalies during the wet season

To evaluate how the seamless forecast can help at the anticipation of atypical events during the wet season, we will consider three basins as case study: HPP Dona Francisca (South region), HPP São Simão (Southeast region) and HPP Tucurui (North region). We will consider the month of January 2019 (wet season), when a clear negative anomaly of precipitation happened in the North and Southeast regions, just after the occurrence of normal precipitations on the trimester

OND (anomalies of -7% at Tucurui and +16% at São Simão). At the same time, a positive anomaly happened in the South region.

In this case study, we evaluate how the predictability/assertiveness vary at each initialization of the sub-seasonal model when coupled with the seasonal model to generate the seamless forecast. We also evaluate the capacity of the forecasts to anticipate precipitation anomalies, when the seamless forecast model is compared with the seasonal forecast model.

6.2.5 Metrics to assess the forecast performances

The metrics used are the same that were presented in Chapter 4, section 4.2.4 for the evaluation of the precipitation forecasts, i.e., CRPS, RME, BSrel, BSres, Correlation coefficient. The reader is invited to refer to it.

Another metric used to evaluate the dispersion will be inter-quantiles distance, considering the quantiles of precipitation with probability of exceedance of 5% and 95% .

$$IQD = P(0.05) - P(0.95) \qquad (6.2)$$

6.2.6 The dataset and study area

The case study (41 river basins) and the observed precipitation data, averaged over the river basins' areas, used here are the same that were presented in chapter 4, section 4.2.1. The reader is invited to refer to it. We also remind that the combined real-time observed precipitation dataset was developed in chapter 3, by blending the gauged observed precipitation from CPC - NOAA (Chen et al., 2008) and the precipitation from TRMM-MERGE (Rozante et al., 2010). The combined precipitation, weighted by the uncertainty of the individual data sources, presented better results than the isolated use of each. The availability of the dataset is for the period from 1979 to 2020. This combined dataset was used in this chapter to evaluate the seamless precipitation forecasts. The ECMWF SEAS5 – seasonal forecast with 7 months horizon (ECMWF, 2017), used here is the same present in chapter 4, section 4.2.2. The ECMWF EPS (15days horizon) and the ECMWF S2S (46 days horizon) (ECMWF, 2017), used here are the same present in chapter 5, section 5.2.2. The reader is invited to refer to it. The ECMWF forecast models were used in this chapter to build the seamless precipitation forecasts.

6.3 RESULTS

6.3.1 Selection of the best coupling method

Figure 6.3 shows the CPRSS results for the five coupling methods. For each graph in the sequence: Euclidean distance 15 days (red), Euclidean distance 30 days (brown), Member-to-Member (green), Volume of last 15 days (blue) and Volume of last 30 days (pink), for the window of days 30 to 60 (the five graphs on the left) and days 40 to 50 (the graphs on the right). The analyses are for the complete year (first row) and also the four seasons (second to fifth rows) (October, November, and December - OND; January, February, and March - JFM; April, May, and June - AMJ; July, August, and September - JAS). The box-plots summarize the results of the 41 basins pulled all together.

From this figure, there is no visible difference in performance between the methods; the results in terms of median and quartiles are very close for all the methods analyzed. The same pattern is observed when we analyze the results individually at each basin (not shown here).

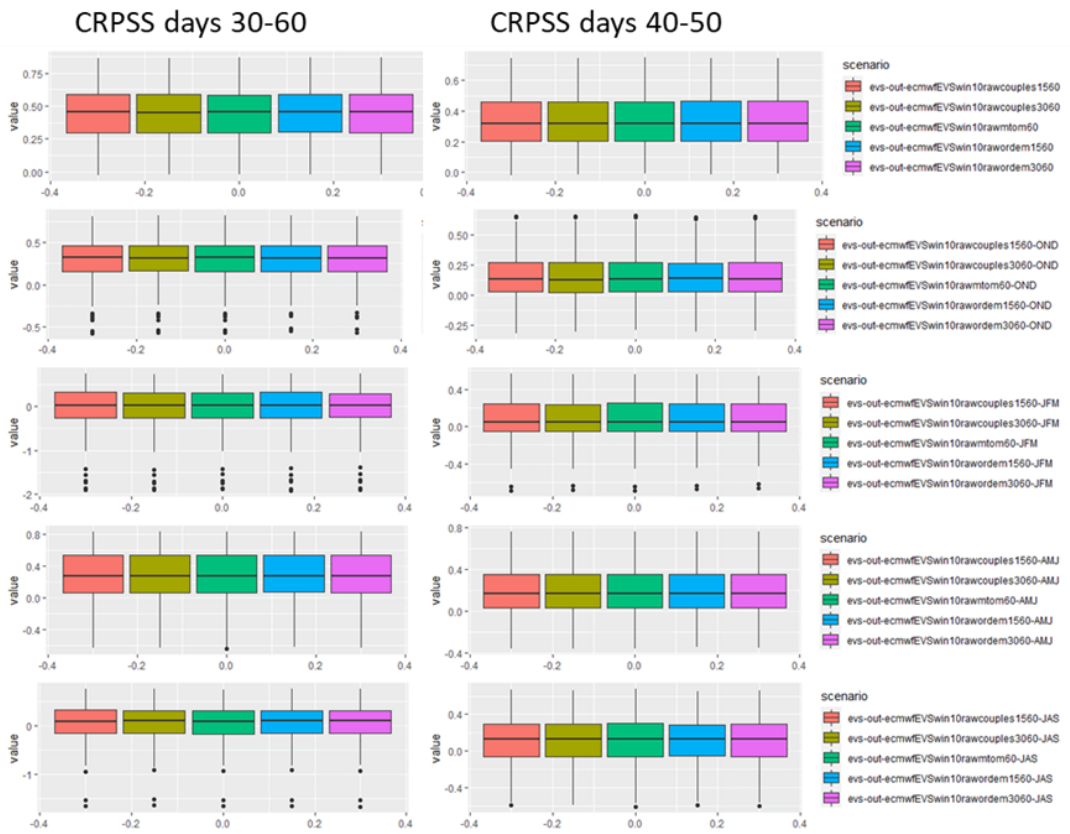

Figure 6.3– CPRSS for the coupling time window of 30 days (left column) and 10 days (right column), for the complete year (first row) and for the seasons OND, JFM, AMJ, JAS (second to

fifth row), and the methods Euclidean distance 15 days (red), Euclidean distance 30 days (brown), Member-to-Member (green), Volume of last 15 days (blue) and Volume of last 30 days (pink).

To have an overall visualization of the results, figure 6.4 summarizes the results for the five coupling methods (1-Euclidean distance 15 days, 2-Euclidean distance 15 days, 3-Member-to-Member, 4-Volume last 15 days and 5-Volume last 30 days) tested for the metrics CRPSS, Coefficient of correlation, Relative resolution, Relative reliability and RME. The values are dimensionless, i.e., they were divided by the mean of the results for each season, and are represented by the lines with different colors (light blue represents the complete year, dark blue OND season, yellow for JFM, orange for AMJ and gray for JAS seasons).

For the CRPSS, the relative differences are lower than 10% compared to the average of the coupling method performances. The performance varies depending on the season and there is not a method that performs better than the others in all periods. The coefficient of correlation, the relative resolution and the relative reliability show average differences in performance of around 5%, and again there is not a method that performs better than the others in all periods. The RME shows that the differences in terms of accuracy are lower than 3% between the methods. Therefore, this figure indicates that, when the different seasons and metrics are compared, there is not a visible difference that could indicate a clear superiority of one of the coupling methods tested.

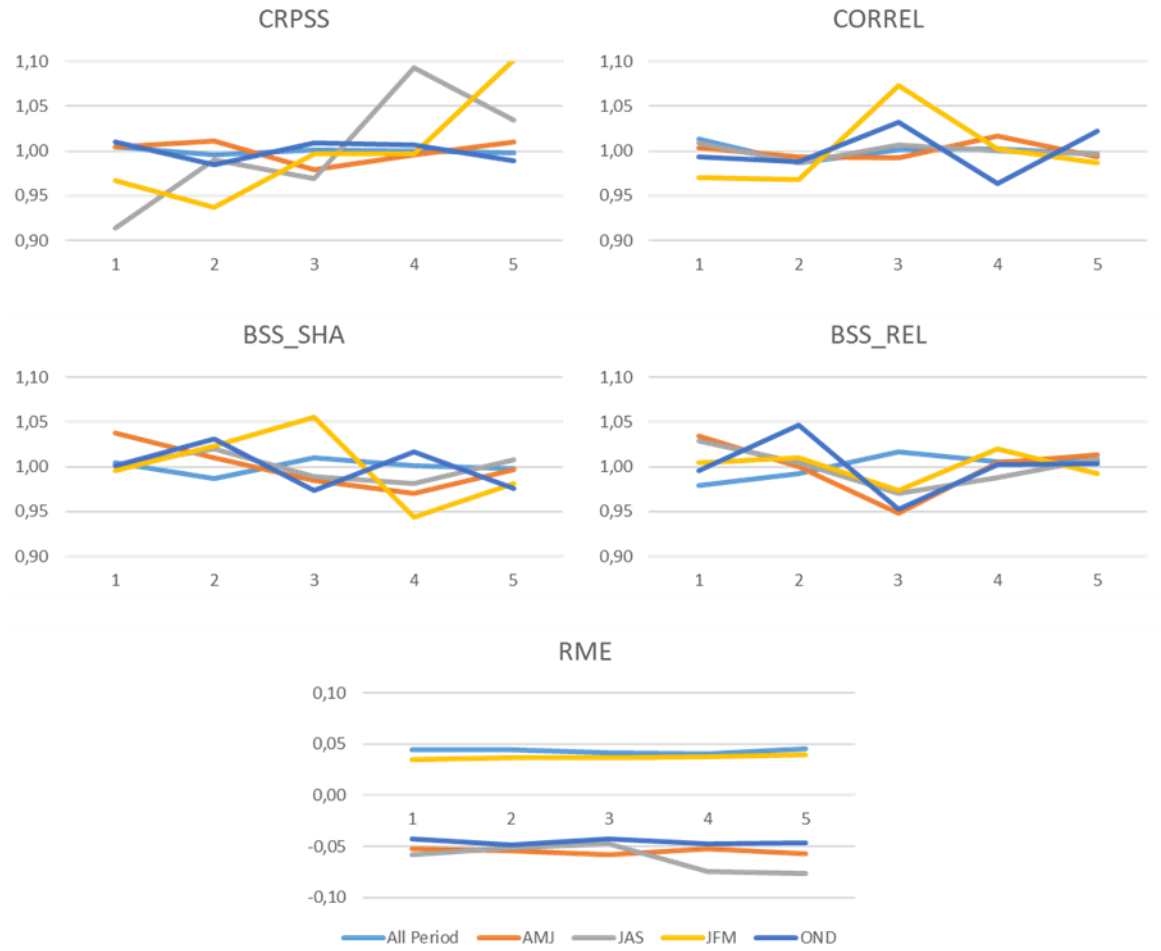

Figure 6.4– Evaluation of the five performance metrics, for the coupling time window of 30 days, the four first metrics the values are divided by the mean value, with different colors for the results considering the complete year and the seasons OND, JFM, AMJ, JAS; the x-axis represents the different coupling methods (1-Euclidean distance 15 days, 2-Euclidean distance 15 days, 3-Member-to-Member, 4-Volume last 15 days and 5-Volume last 30 days).

The last metric applied to evaluate the performance of the coupling method is the inter-quantile distance, applied to all 41 basins. Figure 6.5, shows examples for 3 basins representing the regions South (HPP Dona Francisca), Southeast (HPP São Simão) and North (Tucurui), for the results of the inter-quantile distance, considering the percentiles of 5% and 95% of exceedance, for the coupling windows of 10, 20 and 30 days; the values were dimensionless by the mean precipitation of each window.

We can see that the dispersion of the ensemble members, at each window of analysis for 10, 20 or 30 days, does not change significantly when the coupling method applied changes; the median and the quartiles remain very similar. This behavior observed at these three basins is the same observed at the other 38 basins studied.

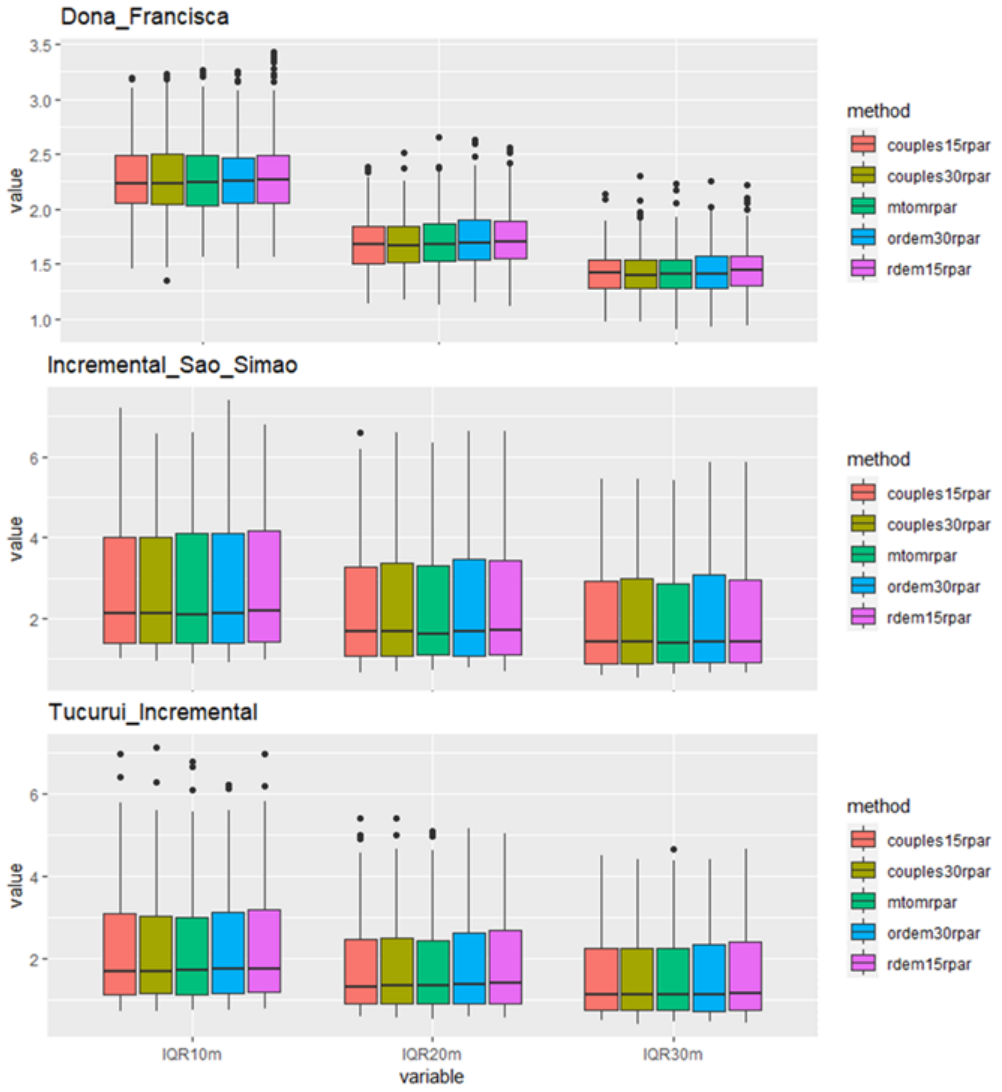

Figure 6.5– A sample of three basins, of the evaluation of the inter-quantiles distance (P 0.05 and 0.95), the values are dimensionless by the mean of each period of 10, 20 or 30 days, for the five methods: Euclidean distance 15 days (red), Euclidean distance 30 days (brown), Member-to-Member (green), Volume of last 15 days (blue) and Volume of last 15 30 days (pink).

When we compare the six metrics presented before, the results are very similar, independently of the coupling method. This can rises a doubt if the coupled members are really different for each method. Table 6.1 shows the degree of coincidence between the members of each method applied. As we can see, the coupling order is very different at each method, and the degree of coincidence varies by 2% to 4%, which is very small. Considering the 51 members available, this translate into having one or two coupled members identical in the methods, while all the others are completely different. Therefore, the similarity observed in the performance results cannot be due to a coincidence of having the same coupled members in all methods.

After comparing all the results presented previously, we can say that there is no significant difference between the coupling methods applied. The method which presents the best cost-benefit ratio for operational uses is thus the Member-to-Member method, since there is no high computational or mathematical cost to apply it and, in addition, it is a simple method that avoids intense data manipulation to create the seamless forecast, which could be another source of errors brought into the process.

Table 6.1 – Matrix with the degree of coincidence between the members of each coupling method applied.

	Member to member	Volume 15 days	Volume 30 days	Euclidean Similarity 15 days	Euclidean Similarity 30 days
Member to member	100.0%	2.0%	2.0%	2.0%	2.0%
Volume 15 days	2.0%	100.0%	4.1%	3.8%	2.3%
Volume 30 days	2.0%	4.1%	100.0%	2.4%	3.8%
Euclidean Similarity 15 days	2.0%	3.8%	2.4%	100.0%	2.8%
Euclidean Similarity 30 days	2.0%	2.3%	3.8%	2.8%	100.0%

6.3.2 Comparison of the seamless forecast with the seasonal forecast

Figure 6.6 shows the CRPSS performance comparison, for the raw forecast, between the seamless forecast (in red) created by the member-to-member method and the Seasonal forecast (in blue), for three time windows, the first 10 days, the first month and the second month, considering the runs of the seamless along the first month of the seasonal model. The analysis are separated in complete year and the four seasons (OND, JFM, AMJ and JAS) to facilitate the evaluation of the wet season.

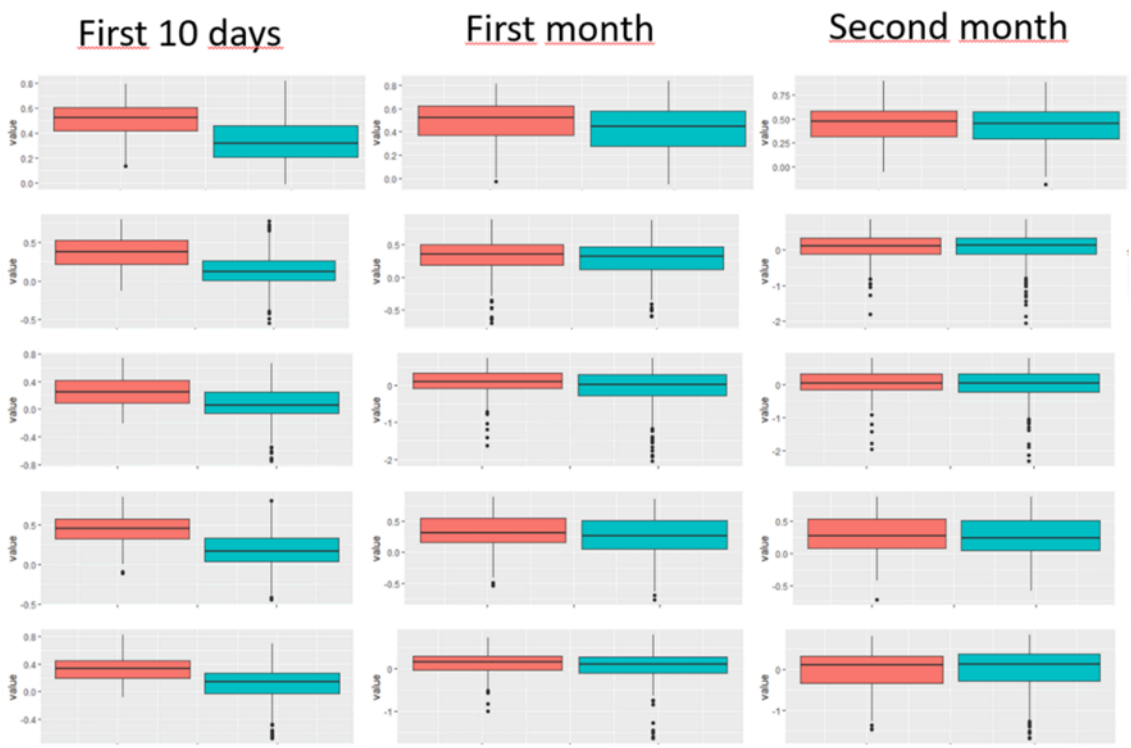

Figure 6.6– The CRPSS performance comparison between the seamless (in red) and the seasonal (in blue) forecasts, for three time windows, the first 10 days, the first month and the second, considering the runs of the seamless along the first month of the seasonal model. The first line of graphs represents the total year analyzes and the other four lines of graphs represent the seasons OND, JFM, AMJ and JAS, sequentially.

As we can see, the highest difference between the seamless and the seasonal forecast appears when we evaluates a shorter time window of 10 days, where we have the highest accuracy of the models. When the first month lead-time is analyzed, the difference in performance reduces but the seamless model still better than the seasonal. When we look at the second month lead time the two models have similar performance, with the seamless slightly better than the seasonal. The results are very similar when we evaluate only the wet season, but at the second month lead time the results becomes closer.

The same analysis was done for RME, the behavior of the performance is very similar to the CRPSS, with the difference between the seamless and the seasonal reducing with a longer lead-time. However, when we look at the wet season, this difference of performance at the shorter lead-time is less evident than we find at the CRPSS. The relative reliability presents the same behavior of the RME metric.

When we evaluate the relative sharpness and the correlation, the results become more similar to the CRPSS metric, with a clear better performance at a shorter lead-time, reducing the differences

when the horizon increases and at the second month lead time the performance becomes very similar.

The results are then evaluated after apply the bias correction at the forecasts. Figure 6.7 shows the CRPSS and RME performance comparison, for the first month lead time and for the wet season, between the Seamless (in red) and the Seasonal (in blue) forecasts, the bias corrected forecast graphs are in the first column and the raw forecasts results are presented at the second column, considering the runs of the seamless, along the first month of the seasonal model, for the period of January/2017 to May/2020.

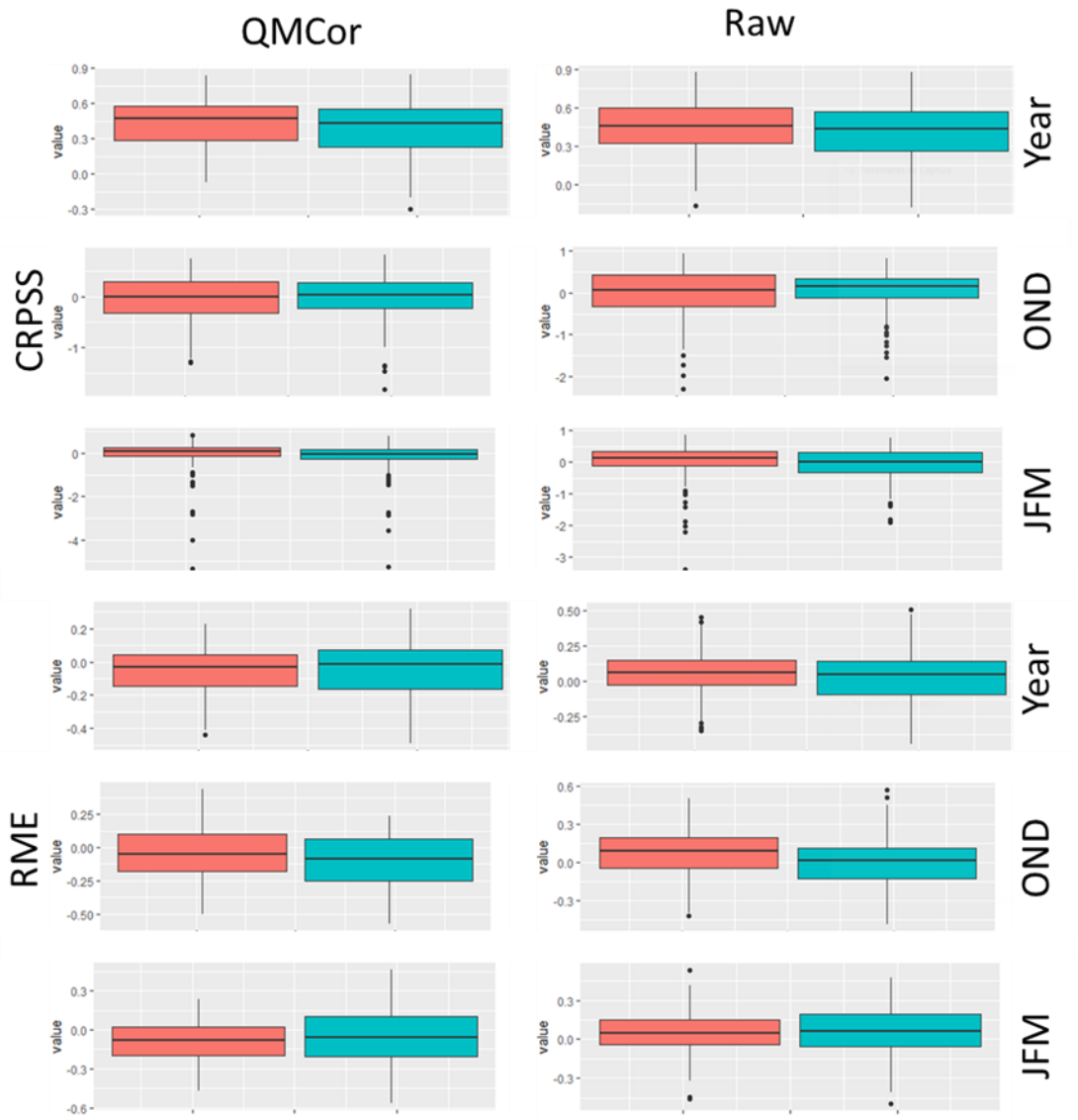

Figure 6.7– The CRPSS and RME performance comparison, for the first month lead time and the wet season, between the Seamless (in red) and the Seasonal (in blue) forecasts, with the bias corrected forecast in the first column and the raw forecast at the second column, considering the runs of the seamless along the first month of the seasonal model.

As we can see at the figure, the CRPSS of the bias corrected forecast did not improved significantly in the analyzed period, but the corrected seamless forecast still performing better than the corrected seasonal forecast. On the other side, the RME was improved in both forecasts reducing the errors. At the trimester OND, after the bias correction, the seamless improves its performance showing more values closer to zero. At the trimester JFM, the correction changes a slightly overestimation to an slightly underestimation in both models. The seasonal forecast presents the median closer to zero but with a higher dispersion, in other hand the seamless shows a lower dispersion of the errors.

The analyzes of the other metrics relative sharpness, relative reliability and correlation showed that the bias correction did not improved this parameters, which still performing similar to the raw forecast, and the seamless forecast still slightly better than the seasonal model.

6.3.3 Case study: an application of a seamless forecast in January 2019

Figure 6.8 shows how the seamless forecast can help in the anticipation of high precipitation anomalies. We present a forecast of the accumulated precipitation for the month of January 2019, with (i) the run of the ECMWF seasonal model started on 1 December 2018 and (ii) the runs of the seamless forecast, with their nine initializations (twice every week) along December. The first column (left) shows the results for the seasonal precipitation forecast and the second column (right), the results for the seamless forecast. Results are for the HPP Tucurui in the North region (first row), the HPP São Simão in the Southeast region (second row), HPP Dona Francisca in the South region (third row). The box-plots indicate the distribution of the 51 members of the ensemble model and the red dots represent the observed precipitation for January 2019.

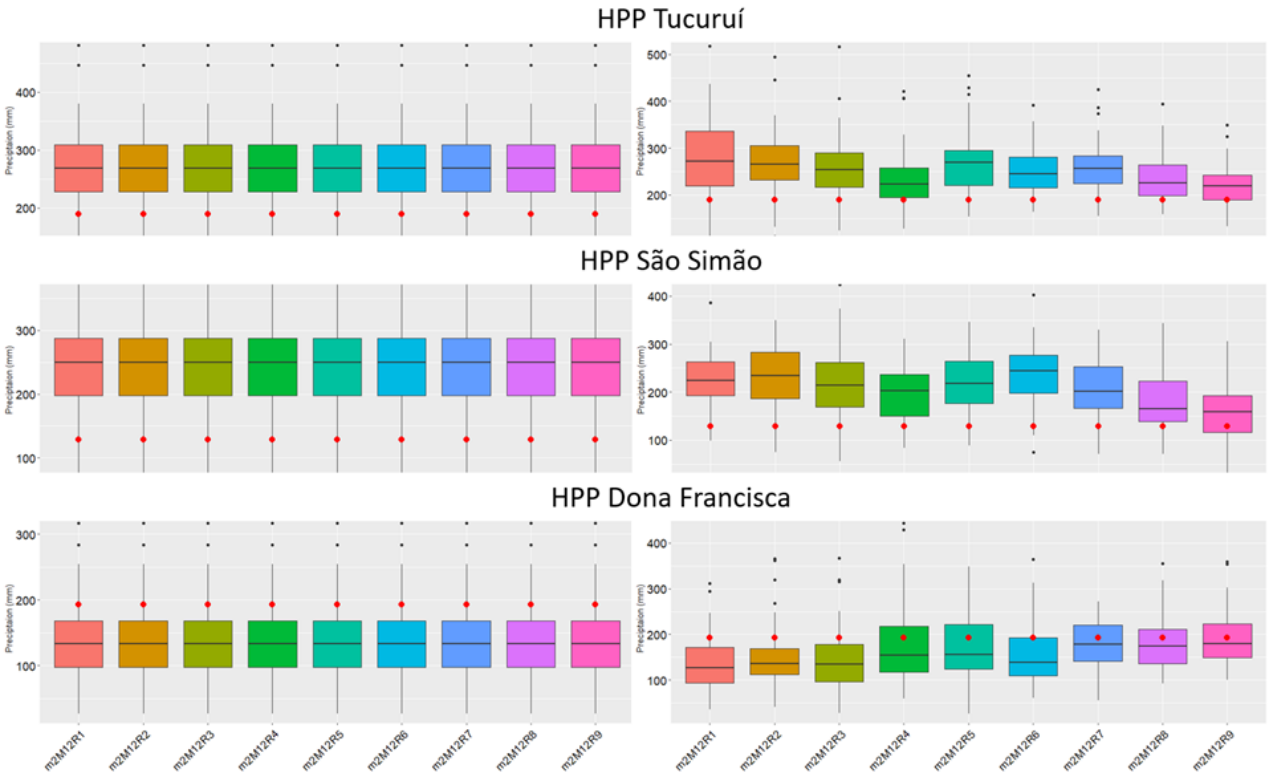

Figure 6.8 – Precipitation for the month of January 2019, with the comparison between the seasonal forecast (left column) and the seamless forecast (right column), for three basins representing the regions North (HPP Tucurui), Southeast (HPP São Simão) and South (Dona Francisca), considering 9 runs of the seamless model and the run of the seasonal along December 2018, the box-plot graphs show the distribution of the 51 members of each run and the red dots represent the observed precipitation in each basin.

As we can see, when we try to forecast the second month lead time (January 2019) with the seasonal model (box-plot m2M12R1, in red), which initializes on 1 December 2018 and remains unchanged, with the same forecast, until the next run on 1 January, the model forecasts an anomaly of precipitation opposite to what actually happened. On the other hand, the seamless forecast, which has new initializations along December (in this example, we show initializations twice a week in December, totalizing nine runs) captures better the anomaly. The first run of the seamless model (m2M12R2, in brown) is very similar to the seasonal model, however the subsequent runs (m2M12R3 to m2M12R9) tend to get closer to the observed value, with the median of the box-plot becoming near to the observation at each run. The seamless forecast presents fluctuations intrinsic to the model's behavior, as the model tries to capture the variations of the chaotic atmosphere in its runs. However, it is still possible to see that the forecast captures well the tendency of the negative anomaly for the basins of the HPP Tucurui (observed precipitation 28% below the average, considering the observed period from 1979-2017) and HPP São Simão (observed precipitation 47% below the average), as well as the positive anomaly at the HPP Dona Francisca (observed precipitation 19% above the average). After the third run of

the seamless forecast (m2M12R4), the model starts to show the correct tendency of the precipitation for the next month, and in the last three runs the signal of the anomaly becomes clear as well as its magnitude. The seamless forecast can anticipate the anomaly of the next month and its amplitude with almost two weeks in advance to the next run of the seasonal model (which in this example only comes on 1 January 2019).

6.4 DISCUSSION

We analyzed different ways to create a seamless seasonal forecast, coupling the three available horizons of the ECMWF models, and we evaluated the performance of each method to choose the best one. We also evaluated the capacity of the seamless forecast to anticipate precipitation anomalies when compared with the forecasts of the seasonal model. In the next paragraphs, the main results are discussed.

6.4.1 Selection of the best coupled method

To couple the three different horizons of the ECMWF models, five different methods to combine each ensemble member were tested. The simpler method is the member-to-member method, and the other four methods are based on the similarity of the model forecasts days before the moment of the coupling. Two methods are based on the accumulated volume of the precipitation considering the last 15 and 30 days, and the other two methods are based on the Euclidean distance of daily precipitations of the last 15 and 30 days.

To compare the performance of the different coupling methods, forecast evaluation metrics were used considering two time windows (10 and 30 days). The results from all metrics showed that in both time windows the performance was very similar. When we visualize the results over a whole year or even during each season, the results of the median and the quartiles of the ensemble forecasts are extremely close for the five coupling methods. Even when river basins are analyzed individually, the same behavior is observed. Differences in the mean CRPSS obtained with each method were lower than 10%, while other metrics indicated differences lower than 5% or even 3%. In addition, differences vary according to the seasons, with some times of the year one method performing better than the other. Therefore, it becomes clear that it is not possible to indicate that one method performs much better than the other, when considering all seasons and the analyzed metrics.

To investigate if the similar performance of the different methods was not due to the fact that, coincidently, they were coupling the same members, we evaluated the degree of coincidence of coupled members between the methods. The results showed that the couples formed within each method are extremely different, with a degree of similarity varying between only 2% to 4%. Considering the 51 members available, the coincidence is of 1 couple or at most 2 couples. The higher rate of same couples occur when the methods are based on the same method for defining similarity (volume or Euclidean distance) or with the time window (15 or 30 days).

With this observed evidences, the member-to-member method presents the best cost-benefit ratio for an operational use, since it presents equivalent performance when compared with more sophisticated methods and has low computational or mathematical cost, while it also avoids complex data manipulation procedures, which could bring additional sources of errors to the process.

Since the ECMWF EPS and the ECMWF S2S are the same model with only the forecast horizon extended (ECMWF, 2015), it was assumed that the coupling between them should be based on the member-to-member method, with no necessity to comparison its performance with other methods. This strategy also makes sense in the light of the results from the assessment of the coupling of the ECMWF S2S with the seasonal model, which showed that there is no reduction in performance when the member-to-member method is used.

6.4.2 Comparison of the seamless forecast with the seasonal forecast

After the definition of the best way to couple the different horizons, the member-to-member method was applied to the three ECMWF precipitation forecasts. The performance of the seamless forecast obtained was evaluated against the seasonal forecast for three different horizons (10 days, 1 month, and 2 months ahead), considering the raw and the QM bias corrected forecasts.

The analysis of the CRPSS metrics showed a clear superiority of the seamless over the seasonal, considering the first 10 days of forecast horizon. The superiority remains until the first month of lead time, but in a lower level. At the second month of lead time, the two forecasts practically exhibit the same performance, with a slight superiority of the seamless forecast. Other evaluation metrics exhibit the same general behavior, metrics evaluating accuracy and reliability exhibiting lower differences in performance at the shorter lead times during the wet season. These results

are in line with other authors who also found improvements in the predictability when coupling sub-seasonal to seasonal forecasts, and are explained by the higher number of initializations of the seamless forecast over the seasonal forecast (Wetterhall and Di Giuseppe, 2017; Wastl et al., 2018; Ye et al., 2017).

When we analyzed the QM bias corrected forecasts, the seamless forecast still performed better than the seasonal forecast, and followed the same behavior of the raw forecasts, but the differences in performance were smaller during the short period analyzed (January 2017 - May 2020).

6.4.3 Case study using the seamless forecast in January 2019

To evaluate how the seamless forecast can anticipate an anomalous event occurring during the wet season, in January 2019, in basins under different climates, we selected three basins to compare the results with the seasonal forecast, with the initializations occurring in December 2018. The seamless forecast was able to predict the negative precipitation anomaly that occurred in January in the basins of HPP Tucurui in the North region and HPP São Simão in the Southeast region, two weeks before the next run of the seasonal forecast, while the seasonal forecast predicted a positive anomaly, i.e., an anomaly with the opposite sign of the actual occurrence. For the basin HPP Dona Francisca in the south region, the seamless forecast was able to capture the signal of the positive anomaly earlier than it did in the other basins, with near three weeks before the next run of the seasonal model. Here again the seasonal model forecasted the opposite anomaly. The two forecasts showed similar performance only at the first or second weeks of lead time. However, with more initializations, the seamless forecast was able to capture better the tendency of the forecasts and also the amplitude of the anomalies. This result is in line with the results obtained by Andrade et al. (2018). The authors studied a group of S2S forecast models and obtained good results in the correlation between the observed precipitation anomalies and the mean of the ensemble forecasts until the second week of lead time for most of the studied models. For the ECMWF S2S, they found remarkable results until week three for the south region of Brazil, and until week four over the northern part of the northeast region of Brazil.

6.5 CONCLUSIONS

The first conclusion is that the seamless forecast can be done by coupling the three ECMWF forecast models (EPS, S2S and seasonal), to have a continuous daily precipitation forecast, with

a daily actualization. We recommend the use of the member-to-member coupling, which presents the best cost-benefit ratio, due the fact that other more sophisticated methods did not perform better than this simple method, which does not require a high computational effort or complex data manipulation.

The seamless precipitation forecast system presents better performance than the seasonal forecast model, and showed a better ability to anticipate, weeks ahead, the occurrence of high anomalies of precipitation during the wet season in Brazil. This capacity brings great opportunities for this category of forecast to future applications in hydrological models, in order to generate flow forecasts to improve the hydropower operation.

CHAPTER 7:

DEVELOPING SEAMLESS MEDIUM- TO LONG-RANGE FLOW FORECAST TO IMPROVE THE PREDICTION OF HYDROPOWER PRODUCTION IN BRAZIL

This chapter will inspire a paper to be submitted at HESS - Hydrological Earth System Sciences Journal

7 DEVELOPING SEAMLESS MEDIUM- TO LONG-RANGE FLOW FORECAST TO IMPROVE THE PREDICTION OF HYDROPOWER PRODUCTION IN BRAZIL

7.1 INTRODUCTION

The management of the water supply is of great importance for many human activities, as navigation, water supply, agriculture, tourism and especially in the context of operations in the Brazilian electricity sector, where the majority of its production comes from hydroelectric generation. Therefore, flow forecast is one of the main information to optimize the electric system. To obtain a trustworthy flow forecast is necessary to deal with many different sources of uncertainties. We have uncertainties from the observed precipitation data, which is one of the most difficult variable to estimate (Herold et al. 2015), where different sources of precipitation can presents huge differences depending on the cover density of the gage stations (Juárez et al., 2009; Demaria et al., 2011; Scheel et al., 2011; Falck et al., 2015; Mantas et al., 2015; Reis et al., 2019) and an way to deal with this, it is to combine different sources based on their individual uncertainty obtaining a more robust estimation of the precipitation, as done in chapter 3, where were combined the precipitation from the CPC-NOAA (Chen et al., 2008) and TRMM-MERGE (Rozante et al., 2010) to obtain a more reliable estimation of the precipitation over basins in South America. In the flow forecasts based on the GCM - General Circulation Models, the precipitation forecast is another important uncertainty source, due the chaotic behavior of the atmosphere the models are affected by the initial conditions (Kalnay, 2003; ECMWF 2015), to deal with this, the models migrated from the deterministic to probabilistic forecast, presenting better prediction results (e.g. Fan and Van de Doll, 2011; ECMWF, 2015; Hamill et al., 2006; Su et al. 2008; Medina et al. 2019). The GCM models are in constant improvement, but still remaining some uncertainties and systematic bias, and an application of post processors are an interesting way to improve the results of the forecasts (Verkade et al. 2013; Crochemore et al. 2016). In chapters 4 and 5, assessing the performance of the ECMWF models, over basins in South America, with interest to power generation, were applied different bias correction methods, and obtained better forecast results with the application of QM – Quantile Mapping method, for bias correction of the daily precipitation forecasts.

Another way to improve the forecasts, based om GCM models, it is to build a seamless forecast, this concept can be translated into concatenation of the best forecast model at each lead-time (Palmer and Webster, 1993). This method is used since in now-casting predictions (Wastl et al.

2018) or in a long time horizon like, applications in climate change studies (Solomon et al., 2007). In chapter 6 were explored on a wide forecast horizon, from days to months and applying different coupling methods, was selected the better way to joining the 3 different horizons of the ECMWF forecast models (EPS, Extended and Seasonal), building a seamless seasonal precipitation forecast for basins in South America, presenting better results in predictability than the original seasonal forecast, for the first two months horizon.

Invest in the treatment of the precipitation uncertainties is only the first part of the problem, still necessary to deal with the hydrological model uncertainty to have better results in flow forecast. It can be treated lumping this with the other uncertainties or separately from the meteorological uncertainties (Regonda et al., 2013), because it depends on the hydrological modeling process, caused, for example, by measurement and sampling errors, climate variability and determination of the initial and boundary conditions (Kim et al., 2021). There are some authors applying this approach, Krzysztofowicz (2002), Seo et al. (2006), and Demargne et al. (2014). There are different post processing techniques available to improve model prediction. The QM based on the cumulative distributions is one of the approaches (Shi et al., 2008; Madadgar et al., 2014), some approaches based on the Bayesian models (Krzysztofowicz and Maranzano, 2004 ;Brown and Seo 2010, 2013), and the generalized linear regression (Zhao et al., 2011). Besides of the existence of various studies on post processing of flow forecast, still necessary studies to evaluate its performance in big basins in a context of seasonal forecast.

Besides the flow post processing approach may corrects the hydrological model, still remaining the uncertainty of the observed precipitation, which affects the initial conditions of the forecasts. The data assimilation is an interesting technique to improve the real-time flow forecasts. In general, the assimilation of data can be grouped into three approaches, (1) where the inputs are changed, (2) the model parameters or (3) state update. In this two first approaches the Kalman filter is widely used to update the internal state and parameters of the system (e.g. Hsu et al., 2003; Moradkhani et al., 2005; Bloschl et al., 2008) and the last directly adjusts the outputs of the models regardless of what is happening internally (e.g. Lundberg, 1982; Lekkas et al., 2001; Xiong and O 'Connor, 2002; Broersen, 2007; Romanowicz et al., 2008; Wu et al., 2012; Liu et al., 2016; Tiwari et al., 2021; Yassin et al. 2021). Xiong and O 'Connor (2002) studied some data assimilation methodologies for error correction and verified that Auto-Regressive (AR) models presented better performance in correcting errors in flow prediction. Later, studies have shown that lower order models (2 or 1) were more applicable in predictions (Wu et al., 2012). The post

processors can improve the predictability of the forecasts and the use of a trustworthy flow forecast can help on the water resources management, especially when it is necessary to take anticipatory measures during the extreme events like droughts and floods.

The Brazilian electric system has a hydrothermal structure with centralized operation, where ONS – System National Operator defines the rules and the normalization to have an harmonic operation of the system, to attend the energy demand at the lowest price. This set of rules are in the Network Procedures, which organize all the information of the system operation, with the obligations of all agents involved at the operation of the system, the optimization and forecast models used, the consistence of all information, etc. (ONS, 2021). To sell all the energy produced, Brazil has two main energy markets, the ACR – Regulated Contract Environment, where the Federal Government, with energy auctions, attend the structural demand of the electric system and the demand of the distribution companies, responsible to sell energy direct to the captive consumers, and the ACL – Free Contract Environment, where the bigger consumers, with bilateral contracts buy the energy directly to the generators (CCEE, 2021). The commercial part of the Energy System is under the responsibility of the CCEE – Electric Energy Commercialization Chamber, where all the contracts are registered and also run the same models used by ONS to optimize the energy production, with a similar deck of information, but with the objective to calculate the PLD – Settlement Price of Differences, which is the price of the energy spot market, where all the energy produced attend the demand, but without contract with the ACL or the ACR, is remunerated by the PLD (CCEE, 2021). The optimization models take in account the predictions of the energy demand, the energy production of all available sources, hydraulic, thermal, solar, wind and others, the level of the reservoirs, and other information (Nascimento, 2021).

Besides the Brazilian electric system be hydrothermal, and year after year it is increasing the participation of other sources as solar and wind power, the energy production and its price still strongly dependent of the of the hydropower generation. Even during the sequence of drought years at the system, observed since the year of 2013, the majority of the energy still coming from hydropower, responsible for 76% of the energy production in 2016 (Paiva et al., 2020). In terms of time horizon, as shown in Figure 7.1, the needs of the hydroelectric system for accurate and reliable forecasts extent from forecasts up to a few days ahead for the balance of the electric grid (ONS, 2019), short-range from 1-7 days for flood control depending on the basin size, medium-range forecasts up to 7–30 days ahead for energy trading in the spot-market (CCEE, 2021), and

seasonal (months ahead) streamflow forecasts for electric system optimization, maintenance planning, water multiple uses management, long-term energy trading strategies.

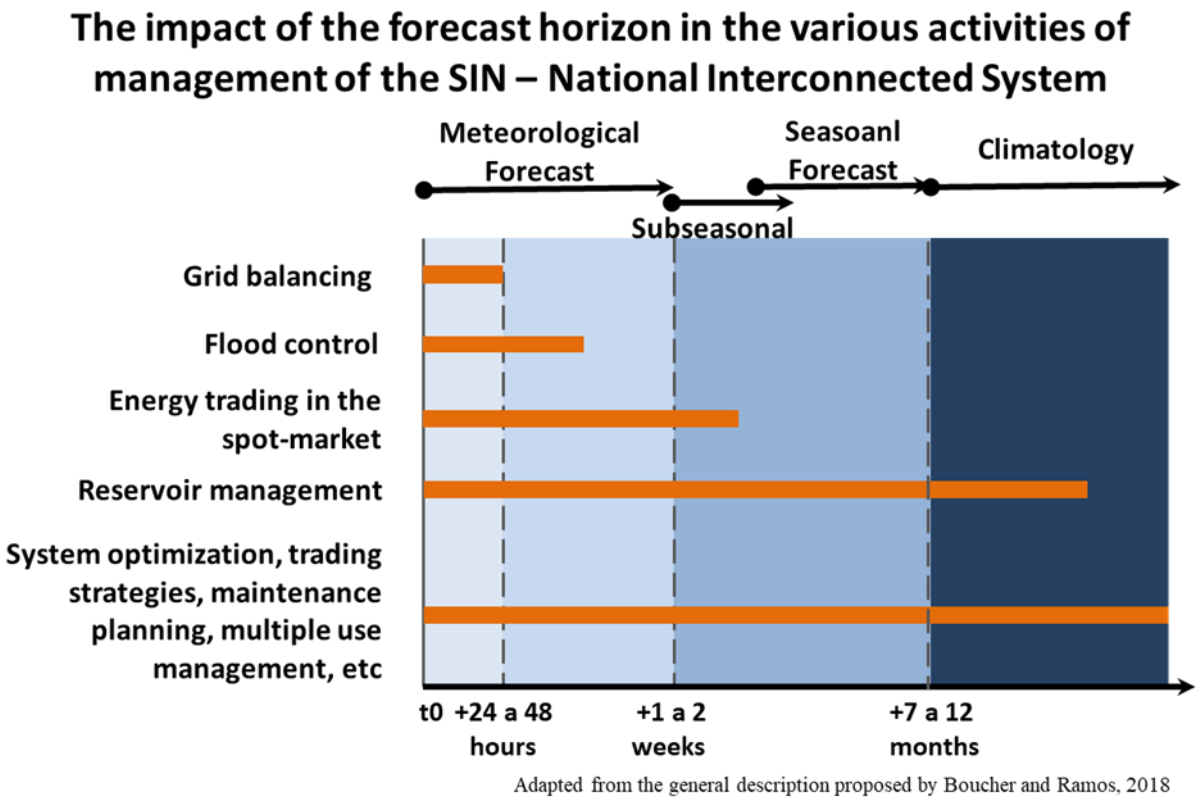

Figure 7.1– The impact of the forecast horizon in the various activities of management of the SIN – National Interconnected System (adapted from Boucher et Ramos, 2018).

At this experiment we explore some techniques to deal with uncertainties faced by hydrologists during the forecast activity, with the goal to generate a seamless seasonal flow forecast. Some of the steps as the treatment of the observed precipitation, the hydrological model calibration, the bias correction of the meteorological models and the coupling of the different horizons of the ECMWF models, after the application of the bias correction on the precipitation forecast were done in previous chapters. In this chapter we deal with hydrological uncertainty exploring some flow post-processors to improve the results of the flow forecasts and apply the results to predict the hydropower generation at the Brazilian electric system.

According the objectives, we answer the following research questions:

i. Can the application of the QM method correct the hydrological bias and improve the simulated flows?

ii. Can the application of the flow data assimilation at the output-error- correction technique deal with the uncertainty of the initial conditions and improve the flow forecasts?

iii. Does the proposed seamless flow forecast perform better than the traditional seasonal flow forecast?

iv. Can the use of the seamless flow forecast improve the prediction of the hydropower production in Brazil?

The chapter is organized with the following sequence, the materials and methods are presented in section 7.2, section 7.3 describe the results and section 7.4 presents the discussion. Finally, section 7.5 bring the conclusions of the study.

7.2 MATERIALS AND METHODS

7.2.1 The dataset and study area (the HPP Brazilian basins)

a. Precipitation forecasts

We use the precipitation forecasts obtained in chapters 4 (section 4.2.2) and 5 (section 5.2.2), based on the application of the QM bias correction method, at the daily precipitation, at the three forecast horizons of ECMWF models:

- The ECMWF seasonal SEAS5 (7 months), with the correction parameters calibrated with the reforecast from 1981 to 2016;

- Extended forecast ECMWF S2S (46 days), applying an on-the-fly bias correction with the parameters being calibrated every run with the 20 years on-the-fly hindcast and;

- The medium term ECMWF EPS model (15 days), correction using the parameters calibrated with the ECMWF S2S hindcast.

The three bias corrected ECMWF models, are coupled to produce a seamless precipitation forecast, using the member-to-member coupling technique to join the bias corrected precipitation forecasts. (for more details see chapter 6).

b. Observed precipitation

The observed precipitation, with the objective to have a more trustworthy dataset, is a combination of two observed precipitation sources, the TRMM-MERGE, with satellite information (Rozante et al., 2010) and the CPC – NOAA, a gauge based dataset (Chen et al., 2008), weighted by the uncertainty of each source, available from 1979-2021 (see chapter 3).

c. HPP streamflows

Observed flows

Daily natural discharge data were obtained from the ONS (the national operator of the electric system). They correspond to the official HPP natural flow time series, and compiled annually by the national operator (for more details, see ONS, 2005). Overall data availability depends on each river basin. For this study, the discharge dataset used covers the period 1979-2021 for all studied river basins.

Simulated flows

Daily simulated hydropower flows dataset came from the HEC-HMS hydrologic model, with parameters calibrated for the period from 1997-2017, using the combined precipitation weighted by the uncertainty, having as a reference the natural observed flow from ONS (for more details, see chapter 3).

The study area covers part of South America, divided in 41 river basins, to model 30 hydropower plants with great importance for hydroelectric generation in Brazil, with diverse climates and soil uses, with areas ranging from 9300 km² to 382000 km². Figure 7.2 illustrates the study area, with the basins delimited in red and the group with similar behavior in dashed black line.

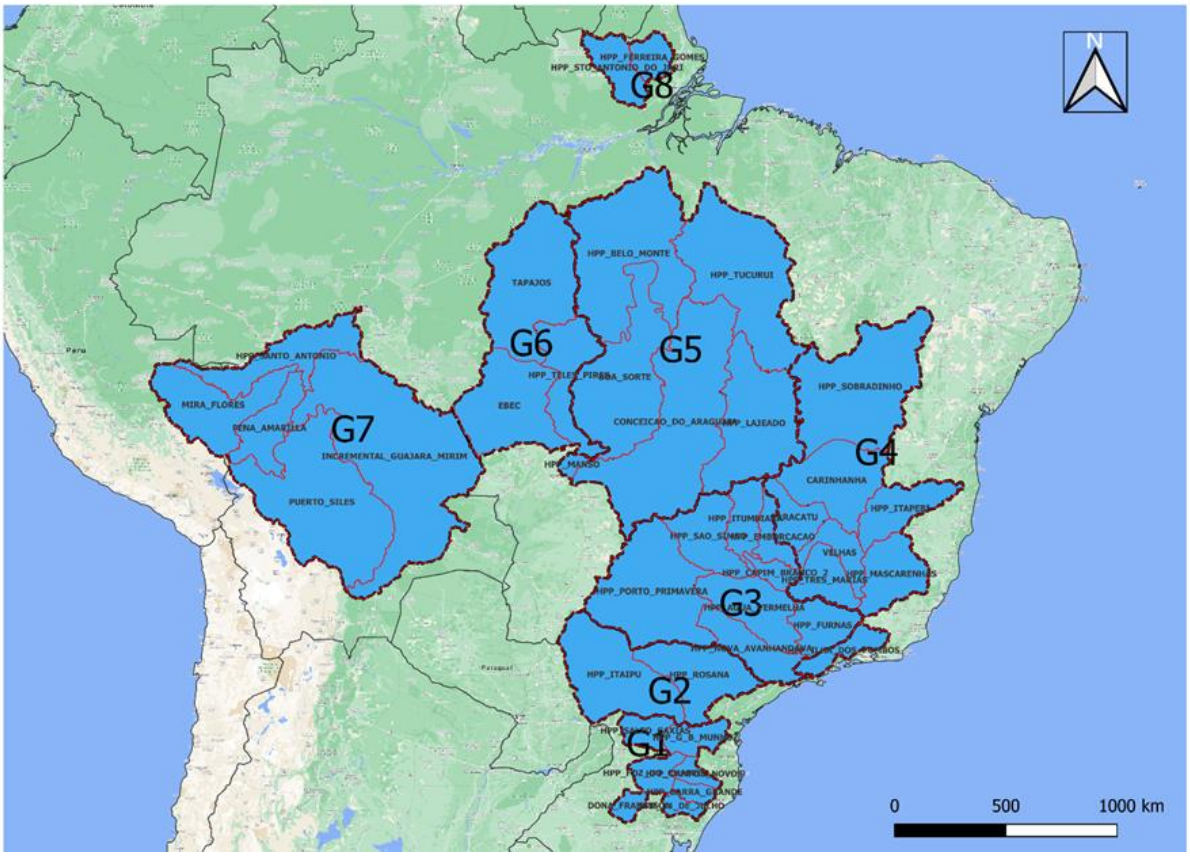

Figure 7.2– Geographic location of the study area composed by 30 HPP, with the basins delimited in red and the groups G1 to G8 delimited in dashed black line.

7.2.2 Applying the QM method to deal with the hydrological uncertainty

The QM bias correction method is classified as distribution-derived transformation, (e.g. Block et al., 2009; Piani et al., 2010; Johnson and Sharma, 2011; Sun et al., 2011; Kim et al., 2016). It is based on correcting the forecasts aiming that their statistical distribution fits to the statistical distribution of observations. There are some ways to adjust the forecast and observed distributions or quantiles, and existing techniques mainly differ in terms of how the cumulative distribution functions (CDFs) are considered (Crochemore et al., 2016). In this study, the empirical CDFs (ECDFs) are used to build the probability distributions of the observed flows and simulated flows of the calibrated HEC-HMS models (see chapter 3).

The QM will be applied with the objective to correct the systematic hydrological model bias. With this technique the bias correction parameters are calibrated applying the split-sample-teste (Klemes, 1986), considering the calibrated periods Cal1-1979/1997, Cal2-1997/2016 and Cal3-1979/2016, the validation periods are Val1-1997/2016 and Val2-1979/2016, and finally the period 2017-2021 is tested with the three calibrations. This bias correction method will be only

month dependent and applied to the daily flows of each basin. Therefore the parameters are calibrated aiming to fit the ECDFs of the Simulated flows with the ECDFs of the observed flows of each calibration period and in sequence checked at the validation period. The bias correction only will be applied if the calibrated parameters presents a performance of correction, at the validation period, similar to the obtained at the calibration period, and also shows a similar performance when applied at the period 2017-2021. To evaluated the performance will be used the MAE, KGE, NSE and R^2 metrics.

7.2.3 Applying the flow data assimilation to update the flow forecast

The selected method is the output-error-correction, AR – Auto Regressive with order 1, with the exponential decay based on the duration of the Clark Unit Hydrograph (Kull and Feldman, 1998) of the calibrated hydrologic models. The hydrological models, in the prediction mode, can adopt a correction of the initial conditions of forecast in the time T_0, in order to have a better assertiveness in the first horizons of the forecast. This correction is based on the errors of the last day of the simulation and from them, the values of the initially predicted flows are corrected. The parameters for this autoregressive correction must be adjusted and are dependent on the flow characteristics of each river basin and the forecast horizon. For this research we apply as the flow post processor the simple output error correction method, defined by the equations 7.1 and 7.2, where we will determine the parameter α that defines the velocity of the exponential decay of the correction.

$$Q_{cor\,(T_{(n+1)})} = Q_{sim\,(T_{(n+1)})} - Er \cdot \alpha^{T_{(n+1)}} \qquad (7.1)$$

$$Er = Q_{Sim\,(T_0)} - Q_{Obs\,(T_0)} \qquad (7.2)$$

where Q_{cor} is the corrected flow, Q_{sim} is the simulated flow, Er is the error of the simulation, T_0 is the time zero with of the last observed flow, and *n* is the number of days ahead after start the correction.

The α parameter will be defined physically, as a function of the duration of the runoff hydrograph for each basin, defined by the Clark Unit Hydrograph calibrated at the HEC-HMS models, for each catchment, to define the time T_n where ends the runoff flow. At this time T_n, the factor $\alpha^{T_{(n+1)}}$, that multiply the correction Er, is equivalent to the average fraction of the total baseflow

divided by the total discharge of the basin, during the total calibration period (1997-2017) of the hydrologic model, obtained from the HEC-HMS models, for each basin.

The α_{phys}, values proposed have their performance compared with the values of α_{math} which are calculated only mathematically, minimizing the RMSE metric, considering the first month horizon, a time window where we have the higher capacity of correction. With this test, we can see how the method proposed to obtain the α, based on physical representation of the flow, has a performance closer to the mathematical method, based only on the best RMSE fit. Once the mathematical α parameters are dependent on the time window to calculate the RMSE, the physical approach has the advantage to be only dependent on the hydrological characteristic of the basin and valid for any horizon. Finally, the simulated flows corrected with the physical α value are compared with RMSE of the simulated flow without AR correction, for the windows of 1, 2 and 4 months, to see how the capacity of correction reduces when the time horizon increases.

7.2.4 Assess the performance of the chosen seamless forecast compared with the traditional seasonal flow forecast

After test the two post processors described in 7.2.2 and 7.2.3, the chosen correction methods, calibrated with the simulated flows and compared to observed values, will be used to correct the seamless flow forecast, running with the seamless precipitation forecast described in 7.2.1. To simulate a real situation of a flow forecast to the Brazilian electric system (detailed in 7.2.5), the performances are checked considering the begin of the simulations happening at the last day of the month 1, therefore we will have six months lead-times ahead instead of the 7 months horizon of the traditional ECMWF seasonal forecast model.

To evaluate the overall performance we will use the metric CRPSS - Cumulative Rank Probability Skill Score, and in terms of assertiveness will be used the RME of the median of the ensemble forecasts. The results are compared with the observed flow as a reference, for the period of Jan/2017 to Jun/2021.

We will compare the performance of the flow forecast running with the traditional ECMWFsn SEAS5 bias corrected and the Seamless bias corrected after the application of the flow post-processor.

7.2.5 Application of the seamless flow forecast to predict the future hydropower energy production of the Brazilian interconnected system

The optimization of the Brazilian electric system operation and the methodology for setting energy prices

The electric energy operation policy and the definition of the prices of the generated energy (CMO - Marginal cost of operation and PLD - Settlement price of differences) is carried out from the chain of computational models (NEWAVE, DECOMP and DESSEM) that seek to optimize the operation of the system, with the lowest operating cost in the period, respecting the requirements of reliability in meeting the load.

NEWAVE is used for planning the operation of the Brazilian hydrothermal system, with a horizon of up to 5 years, in a monthly basis. The thermal plants are represented individually and for the hydroelectric park that is centrally dispatched, the plants are aggregated into Equivalent Energy Reservoirs - REE, the other sources are represented as Individually Not Simulated Plants - UNSI, which come in to meet the submarket's share of the load where they are present. Its objective is to define the hydraulic and thermal generation strategy that minimizes the operating cost for the entire planning period. It defines the future water cost functions that impact the water use policy in the reservoirs, determined by the short-term models.

DECOMP optimizes the operation of the hydrothermal system, with a horizon of up to 2 months and weekly discretization in the first month. In this model, thermal and hydroelectric plants are represented individually and energy exchanges are modeled similarly to NEWAVE. In DECOMP, the dispatch of the hydrothermal park is determined, which minimizes the operating cost in the period analyzed, based on the set of available information (load forecast, reservoir start-up levels, plant availability, flow forecast, future cost function of the NEWAVE, electrical limits, hydraulic restrictions, among others). In it, the future cost function, for coupling to the DESSEM very short-term model, is obtained.

At DESSEM, the hydrothermal system is optimized in the very short term, with a 7-day horizon, with hourly discretization. In this model, thermal plants are represented by generating unit, considering the restrictions of unit commitment, and hydroelectric plants are represented individually. Intermittent sources (solar and wind) have their characteristic variations represented in this model. It determines the dispatch of the system that minimizes the operating cost, the

Marginal Operating Cost - CMO for each period and submarket, with a more detailed set of information (Load forecast, Flow rates, storage, wind generation, solar generation, limits electrical, future cost function of DECOMP, among others).

The CMO is obtained through the aforementioned models, while the PLD is determined from the CMO limited between minimum and maximum values, according to ANEEL Normative Resolution No. 858/19. In addition, the maximum PLD has 2 values, a structural maximum limit and a maximum hourly limit.

The revisions of the operation policy and prices are carried out in the Monthly Operation Planning - PMO meetings, whose energy price and the operating assumptions for the current month are carried out on the last Thursday of the previous month. Prices are revised weekly, every Thursday, based on the rounds of the three operation optimization models. Details of the entire process and the requirements of each of the factors that affect the planning of the operation can be obtained from the network procedures of the ONS - National Electric System Operator (ONS, 2021)

As the Brazilian hydrothermal system has a predominance of hydraulic generation, the analysis of its behavior assumes a probabilistic premise, since the policy for the use of stored water is dependent on future uncertainties such as load, system expansions, present and future storage, but mainly the future affluent flows. Table 7.1 summarizes the operation policy and its consequences, based on the possibilities of future inflows.

Table 7.1 – The impact of the operation policy under the influence of future inflows.

Policy	Future inflows	Consequences of the operation
Use stored water	High (abundance of flows)	**Economically efficient operations**, with optimal use of water, thermal and financial resources (lower energy cost, with the activation of cheaper thermal plants over the period)
	Drops (drought)	**Energy Deficit** (Unoptimized use of resources, leading to depletion of reservoirs, with late activation of thermal resources, leading to the use of more expensive thermal plants for a longer period, with the highest energy costs in the period and, in extreme cases, failure to meet demand, with long-term social and economic repercussions)
Use the Thermals, saving water in the reservoirs.	High (abundance of flows)	**Spillage above necessary** (Deoptimized use of resources, leading to premature filling of reservoirs, with unnecessary activation of thermal resources, increasing energy costs in the period and, in extreme cases, limiting flood control)
	Drops (drought)	**Economically efficient operations**, with optimal use of water, thermal and financial resources (a little higher energy cost, with activation of the necessary thermal plants over the period)

Brazil is a country with a large territorial extension and great climatic variability, which makes it possible to reduce operating costs through the exchange of energy between the four subsystems (North, Northeast, Southeast/Midwest and South). These regions have great complementarity between the affluent flows of the various regions and also between the generation of intermittent wind and solar sources, in which the peak of wind and solar generation is observed during the period of lower flows in most of the country. This exchange is only possible due to the vast transmission system, which interconnects the various regions and allows the abundance of energy in one subsystem to be transferred to the other subsystems, which can be used to supply the load and in cases of excess supply, stored in the various reservoirs of the hydroelectric plants.

Thus, the importance of knowing the future flows to the reservoirs of the Brazilian interconnected system is evident, being essential a reliable and assertive flow forecasting system, which would provide the optimal use of available resources and the lowest energy cost for the whole society.

The calculation of Affluent Natural Energy - ENA, based on affluent flows

ENA is calculated based on natural flows and productibilities equivalent to the storage of 65% of the active storage of the reservoirs of hydroelectric plants. It can be calculated on a daily, weekly, monthly or annual basis and also by basin and by subsystem (ENASUBSYSTEM), according to the existing hydropower systems in the configurations of the hydrographic basins and electrical subsystems, as described in the procedures of network submodule 2.4 (ONS, 2021).

In the present work, the forecasts of 30 projects were modeled, so that it was possible, with these hydroelectric plants, to represent the ENA of the four subsystems and, consequently, the ENA of the complete interconnected system. Thus, to obtain the ENA by subsystem, the parameters of multiple regressions between the observed natural flows, in the plants that make up each subsystem, and the respective ENA of the subsystem were calibrated. Table 7.2 shows the plants used to calculate the ENA in each subsystem.

Table 7.2 – HPP list used to calculate the ENA in each subsystem.

Subsystem	North	Northeast	Southeast / Center-West	South
HPP	Belo Monte Ferreira Gomes Sto. Ant. do Jari Lajeado Tucurui	Itapebi Três Marias Sobradinho	Ilha dos Pombos Manso Mascarenhas Itumbiara Emborcação Capim Branco 2 São Simão Furnas Agua Vermelha Nova Avanhandava Porto Primavera Rosana Itaipu Santo Antônio Teles Pires	Quatorze de Julho Dona Francisca Barra Grande Campos Novos Foz do Chapecó Gov. B. Munhoz Salto Caxias

For the South, Southeast/Center-West and Northeast regions, where the system had a more stable configuration until the actual days, without the entry of new relevant plants, and consequently a longer period of data for the relation Flow versus ENA, greater than 10 years, multiple regressions were used to calculate the ENA for each month of the year. Thus, each of these subsystems presents twelve sets of parameters to model the year's ENA. As for the North subsystem, which more recently had the entry into operation of the Belo Monte HPP, whose number of operating machines allowed us to have the most similar configuration to the current system only after 2015, a multiple regression representing the entirety year was adopted for the relation Flow versus ENA.

The calculation of ENA, based on seamless flow forecast

The Affluent Natural Energy-ENA predicted for each subsystem was calculated from the median of the ensemble of expected flows for the reference month, from the runs of the last Thursday of the previous month, similar to what is done in the actual PMO systematics. For the median predicted flows, a calibrated multiple regression was applied for each subsystem and the ENA forecasts were obtained for a horizon of up to 6 months, for each of the subsystems. The sum of these flows results in the total ENA of the SIN – National Interconnected System.

The performance of these planned ENAs was evaluated for the period from Jun/2017 to Jun/2021, using the performance indicators MAPE, KGE and R2. It will be evaluated how the ENA forecast performance is for each subsystem and for each forecast horizon. In addition, the performance of

the SIN will be evaluated, since it is interconnected, the analysis of the forecast of the SIN, as a whole, will allow to assess whether it is possible to anticipate the most extreme events, especially droughts, which bring the most serious consequences for the price of energy.

Comparison of predicted ENA, based on seamless flow forecast and NEWAVE's first six months forecast

At this part we run the NEWAVE Model, on its latest 2021 version, which were introduced an extension of the stochastic model, adding a new term at the regression equation, referring to the average of the observed flows of the last twelve months, to give to the model a higher capacity to represent a more severe hydrological tendency, for example long droughts (Lima and Oliveira, 2021). NEWAVE is able to simulate the operation of the interconnected system for a horizon of up to 5 years, and will be operated in the forecast module only with the objective to obtain the ENAs of the electric systems, which are statistical forecasts based on the past of observed flows, which results are determinant for the future cost function of water and, consequently, for the price of energy. The first six months of NEWAVE forecast will be evaluated with the six months of ENA obtained by the proposed methodology, comparing the assertiveness of the median of Seamless forecast versus the NEWAVE, based on the performance metric MAPE Skill Score. If the forecasts based on the seamless flow forecast are more assertive, we will have an excellent indicative that the proposed methodology can contribute to a better operation of the system.

7.2.6 Metrics to assess the forecast performances

The metrics used are the same that were presented in Chapter 4, section 4.2.4 for the evaluation of the precipitation forecasts, i.e., CRPS, RME, BSrel, BSres, Correlation coefficient, and skill score. Also the same that were presented in chapter 3, section 3.2.6, for the evaluation of the hydrological simulations, i.e., NSE, KGE, MAE and R^2. The reader is invited to refer to it.

The mean absolute percentage error (MAPE), is a measure of prediction accuracy of a forecasting method in statistics. It usually expresses the accuracy as a ratio defined by the formula:

$$MAPE = \frac{100}{n}\sum_{i=1}^{n}\left|\frac{Y_i - x_i}{x_i}\right| \qquad (7.3)$$

where x_i is the observed value, n is the number of events, and Y_i is the forecast value. The absolute value in this ratio is summed for every forecasted point in time and divided by the number of fitted points n.

The root mean square error (RMSE), is a measure of the standard deviation of the residuals. It usually expresses the accuracy as a ratio defined by the formula:

$$RMSE = \sqrt[2]{\frac{1}{n}\sum_{i=1}^{n}(Y_i - x_i)^2} \qquad (7.4)$$

7.3 RESULTS

7.3.1 Application of the QM method to deal with the hydrological uncertainty

The parameters calibrated to perform the QM bias correction of the flows was calibrated with 3 different periods applying the split-sample-test (Klemes, 1986) to have more robust parameters. Figure 7.3 shows the boxplots with the performance results of the application of the QM method in three different periods of calibration (1979-1997, 1997-2016 and 1976-2016) and validation (1997-2016, 1979-1997, and 2017-2021), considering the four metrics (MAE, KGE, NSE, and R^2) with analysis of the bias corrected simulated flows of the HMS-models considering as a reference the observed daily flow, for the 30 HPP.

When we observe the three calibration periods (first row of graphs), it is clearly visible an improvement of the performance of the corrected flow (left boxplot) compared with the raw simulated flow (right boxplot), at all the four metrics, with emphasis on KGE, NSE, and R2, where they presents a better median of the performance and also reduces the variability, especially for the calibration period 1979-1997. Otherwise when we look at the validation periods, those improvements do not appear, the median of the performance of the corrected flows tends to be equal or worse than the raw flows, also is noted a bigger dispersion of the results presenting more basins with worse performance after the correction.

Finally, when we observe the recent period 2017-2021, the parameters calibrated for the periods 1979-1997 and 1979-2016 generate corrected flows with a median of the performances similar to the raw flows, but with a higher dispersion, presenting more basins with worse performance for the corrected flows. The calibration for the period 1997-2016, had the worst performance of

the corrected flows, showing a lower median of the performances and also a higher dispersion, with worst performance in more basins.

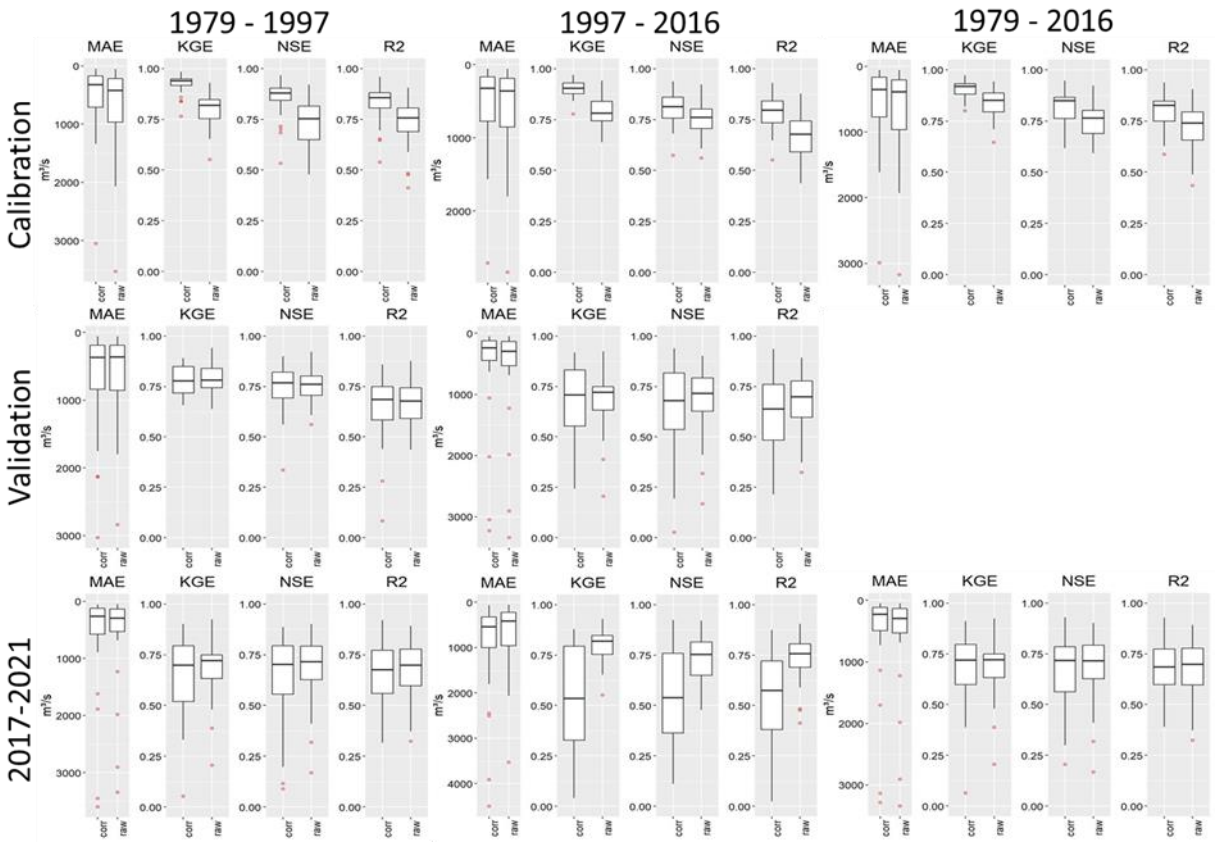

Figure 7.3– Graphs with the performance indicators (MAE, KGE, NSE and R2) of the bias corrected flows (right boxplot in each graph), obtained with parameters calibrated in three different periods (1979-1997, 1997-2016 and 1976-2016) and validated in two validation periods (1997-2016 and 1979-1997) and verified in the recent period 2017-2021, compared with the raw simulated flows (left boxplot in each graph).

7.3.2 Application of the output-error-correction technique at the simulated flow

In Table 7.3 we can see the α parameters, first with the best RMSE of the corrected simulated flows, obtained only mathematically (α_{math}) compared with the hydrologically proposed method (α_{phys}) with the correspondent RMSE of the daily corrected flows, considering the first month horizon, with the observed flow as a reference. Also is presented the comparison of the performance of the corrected daily simulated flows, with the raw simulated flows for the horizons of one, two and four months ahead.

In this table is possible to see that the RMSE of the hydrological α is very closer to the best RMSE, the differences show that the chosen values are in average 2% worse than the best performance, and the biggest difference is 10%, in more of 80% of the basins the difference is

equal or lower than 2% for the first month horizon. When we compare the performance of the flows corrected with the physical α, is possible to see that method improves the RMSE metric in 20% in average, and the maximum improvement is 39%. For the second month horizon the mean improvement of the performance is around 12%, with the best value of 24%. Finally, at the fourth month horizon, the improvement of the corrected flows is near 6%, with the best value of 12%. For longer horizons the improvement tends to zero due the exponential decay factor of the correction.

Table 7.3 – Comparison of the α values and the RMSE performance of the corrected flows using the mathematical α and the proposed physical α, considering the first month (1M) horizon (first 5 columns). In sequence corrected simulated flows with Physical α compared with the performance of the raw simulated flows for 1, 2 and 4 months horizon.

HPP	α_{math}	RMSE 1M	α_{phys}	RMSE 1M	diff.	Raw RMSE 1M	RMSE 2M	Raw RMSE 2M	RMSE 4M	Raw RMSE 4M	diff 1M	diff 2M	diff 4M
14_DE_JULHO	0.728	231	0.887	233	1%	241	258	261	278	280	-3%	-1%	-1%
AGUA_VERMELHA	0.975	301	0.964	305	1%	428	373	448	441	478	-29%	-17%	-8%
BARRA_GRANDE	0.809	177	0.778	177	0%	186	195	199	209	211	-5%	-2%	-1%
BELO_MONTE	0.973	1206	0.973	1206	0%	1953	1628	2085	2081	2344	-38%	-22%	-11%
CAMPOS_NOVOS	0.939	125	0.887	127	2%	145	145	154	160	164	-13%	-6%	-3%
CAPIM_BRANCO_2	0.961	75	0.959	75	0%	89	86	94	99	103	-15%	-9%	-4%
DONA_FRANCISCA	0.939	176	0.868	179	2%	197	202	210	219	223	-9%	-4%	-2%
EMBORCACAO	0.981	100	0.957	103	3%	141	125	148	148	160	-27%	-16%	-8%
FERREIRA_GOMES	0.966	225	0.949	228	1%	296	268	310	311	334	-23%	-14%	-7%
FOZ_DO_CHAPECO	0.927	622	0.824	638	3%	696	714	742	772	786	-8%	-4%	-2%
FURNAS	0.963	186	0.953	203	10%	228	216	241	249	262	-11%	-10%	-5%
G_B_MUNHOZ	0.961	217	0.923	222	2%	271	262	289	294	306	-18%	-9%	-4%
ILHA_DOS_POMBOS	0.967	109	0.956	110	0%	138	127	144	144	152	-20%	-12%	-5%
ITAIPU	0.971	1479	0.971	1479	0%	2058	1780	2142	2064	2248	-28%	-17%	-8%
ITAPEBI	0.927	162	0.963	165	2%	183	189	200	222	227	-10%	-6%	-2%
ITUMBIARA	0.973	258	0.958	263	2%	355	320	376	383	413	-26%	-15%	-7%
LAJEADO	0.945	702	0.978	725	3%	732	723	777	845	862	-1%	-7%	-2%
MANSO	0.841	70	0.696	70	1%	74	77	79	87	89	-5%	-2%	-2%
MASCARENHAS	0.963	219	0.938	224	2%	277	263	294	304	320	-19%	-11%	-5%
NOVA_AVANHANDAVA	0.961	200	0.963	203	2%	246	228	256	256	271	-17%	-11%	-6%
PORTO_PRIMAVERA	0.978	929	0.962	942	1%	1293	1145	1352	1332	1437	-27%	-15%	-7%
ROSANA	0.951	387	0.947	388	0%	466	449	492	504	524	-17%	-9%	-4%
SALTO_CAXIAS	0.965	428	0.896	462	8%	554	539	587	600	623	-17%	-8%	-4%
SANTO_ANTONIO	0.979	2122	0.984	2125	0%	3458	2730	3592	3335	3792	-39%	-24%	-12%
SAO_SIMAO	0.979	364	0.970	367	1%	522	453	553	551	604	-30%	-18%	-9%
SOBRADINHO	0.977	451	0.979	452	0%	655	556	693	683	762	-31%	-20%	-10%
STO_ANTONIO_DO_JARI	0.979	222	0.950	240	8%	353	303	371	367	404	-32%	-18%	-9%
TELES_PIRES	0.978	330	0.983	331	0%	534	438	565	557	622	-38%	-22%	-10%
TRES_MARIAS	0.950	222	0.960	223	0%	267	260	286	308	322	-16%	-9%	-4%
TUCURUI	0.969	1257	0.961	1274	1%	1892	1639	1998	2004	2200	-33%	-18%	-9%
Mean					2%						-20%	-12%	-6%

7.3.3 Evaluate the performance of the seamless forecast compared with the traditional seasonal flow forecast

After the definition of the AR output-error-correction as the flow postprocessor, we compare the performance between the original bias corrected ECMWFsn and the proposed flow forecast with the Seamless ARpost (with the flow data assimilation). Figure 7.4 shows the heat map graphs of CRPSS metric, with six months horizon, divided in four seasons, for a best evaluation of the dry and wet periods. We are considering the run at the last day of the month, to simulate a real forecast situation for the PMO of the Brazilian Electric System. In each column we have the seasons, starting with the months OND (October, November and December) representing the begin of the wet season, at the last column we have the months JAS (July, August and September), representing the end of the dry season. At the rows we have the different seasonal forecasts, the ECMWFsn bias corrected, at the first row, and the proposed methodology, the Seamless ARpost at the end, with the application of the post processor the AR output-error-correction. The results are divided in eight groups from South to North direction (G1 to G8) with hydrological similarity.

It is possible to observe in this figure that the South region represented by the group G1, it is pretty hard to predict the flows, even in the first month horizon, only at the seasons AMJ and JAS is possible to be better than the climatology, only with the Seamless ARpost forecast improving the performance, fortunately the highest flows happens at this seasons. After the second month horizon is not possible to beat the climatology.

For the group G2 which still under some influence of the South weather, the result is similar, but with the Seamless ARpost, it is possible to have a performance higher than the climatology in all seasons for the first month horizon.

In group G3, which is located in the center of Brazil, the Seamless ARpost present a visible improvement at the first month horizon, being possible to beat the climatology in all seasons. And for the seasons OND and JAS, it is possible to extend the viability to longer horizons.

In group G4, with great part of the basins under influence of the semi-arid weather, it is only possible go best than the climatology at the first month horizon with the Seamless ARpost, except in the JAS season, the driest period of the basins, when it is not possible to perform better than the climatology in any horizon.

In the groups G5, G6 and G7, located in the north region, and with the biggest basins, the Seamless ARpost forecast can beat the climatology in all seasons at the first two months horizon, and in the seasons OND, AMJ and JAS we can extend this better performance for longer horizons. Finally at group G8, at the extreme North region, the Seamless ARpost flow forecast has a good performance and in a longer horizon at the seasons OND, JFM, and JAS than the ECMWFsn.

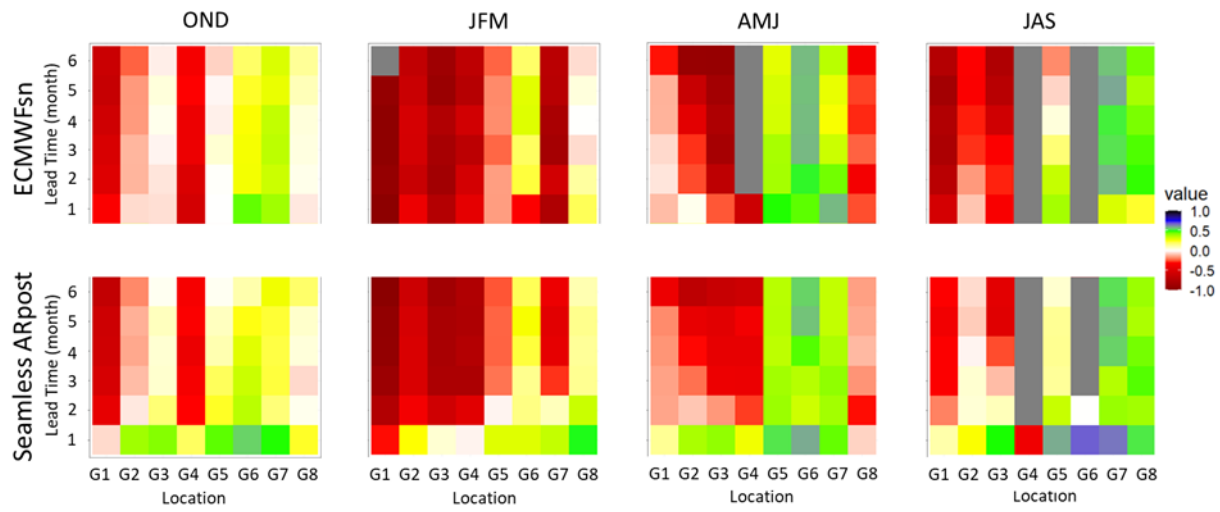

Figure 7.4– CRPSS results of the two flow forecasts (ECMWFsn and Seamless ARpost), considering the run at the last day of the month, the six months lead times and the four seasons. Divided in 8 groups with hydrological similarity (G1 to G8). The gray and the red color represents a performance worse than the climatology, the colors yellow, green and blue represents different degrees of performance better than the climatology.

Figure 7.5, shows a spatial vision of the CRPSS performance, with maps of the first month horizon, for all four seasons in each column of maps, starting by the begin of the wet seasons (OND) and at the rows of maps we have each seasonal flow forecast (ECMWFsn and Seamless ARpost). With this figures is possible to see a clear improvement of the flow forecasts with the proposed method Seamless ARpost, illustrated by the stronger blue when we compare with the ECMWFsn. It happens in all seasons and in all basins. This is an evidence that the flow post processor applied with the seamless forecast produces more viable flow forecasts.

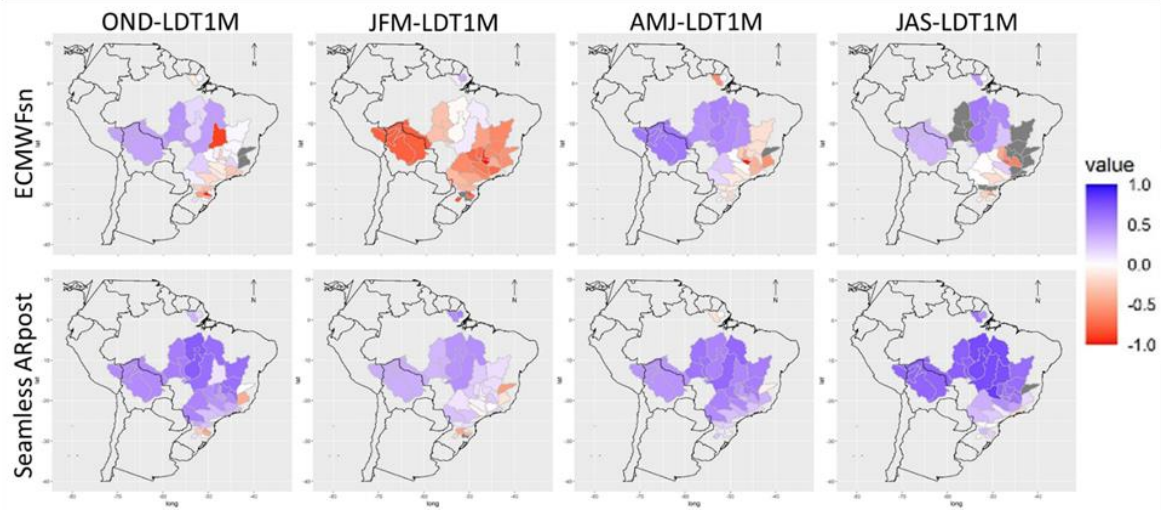

Figure 7.5– Maps with CRPSS results of the two forecasts (ECMWFsn and Seamless ARpost), considering the run at the last day of the month, for the first month lead-time (LDT1M) and the four seasons. The blue represent a performance better than the climatology and the red a worse performance.

Figure 7.6 shows the heat map graphs of RME metric, to give an idea of the assertiveness of the forecasts, with six months lead-time horizons, divided in the four seasons, for a best evaluation of the dry and wet periods, with exactly the same structure and scenarios presented in figure 7.4. But in this case, at the RME figures, the best performance is the white color (zero bias), a red color represents and underestimation of the forecasts and the blue represents an overestimation of them.

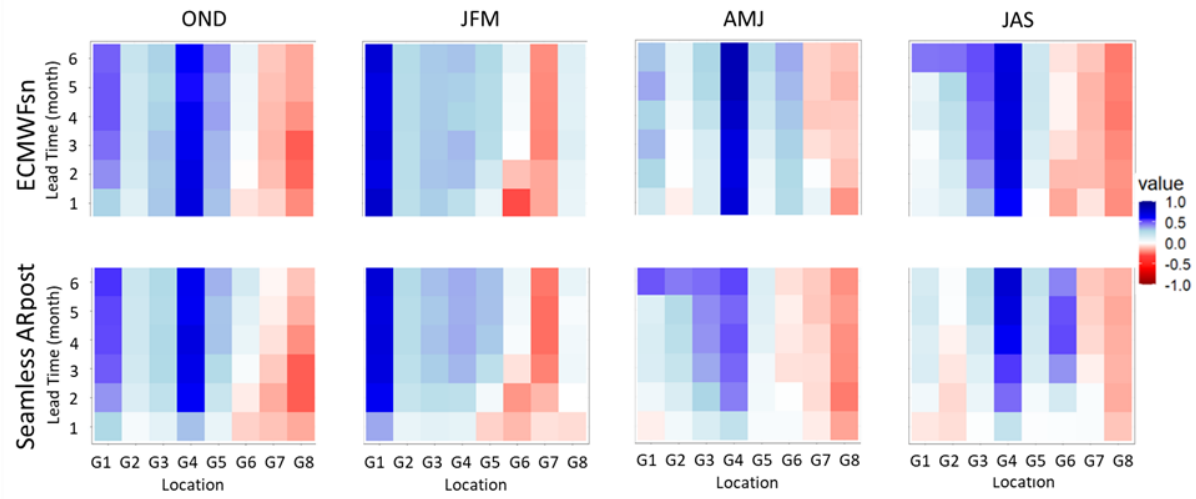

Figure 7.6– RME results of the two forecasts (ECMWFsn and Seamless ARpost), considering the run at the last day of the month, the six months lead times and the four seasons. The blue represent an overestimation, the red an underestimation of the forecast flows, and white is the best performance.

At this figure we can see a tendency of overestimation of the forecast flows for groups G1 to G5, in all seasons and forecast methods, with the Seamless ARpost being able to reduce this

overestimation at the first month horizon, and sometimes generating a small underestimation. For group G6 appears a tendency of underestimation during the wet seasons at the first lead time horizons with the Seamless ARpost being able to improve the results.

For groups G7 and G8 appears a tendency of underestimation in practically all seasons and again the Seamless ARpost was able to improve the forecasts at first horizons.

After the second month horizon the both forecasts tend to have a similar performance due the fact that the Seamless and the flow post processor acts stronger only at these initial periods, decreasing the influence along the higher lead-times.

Figure 7.7, shows a spatial vision of the RME performance with maps of the first month horizon, for all four seasons in each column of maps, starting by the begin of the wet seasons (OND), and at the lines of maps, we have each seasonal flow forecast (ECMWFsn and Seamless ARpost). With this figures is possible to see that the basins at the West region have a tendency to present underestimation of the flows and in the east region inverts this tendency to an overestimation at the ECMWFsn flow forecast. But after the application of the complete Seamless ARpost flow forecast, the method was able to reduce significantly this bias of the underestimations and also at the overestimations, represented by the colors near to white, generating forecasts with lower bias, and consequently with more assertiveness.

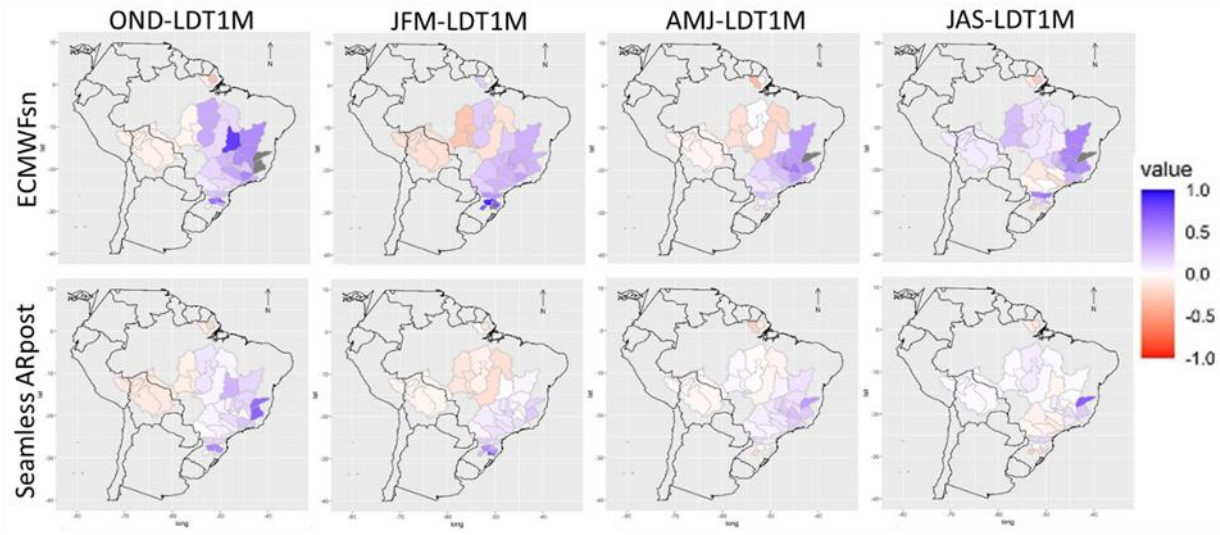

Figure 7.7– Maps of RME results of the two forecasts (ECMWFsn and Seamless ARpost), considering the run at the last day of the month for the first month lead-time (LDT1M) and the four seasons. The blue represent an overestimation, the red an underestimation of the forecast flows, and white is the best performance.

7.3.4 Application of the Seamless flow forecast to predict the hydropower energy production for the Brazilian electric system

The transformation of the hydropower energy production in each subsystem involves the calculation of the generation of each HPP in the system. But at this experiment we work with a specific group of HPP that can represent the energy production of the subsystem. To calculate the energy production for the subsystem a multiple regression was calibrated to calculate the ENA – *Energia Natural Afluente* (Affluent Natural Energy) of the subsystems. In Figure 7.8, we can see the result of the coefficient of correlation between the calculated ENA and the real observed ENA, for each of the four subsystems of the Brazilian interconnected system. It is possible to see a very good fit between the calculated and observed values, with a R^2 near to one. The lower value appears at the North region where we have a shorter period of the actual configuration of the subsystem to calibrate the parameters. This results indicates that the 30 chosen HPP can represent the complete electric system with a high degree of confidence.

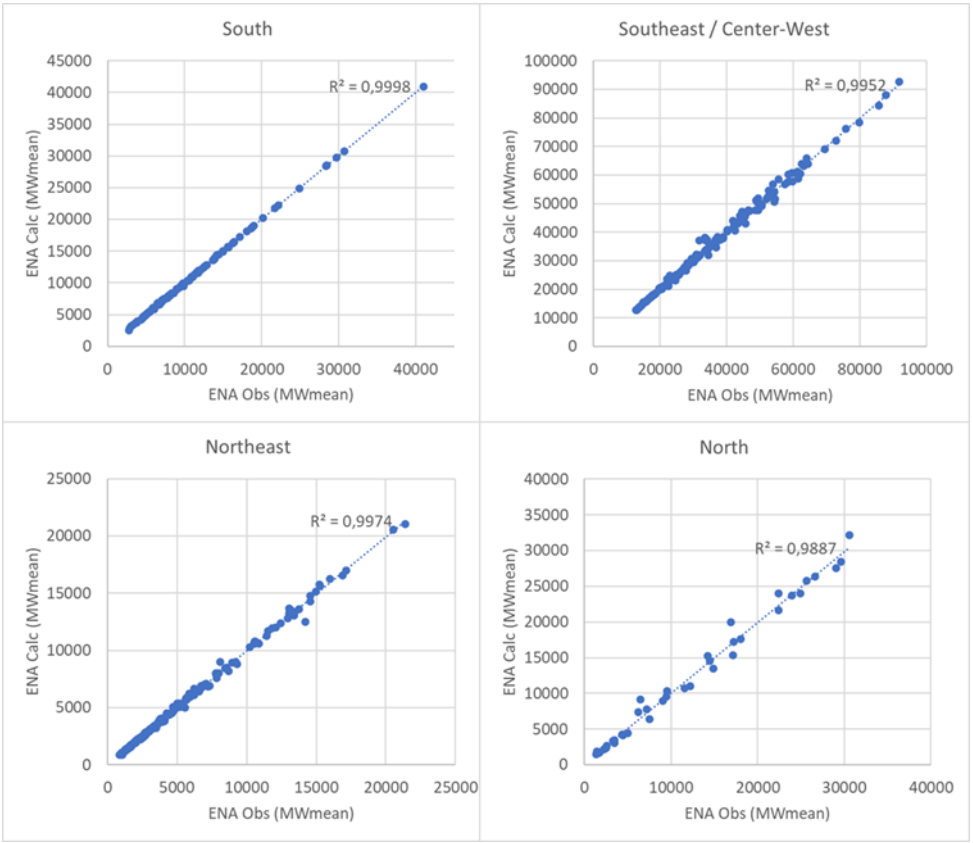

Figure 7.8– Graphs with the ENA calculated versus ENA observed and the correlation coefficient of the calibrated multiple linear regression of observed flow and ENA for the subsystems South, Southeast/Center-West, Northeast, and North.

The calibrated multiple regressions parameters were applied at the median of the Seamless ARpost flow forecasts to predict the hydropower energy production at each subsystem, until six month lead-time. In Figure 7.9 we have the HPP energy production forecast for the subsystems South and Southeast / Center-West, for the period from July/2017 to June/2021, with the LTM (long term mean) of the ENA in blue dots line, the observed ENA in dashed black line, the green lines represent the forecasted ENA in different horizons, the thickest and darkest lines are the closer lead time horizons, and the red bars indicates the error for the first month lead-time. The table 4 indicates the performance of the predictions, for the six lead-times, and for the metrics MAPE, NSE and R^2. At this figure, on the first graph, we can see that the South region is the most difficult to predict, even for the first month. When the observations are far to the climatology, the forecasts cannot predict the intensity of the extremes or a sudden change of the conditions from dry to wet or at the opposite direction. But the model still with the capacity to forecast if we will have production above or below the climatology for almost all months of the analyzed period. When we look to the bars of errors of the first month lead-time we can see a tendency of overestimation of the forecasts. Table 7.4, with the performance metrics, shows in numbers this behavior with a strong degradation of the performance after the first month horizon, with MAPE near to 50%, NSE below zero and R^2 below 0.2 after the first month horizon.

In the second graph of this figure, we have the representation of the Southeast / Center-West subsystem, with the bigger production of the SIN. At this subsystem the results are much better than the previous, showing ability to predict the energy production in a longer horizon and with more sensibility to predict the intensity of the more extreme situations. This become more evident during the recession period which goes from April to October where the observed initial conditions are known and the hydrological model predict well the future conditions. The model exhibits a good performance to forecast the energy production below or above the average for the majority of the observed period and in a long horizon, more than 5 months during the recession and near 3 months during the wet period. The red bars with the errors of the first month shows the lower errors at this period and the highest values appear during the wet season, especially when happens a break in the trend of the flows. At table 7.4 we can see the best results at the first two months, with MAPE below 30%, NSE higher than 0.6 and R^2 higher than 0.8, we have a small degradation on the third month, and after this we have the lowest performance with MAPE higher than 40%, NSE below 0.4 and R^2 around 0.76.

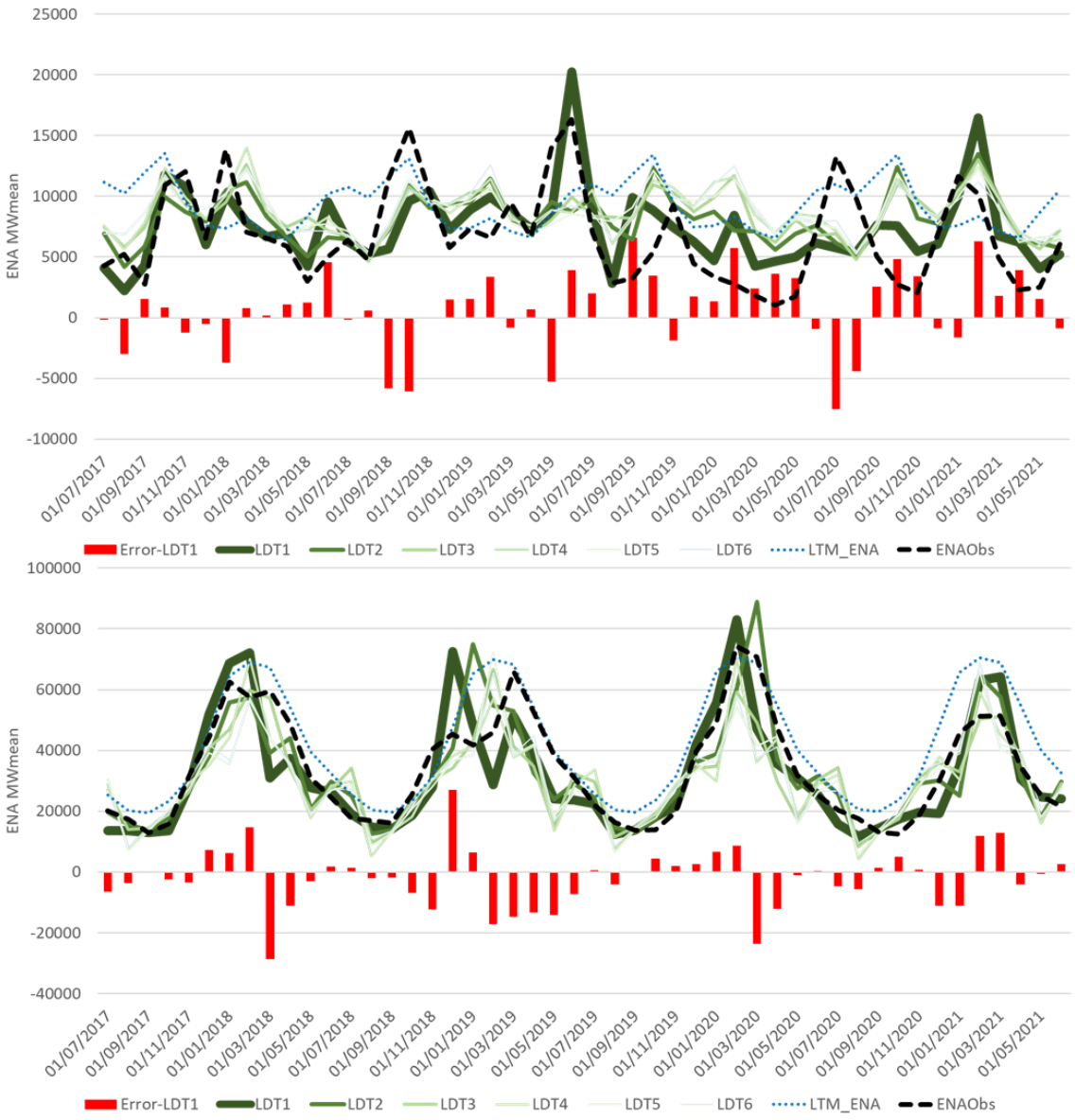

Figure 7.9– Hydrographs of ENA for the subsystems South and Southeast/Center-West, for the period from July/2017 to June/2021, with the LTM (long term mean) of the ENA in blue dots line, the observed ENA in dashed black line, the forecasted ENA for each lead-time in green, the thinner and clearer line is the farther lead time horizon, and the red bars indicates the error for the first month lead-time.

Table 7.4 – The performance of the forecast for the ENA of the subsystems South and Southeast / Center-West with the metrics MAPE, NSE and R^2, for six months lead-time.

	South			Southeast / Center-West		
LDT	MAPE	NSE	R^2	MAPE	NSE	R^2
1	37%	0.15	0.37	30%	0.61	0.81
2	47%	-4.92	0.20	25%	0.63	0.82
3	47%	-6.59	0.17	33%	0.39	0.79
4	48%	-6.28	0.11	46%	0.36	0.76
5	47%	-8.03	0.09	40%	0.32	0.76
6	47%	-8.03	0.09	34%	0.33	0.77

In Figure 7.10 we have the HPP energy production forecast for the subsystems Northeast and North, for the period from July/2017 to June/2021, with the same configuration of the Figure 7.9. The table 7.5 indicates the performance of the predictions, for the six lead-times, and for the metrics MAPE, NSE and R^2. At this figure, on the first graph, we can see that the Northeast region have a good capacity of prediction, especially on the first two months lead time. When the observations are far to the climatology, the forecasts can predict the intensity of the extremes or a sudden change of the conditions dry to wet or the opposite on the first month lead time. The model exhibits a great capacity to forecast if we will have production below the climatology for almost all months of the analyzed period and in a long lead-time horizon. When we look to the bars of errors of the first month lead-time, we can see a tendency of overestimation of the forecasts, but during the recession period, from April to October, the errors are very small showing the good ability of the hydrological model to reproduce the recession of the basins. Table 7.5 shows the best results at the first month, with MAPE of 16%, NSE higher than 0.85 and R^2 higher than 0.95, we have a degradation on the second month (MAPE=0.29, NSE=0.39, and R^2=0.75), and after this we have the lowest performance with MAPE higher than 35%, NSE below 0.3 and R^2 below 0.75.

In the second graph of this figure, we have the representation of the North subsystem, with the bigger basins, that represent part of the Amazon river basin. At this subsystem the results are the best of the subsystems, showing ability to predict the energy production in a longer horizon (even six months ahead) and with more sensibility to predict the intensity of the high and low inflows. This become more evident during the recession period which goes from May to October, where the observed initial conditions are known and the hydrological model predict well the future conditions especially at the big basins. The model exhibits a good performance to forecast the energy production below or above the average for all observed period and in a long horizon, more than six months during the recession and near 3 months during the wet period. The red bars with the errors of the first month horizon, show the lower errors at this period and the highest values appear during the wet season, especially when happens a break in the trend of the flows. At table 7.5 we can see good results in practically all horizons, with performance starting with MAPE equal 21%, NSE higher than 0.8 and R^2 higher than 0.9, we have a small degradation along the higher lead-times, with MAPE below than 28%, NSE above 0.75 and R^2 above 0.9.

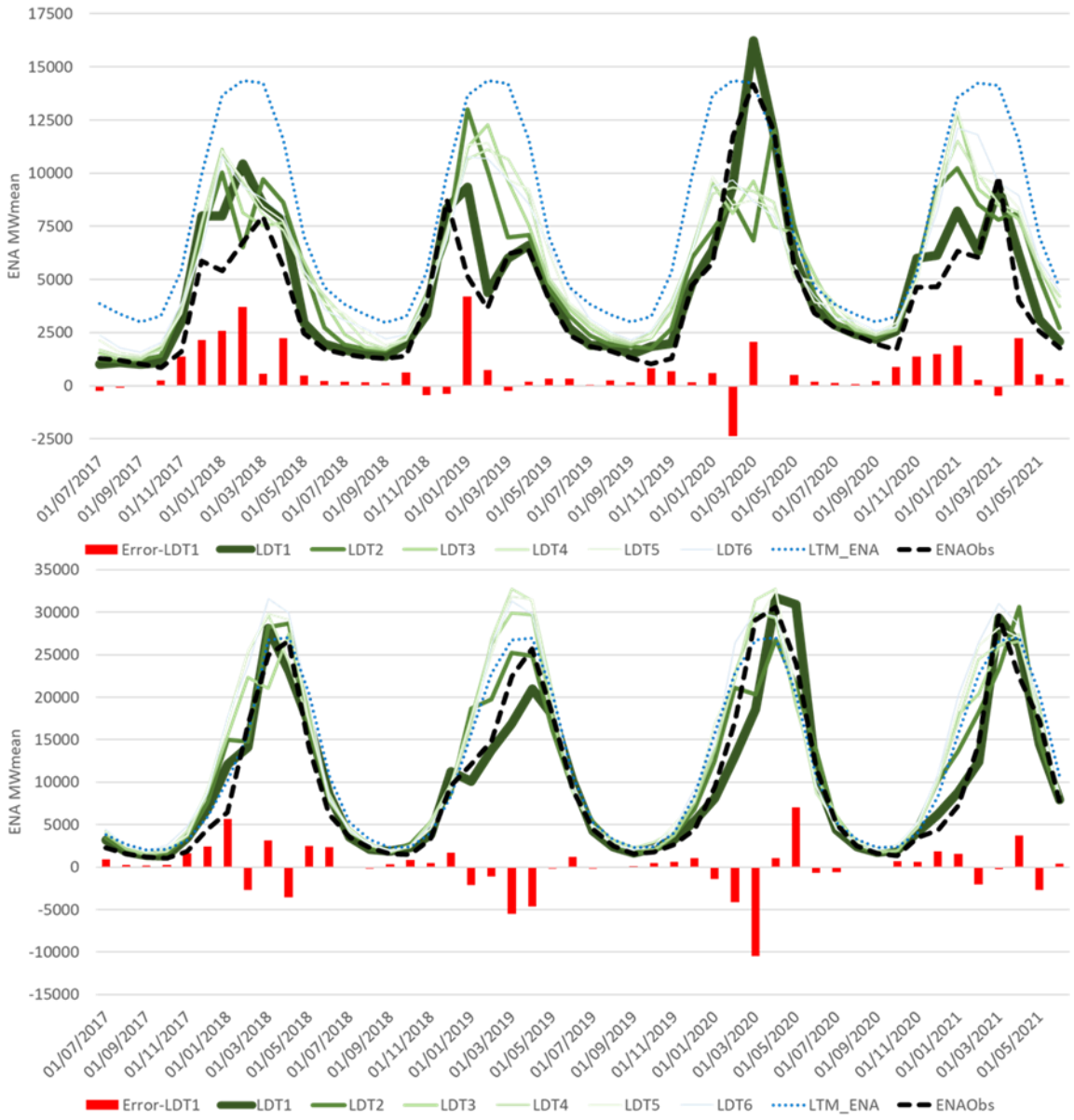

Figure 7.10– Hydrographs of ENA for the subsystems Northeast the first and in second the North, for the period from July/2017 to June/2021, with the LTM (long term mean) of the ENA in blue dots line, the observed ENA in dashed black line, the forecasted ENA for each lead-time in green, the thinner and clearer line is the farther lead time horizon, and the red bars indicates the error for the first month lead-time.

Table 7.5 – The performance of the forecast for the ENA of the subsystems Northeast and North with the metrics MAPE, NSE and R^2, for six months lead-time.

	Northeast			North		
LDT	MAPE	NSE	R^2	MAPE	NSE	R^2
1	16%	0.86	0.95	21%	0.81	0.91
2	29%	0.39	0.75	24%	0.75	0.89
3	35%	0.23	0.71	26%	0.78	0.92
4	36%	0.26	0.75	28%	0.78	0.93
5	37%	0.21	0.72	27%	0.81	0.94
6	38%	0.18	0.73	27%	0.79	0.94

Finally, in figure 7.11, we have the representation of the complete interconnected system. Once the Brazilian electric system is interconnected with big power transmission lines, we can take advantage of the aggregation of the forecast results. The forecasts show ability to predict the energy production in a longer horizon (even six months ahead) and with more sensibility to predict the intensity of the high and low inflows especially at the first three months horizon. At this global forecast, the model exhibits a good performance to forecast the energy production below or above the average for all observed period and in a long horizon, more than six months during the recession, but also is able to do good predictions during the wet period. The red bars, with the errors of the first month, show a more equilibrated distribution along the observed period, with lower errors during the recession and the highest values appearing during the wet season, especially when happens a break in the trend of the flows. At Table 7.6 we can see good results in practically all horizons, with performance starting with MAPE equal 18%, NSE higher than 0.8 and R^2 higher than 0.9, we have a small degradation along the lead-times, with MAPE below than 23%, NSE above 0.72 and R^2 above 0.87.

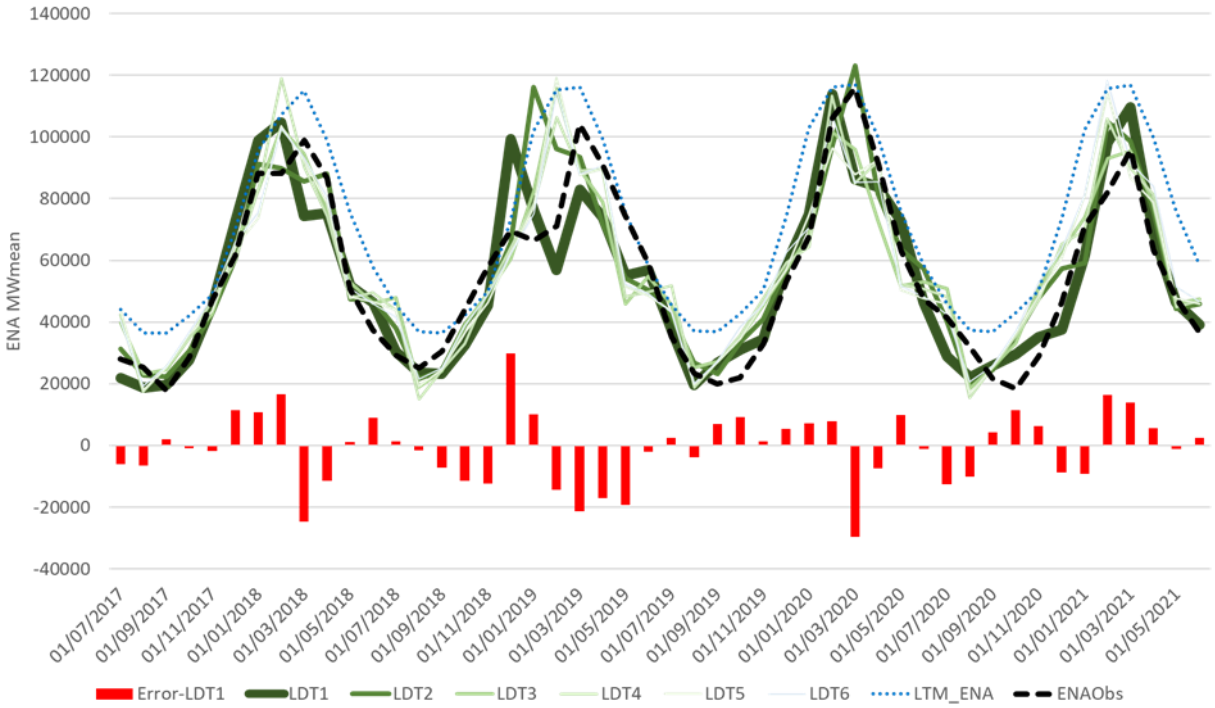

Figure 7.11– Hydrographs of ENA for the SIN (Interconnected Electric System), for the period from July/2017 to June/2021, with the LTM (long term mean) of the ENA in blue dots line, the observed ENA in dashed black line, the forecasted ENA for each lead-time in green, the thinner and clearer line is the farther lead time horizon, and the red bars indicates the error for the first month lead-time.

Table 7.6 – The performance of the forecast for the ENA of the complete Interconnected Electric System with the metrics MAPE, NSE and R^2, for six months lead-time.

	Complete SIN		
LDT	MAPE	NSE	R^2
1	18%	0.82	0.91
2	17%	0.80	0.90
3	20%	0.74	0.89
4	23%	0.74	0.87
5	22%	0.72	0.87
6	20%	0.72	0.87

At Table 7.7 we have the comparison of the assertiveness performance, with the metric MAPE Skill Score, between the ENA calculated with the median of the Seamless forecast and with the reference model NEWAVE, for the period 07/2017 to 06/2021, for each subsystem and for the complete interconnected system (SIN), for the six months lead time. We ca see that in three of the four subsystems the performance of the Seamless forecast is superior than the reference NEWAVE, only at the Southeast/Center-West the NEWAVE performs better at the analyzed period. Besides the NEWAVE has the best performance at the biggest subsystem, was not enough to compensate the superiority of the seamless forecast at the other subsystems. When analyze the complete interconnected system the Seamless forecast have a best performance in all six months horizon.

Table 7.7 – Comparison of the MAPE Skill Score performance of the forecast for the ENA, calculated with the Seamless forecast versus the NEWAVE, at the four subsystems and the complete SIN, for six months lead-time.

	MAPE Skill Score				
LDT	Northeast	North	South	Southeast / Center-West	SIN
1	0,47	0,05	0,52	-0,96	0,08
2	0,37	0,16	0,54	-0,21	0,40
3	0,40	0,20	0,57	-0,38	0,33
4	0,47	0,21	0,57	-0,82	0,27
5	0,52	0,29	0,55	-0,57	0,32
6	0,54	0,34	0,56	-0,30	0,40

7.4 DISCUSSION

At this experiment we tested some methods to deal with some of the uncertainties related with the hard job of produce a flow forecast, and we define a consistent methodology for a seamless flow forecast with potential application to predict the hydropower energy production in the

Brazilian electric system. The steps related to the uncertainty of the observed precipitation and the forecast precipitation was done by the author previous studies, now is presented the final part related with the flow forecast uncertainties and the final proposed methodology.

7.4.1 Application of the QM method to deal with the hydrological uncertainty

In previous chapters (4 and 5) the we applied with success the QM bias correction to improve the precipitation forecast at the ECMWF meteorological model. The same method was applied here, aiming to correct the bias of the hydrological model, calibrating the parameters to fit the simulated flows ECDF - Empirical Cumulative Density Function with the ECDF of the observed flows, applying the split-sample-test (Klemes, 1986).

For the three calibration periods, as we can see at the first graphs of figure 7.3, the correction was able to improve all the results for all basins for the metrics MAE, KGE, NSE and R^2. Initially it seemed to be a good indication of success, but when we applied the calibrated parameters at the validation period, the results are not good enough. The calibration with the period 1979-1997 did not produce the same good correction at the validation, the metrics of performance presented the same average of the raw simulated flow, but with a higher dispersion, showing more basins with worse performance. Parameters of the period 1997-2016, during the validation step, showed worse performance than the raw simulated flows at the average values and in the dispersion with more basins with worse performance.

At the analyze of the recent period 2017-2021, the results was very similar with the validation period with no improvement of the simulated flows after the bias correction. The best result was obtained with the parameters the calibration of the total period 1979-2016, with a slight lower MAE, but with KGE, NSE and R^2 with average very similar but with higher dispersion in the results.

The application of the QM method, brings one inconvenient at the application at daily flows, once the parameters are month dependent due the big variation of the scale of the flows in each season, the application of the bias correction can create a discontinuity at the daily flows. Every time we manipulate the dataset trying to reduce the errors, we add some new uncertainty, and only make sense apply the correction if the benefit is really bigger than the uncertainty.

In this case, there is no evident benefit and the discontinuity created with the method can generate a worse forecast, for this reason the application of the QM bias correction at the flows was discarded as a flow post processor in this study.

7.4.2 Application of the flow data assimilation to update the flow forecast

The second flow post processor was the data assimilation, where we use an AR – Auto Regressive output-error-correction, with degree 1, to correct the forecasted flows and improve the results. To define the parameters of the AR models was tested a hydrological approach with the α parameters, which defines the exponential decay of the correction, dependent of the characteristics of the basins, taking as a reference the characteristics of Clark Unit Hydrograph and the base flow calibrated at the HEC-HMS models with daily flows. The advantage of this technique is that the parameters are not time dependent.

The physical α is compared with the parameter calibrated mathematically, with the objective function to reduce the RMSE of the daily simulated flows, this approach is time dependent, therefore the result can be different if you take a time window of one, two or three months to calculate the RMSE and obtain the optimum α that minimize the error. The results obtained with one month horizon (Table 7.3), showed that the performance of the physical α is very close to the best mathematical value in average 2% worse, with more than 80% of the differences below 2%. With this result we can conclude that the parameter based on the hydrological characteristic of the basin make sense and can improve the simulated flows.

At table 7.3, we also can see that the proposed α can improve the simulated flows reducing the RMSE in 20% in average at the first month horizon, at the second month the average improvement reduces to 12%, and four months ahead the average improvement is 6%. This reduction of performance makes sense with the characteristic of the correction that is maximum at the first day and tends to zero in a longer lead-time. With this method we aim to treat some part of the error of the observed precipitation that affect the initial conditions of the hydrological model, we assume the hypothesis that the error of the last observed precipitation affect the flows strongly at the first days and reduces along the time of the runoff hydrograph and become equivalent of the base flow at the end.

With this results this post-processor has a great potential to correct the seamless flow forecast and improve the performance specially at the shorter lead-times, where the initial conditions of the hydrological model affects more the predicted flows.

7.4.3 Evaluate the performance of the seamless forecast compared with the traditional seasonal flow forecast

After test the methods to deal with some uncertainties related to flow forecast, at figure 7.12 we present a flowchart of the proposed methodology, with each step suggested to produce the seamless flow forecast at this study.

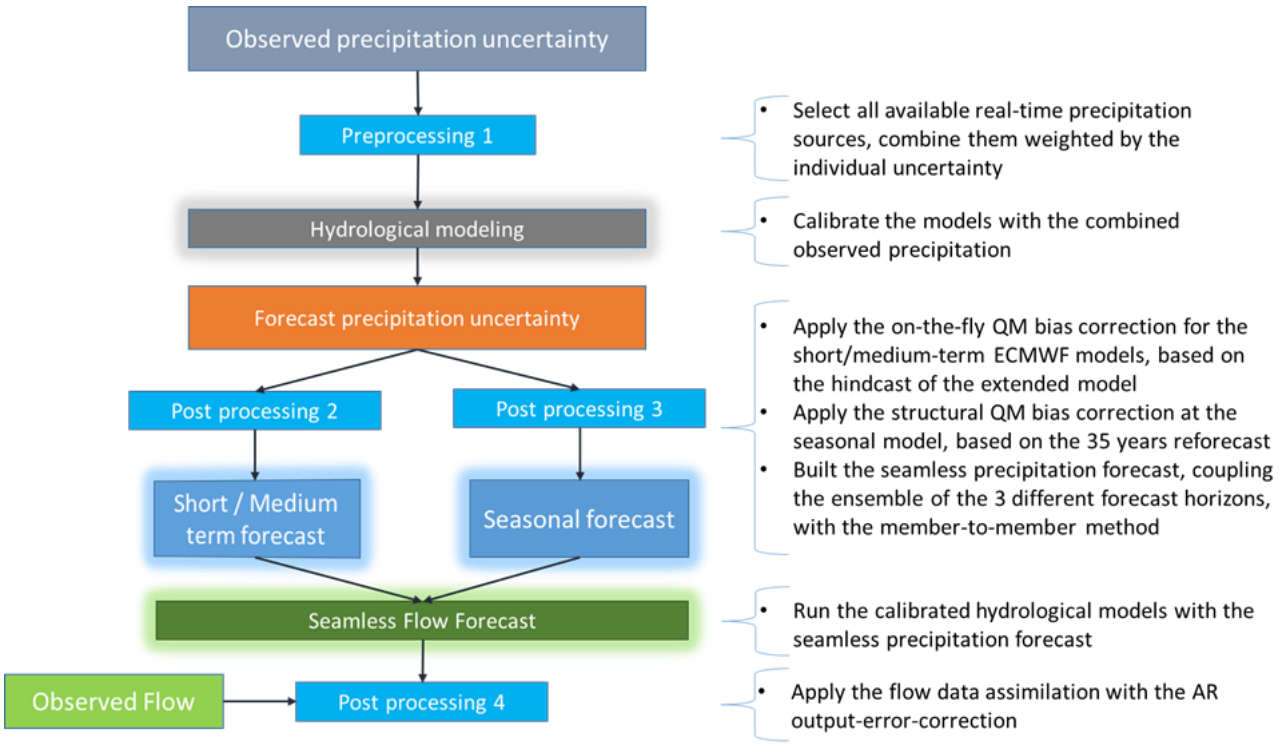

Figure 7.12– The methodological steps defined from the works of this thesis to build a seamless flow forecast.

Each step was detailed at the methodology (item 7.2) and the details and references can be obtained there.

After apply this proposed method for the flow forecast of the period 2017-2021 we evaluate the performance of this forecasts. In terms of overall performance the CRPSS indicates that the proposed seamless forecast can produce forecasts with a better results than the traditional seasonal forecast. Considering the assertiveness, the RME metric shows that the proposed

seamless forecast can reduce the error of the predictions, especially at the first month horizons, producing forecasts with less bias than the traditional seasonal forecast.

For the basins closer to the South region (group G1 and G2), only the proposed seamless forecast is able to produce forecasts more viable than the climatology, and RME showed a reduction of the tendency of overestimation only at the first month. The weather of the south region is more unstable, with no seasonality of wet and dry season, dominated by the passage of the cold fronts, that can depending on the atmospheric conditions, change dramatically the weather with strong convective storms causing big variations at the flows. This characteristic can be associated with the difficult of the models to forecast the region, generally the models have reasonable results at the first two weeks, but the performance presents a big degradation in longer horizons (see chapter 5).

For the basins of group G3, located more in the center of Brazil, we have a clear seasonality between the dry and the wet season. During the wet season the big precipitations are associated with the South Atlantic Convergency Zone - ZCAS, which creates a moisture pathway between the Amazon region and the Atlantic Ocean. This kind of precipitation has a more inertial atmosphere conditions and the models can predict this events with more antecedence, its permits the model a better performance and for a longer horizon especially at the end of the wet season and the proposed seamless forecast was able the reduce the tendence of the overestimation of the flows until the third month horizon.

In group G4, with great part of the basins under influence of the semi-arid weather, it is only possible go best than the climatology at the first month horizon with the Seamless ARpost and the proposed method was able to reduce the tendency of overestimation of the flows. Probably the reasons for the difficult of the models to forecast at this region, can be related with the strong reduction of the flows and of part of the precipitations during the last twenty years. The models was calibrated to correct the precipitation bias considering the a window of 35 years started forty years ago, when the precipitations and flows was higher than the recent years, with this situation the calibrated parameters are not able to correct so strong reduction.

In the groups G5 to G8, with basins located in the north region, and with the biggest basins, the Seamless forecast can produce more viable predictions and have a CRPSS better than the climatology in all seasons at the first two months horizon, and in the seasons OND, AMJ and

JAS we can extend this better performance for longer horizons. Considering the assertiveness, the proposed method was able to reduce the bias at the first two months and at the big basins until the third month horizon.

After the second month horizon, for the majority of the basins, the both forecasts tend to have a similar performance due the fact that the Seamless and the flow post processor acts stronger only at the initial periods, decreasing the influence along the higher lead-times.

This capacity to improve the forecasts at the initial lead times can be observed at the figures 7.5 and 7.7, where the basins with a clear seasonality between wet and dry season and with bigger drainage areas, which increase the inertia of the flows, presents a better performance of the CRPSS and with lower RME after the application of the proposed method. The smaller basins located in a region with no seasonality and with a more unstable weather, the proposed method improves the results but in a lower degree, especially in the south region of Brazil.

7.4.4 Application of the Seamless flow forecast to predict the hydropower energy production on the Brazilian electric system

At the daily activities of the ONS are calculated the ENA of more than 160 HPP of the Brazilian electric system, considering the observed inflows and the producibility at 65% of the operational volume (ONS, 2021). In this study we use a simplification to represent the ENA of each of the four main subsystem, in which the electric system is divided. We perform a flow forecast of 30 main HPP and calibrate the multiple linear regressions with the HPP inside of each of the energetic regions. At figure 7.8 was possible to see a very good fit between the calculated ENA and the observed ENA with an R^2 above 0,99 for the regions South, Southeast/Center-West and Northeast, with a value superior to 0.98 to North region, confirming how representative they are of the real ENA. With this result, we have a simplified tool to convert flow in energy and have an good idea how the forecasted flows can reflect at the HPP energy production and evaluate its potential to help on the policies of energy and water management.

Applying the conversion tool at the median of the HPP seamless flow forecasts, from the period of 2017-2021, was obtained the forecasted ENA of each subsystem. The first region, and the most difficult to predict, the South region, where we have a more unstable weather, governed by the passage of cold fronts, which depending on the atmospheric conditions can create big convective storms, which reflects in big changes of the flows and with sudden floods. The chaotic

weather, the mountainous relief and the small size of the basins, when compared with the others of the electric system, can explain why is so difficult to forecast at this subsystem. The results showed that only at the first month lead time the forecasts are viable, with lower error and with a tendency of overestimation under the studied period. For a period superior to that the errors are too high, and cannot bring a very usable information.

The second subsystem the Southeast/Center-West, with the biggest energy production in Brazil, and it is the area where is concentrated the majority of the energy consumers. This subsystem is distributed in a large geographic area, with the South Atlantic Convergency Zone (ZCAS) as the main mechanism responsible for the big precipitations during the wet season, and consequently the big flows. This precipitation system has a high inertia of the formation at the atmosphere and a longer horizon predictability. For this reasons we have better results of the forecast at this region with lower errors and viable for a longer lead time with the forecasts able to capture better the variations of the energy production. Besides to have a clear seasonality, with a dry and wet season, sometimes the strongest cold fronts from the South, affects some important basins at the Southeast region, and change the natural recession of the energy production during the dry season, driving more difficult for the forecast even during the dry season.

At the Northeast subsystem, the main mechanism responsible for the big precipitations still the ZCAS, and here we have a more clear seasonality, with practically zero precipitation during the months of the dry period. Due the absence of the precipitation forecast uncertainty at his period, the forecast recession of the hydrological model, based on the initial conditions of the basins, can have a much higher accuracy of the flows and the energy production during this season. The highest difficult appears at the wet season, with the model able to forecast the precipitation events, but the intensity is harder hit. This basin is passing for a long period of flows below the average since the last two decades, and besides the models be bias corrected and be able to reduce the overestimation, the parameters calibrated with the 35 years reforecasts (1981-2016) (see chapter 4), are not able to reproduce so strong drought and this explain the tendency of overestimation of the energy forecast at the analyzed period.

The North System, formed by big basins, is located on the equatorial region, and because of that we have the equatorial weather with convective precipitation on the major part of the basin, but at the upstream part of the basins, the precipitation still under some effect of the ZCAS. At this subsystem, the prediction of the energy production showed the major accuracy and with a longer

lead-time horizon. During the dry period, at the recession of the basins, the error is very low, evidencing the ability of the hydrological model to reproduce the baseflow, controlled by the initial conditions of the begin of the dry season. The bigger errors happens exactly during the wet season, but the model can predict with an acceptable accuracy, especially at the first two months horizon. A good signal of the accuracy of this system are the NSE near 0.8 and R^2 higher than 0.9 in practically all the six months horizon.

Finally, we have the complete SIN, where we sum the energy production of the four subsystems. Generally when aggregate the forecast in big areas the results tends to improve, therefore in the case of the Brazilian electric system, which is strongly interconnected by power lines, make sense this systemic analysis because the excess of flow/energy in one region can be transported to other region to be used or stored at the reservoirs. At this complete system, the difficult of forecast at the South region is compensated by the accuracy of the North region forecast. At figure 7.11 is possible the see that the proposed methodology is able to capture the variation of the energy production, predicting the wet period and capturing part of the intensity, even in a long forecast horizon, giving a good view of the future scenarios of the HPP energy production of the interconnected system. It is possible to see that the model was able to predict this sequence of years of energy production below the average during the wet period, and during the recession periods, where the production reached near to 50% of the mean, at the driest month. Other advantage of this systemic analysis is that the distribution of the errors became more homogeneous along the analyzed period, practically without a bias (near -2%).

When we compare the results of ENA prediction obtained with the Seamless forecast versus the reference model NEWAVE the seamless has superiority in 3 of the four subsystems, but at the analysis of the complete electric system The proposed forecast has superior performance in all six months horizon. Besides the newest NEWAVE, tried to solve the tendency to quick converge to the climatology in longer horizons, and give more capacity to represent a severe hydrological tendency, based on the short past tendency (last 12 months) (Lima and Oliveira, 2021), the reference model still exhibiting a tendency of overestimation of the ENA at the analyzed period and still converging to the climatology after the third month horizon with predicted values closer to the historical mean flows than to observed values in all subsystems and at the SIN. The seamless forecast presents as lower bias, for a longer horizon, even at the Southeast/Center-West subsystem where the NEWAVE has a better MAPE skill score, Therefore the Seamless forecast shows a better capacity to predict the more extreme events (droughts and floods) giving the

possibility to have a more conservative policy of energy production, and save water on the reservoirs once the models indicates the production below the average months before. This indicates that the proposed forecast can be a promising information to help on the energy production policy.

7.5 CONCLUSIONS

A sequence of steps was described that can be used to obtain a better flow forecast to be applied at the prediction of the HPP energy production in Brazil. The main conclusion is that the seamless flow forecast, with the proposed postprocessors, can improve the predictability of the flows at the basins studied to perform the forecast at the main 30 HPP in the Brazilian electric system, and consequently improve the prediction of the HPP energy production. This shows a great potential to help on the optimization of the energy generation and on the management of the water resources of the HPP reservoirs.

At this study, we show that the QM bias correction method, applied to deal with the uncertainty of the hydrological model, may be not enough robust to be applied on the correction of the simulated flows, neither at the flow forecast. Being able only to correct at the calibrated period, when the same parameters are applied in a validation period the correction does not exhibit the same capacity off correction, and in some basins get worse results.

Another postprocessor, the data assimilation of the observed flow, with the output-error-correction method, proved to be very effective at the correction of the seamless flows forecasts, especially at the first month horizon, reducing significantly the error and generating forecast more viable.

The proposed seamless flow forecast was tested against the traditional seasonal flow forecast showing a clear improvement at the flow forecast performance. The proposed seamless forecast shows the advantage of the more frequent initializations of the meteorological models, and the benefit of the suggested post processor to correct the flow forecast and improve the accuracy and the reliability.

The seamless forecast proposed at this study shows a great potential to help on the prediction of the HPP energy production at the Brazilian electric system. With application at each of four subsystems (South, Southeast/Center-Wes, North, and Northeast) shows how is the predictability

in each of them and also in conjunctural application, when we analyze the complete interconnected system, in terms of HPP energy production, the proposed forecast shows the capacity to forecast this observed sequence of years with energy production below the average at the analyzed period. Presenting a better performance to predict the HPP energy production of the interconnected electric system – SIN, at the six months horizon, at the period analyzed, than the reference model NEWAVE, the official software of Brazilian energy planning.

CHAPTER 8:

FINAL CONSIDERATIONS

8 FINAL CONSIDERATIONS

With the results obtained it is possible to answer the scientific questions proposed at the begin of the research.

1. *How to improve the representativeness of Brazilian climatology as an way of guaranteeing energy security in the context of hydroelectric generation?*

    a. *How representative of local climatology is the daily grid observed precipitation data provided by the TRMM-MERGE and by the CPC-NOAA for their use in rainfall-runoff models and inflow forecasting to a group of hydropower plants in Brazil?*

The first part of the research showed that for some basins the two sources show considerable differences, notably in terms of daily and monthly precipitation values, with an expected impact on the simulation of daily streamflows. In addition, a spatial behavior of the differences between the precipitation sources was detected, with differences becoming more positive (i.e., TRMM-MERGE values are higher than CPC values) as we move to north and west in the study area.

With the results of this study, we recommend being cautious when working with a unique source of historic precipitation data to calibrate hydrological models, since this source can displays uncertainties and errors that vary in space and time. In our study, we showed that it is a complex problem to determine a precipitation data source that could be the best for all situations, especially when no observed data set can be used as ground truth or reference, as in the case of large continental areas, such as South America.

    b. *Can this information be blended to have a better precipitation forcing and reduce the uncertainty of the observed precipitation while providing a better initial condition for the hydrological models?*

The experiment described in chapter 3 showed that the combination of the real-time precipitation (TRMM-MERGE and CPC), weighted by the uncertainty of the original sources, performs better than the isolated use of them, and is possible to have a longer time series using double-mass curve correlation and hydrological models to validate it. This time series can be used to have a

better calibration of the hydrological models and to give better initial condition for hydrological models, in a forecast mode, than the use of only one of the sources.

c. *Can this new observed precipitation data be used to perform bias correction to the meteorological forecasts?*

On the experiment showed in chapter 3, when comparing the uncertainty of the obtained blended precipitation dataset with the reanalysis product MSWEP, the uncertainties are in a similar magnitude, a good result for a real-time dataset. Therefore, this blended precipitation can be used to perform the analysis and the bias correction of the forecast models. Once the hydrological models are calibrated with this dataset, the blended precipitation should be the reference to assess the precipitation forecasts performance and calibrate the bias correction methods, with the objective to obtain a better flow forecast.

2. *How good is the performance of the weather forecasting models made available by the meteorological center of ECMWF (UK) for short (days to weeks) to long (months to seasons) forecast ranges in the Brazilian context of hydropower production?*

    a. *Can the application of bias correction techniques improve the performance of the forecasts for the Brazilian basins?*

About the seasonal forecast, the experiment described in the chapter 4, the raw seasonal forecast presented a clear bias and the methods of correction (QM- Quantile Mapping and LS – Linear Scaling) were very effective to correct the precipitations, improving the assertiveness and the reliability. To separate only the effect of the precipitation bias correction on the flow forecast, the predictions were compared with the simulated flows, the precipitation correction converts in a better flow forecast, reducing the errors and presenting viable results in the seven months horizon for almost all basins. The uncertainties of the observed precipitation, affects the hydrologic model calibration and the initial conditions of the forecast, reducing the improvement in quality at the first month horizon. Despite of that, the flow forecast have enough quality and with potential to contribute in operational decisions for hydropower operation.

    a. *For the short-term forecasts, does the 'on-the-fly' bias correction based on the seasonal hindcasts perform better than the structural bias correction based on the short-range reforecasts?*

For the short-term and the extended model, the study described in chapter 5, shows that the ECMWF S2S models was able to produce viable forecasts at least at the first three weeks horizon and the on-the-fly bias correction was able to improve the precipitation forecasts, especially at the cases where was observed systematics overestimations or underestimations of the precipitations. When we compare the recent period 2017-2020, the on-the-fly bias correction exhibited results equal or superior than the traditional bias correction based on ten years reforecast parameters calibration period to correct the ECMWF EPS, the short term model. One other clear advantage of this on-the-fly bias correction, it is that we are able to follow any change of the forecast model, being able to calibrate the bias correction parameters without the necessity wait for a long period to have a reasonable reforecast to calibrate the bias correction parameters.

b. *How can we build a seamless hydrometeorological forecast for hydropower decision-making, ranging from short to seasonal scales?*

In chapter 6 we study the seamless precipitation forecast, and this approach can be done coupling the three ECMWF forecast models (EPS, S2S and Seasonal), to have a continuous daily precipitation forecast, with a daily actualization. We recommend the use of the member-to-member coupling, which presents the best cost-benefit ratio, due the fact that other more sophisticated methods did not perform better than this simple method, which does not have a computational effort or data manipulation. The seamless precipitation forecast presents a performance superior than the seasonal model, and showed a great capacity to anticipate, in some weeks, the occurrence of higher anomalies of precipitation during the wet season in Brazil. This capacity brings great opportunities for this category of forecast to future applications in hydrological models, to generate flow forecasts to improve the hydropower operation.

3. *Can the benefits of the seamless precipitation forecast be translated into a better seasonal flow forecast and even into a better driver for decision making in the electric sector?*

   a. *Can the Quantile Mapping bias correction method correct the systematic hydrological calibration bias?*

In chapter 7, we show that the QM bias correction method is not enough robust to be applied on the correction of the simulated flows, neither at the flow forecast. Being able only to correct at the calibrated period, when the same parameters are applied in a validation period the correction does no exhibit the same capacity off correction.

b. Can flow data assimilation improve the performance of the streamflow forecasts?

To deal with the uncertainty of the initial conditions we suggest the post processor that uses the data assimilation of observed flow, and the output-error-correction method proved to be very effective at the correction of the seamless flows forecasts, especially at the first month horizon, reducing significantly the error and generating forecast more viable.

c. Can the seamless forecasts help on building decision-making guidance for hydropower generation?

The proposed seamless flow forecast shows a clear improvement at the flow forecast performance when compared with the traditional seasonal flow forecast. Being clear the advantage of the more frequent initializations of the meteorological model, and the benefit of the suggested post processor to correct the flow forecast and improve the accuracy and the reliability. When it was applied at each electric subsystems shows how the predictability of the hydropower energy production is in each of them and also in conjunctural application, when we analyze the complete interconnected system, the proposed flow forecast shows the capacity to forecast the observed sequence of years with energy production below the average at four years analyzed. The seamless forecast proposed at this study shows a great potential to help on the prediction of the HPP energy production at the Brazilian electric system. The results of this study shows that we can extend the application of the meteorological models to predict the hydropower energy production, for period superior than those actually practiced by the ONS, which uses practically only at the first month horizon.

Recommendations:

This study is only the begin of a long research line and there are a lots of questions that need to be answered with more research, as the performance new post processors based on the climatic teleconnections as a drivers, extend the forecast period with the use of the ESP – Ensemble streamflow prediction, with the selection of the years based on the similarity of the last years or with the current meteorological forecast, apply the method suggested to produce the seamless forecast with other group models and create a super-ensemble. There is a long road to be covered by those who want to follow this challenge, which is generate a flow forecasting.

BIBLIOGRAPHIC REFERENCES

BIBLIOGRAPHIC REFERENCES

ADLER, R. F.; HUFFMAN, G. J.; CHANG, A.; FERRARO, R.; XIE, P.; JANOWIAK, J.; RUDOLF, B.; SCHNEIDER, U; CURTIS, S.; BOLVIN, D.; GRUBER, A.; SUSSKIND, J.; ARKIN, P. and NELKIN, E. – The Version-2 Global Precipitation Climatology Project (GPCP) Monthly Precipitation Analysis (1979-Present). American Meteorological Society – Vl. 4, 1147-1167, - doi.org/10.1175/1525-7541, 2003.

ALFIERI, L.; BUREK, P., DUTRA; E., KRZEMINSKI, B.; MURARO, D.; THIELEN, J.; and PAPPENBERGER, F.: GloFAS – Global Ensemble Streamflow Forecasting and Flood Early Warning, Hydrol. Earth Syst. Sci., 17, 1161-1175, doi.org/10.5194/hess-17-1161-2013, 2013.

ANDRADE, F. M., COELHO, C. A. S., and CAVALCANTI, I. F. A.: Global precipitation hindcast quality assessment of the Subseasonal to Seasonal (S2S) prediction project models, Climate Dynamics, https://doi.org/10.1007/s00382-018-4457-z, 2018.

ANGHILERI, D.; VOISIN, N.; CASTELLETTI, A.; PIANOSI, F.; NIJSSEN, B. and LETTENMAIER, D. P.: Value of long-term streamflow forecasts to reservoir operations for water supply in snowdominated river catchments. Water Resources Research, 52, 4209–4225. doi:10.1002/2015WR017864, 2016.

ARNAL, L.; WOOD, A. W.; STEPHENS, E.; CLOKE, H. L. and PAPPENBERGER, F.: An efficient approach for estimating streamflow forecast skill elasticity. Journal of Hydrometeorology, 18 (6). pp. 17151729. ISSN 15257541 doi: https://doi.org/10.1175/JHMD160259.1, 2017

ARNAL, L.; CLOKE, H. L.; STEPHENS, E.; ETTERHALL, F.; PRUDHOMME, C.; NEUMANN, J.; KRZEMINSKI, B.; and PAPPENBERGER, F.: Skillful seasonal forecasts of streamflow over Europe?, Hydrol. Earth Syst. Sci., 22, 2057-2072, https://doi.org/10.5194/hess-22-2057-2018, 2018.

ALLEN, R. G.; PEREIRA, L. S.; RAES, D.; and SMITH, M.: Crop evapotranspiration - Guidelines for computing crop water requirements - FAO Irrigation and drainage paper 56., FAO - Food and Agriculture Organization of the United Nations, Rome, M-56, ISBN 92-5-104219-5, 1998.

ARKIN, P. A.; and MEISNER, B. N.: The relationship between large-scale convective rainfall and cold cloud over the western hemisphere during 1982–84. Mon. Weather Rev. 115, 51–74 (1987).

BALSAMO, G.; BELJAARS, A.; SCIPAL, K.; VITERBO, P.; VAN DEN HURK, B.; HIRSCHI, M. and BETTS, A. K.: A Revised Hydrology for the ECMWF Model: Verification from Field Site to Terrestrial Water Storage and Impact in the Integrated Forecast System, Journal of Hydrometeorology, 10, 623-643, 10.1175/2008jhm1068.1, 2009.

BARNSTON, A. G., and MASON, S. J.: Evaluation of IRI's seasonal climate forecasts for the extreme 15% tails. Wea. Forecasting, 26, 545–554, https://doi.org/10.1175/WAF-D-10-05009.1, 2011.

BAUER, P., THORPE, A., and BRUNET, G.: The quiet revolution of numerical weather prediction.Nature,525, 47–55, https://doi.org/10.1038/nature14956, 2015

BECK, H. E.; VAN DIJK, A. I. J. M.; LEVIZZANI, V.; SCHELLEKENS, J.; MIRALLES, D. G.; MARTENS, B. and DE ROO, A.: MSWEP: 3-hourly 0.25_ global gridded precipitation (1979–2015) by merging gauge, satellite, and reanalysis data, Hydrol. Earth Syst. Sci., 21, 589–615, 2017 - doi:10.5194/hess-21-589-2017.

BECK, H. E.; WOOD, E. F.; MCVICAR, T. R.; ZAMBRANO-BIGIARINI, M.; ALVAREZ-GARRETION, C.; BAEZ-VILLANUEVA, O. M.; SHEFFIELD, J.; and KARGER, D. N.: Bias correction of Global High-Resolution Precipitation Climatologies Using Streamflow Observations from 9372 Catchments. Journal of Climate, vol33, Issue4, DOI: 10.1175/JCLI-D-19-0332.1, 2020.

BECK, H. E.; WOOD, E. F.; PAN, M.; FISHER, C. K.; MIRALLES, D. G.; VAN DIJK, A. I. J. M.; MCVICAR, T. R.; and ADLER, R. F.: MSWEP V2 Global 3-Hourly 0.1° Precipitation – Methodology and Quantitative Assessment. American Meteorological Society, DOI:10.1175/BAMS-D-17-0138.1, 2019.

BECKERS, J. V. L.; WEERTS, A. H.; TIJDEMAN, E. and WELLES, E.: ENSO-conditioned weather resampling method for seasonal ensemble streamflow prediction, Hydrol. Earth Syst. Sci., 20, 3277–3287, 2016 - doi:10.5194/hess-20-3277-2016.

BELLIER, J., ZIN, I., and BONTRON, G.: Generating Coherent Ensemble Forecasts After Hydrological Postprocessing: Adaptations of ECC-Based Methods. Adaptations of ECC-based methods. Water Resources Research, 54, 5741–5762. https://doi.org/10.1029/2018WR022601, 2018.

BENNETT, J. C.; WANG, Q. J.; ROBERTSON, D. E., SCHEPEN, A.; LI, M., and MICHAEL, K.: Assessment of an ensemble seasonal streamflow forecasting system for Australia, Hydrol. Earth Syst. Sci., 21, 6007-6030, https://doi.org/10.5194/hess-21-6007-2017, 2017

BENNETT, T. H.: Development and application of a continuous soil moisture accounting algorithm for the Hydrologic Engineering Center Hydrologic Modeling System (HEC-HMS). MS thesis, Dept of Civil and Environmental Engineering, University of California, Davis, 1998

BERGSTRÖM, S., The HBV model. In: Singh, V.P. (Ed.) Computer Models of Watershed Hydrology. Water Resources Publications, Highlands Ranch, CO., pp. 443-476. 1995.

BITEW, M. M.; GEBREMICHAEL, M.; GHEBREMICHAEL, L. T. and BAYISSA, Y. A.: Evaluation of high-resolution satellite rainfall products through streamflow simulation in a hydrological modeling of a small mountainous watershed in Ethiopia, Journal of Hydrometeorology, 13, 338–350, 2012.

BLOCK, P. J.; SOUZA FILHO, F. A.; SUN, L.; and KWON, H. H.: A Streamflow Forecasting Framework using Multiple Climate and Hydrological Models1, J. Am. Water Resour. Assoc., 45, 828–843, 2009.

BLOSCHL, G., RESZLER, C. and KOMMA, J.: A spatially distributed flash flood forecasting model, Environmental Modelling & Software, Volume 23, Issue 4, April 2008, Pages 464-478, https://doi.org/10.1016/j.envsoft.2007.06.010, 2008.

BOUCHER, M. A.; RAMOS, M. H.: Handbook of Hydrometeorology Ensemble Forecasting, cap – Ensemble Streamflow Forecasts for Hydropower Systems, pg 1-19, Ed. Springer Berlin Heidelberg, 2018

BREMNES, J. B.: Probabilistic Forecasts of Precipitation in Terms of Quantiles Using NWP Model Output, Monthly Weather Review, 132, 338– 347, doi:10.1175/1520-0493(2004)132%3C0338:PFOPIT%3E2.0.CO;2, 2004.

BRIER, G. W.: Verification of forecasts expressed in terms of probability. Monthly Weather Review, **78**, 1-3. 1950

BROERSEN, P. M. T.: Error correction of rainfall-runoff models with the ARMAsel program. IEEE Trans. Instrum. Meas. 56(6): 2212–2219, 2007.

BROWN, J. D. and SEO, D.-J.: A Nonparametric Postprocessor for Bias Correction of Hydrometeorological and Hydrologic Ensemble Forecasts, Journal of Hydrometeorology, 11, 642–665, doi:10.1175/2009JHM1188.1, 2010.

BROWN, J. D.; DEMARGNE, J.; SEO, D.-J.; and LIU, Y.: The Ensemble Verification System (EVS): a software tool for verifying ensemble forecasts of hydrometeorological and hydrologic variables at discrete locations, Environ. Modell. Software, 25, 854–872, 2010.

BROWN, J. D. and SEO, D.-J.: Evaluation of a nonparametric postprocessor for bias correction and uncertainty estimation of hydrologic predictions, Hydrological Processes, 27, 83–105, doi:10.1002/hyp.9263, 2013.

CASSAGNOLE, M., RAMOS, M.-H., ZALACHORI, I., THIREL, G., GARÇON, R., GAILHARD, J., and OUILLON, T.: Impact of the quality of hydrological forecasts on the management and revenue of hydroelectric reservoirs – a conceptual approach, Hydrol. Earth Syst. Sci., 25, 1033–1052, https://doi.org/10.5194/hess-25-1033-2021, 2021

CASSALHO, F.; RENNÓ, C. D.; REIS, J. B. C.; and SILVA B. C.: Hydrologic Validation of MERGE Precipitation Products over Anthropogenic Watersheds. Water 2020, 12(5), 1268; https://doi.org/10.3390/w12051268, 2020.

CCEE: O SIN e os modelos NEWAVE e DECOMP utilizados no planejamento da operação energética e no cálculo do PLD Junho. CEUR Workshop Proceedings, 2016.

CCEE – CAMARA DE COMERCIALIZAÇÃO DE ENERGIA ELÉTRICA: Regras de Comercialização. https://www.ccee.org.br/ccee/documentos/CCEE_653095 , Access at May 6th 2020.

CCEE. Camara de Comercialização de E. E. Metodologia. 2021. Disponível em <https://www.ccee.org.br/portal/faces/pages_publico/o-que-fazemos/como_ccee_atua/precos/metodologia_de_precos?_afrLoop=104858829549211&_adf.ctrl-state=19bttq07jq_1#!%40%40%3F_afrLoop%3D104858829549211%26_adf.ctrl-state%3D19bttq07jq_5>. Accessed on 06/09/2021.

Centro de Previsão do Tempo e Estudos Climáticos – Instituto Nacional de Pesquisas Espaciais – CPTEC - INPE. (2018). TRMM-MERGE Dataset ftp. Retrieved in 2018, January 22, from ftp:ftp1.cptec.inpe.br/modelos/io/produtos/MERGETRMM-MERGE

CHEN, M.; XIE, P.; SHI, W.; SILVA, V., KOUSKY; V., HIGGINS, W.; and JANOWIAK, .J. E.: Quality control of daily precipitation reports at NOAA/CPC. In autor (es). Quality control working group climate prediction center (CPC)/NCEP/NOAA (pp. 1-7). 12th Conference on IOAS-AOLS Adjourns. Maryland: NOAA, 2008.

CHEN, M.; XIE P.; and CPC Quality Control Working Group Climate Prediction Center (CPC)/NCEP/NOAA: Quality Control of Daily Precipitation Reports at NOAA/CPC, CPC-NOAA GTS QC AMS, 2008.

CHEN, Y.; WENG, F.; HAN, Y.; and LIU, Q.: Validation of the Community Radiative Transfer Model by using CloudSat data. JOURNAL OF GEOPHYSICAL RESEARCH, VOL. 113, D00A03, doi:10.1029/2007JD009561, 2008.

COELHO, C. A. S.; FIRPO, M. A. F.; and ANDRADE, F. M.: A verification framework for South American sub-seasonal precipitation predictions, Meteorologische Zeitschrift, PrePub DOI 10.1127/metz/2018/0898, 2018.

COLLISCHONN, B.; COLLISCHONN, W. and TUCCI, C. E. M.: Daily hydrological modeling in the Amazon basin using TRMM rainfall estimates. J. Hydrol., 360, 207–216, https://doi.org/10.1016/j.jhydrol.2008.07.032, 2008.

CLOKE, H. L. and PAPPENBERGER, F.: Ensemble flood forecasting: A review. Journal of Hydrology, v.375, n. 3–4, p.613–626, 2009.

CROCHEMORE, L.; RAMOS, M.-H.; and PAPPENBERGER, F.: Bias correcting precipitation forecasts to improve the skill of seasonal streamflow forecasts, Hydrol. Earth Syst. Sci., 20: 3601-3618, doi:10.5194/hess-20-3601-2016, 2016.

CROCHEMORE, L., RAMOS, M.-H., PAPPENBERGER, F., and PERRIN, C.: Seasonal streamflow forecasting by conditioning climatology with precipitation indices, Hydrol. Earth Syst. Sci., 21, 1573-1591, DOI: 10.5194/hess-21-1573-2017, 2017.

DAY, G. N.: Extended streamflow forecasting using NWSRFS, J. Water Res. Pl.-ASCE, 111, 157–170, https://doi.org/10.1061/(ASCE)0733-9496(1985)111:2(157), 1985.

DELGADO, J. M., VOSS, S., BÜRGER, G., VORMOOR, K., MURAWSKI, A., RODRIGUES PEREIRA, J. M., MARTINS, E., VASCONCELOS JÚNIOR, F., and FRANCKE, T.: Seasonal drought prediction for semiarid northeastern Brazil: verification of six hydro-meteorological forecast products, Hydrol. Earth Syst. Sci., 22, 5041–5056, https://doi.org/10.5194/hess-22-5041-2018, 2018.

DEMARGNE, J., WU,L., REGONDA, S.K., BROWN, J. D., LEE, H. HE, M., SEO, D.J., HARTMAN, R., HERR, H. D., FRESCH, M., SCHAAKE, J., and ZHU. Y.: The Science of NOAA's Operational Hydrologic Ensemble Forecast Service, Bulletin of the American Meteorological Society, HTTPS://DOI.ORG/10.1175/BAMS-D-12-00081.1, 2014.

DEMARIA, E. M. C.; RODRIGUEZ, D. A.; EBERT E. E.; SALIO, P.; SU, F. and VALDES, J. B.: Evaluation of mesoscale convective systems in South America using multiple satellite products and an object-based approach. J. Geophys. Res., 116, D08103, doi:10.1029/2010JD015157 – 2011.

DÉQUÉ, M.; ROWELL, D.; LÜTHI, D.; GIORGI, F.; CHRISTENSEN, J.; ROCKEL, B.; JACOB, D.; KJELLSTRÖM, E.; DE CASTRO, M. and VAN DEN HURK, B.: An intercomparison of regional climate simulations for Europe: assessing uncertainties in model projections, *Climatic Change*, 81, 53–70, 2007.

DISKIN, M. H. and SIMON, E.: A procedure for the selection of objective functions for hydrologic simulation models, Journal of Hydrology, 34, 129-149, https://doi.org/10.1016/0022-1694(77)90066-X , 1977.

DOLL, P.; FIEDLER, K. and ZHANG, J.: Global-scale analysis of river flow alterations due to water withdrawals and reservoirs, Hydrology and Earth System Sciences, 13, 2413-2432, https://doi.org/10.5194/hess-13-2413-2009, 2009.

ECMWF – European Centre for Medium-Range Weather Forecasts.: User Guide to ECMWF Forecast Products – pp 1 – 121, UK. 2015.

ECMWF – European Centre for Medium-Range Weather Forecasts.: System 5 user guide, Version 1.0, October. 2017.

ECMWF – European Centre for Medium-Range Weather Forecasts. https://confluence.ecmwf.int/display/COPSRV/GloFAS+v2.1. Access at January15th 2020.

ELMORE, L. K. and RICHMAN, M. B.: Euclidean Distance as a Similarity Metric for Principal Component Analysis, Monthly Weather reviews, 129, 540-549, 2001.

EMERTON, R. E.; STEPHENS, E. M.; PAPPENBERGER, F.; PAGANO, T. C.; WEERTS, A. H.; WOOD, A. W.; SALAMON, P.; BROWN, J. D.; HJERDT, N.; DONNELLY, C.; BAUGH, C. A.; and CLOKE, H. L.: Continental and global scale flood forecasting systems, Wiley Interdiscip. Rev. Water, 3, 391–418, https://doi.org/10.1002/wat2.1137, 2016.

EMERTON, R., ZSOTER, E., ARNAL, L., CLOKE, H. L., MURARO, D., PRUDHOMME, C., STEPHENS, E. M., SALAMON, P., and PAPPENBERGER, F.: Developing a global operational seasonal hydro-meteorological forecasting system: GloFAS-Seasonal v1.0, Geosci. Model Dev., 11, 3327–3346, 2018 - https://doi.org/10.5194/gmd-11-3327-2018.

EMPRESA DE PESQUISA ENERGÉTICA - EPE: Balanço Energético Nacional 2019: Ano base 2018– 292 p., Rio de Janeiro, Brasil, 2019.

FALCK, A. S.; MAGGIONI, V.; TOMASELLA, J.; VILA, D. A. and DINIZ, F. L. R.: Propagation of satellite precipitation uncertainties through a distributed hydrologic model: A case study in the Tocantins-Araguaia basin in Brazil, J. Hydrol., 527, 943–957, doi:10.1016/j.jhydrol.2015.05.042, 2015.

FAN F. M.; COLLISCHONN, W.; MELLER, A.; and BOTELHO, L. C. M. Ensemble streamflow forecasting experiments in a tropical basin: The São Francisco river case study, Journal of Hydrology, Volume 519, Part D, 2014, Pages 2906-2919, ISSN 0022-1694, http://dx.doi.org/10.1016/j.jhydrol.2014.04.038.

FAN, F. M.; SCHWANENBERG, D. ; COLLISCHONN, W.; WEERTS, A. Title: Verification of Inflow into Hydropower Reservoirs using Ensemble Forecasts of the TIGGE Database for

Large Scale Basins in Brazil. Journal of Hydrology: Regional Studies. EJRH-D-14-00159R1. 2015.

FAN, F. M.; COLLISCHONN, W.; JIMÉNEZ, K. Q.; SORRIBAS, M. V.; BUARQUE, D.; SIQUEIRA, V. Flood forecasting on the Tocantins River using ensemble rainfall forecasts and real-time satellite rainfall estimates. Journal of Flood Risk Management. 10.1016/j.jhydrol.2014.04.038, 2016.

FAN, F. M.: Previsão por conjunto de vazões afluentes a reservatórios em grandes bacias hidrográficas brasileiras. Tese de Doutorado - Universidade Federal do Rio Grande do Sul. Instituto de Pesquisas Hidráulicas. Programa de Pós-Graduação em Recursos Hídricos e Saneamento Ambiental – pp. 1 – 364, Porto Alegre - RS, 2015

FAN, F. M.; SCHWANENBERG, D.; ALVARADO, R.; REIS, A. A. D.; COLLISCHONN, W.; and NAUMMAN, S.: Performance of Deterministic and Probabilistic Hydrological Forecasts for the Short-Term Optimization of a Tropical Hydropower Reservoir. Water Resour. Manage. - 2016 - 30:3609–3625 - DOI 10.1007/s11269-016-1377-8

FAN, Y.; VAN DEN DOLL, H.: Bias correction and forecast skill of NCEP GFS Ensemble Week-1 and Week-2 precipitation, 2-m surface temperature, and soil moisture forecasts. American Meteorological Society, DOI: 10.1175/WAF-D-10-05028.1 , 2011

FELDMAN, A. D.: Hydrologic Modeling System – HEC-HMS – Technical Reference Manual, USACE – US Army Corps of Engineers - Hydrologic Engineering Center, CA, USA, 2000.

FERREIRA, S. A. and GAN, M. A.: Intraseasonal variability in the South American monsoon system. Royal Neteorological Society, Atmos. Sci. Let. 12: 253–260, (wileyonlinelibrary.com) DOI: 10.1002/asl.328, 2011.

GARREAUD, R. D., VUILLE, M., ROSA, C. and MARENGO, J.: Present-day South America Climate. Palaeogeography, Palaeoclimatology, Palaeoecology Journal, 281, 180–195, doi:10.1016/j.palaeo.2007.10.032, 2009.

GIBERTONI, R. F. C.; SABOIA, J. P. J.; DARU, R. L.; KAN, A.; OENING, A. P.; DETZEL, D. H. M.; TALSMA, J. and REIS, A. A.: Previsão de Vazões e Operação de Reservatórios Através do Sistema Fews-CEMIG. IX CITENEL – Congresso de Inovação Tecnológica em Energia Elétrica, João Pessoa, PB – 2017, editora: CITENEL.

GILEWSKI, P. and NAWALANY, M.: Inter-Comparison of Rain-Gauge, Radar, and Satellite (IMERG GPM) Precipitation Estimates Performance for Rainfall-Runoff Modeling in a Mountainous Catchment in Poland. Water, 10, 1665. https://doi.org/10.3390/w10111665, 2018.

GILL, J.; RUBIERA, J.; MARTIN, C.; CACIC, I.; MYLNE K.; DEHUI, C.; JIAFENG, G.; XU, T.; YAMAGUCHI, M.; FOAMOUHOUE, A. K.; POOLMAN, E. AND GUINEY, J.: Guidelines on communication forecast uncertainty. WMO – Word Meteorological Organization. WMO/TD No. 1422, 2008

GNEITING, T., RAFTERY, A., WESTVELD, A., and GOLDMAN, T.: Calibrated probabilistic forecasting using ensemble model output statistics and minimum CRPS estimation, Monthly Weather Review, 133, 1098–1118, 2005.

GOLDING, B. W.: Long lead time flood warnings: reality or fantasy?. Meteorol. Appl., 16, 3–12, https://doi.org/10.1002/met.123 , 2009.

GUBLER, S.; SEDLMEIER, K.; BHEND, J.; AVALOS, G.; COELHO, C. A. S.; ESCAJADILLO, Y.; JACQUES-COPER, M.; MARTINEZ, R.; SCHWIERZ, C.; DE SKANSI, M.; and SPIRIG, CH.: Assessment of ECMWF SEAS5 Seasonal Forecast Performance over south America, American Meteorological Society, 35, 561-584, DOI: 10.1175/WAF-D-19-0106.1, 2020.

GUDMUNDSSON, L.; BREMNES, J. B.; HAUGEN, J. E. and ENGEN-SKAUGEN, T.: Technical Note: Downscaling RCM precipitation to the station scale using statistical transformations – a comparison of methods, Hydrol. Earth Syst. Sci., 16, 3383–3390, doi:10.5194/hess-16-3383-2012, 2012.

GUPTA, H. V.; KLING, H.; YILMAZ, K. K.; and MARTINEZ, G. F.: Decomposition of the mean squared error and NSE performance criteria: Implications for improving hydrological modeling. JOURNAL OF HYDROLOGY, VOLUME 377, ISSUES 1-2, 20 OCTOBER 2009, PAGES 80-91. DOI: 10.1016/J.JHYDROL.2009.08.003. ISSN 0022-1694, 2009.

HAGEDORN, R., HAMILL, T., and WHITAKER, J.: Probabilistic forecast calibration using ECMWF and GFS ensemble reforecasts. Part I: Two-meter temperatures, Monthly Weather Review, 136, 2608–2619, 2008.

HAGEMANN, S.; CHEN, C.; HAERTER, J. O.; HEINKE, J.; GERTEN, D. and PIANI, C.: Impact of a Statistical Bias Correction on the Projected Hydrological Changes Obtained from Three GCMs and Two Hydrology Models, Journal of Hydrometeorology, Water and Global Change (WATCH), vol 12, pg 556-578, DOI: 10.1175/2011JHM1336.1, 2011.

HAMILL, T.M., WHITAKER, J.S., and MULLEN, S.L.: Reforecasts: An important dataset for improving weather predictions. Bull. Am. Meteorol. Soc. 87 (1), 33–46. https://doi.org/10.1175/BAMS-87-1-33, 2006.

HAMILL, T.; HAGEDORN, R.; and WHITAKER, J.: Probabilistic forecast calibration using ECMWF and GFS ensemble reforecasts. Part II: Precipitation, Monthly Weather Review, 136, 2620–2632, 2008.

HAMILL, T. M.; BATES, G. T.; WHITAKER, J. S.; MURRAY, D. R.; FIORINO, M.; GALARNEAU JR., T. J.; ZHU, Y.; and LAPENTA, W.: NOAA's second-generation global medium-range ensemble reforecast; dataset. Bull. mer. Meteor. Soc.,94, 1553–1565, https://doi.org/ 10.1175/BAMS-D-12-00014.1, 2013.

HARRIGAN, S.; PRUDHOMME, C.; PARRY, S.; SMITH, K.; and TANGUY, M.: Benchmarking ensemble streamflow prediction skill in the UK, Hydrol. Earth Syst. Sci., 22, 2023-2039, https://doi.org/10.5194/hess-22-2023-2018, 2018.

HAY, L. E. and CLARK, M. P.: Use of statistically and dynamically downscaled atmospheric model output for hydrologic simulations in three mountainous basins in the western United States, J. Hydrol., 282, 56–75, doi:10.1016/s0022-1694(03)00252-x, 2003.

HENN, B.; CLARK, M. P.; KAVETSKI, D. and LUNDQUIST, J. D.: Estimating mountain basin-mean precipitation from streamflow using Bayesian inference, Water Resour. Res., 51, 8012– 8033, doi:10.1002/2014WR016736, 2015

HEROLD, N.; ALEXANDER, L. V.; DONAT, M. G.; CONTRACTOR, S. and BECKER, A.: How much does it rain over land?, Geophys. Res. Lett., 43, 341–348, https://doi.org/10.1002/2015GL066615, 2015.

HERSBACH, H.: Decomposition of the continuous ranked probability score for ensemble prediction systems, Weather Forecast., 15, 559–570, https://doi.org/10.1175/1520-0434(2000)015<0559:DOTCRP>2.0.CO;2 , 2000.

HONG, Y.; TANG, G.; MA, Y.; HUANG, Q.; HAN, Z.; ZENG, Z.; YANG, Y.; WANG, C.; and GUO X.: Remote Sensing Precipitation: Sensors, Retrievals, Validations, and Applications. Observation and Measurement, Ecohydrology, https://doi.org/10.1007/978-3-662-47871-4_4-1, 2018.

HSU, M. H., FU, J. C., and LIU, W. C.: Flood routing with real-time stage correction method for flash flood forecasting in the Tanshui River, Taiwan. J Hydrol 283:267–280, 2003.

HUFFMAN, G. J.; ADLER, R. F.; ARKIN, P.; CHANG, A.; FERRARO, R.; GRUBER, A.;JANOWIAK, J.; MCNAB, A.; RUDOLF, B. and SCHNEIDER, U. – The Global Precipitation Climatology Project (GPCP) Combined Precipitation Dataset. American Meteorological Society – vl 78, nº1, 5-20, - doi.org/10.1175/15200477, 1997.

HUFFMAN, G. J.; BOLVIN, D. T.; and NELKIN, E. J.: Integrated Multi-satellite Retrievals for GPM (IMERG) Technical Documentation, NASA Goddard Space Flight Center, USA, 2017.

JIANG-SHAN, Z.; FAN-YOU, K., and HENG-CHI, L.: Bias-Corrected Short-Range Ensemble Forecasts for Near-Surface Variables during the Summer Season of 2010 in Northern China, Atmospheric and Oceanic Science Letters, vol 7: n° 4, 334-339, http://dx.doi.org/10.3878/j.issn.1674-2834.13.0098, 2014

JOHNSON, F. and SHARMA, A.: Accounting for interannual variability: A comparison of options for water resources climate change impact assessments, Water Resour. Res., 47, W04508, doi:10.1029/2010WR009272, 2011.

JOHNSON, S. J.; STOCKDALE, T. N.; FERRANTI, L.; BALMASEDA, M. A.; MOLTENI, F.; MAGNUSSON, L.; TIETSCHE, S.; DECREMER, D.; WEISHEIMER, A.; BALSAMO, G.; KEELEY, S. P. E.; MOGENSEN, K.; ZUO, and MONGE-SANZ B. M.: SEAS5: the new ECMWF seasonal forecast system, Geosci. Model Dev., 12, 1087–1117, 2019 https://doi.org/10.5194/gmd-12-1087-2019

JUÀREZ, R. I. N.; LI, W.; FU, R.; FERNANDES, K. and CARDOSO, A. O.: Comparison of Precipitation Datasets over the Tropical South American and African, Journal of Hydrometeorology, vl 10, 289–299, https://doi.org/10.1175/2008JHM1023.1 , 2009.

KALNAY, E.: Atmospheric modeling, data assimilation and predictability. Cambridge University Press, New York, 2003

KIRCHNER, J. W.: Catchments as simple dynamical systems: Catchment characterization, rainfall-runoff modeling, and doing hydrology backward, Water Resour. Res., 45, W02429, doi:10.1029/2008WR006912, 2009.

KIM, K. B.; KWON, H. and HAN, D.: Precipitation ensembles conforming to natural Variations derived from a regional climate model using a new bias correction scheme, Hydrol. Earth Syst. Sci., 20, 2019–2034, 2016, doi:10.5194/hess-20-2019, 2016.

KIM, K. B., KWON, H. H. and HAN, D.: Bias-correction schemes for calibrated flow in a conceptual hydrological model, Hydrology Research, 52.1, doi: 10.2166/nh.2021.043, 2021.

KLEMES, V.: Operational testing of hydrological simulation models. Hydrological Sciences Journal, 31:1, 13-24, DOI: 10.1080/02626668609491024, 1986 http://dx.doi.org/10.1080/02626668609491024.

KRZYSZTOFOWICZ, R.: Bayesian system for probabilistic river stage forecasting, Journal of Hydrology 268(1-4):16-40, DOI:10.1016/S0022-1694(02)00106-3. 2002.

KRZYSZTOFOWICZ, R. and MARANZANO, C.: Hydrologic uncertainty processor for probabilistic stage transition forecasting. Journal of Hydrology 293 (1–4), 57–73, 2004.

KUCERA, P. A.; EBERT, E. E.; TURK, F. J.; LEVIZZANI, V.; KIRSCHBAUM, D.; TAPIADOR, F. J.; LOEW, A.; and BORSCHE, M.: Precipitation from space: Advancing Earth system science, B. Am. Meteorol. Soc., 94, 365–375, 2013.

KUCZERA, G. and PARENT, E.: Monte Carlo assessment of parameter uncertainty in conceptual catchment models: The Metropolis algorithm. Journal of Hydrology 211: 69—85, 1998.

KULL, D. and FELDMAN, A.: Evolution of Clark's unit graph method to spatially distributed runoff. Journal of Hydrologic Engineering, ASCE, 3(1), 9-19, 1998.

KUMMEROW; C. AND COAUTHORS: The status of the Tropical Rainfall Measuring Mission (TRMM) after two years in orbit, Journal of Applied Meteorology and Climatology, 39, 1965-1982, 2000

LEKKAS, D. F., IMIRE, C. E., and LEES, M. J.: Improved non-linear transfer function and neural network method of flow routing for real-time forecasting. J Hydroinform 3(3):153–164, 2001

LETTENMAIER, D. P.; ALSDORF, D.; DOZIER, J.; HUFFMAN; G. J., PAN, M. and WOOD, E. F.: Inroads of remote sensing into hydrologic science during the WRR era, Water Resour. Res., 51, 7309–7342, https://doi.org/10.1002/2015WR017616 , 2015.

LEVY M. C.; COHN A.; LOPES A. V. and THOMPSON S. E.: Addressing rainfall data selection uncertainty using connections between rainfall and streamflow. www.nature.com/scientificreports, pg. 1-12, Scientific Reports, 7: 219, DOI:10.1038/s41598-017-00128-5, 2017.

LI, L.; NGONGONDO, C. S.; XU, C.-Y. and GONG, L.: Comparison of the global TRMM and WFD precipitation datasets in driving a large-scale hydrological model in southern Africa, Hydrol. Res., 44, 770–788, DOI:10.2166/nh.2012.175 , 2013.

LIMA, A. L. D. and OLIVEIRA, C. B. C.: Revisão da construção dos cortes de Benders ao considerar o Modelo Autorregressivo Periódico Anual (PAR(p)-A) no Algoritmo de Programação Dinâmica Dual Estocástica, Relatório de Projeto – DEA - 1941 /2021, Eletrobras – CEPEL, Rio de Janeiro, RJ, 2021.

LIU, Y., and GUPTA, H. V. , Uncertainty in hydrologic modeling: Toward an integrated data assimilation framework, Water Resour. Res., 43, W07401, doi:10.1029/2006WR005756. 2007.

LIU. Z., GUO. S., and ZHANG. H.: Comparative Study of Three Updating Procedures for Real-Time Flood Forecasting. Water Resour. Manage 30. 2111–2126 https://doi.org/10.1007/s11269-016-1275-0, 2016.

LUCATERO, D.; MADSEM, H.; REFSGAARD, J. C.; KIDMOSE, J. and JENSEN, K. H.: Seasonal streamflow forecasts in the Ahlergaarde catchment, Denmark: effect of preprocessing and postprocessing on skill and statistical consistency, Hydrol. Earth Syst. Sci. Discuss., https://doi.org/10.5194/hess-2017-379, 2017.

LUNDBERG, A.: Combination of a conceptual model and an autoregressive error model for improving short time forecasting. Nord Hydrol 13:233–246, 1982

MADADGAR, S., MORADKHANI, H., and GAREN, D.: Towards improved post-processing of hydrologic forecast ensembles. Hydrol. Process. 28 (1), 104–122. https://doi.org/10.1002/hyp.9562, 2014

MAGGIONI, V.; MAYERS, P. C. and ROBINSON, M. D.: A Review of Merged High-Resolution Satellite Precipitation Product Accuracy during the Tropical Rainfall Measuring Mission (TRMM) Era, Journal of Hydrometeorology, Vol. 17, p.1101- 1117, 2016. - DOI: 10.1175/JHM-D-15-0190.1

MANTAS, V. M.; LIU, Z.; CARO, C. and PEREIRA, A. J. S. C.: Validation of TRMM Multi-satellite Precipitation Analysis (TMPA) products in the Peruvian Andes. Atmos. Res., 163, 132–145, doi:10.1016/j.atmosres.2014.11.012. – 2015.

MASON, S. J. and GRAHAM N. E.: Areas beneath the relative operating characteristics (ROC) and relative operating levels (ROL) curves: Statistical significance and interpretation, Quarterly Journal of the Royal Meteorological Society, 30, 291-303, https://doi.org/10.1256/003590002320603584, 2002.

MEDINA, H.; TIAN, D.; MARIN, F. R.; and CHIRICO, G. B.: Comparing GEFS, ECMWF, and Postprocessing Methods for Ensemble Precipitation Forecasts over Brazil. Journal of Hydrometeorology, vol 20, 773-790, DOI: 10.1175/JHM-D-18-0125.1, 2019.

MEHROTRA, R., and SHARMA, A.: A multivariate quantile matching bias correction approach with auto- and cross dependence across multiple time scales: Implications for downscaling. J. Climate, 29, 3519–3539, https://doi.org/10.1175/JCLI-D-15-0356.1, 2016.

MICHELSON, D. B.: Systematic correction of precipitation gauge observations using analyzed meteorological variables. Journal of Hydrology 290, pg 161–177, doi:10.1016/j.jhydrol.2003.10.005, 2004.

MINGYUE CHEN, XIE P., and CPC Quality Control Working Group Climate Prediction Center (CPC)/NCEP/NOAA: Quality Control of Daily Precipitation Reports at NOAA/CPC, CPC-NOAA GTS QC AMS, 2008.

MORADKHANI, H., SOROOSHIAN, S., GUPTA, H., and HOUSER, P. R.: Dual state parameter estimation of hydrological models using ensemble Kalman filter. Advances in Water Resources, 28(2), 135–147. https://doi.org/10.1016/j.advwatres.2004.09.002, 2005.

MSWEP V2.8, Technical Documentation, February 14, 2021, available in https://www.dropbox.com/s/5r4nnicfe3ft12d/MSWEP_V2_doc.pdf?dl=1, accessed in 2021/10/30.

MURPHY, A. H.: New Vector partition of the probability score. Journal of applied Meteorology and Climatology, 12, 595-600, https://doi.org/10.1175/1520-0450(1973)012<0595:ANVPOT>2.0.CO;2, 1973.

MURPHY, A.H.: General decompositions of MSE-based skill scores: Measures of some basic aspects of forecast quality. Monthly Weather Review, **124**, 2353-2369, 1996.

NAGHETTIN, M.; and PINTO, E. J. A.: Hidrologia Estatística. Belo Horizonte: CPRM, 2007

NAJIM, M. M. M. D.: Application of the HEC-HMS model for runoff simulation in a tropical catchment. Environmental Modeling & Software. Vl 46, pg 155-162 http://dx.doi.org/10.1016/j.envsoft.2013.03.006, 2013.

National Oceanic and Atmospheric Administration – NOAA. (2018). Gauge Global Dataset ftp. Retrieved in 2018, January 18, from ftp://ftp.cpc.ncep.noaa.gov/precip/CPC_UNI_PRCP/GAUGE_GLB

NASH, J. E. and SUTCLIFFE, J. V.: River flow forecasting through conceptual models part I - A discussion of principles, Journal of Hydrology, 10 (3), 282-290, 1970.

NASCIMENTO, F. B.: Estratégias de Predição de Preços do Mercado Livre de Energia por Redes Neurais Artificiais e Filtragem Estocástica, Dissertação de Mestrado, Programa de Pós-Graduação em Engenharia Elétrica, Faculdade de Engenharia da Universidade Federal de Juiz de Fora, 2021.

ONS - OPERADOR NACIONAL DO SISTEMA ELÉTRICO. Revisão das Séries de Vazões Naturais nas Principais Bacias do SIN – Relatório Executivo – Dezembro/2005. 126p. Rio de Janeiro, 2005

ONS – OPERADOR NACIONAL DO SISTEMA ELÉTRICO: Procedimentos de Rede. 2016, available in: http://apps05.ons.org.br/procedimentorede/procedimento_rede/procedimento_rede.aspx. Accessed at September 20th 2016.

ONS - OPERADOR NACIONAL DO SISTEMA ELÉTRICO. NT 0053-2019-Metodologia de Previsão de Precipitação por Conjunto e Remoção de Viés com Histórico de Curto Prazo Rio de Janeiro, 2019.

ONS – OPERADOR NACIONAL DO SISTEMA ELÉTRICO: Procedimentos de Rede. 2021. available in: http://www.ons.org.br/paginas/sobre-o-ons/procedimentos-de-rede/vigentes. Access on September 6th. 2021.

PAIVA L. F. G., MONTENEGRO, S. M. and CATALDI, M.: Prediction of monthly flows for Três Marias (São Francisco river basin) using CFS climate forecast model, Brazilian Journal of Water Resources, v. 25, e16, https://doi.org/10.1590/2318-0331.252020190067, 2020

PALMER, T. and WEBSTER, P.: Towards a unified approach to climate and weather prediction, in: Proceedings of 1st Demetra Conference on Climate Change, 1993.

PAPPENBERGER, F.; WETTERHALL, F.; DUTRA, E.; DI GIUSEPPE, F.; BOGNER, K.; ALFIERI, L.; and CLOKE, H. L.: Seamless forecasting of extreme events on a global scale, pp. 3–10, Proceedings of H01, IAHS-IAPSO-IASPEI Assembly, Gothenburg, Sweden, July 2013 (IAHS Publ. 359, 2013), 2013.

PALMER, T. N.; DOBLAS-REYES, F. J.; WEISHEIMER, A. and RODWELL, M. J..: TOWARD SEAMLESS PREDICTION - Calibration of Climate Change Projections Using Seasonal Forecasts, AMERICAN METEOROLOGICAL SOCIETY, APRIL, 450-470, 2008.

PIANI, C.; HAERTER, J.; and COPPOLA, E.: Statistical bias correction for daily precipitation in regional climate models over Europe, Theor. Appl. Climatol., 99, 187–192, 2010.

PILZ, T., DELGADO, J. M., VOSS, S., VORMOOR, K., FRANCKE, T., COSTA, A. C., MARTINS, E., and BRONSTERT, A.: Seasonal drought prediction for semiarid northeast Brazil: what is the added value of a process-based hydrological model?, Hydrol. Earth Syst. Sci., 23, 1951–1971, https://doi.org/10.5194/hess-23-1951-2019, 2019.

PINTO, R. B.; GIBERTONI, R. F. C.; REGO, J. L.; SCHWANENBERG, D.; and REIS A. A.: Sistema Integrador DELFT_FEWS: usos e aplicações no cenário brasileiro. XX Simpósio Brasileiro de Recursos Hídricos, Bento Gonçalves-RS, 2013, editor: ABRH.

POZZI, W.; SHEFFIELD, J.; STEFANSKI, R.; CRIPE, D.; PULWARTY, R.; VOGT, J. V.; HEIM, R. R.; BREWER, M. J.; SVOBODA, M.; WESTERHOFF, R.; VAN DIJK, A. I. J. M.; LLOYD-HUGHES, B.; PAPPENBERGER, F.; WERNER, M.; DUTRA, E.; WETTERHALL, F.; WAGNER, W.; SCHUBERT, W.; MO, K.; NICHOLSON, M.; BETTIO, L.; NUNEZ, L.; VAN BEEK, R.; BIERKENS, M.; GONCALVES DE GONCALVES, L. G.; ZELL DE MATTOS, J. G. and LAWFORD, R.: Toward global drought early warning capability: expanding international cooperation for the development of a framework for monitoring and forecasting. B. Am. Meteorol. Soc., 94, 776–785, DOI:10.1175/BAMS-D-11-00176 , 2013.

PRUDHOMME, C.; HANNAFORD, J.; HARRIGAN, S.; BOORMAN, D.; KNIGHT, J.; BELL, V.; JACKSON, C.; SVENSSON, C.; PARRY, S.; BACHILLER- JARENO, N.; DAVIES, H.; DAVIS, R.; MACKAY, J.; MCKENZIE, A.; RUDD, A.; SMITH, K.; BLOOMFIELD, J.; WARD, R.; and JENKINS, A.: Hydrological Outlook UK: an operational streamflow and groundwater level forecasting system at monthly to seasonal time scales, Hydrol. Sci. J., 62, 2753–2768, https://doi.org/10.1080/02626667.2017.1395032, 2017

RATRI, D. N.; WHAN, K.; and SCHMEITS, M.: A Comparative Verification of Raw and Bias-Corrected ECMWF Seasonal Ensemble Precipitation Reforecasts in Java (Indonesia), American Meteorological Society, DOI: 10.1175/JAMC-D-18-0210.1, 2019.

REBOITA, M. S.,. DIAS, C. G., DUTRA, L. M. M., ROCHA, R. P., and LLOPART, M.: Seasonal climate forecast to Brazil obtained through global and regional climate models. Revista Brasileira de Meteorologia, v. 33, n. 2, 207-224, DOI: http://dx.doi.org/10.1590/0102-7786332001, 2018.

REGONDA, S. K., SEO, D. J., LAWRENCE, B., BROWN, J. D. and DEMARGNE, J.: Short-term ensemble streamflow forecasting using operationally-produced single-valued streamflow forecasts – A Hydrologic Model Output Statistics (HMOS) approach, Journal of Hydrology Volume 497, 8 August 2013, Pages 80-96, https://doi.org/10.1016/j.jhydrol.2013.05.028, 2013.

REIS, A. A.; FERNANDES, W. S.; and RAMOS, M. H.;Assessing two precipitation data sources at basins of special interest to hydropower production in Brazil. RBRH - Brazilian Journal of Water Resources, RBRH-2019-0068, 2019. http://dx.doi.org/10.1590/2318-0331.252020190068.

ROMANOWICZ, R. J., YOUNG, P. C., BEVEN, K. J. and PAPPENBERGER F.: A data based mechanistic approach to nonlinear flood routing and adaptive flood level forecasting. Adv Water Resour 31(8):1048–1056, 2008.

ROZANTE, J. R.; SOARES, M. D.; GONÇALVES, L. G. G. and VILA, D. A.: Combining TRMM and Surface Observations of Precipitation: Technique and Validation over South America. American Meteorological Society, vl 25,885-894, https://doi.org/10.1175/2010WAF2222325.1 , 2010.

ROZANTE, J. R.; VILA, D. A.; CHIQUETO, J. B.; FERNANDES, A. A.; and ALVIM, D. S.: Evaluation of TRMM/GPM Blended Daily Products over Brazil, Remote Sensing 2018, 10, 882; doi:10.3390/rs10060882, 2018.

ROZANTE, J. R.; GUTIERREZ, E. R.; FERNANDES, A. A.; and VILA, D. A.: Performance of precipitation products obtained from combinations of satellite and surface observations. International Journal of Remote Sensing 2020, VOL. 41, NO. 19, 7585–7604, https://doi.org/10.1080/01431161.2020.1763504, 2020.

SÁNCHEZ-GARCÍA, E.; VOCES-ABOY, J.; NAVASCUÉS, B.; and RODRÍGUEZ-CAMINO E.: Regionally improved seasonal forecast of precipitation through Best estimation of winter NAO, Adv. Sci. Res., 16, 165–174, 2019 https://doi.org/10.5194/asr-16-165-2019.

SANT'ANNA NETO, J. L.: Ritmo Climático e a gênese das chuvas na Zona Costeira Paulista. Dissertação (Mestrado em Geografia). São Paulo: FFLCH/USP- Programa de Pós-Graduação em Geografia, 1990. 168p

SCHARFFENBERG, W.: Hydrologic Modeling System – HEC-HMS – User's Manual, version 4.2, USACE – US Army Corps of Engineers - Hydrologic Engineering Center, CA, USA, 2016.

SCHEEL, M. L. M.; ROHRER, M.; HUGGEL, C.H.; VILLAR, D. S.; SILVESTRE, E.; and HUFFMAN, G. J.: Evaluation of TRMM Multi-satellite Precipitation Analysis (TMPA)

performance in the Central Andes region and its dependency on spatial and temporal resolution. Hydrol. Earth Syst. Sci., 15, 2649–2663, doi:10.5194/hess-15-2649-2011.

SCHEFZIK, R., THORDIS L. T., and GNEITING, T.: Uncertainty Quantification in Complex Simulation Models Using Ensemble Copula Coupling. Statist. Sci. 28 (4) 616 - 640, https://doi.org/10.1214/13-STS443, 2013

SCHEFZIK, R.: Ensemble calibration with preserved correlations: unifying and comparing ensemble copula coupling and member-by-member postprocessing, Q. J. R. Meteorol. Soc. 143: 999–1008, January 2017 B DOI:10.1002/qj.2984.

SCHUMANN, G. J-P.; BATES, P. D.; APEL, H. and ARONICA, G. T.: Global Flood Hazard: Applications in Modeling, Mapping and Forecasting, 300 pp., ISBN: 978-1-119-32586-4, 2018.

SCHWANENBERG, D; FAN, F. M.; NAUMANN, S; KUWAJIMA, J. I.; MONTERO, R. A. and REIS, A. A.: Short-Term Reservoir Optimization for Flood Mitigation under Meteorological and Hydrological Forecast Uncertainty - Application to the Três Marias Reservoir in Brazil. Water Resources Management, 2015 - 29:1635–1651 - DOI 10.1007/s11269-014-0899-1, 2015.

SEARCY, J. K.; HARDISON C. H. and LANGBEIN, W. B.: Double-mass curves – Manual of Hydrology: Part 1. General Surface-water techniques. USGS – Geological Survey Water-Supply – Paper 1541-B, 66p, Washington, USA, 1960.

SEO, D. J., HERR, H. D., and SCHAAKE, J. C.: A statistical post-processor for accounting of hydrologic uncertainty in short-range ensemble streamflow prediction. Hydrol. Earth Syst. Sci. Discuss. 2006, 1987–2035. https://doi.org/10.5194/hessd-3-1987- , 2006.

SERRAT-CAPDEVILA, A.; VALDES, J. B. and STAKHIV, E. Z.: Water management applications for satellite precipitation products: synthesis and recommendations, J. Am.Water Resour. Assoc., 50, 509– 525, https://doi.org/10.1111/jawr.12140 , 2013.

SHAO, Q.; TRAYLEN, A.; and ZHANG, L.: Nonparametric method for estimating the effects of climatic and catchment characteristics on mean annual evapotranspiration, Water Resour. Res., 48, W03517, doi:10.1029/2010WR009610, 2012.

SHARMA, D.; DAS GUPTA, A.; and BABEL, M. S.: Spatial disaggregation of bias-corrected GCM precipitation for improved hydrologic simulation: Ping River Basin, Thailand, Hydrol. Earth Syst. Sci., 11, 1373–1390, doi:10.5194/hess-11-1373-2007, 2007.

SHI, X.; WOOD, A. W.; and LETTENMAIER, D. P.: How essential is hydrologic model calibration to seasonal streamflow forecasting? Journal of Hydrometeorology, 9 (6), 1350–1363, 2008.

SHIMIDT, J.; CANCELLA, R.; and PEREIRA JUNIOR, A. O.: The effect of wind power on long-term variability of combined hydro-wind resources: The case of Brazil. Renewable and Sustainable Energy Reviews 55, p. 131–141, 2016

SHUKLA, J.: Predictability in the midst of chaos: a scientific basis for climate forecasting. Science 282:728–731, 1998.

SIMPSON, J., ADLER, R. F., NORTH, G. R.: A Proposed Tropical Rainfall Measuring Mission (TRMM) Satellite. Bull. Amer. Meteor. Soc., 69, 278–278, Simpson, J., R.F., and Adler, G.R.: A Proposed Tropical Rainfall Measuring Mission (TRMM) Satellite. Bull. Amer. Meteor. Soc., 69, 278–278, https://doi.org/10.1175/1520-0477(1988)069<0278:APTRMM>2.0.CO;2, 1988.

SIQUEIRA, V. A..; PAIVA, R. C. D.; FLEISCHMANN, A. S.; FAN, F. M.; RUHOFF A. L.; PONTES, P. R. M.; PARIS, A.; CALMANT, S. and COLLISCHONN. W.: Toward continental hydrologic-hydrodynamic modeling in South America. Hydrol. Earth Syst. Sci. Discuss., https://doi.org/10.5194/hess-2018-225, 2018.

SKOFRONIK-JACKSON, G.; KIRSCHBAUM, D.; PETERSEN, W.; HUFFMAN, G.; KIDD, C.; STOCKER, E.; and KAKAR, R.: The Global Precipitation Measurement (GPM) mission's scientific achievements and societal contributions: reviewing four years of advanced rain and snow observations. Q. J. R. Meteorol Soc. 2018;144 (Suppl. 1):27–48, ADVANCES IN REMOTE SENSING OF RAINFALL AND SNOWFALL, DOI: 10.1002/qj.3313, 2018.

SOLOMON, S.; QIN, D.; MANNING, M.; MARQUIS, M.; AVERYT, K.; TIGNOR, M. M. B.; MILLER JR., H. L. and CHEN. Z.: Climate Change 2007: The Physical Science Basis. Cambridge University Press, 996 pp., 2007

SU, F.; HONG, Y. and LETTENMAIER, D. P.: Evaluation of TRMM Multisatellite Precipitation Analysis (TMPA) and its utility in hydrologic prediction in the La Plata Basin, J. Hydrometeorol., 9, 622– 640, https://doi.org/10.1175/2007JHM944.1, 2008.

SUN, F.; RODERICK, M. L.; LIM, W. H.; and FARQUHAR, G. D.: Hydroclimatic projections for the Murray-Darling Basin based on an ensemble derived from Intergovernmental Panel on Climate Change AR4 climate models, Water Resour. Res., 47, W00G02, doi:10.1029/2010WR009829, 2011.

SUN, Q.; MIAO, C.; DUAN, Q; ASHOURI, H.; SOROOSHIAN, S.; and HSU H.-L..: A Review of Global Precipitation Data Sets: Data Sources, Estimation and Inter-comparisons. Reviews of Geophysics, 56, 79-107. https://doi.org/10.1002/2017RG000574, 2017.

TANG, G.; ZENG, Z.; LONG, D.; GUO, X.; YONG, B.; ZHANG, W. and HONG, Y.: Statistical and hydrological comparisons between TRMM and GPM Level-3 products over a mid-latitude basin: Is day-1 IMERG a good successor for TMPA 3B42V7?, J. Hydrometeorol., 17, 121–137, https://doi.org/10.1175/JHM-D-15-0059.1, 2016.

TEUTSCHBEIN, C. and SEIBERT, J.: Is bias correction of regional climate model (RCM) simulations possible for non-stationary conditions? Hydrol. Earth Syst. Sci., 17, 5061–5077, 2013 www.hydrol-earth-syst-sci.net/17/5061/2013/ doi:10.5194/hess-17-5061-2013

THIELEN, J., BARTHOLMES, J., RAMOS, M.-H., and DE ROO, A.: The European Flood Alert System Part 1: Concept and development, Hydrol. Earth Syst. Sci., 13, 125–140, https://doi.org/10.5194/hess-13-125-2009, 2009.

TINÔCO, I. C. M., BEZERRA, B. G., LUCIO, P. S., and BARBOSA, L. M.: Characterization of Rainfall Patterns in the Semiarid Brazil. Anuário do Instituto de Geociências – UFRJ, DOI: http://dx.doi.org/10.11137/2018_2_397_409, 2018.

TIWARI. A. D.. MUKHOPADHYAY. P.. and MISHRA. V.: Influence of bias correction of meteorological and streamflow forecast on hydrological prediction in India. Journal of Hydrometeorology . Published-online: 25 Jan 2021. https://doi.org/10.1175/JHM-D-20-0235.1. 2021.

TWEDT, T. M.; SCHAAKE, J. C. and PECK, E. L.: National weather service extended streamflow prediction, Proc. Western Snow Conference, Albuquerque, NM, 52–57, https://westernsnowconference.org/node/1106, 1977.

TWIGT, D.; REGO, J. L.; TYRRELL, D.; and TROOST, T.: Water Quality Forecasting Systems: Advanced Warning of Harmful Events and Dissemination of Public Alerts. Proceedings of the 8th International Conference on Information Systems for Crisis Response and Management, in Lisbon, Portugal, 8-11. 2011.

VAN DER KNIJFF, J. M.; YOUNIS, J. and DE ROO, A. P. J.: LISFLOOD: a GIS-based distributed model for river basin scale water balance and flood simulation, International Journal of Geographical Information Science, 24, 189-212, 10.1080/13658810802549154, 2010.

VAN OSNABRUGGE, B., WEERTS, A. H., and UIJLENHOET, R.: genRE - A Method to Extend Gridded Precipitation Climatology Data Sets in Near Real-Time for Hydrological Forecasting Purposes, Water Resources Research, 53(11), doi: 10.1002/2017WR021201, 2017.

VERKADE, J. S., BROWN, J. D., REGGIANI, P., and WEERTS, A. H.: Postprocessing ECMWF precipitation and temperature ensemble reforecasts for operational hydrologic forecasting at various spatial scales, Journal of Hydrology, 501, 73–91, doi:10.1016/j.jhydrol.2013.07.039, 2013.

VERKADE, J. S.: Estimating the real-time predictive hydrological uncertainty, Doctorate thesis, printed by Gildeprint Drukkerijen, p 1-177, Delft, the Netherlands, 2015.

VIGAUD, N., ROBERTSON, A. W., and TIPPETT M. K.:Multimodel ensembling of subseasonal precipitation forecasts over North America. Mon Weather Rev 145:3913–3928, 2017a

VIGAUD, N., ROBERTSON A. W., TIPPETT M. K., and ACHARYA, N.: Subseasonal predictability of boreal summer monsoon rainfall from ensemble forecasts. Front Environ Sci. https://doi.org/10.3389/fenvs.2017.00067, 2017b

VITART, F., ROBERTSON, A.W., and ANDERSON D.L.T.: Subseasonal to seasonal prediction project: bridging the gap between weather and climate. Bull World Meteorol Organ 61:23–28, 2012.

VOISIN, N.; WOOD, A. W. and LETTENMAIER, D. P.: Evaluation of precipitation products for global hydrological prediction, J. Hydrometeorol., 9, 388–407, https://doi.org/10.1175/2007JHM938.1, 2008.

WANG, S., ANICHOWSKI, A., TIPPETT, M. K., and SOBEL, A.H.: Seasonal noise versus subseasonal signal: forecasts of California precipitation during the unusual winters of 2015–2016 and 2016–2017. Geophys Res Lett 44:9513–9520, 2017.

WANG, Y., DE CONNING, E.; HAROU, A.; JACOBS, W.; JOE, P.; NIKTINA, L.; ROBERSTS, R.; J. WANG, WILSON, J.; ATENCIA, A.; BICA B.,; BROWN, B.; GOODMANN, S.; KANN, A.; LI, P.-W.P.; MONTEIRO, I.; PARRISH, P.; SCHMID, F.; SEED, A.; and SUN, J.: Guidelines for nowcasting techniques WMO publication 1198, 82 pp, ISBN: 978-92-63-11198-2, 2017.

WASTL, C.; SIMON, A.; WANG, Y.; KULMER, M.; BAÁR, P.; BÖLÖNI, G.; DANTINGER, J.; EHRLICH, A.; FISCHER, A.; FRANK, A.; HEIZLER, Z.;, KANN, A.; STADLBACHER, K.; SZINTAI, B.; MIHÁLY SZ″UCS, M.; and WITTMANN, C.: A seamless probabilistic forecasting system for decision making in Civil Protection, Meteorologicshe Zeitschrift, Vol. 27, No. 5, 417–430, DOI 10.1127/metz/2018/902, 2018.

WERNER, M.; HEYNERT, K.: Open model integration - A review of practical examples in operational flood forecasting, 7th International Conference on Hydroinformatics, Nice, France, Vol. 1, 155-162, 2006.

WERNER, M.; SCHELLEKENS J.; GIJSBERS, P.; VAN DIJK, M.; VAN DEN AKKER, O. and HEYNERT, K.: The Delft-FEWS Flow Forecasting System. Environmental Modelling & Software, 40, p. 65–77,.-doi:10.1016/j.envsoft.2012.07.010., 2013.

WETTERHALL, F. and DI GIUSEPPE, F.: The benefit of seamless forecasts for hydrological predictions over Europe, Hydrol. Earth Syst. Sci. Discuss., https://doi.org/10.5194/hess-2017-527, 2018.

WILKS, D. S.: Statistical methods in the atmospheric sciences, Academic Press, Oxford, United Kingdom, 2011.

World Meteorological Organization. Seamless Prediction of the Earth System: From Minutes to Months. WMO No. 1156 (World Meteorological Organization, Geneva, 2015) https://library.wmo.int/doc_num.php?explnum_id=3546, 2015.

WOOD, A. W., LEUNG, L. R., SRIDHAR, V., and LETTENMAIER, D. P.: Hydrologic implications of dynamical and statistical approaches to downscaling climate model outputs, Climatic Change, 62, 189– 216, doi:10.1023/B:CLIM.0000013685.99609.9e, 2004.

WOOD, A.W. and LETTENMAIER, D. P.: A testbed for new seasonal hydrologic forecasting approaches in the western US, B. Am. Meteorol. Soc., 87, 1699–1712, doi:10.1175/BAMS-87-12-1699, 2006.

WOOD, A.W. and LETTENMAIER, D. P.: An ensemble approach for attribution of hydrologic prediction uncertainty, Geophys. Res. Lett., 35, L14401, doi:10.1029/2008GL034648, 2008.

WU, S.J.; LIEN, H. C.; CHANG, C. H. and SHEN, J. C.: Real-time correction of water stage forecast during rainstorm events using combination of forecast errors. Stoch Environ Res Risk Assess 26:519–531, DOI 10.1007/s00477-011-0514-4, 2012.

XIONG, L. and O'CONNOR, K.: Comparison of four updating models for real-time river flow forecasting. Hydrol. Science 47(4):621–639, 2002.

YAMAZAKI, D.; KANAE, S.; KIM, H. and OKI, T.: A physically based description of floodplain inundation dynamics in a global river routing model, Water Resources Research, 47, 10.1029/2010WR009726, 2011.

YANG, C. ; YUAN, H.; and SU, X.: Bias correction of ensemble precipitation forecasts in the improvement of summer streamflow prediction skill, Journal of Hydrology, Vol. 588, September 2020, 124955; https://doi.org/10.1016/j.jhydrol.2020.124955, 2020

YASSIM, M., ASFAW, A., SPEIGHT, V. and SHUCKSMITH, J. D.: Evaluation of a data-driven and process-based real-time flow forecasting techniques for informing operation of surface water abstraction. J. Water Resour. Plan Manage., 147(7), DOI: 10.1061/ (ASCE)WR.1943-5452.0001397, 2021.

YE, A.; DENG, X.; MA, F.; DUAN, Q.; ZHOU, Z.; and DU, C.: Integrating weather and climate predictions for seamless hydrologic ensemble forecasting: A case study in the Yalong River basin, Journal of Hydrology, 547, 196–207, http://dx.doi.org/10.1016/j.jhydrol.2017.01.053, 2017

YUAN, X., WOOD, E.F., and LIANG, M.: Integrating weather and climate prediction: toward seamless hydrologic forecasting. Geophys. Res. Lett. 41, 5891–5896, 2014

ZALACHORI, I.; RAMOS, M.-H.; GARÇON, R.; MATHEVET, T. and GAILHARD, J.: Statistical processing of forecasts for hydrological ensemble prediction: a comparative study of different bias correction strategies, Adv. Sci. Res., 8, 135–141, www.adv-sci-res.net/8/135/2012/doi:10.5194/asr-8-135-2012,

ZHAO, T.; BENNET, J. C.; WANG, Q. J.; SCHEPEN, A.; WOOD, A. W.; ROBERTSON, D. E.; and RAMOS, M. H.: How Suitable is Quantile Mapping For Postprocessing GCM Precipitation Forecasts?, Journal of Climate, 3185-3196, DOI: 10.1175/JCLI-D-16-0652.1, 2017.

ZHAO, L., DUAN, Q., SCHAAKE, J., YE, A. and XIA, J.: A hydrologic post-processor for ensemble streamflow predictions. Advances in Geosciences 29, 51–59, 2011.

ZHAO, T., ZHANG, W., ZHANG, Y., LIU, Z., and CHEN, X.: Significant spatial patterns from the GCM seasonal forecasts of global precipitation, Hydrol. Earth Syst. Sci., 24, 1–16, https://doi.org/10.5194/hess-24-1-2020, 2020.